Multi-component Determinations using Sequential Injection Analysis

by

Rosa Elizabeth Taljaard

Submitted in partial fulfilment of the requirements for the degree

PHILOSOPHIAE DOCTOR

in the Faculty of Science
University of Pretoria
Pretoria
October 1999

Multi-component Determinations using Sequential Injection Analysis

by

Rosa Elizabeth Taljaard

Promoter: Professor Jacobus F. van Staden

Department of Chemistry

University of Pretoria

Degree: Philosophiae Doctor

SYNOPSIS

The need to measure several parameters rapidly in the same sample in areas such as clinical chemistry, environmental pollution and industrial control has urged the development of automated methods of analysis. Multiple determinations are feasible, not only because it is more cost-effective, but also because it shortens or eliminates separation steps needed to remove interferences due to closely related species. This results in less sample preparation and eliminates loss of analyte due to long and sometimes ineffective pretreatment methods.

Several multi-component sequential injection systems are proposed. These include a novel tandem application of SIA, which is based on an optimised sequence of samples and reagents in the holding coil, as well as the kinetics of the reactions involved, to determine sulphate and iron sequentially or simultaneously in aqueous samples. The same analytes were used to evaluate a sandwich technique based on the introduction of a very large sample volume, sandwiched between two different reagents. A method based on differential kinetics was used to determine nickel and cobalt with the same reagent (PAR) without prior separation. Three sequential extraction systems were developed for the determination of two up to seven metal ions in the same samples.

Compared to flow injection extraction, the sequential injection extraction manifold is much simpler to design, since no phase segmenters or separators are needed.

For all of these determinations, SIA manifolds with only a single detector were used. The usefulness, cost-effectiveness and advantages of multi-component sequential injection analysis over convential (multi-component) flow injection analysis are demonstrated.

Multi-komponent Bepalings met behulp van Sekwensiële-inspuitanalise

deur

Rosa Elizabeth Taljaard

Promotor: Professor Jacobus F. van Staden

Departement Chemie

Universiteit van Pretoria

Graad: Philosophiae Doctor

SAMEVATTING

Die behoefte om verskeie parameters in dieselfde monster vinnig en effektief te bepaal, het die ontwikkeling van geoutomatiseerde analitiese metodes versnel. Hierdie behoefte het veral op die gebied van kliniese chemie, besoedelingsbeheer asook industriële kwaliteitsbeheer ontstaan. Veelvuldige bepalings is wenslik, nie alleen omdat dit goedkoper is nie, maar ook weens die feit dat die skeidingstap benodig om steurings weens soortgelyke spesies te verwyder, verkort of heeltemal weggelaat kan word. Die resultaat hiervan is dat minder monstervoorbereiding benodig word. Dit opsigself verminder die verlies aan analiet as gevolg van lang en soms oneffektiewe monstervoorbereidingsmetodes.

Verskeie multi-komponent sekwensiële-inspuitanalise sisteme is voorgestel tydens hierdie studie, onder andere 'n nuwe tandem toepassing van SIA vir die agtereenvolgende of gelyktydige bepaling van yster en sulfaat in waterige monsters. Die bepaling is gebaseer op 'n geoptimiseerde volgorde van monsters en reagense in die deurvloeispiraal asook die kinetika van die betrokke reaksies. Dieselfde analiete is gebruik in die evaluering van 'n "toebroodjie-tegniek". Die tegniek is gebaseer op die

gebruik van 'n baie groot monstervolume wat geleë is tussen twee verskillende reagens oplossings. 'n Metode gebaseer op differensiële kinetika is aangewend vir die bepaling van nikkel en kobalt met dieselfde reagens (PAR), sonder die vooraf skeiding van die analiete. Drie sekwensiële-inspuitekstraksie sisteme is ontwikkel vir die bepaling van twee tot en met sewe metaalione in monsters. In vergelyking met vloei-inspuitekstrasie is die sisteemontwerp van die sekwensiële-inspuitekstraksie eenhede baie eenvoudig, aangesien geen fasesegmenteerders of -skeiers benodig word nie.

Al die voorgestelde bepalings het van SIA sisteme met slegs een detektor gebruik gemaak. Die aanwending, ekonomiese en ander voordele van hierdie veelvuldige tegniek bo konvensionele vloei-inspuitanalise (VIA) is aangetoon.

Acknowledgements

First and foremost, I would like to express my gratitude towards the Lord, my God, for the strength and perseverance He gave me to achieve this goal. There were many times that I was on the brink of letting all go, but He was (and is) always there for me to give me strength and courage.

I like to thank my supervisor, Professor Koos van Staden, for his constant enthusiasm, patience and valuable aid during my studies.

A special word of thanks to my husband, Pieter van Jaarsveldt, for all his patience, tolerance and special efforts, especially during the last few months. Pieter, thanks for all the extra tasks you had to perform in and around the house, for all the times you could not go out, because I had to work and for all the evenings you had to spend in front of the television alone. Without you I would definitely not made it thus far.

I also like to thank my parents, Kobus and Marika Taljaard, and sisters, Johanel, Marlie and Jacolene, for their encouragement and motivation. You have, often unknowingly, provide that vital support when it appears that nothing is about to work. To my family-in-law, thanks for your patience and encouragement.

A number of friends and colleagues have helped me in various ways, and I like to thank them all, while mentioning specifically only a few - Adelé Botha and Hanneli du Plessis for their help in finding the correct components (debubblers) for my extraction systems, for always being willing listen to my problems and for their valuable advice. Neels Hattingh, Niel Malan and Marga Stronkhorst for their constant encouragement, tolerance, motivation and advice - even though some of them were not in South Africa the whole time, they still took the effort to phone to show their support. Dr Raluca Stefan, thanks for your help with proofreading some of my articles. I also like to thank my colleagues at Citicol and CAL (Central Agricultural Laboratories) for their understanding and motivation.

I also want to express my gratitude towards the following persons and companies:

- Dr André Scheffer, Frans van Bemmel, Ian Grace and Stefan Toerien from Chemetrix for all their time and effort and advice in getting the diode array spectrophotometer up and running and ready for coupling with FlowTEK.
- Dr Graham Marshall for his advice and assistance with the coupling of the diode array spectrophotometer with the FlowTEK program.
- The FRD and the University of Pretoria for financial support.

To Him who by means of His power working in us is able to do so much more than we can ever asks for, or even think of: to God be the glory.

Ephesians 3 : 20 - 21.

Table of Contents

CHAPTER 1

Multi-Component Sequential Injection - A New Challenge?

1.1 Introduction

Since its introduction in 1990 [1, 2], sequential injection analysis' popularity grew tremendously. Several laboratories and research groups [3 - 10] started to exploit the advantages of this third generation of flow injection analysis. Due to its economical sample and reagent consumption and the simplicity and versatility of the sequential injection system, several traditional 'hand' methods and flow injection systems were adapted to SIA systems [11 - 18] and employed as process analysers. Several reasons can be given for the employment of flow and sequential injection systems as process analysers. These reasons include [9]:

- Reduction in cost (personnel, equipment and consumables).
- High and accurate sample throughput.
- Improvement of the work environment (the use of sealed tubing and reactors when working with hazardous and/or toxic reagents).
- Substantial reduction of waste containing toxic reagents or samples [19].

In laboratory applications manual reconfiguration of the flow channel, high reagent consumption due to continuous flow operation, frequent servicing of peristaltic pumps and frequent recalibration of the system are acceptable. In a process environment these are prohibitive in terms of cost and manpower. Early studies in the field of SIA [1] soon showed that a single manifold was sufficient, irrespective of the chemistry to be employed. The manifold, once optimised, could be 'cast in stone'. There is apparently no limit to how many solutions (reagents, samples and standards) or

devices (reactor coils, mixing chambers and detectors) can be nested around the valve. Indeed, an SI cluster may serve as a single and multichannel analyser. Alternatively, a series of standards can be permanently nested around the valve, being ready for automated recalibration whenever needed [20].

The biggest advantage of the sequential injection system is that there is no need for physical reconfiguration of the flow path. Any changes (injected sample volume, reaction time, sample dilution and reagent : analyte ratio) are accomplished via flow programming, rather than by physical reconfiguration of the flow path. Indeed, SI is fully computer compatible, as it allows all changes including system calibration, to be controlled from a computer keyboard, a feature that will allow its future optimisation through the use of artificial intelligence [20]. The SI system is further robust, reliable and requires a low frequency of maintenance. In comparison with FIA it is also more flexible for stop-flow and reversed flow operations.

There are presently two drawbacks of SI to be mentioned. First, since aspiration of the wash solution and sequencing of the zones in the holding coil take some time (typically 30 seconds), the sampling frequency of the SI system is presently half that of a conventional FI system, where filling of the injection valve is a matter of a few seconds. Secondly, SI requires specialized software, since the sequencing, injection and data collection are entirely computer driven. This, however, is not an obstacle in using the technique [3].

Automatic methods of analysis have been especially influential in clinic chemistry. Since health is one of the major concerns of our society, it is easy to understand the imperative need for hospitals to obtain a large number of analytical data as quickly and inexpensively as possible.

The situation is much the same in most industries, where quality control laboratories become much more important than they were a few decades ago. Most of the process control systems currently used, are based on physical measurements such as flow rate,

pressure, electrical resistance, etc. While this has resulted in processes which are operated under statistical control, verification of the process performance can only really be achieved by chemical analysis, usually in a remote plant laboratory. This approach is seen as unacceptable in the design of quality management systems for the production process. In such systems, the emphasis is on quality assurance during the process rather than after-the-fact. Process analysis brings the process controller a step closer to ensuring excellent control of the plant and real time quality assurance. At this stage, lengthy development times, the cost of these analysers and their maintenance requirements mean that only a few critical streams are monitored. The demands in this field are dictated by the large number of samples to be analysed, especially in on-line control of automized manufacturing processes and the quality now required in manufactured products. It is therefore necessary to control not only the raw products, but also the intermediate and end products.

Sequential injection systems had been proven to be suitable as on-line process analysers for most single component analysis [8, 9, 21]. Studies revealed that reduced numbers of samples can be used when applying SIA systems as process analysers, provided that the correct regression model is used [21]. The flow systems already adapted to SIA systems involved, however, very simple methods and operations and were mainly restricted to single component determinations. Multi-component analysis using SIA systems seemed to be a bit of a headache, since most of these determinations required extraction and the subsequent separation of the aqueous and organic phases, establishment of pH gradients or effective pH control, long and complex procedures, complex mathematical and statistical calculations and/or multiple detectors. To address these and the many other problems which usually showed up along the way, multi-component analysis might be seen as a new challenge in cost effective analysis.

The need to measure several parameters rapidly in the same sample in areas such as clinical chemistry, environmental pollution and industrial control has urged the development of automated methods of analysis, which in both the continuous and discrete modes offer the possibility of carrying out simultaneous determinations. In the

discrete mode, the same sample must be present in as many locations as there are parameters that are going to be determined. In the continuous mode or segmented flow analysis, the sample is split up into as many channels as there are parameters to be determined. Reaction and detection units exists for each of them.

1.2 Single-component sequential injection analysis

Determination of single components can range from simple analysis involving only one zone (the analyte zone) to complex systems using up to six different zones [22]. Single zone determinations involve mainly pH determinations, ion-selective electrodes, amperometric determinations or the use of chemical sensors. The properties of the unknown substance usually dictate the type of sensor needed for the detection. No mixing of analyte and reagent is needed and the analyte is analysed directly without chemical modification. The most important parameter needed to be controlled is the physical dispersion the analyte zone undergoes. In these type of applications it is advisable to work under low dispersion conditions ($D < 3$) in order to minimise the extent of sample dilution by mixing with the carrier, thereby ensuring a minimum decrease in sensitivity.

These methods offer substantial advantages which are noted below [23]:

- Simplicity. No sample pretreatment is necessary. Satisfactory sample dilution is achieved by controlling the dispersion (volume and flow rate) of the aspired zone.
- Rapidity. High sample frequencies are achieved this way.
- Sensitivity. Since it is a micromethod it is of great usefulness for the analysis of samples collected in capillary tubes.
- Reproducibility. The precision is comparable to that of conventional methods.

Determinations that involve chemical modification of the analyte, result in SIA systems where two or more zones must be sufficiently mixed to yield a product with measurable properties. In general, the dispersion is larger than in the case of single zone analysis (D = 2 - 10) and the occurrence of the chemical reaction is one of the major factors contributing to dispersion. Most of these systems employ colorimetric determination, fluorescence or chemiluminescence, since these methods of detection are cost effective and the apparatus are generally available. In photometric determinations parameters governing physical dispersion usually play a lessor role compared to the optimisation of the chemical parameters.

A typical SIA system is represented in Fig. 1.1. It is usually constructed (assembled) from a liquid driver (this can be a peristaltic, piston or electroosmotic pump or a burette [8]), an electrically actuated selection valve, Tygon or Teflon tubing to form holding and reaction coils and a single detector. Additional components can be added to perform specific duties. These components include dialysers (for separation of the analyte from the matrix) [24], hydride generators [25] and mixing chambers (for effective mixing or dilution) [22]. Since these applications are more advanced, it proves to be necessary that when describing it, the following aspects must always be highlighted: (i) the components it was constructed of, (ii) the specific manifold dimensions, as well as (iii) the device sequence or method construction (see addendum 1 for an example).

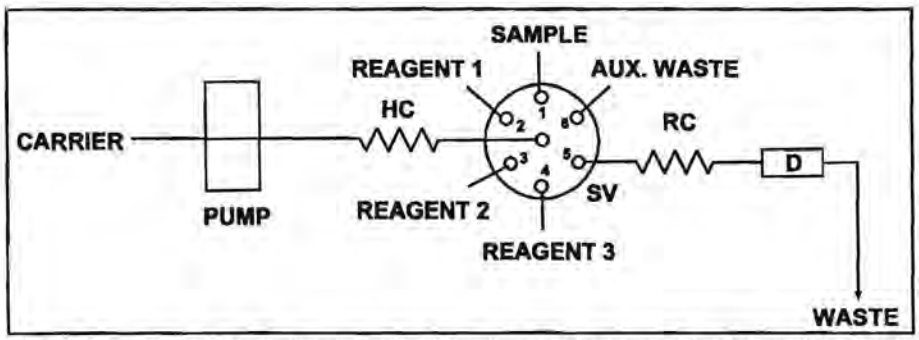

Fig. 1.1 A typical sequential injection system used to determine single analytes (components). HC - holding coil, SV - selection valve, RC - reaction coil and D - detector.

1.3 Multi-component sequential injection analysis

Since most of the SIA systems originate from conventional flow injection methods, it is wise to first highlight the different options possible. There are mainly two groups of FIA methods used: One group of methods in which a detector for each species to be analysed exists and another group in which the number of detectors is lower than the number of species to be determined [26]. The application of pH gradients [27] and differential kinetic determinations [28, 29] dominate the simultaneous determination of two or more closely related species, like cobalt and nickel, in mixtures without prior separation. Using the same reagent, PAR in most cases [27, 28], the different analytes can be determined spectrophotometrically at the same wavelength. In some applications of flow injection analysis to kinetic analysis the, FIA system is used as a sample inlet system whereby the reactants are transported to the detector cell. On arrival the flow is stopped and the rate of the reaction is monitored by change in absorbance. FIA has received growing attention for making catalytic methods of analysis simpler and more reliable and has been used to implement differential kinetic methods for binary mixtures of metals.

Sequential injection multi-detection systems used, include the use of two detectors placed in series [30 - 32], a sandwich technique employing large sample volumes [33], ICP [34], a single detector using two chemiluminescence reactions involving luminol [35, 36], HPLC (SIA systems were used for sample preparation) [37, 38], diode array spectrophotometry [39, 40], redox reactions (nitrate and nitrite) [41], photometry (using the same reagent for Mg(II) and Ca(II)) [42], hydride generation DCP-AES [25], f-AAS [43], potentiometry [44] and other chromatographic detection [45].

Most of the above systems were merely used for sample preparation and detection was done by more expensive apparatus such as ICP, AAS, AES and chromatography. The systems employing the chemiluminescence reactions also seemed to be too expensive, since the instrumental setup included three pumps (one peristaltic pump and two piston pumps) and three valves (one injection valve and two multi-position valves) [35].

The best solution to produce cost effective multi-component SIA systems appeared to be the use of inexpensive detectors in series (if detection is non-destructive) or detectors in parallel (if detection is destructive). Non-destructive detectors include photometric detection (LED) and ion-selective electrodes. Single detector systems will be even cheaper. These type of systems involve reaction of the analytes with the same reagent and the subsequent detection of the formed products. The selectivity of these determinations are controlled by either controlling the pH of the different reactions or by employing the difference in reaction rates of the analytes with the chromophore. Extraction of the analytes into the aqueous or organic phase prior to the reaction will also increase selectivity.

The manifolds used for multi-component systems or systems employing complex chemistries can usually be accommodated with minimal changes to the manifold. The SIA system used for the simultaneous determination of Co(II) and Ni(II) is shown in Fig. 1.2. Programming of the methods used for multi-component detection is more complex as for single component analysis and the mathematical and statistical manipulations of the data also require more skill.

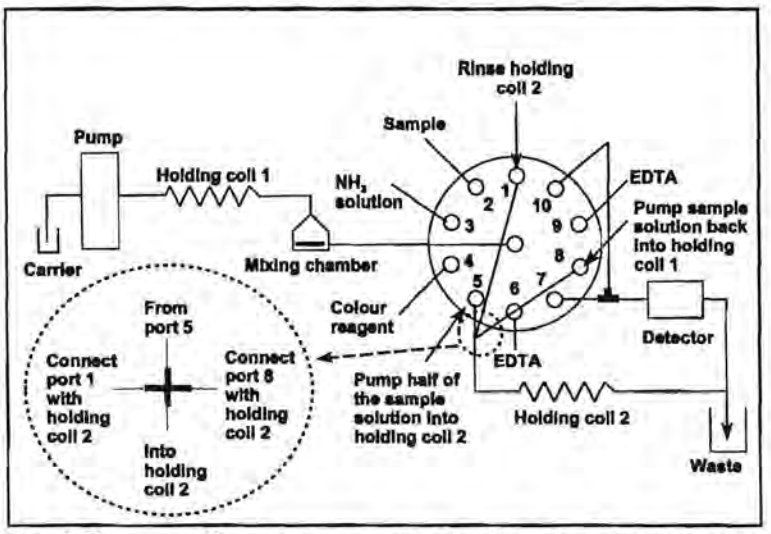

Fig. 1.2 SIA system used for the simultaneous determination of Ni(II) and Co(II).

Since these applications are even more complicated, it proves (like in the case of more advanced single component SIA systems) to be necessary that in its description, the following aspects need special attention: (i) the components it was constructed of, (ii) the specific manifold dimensions, (iii) the device sequence (see addendum 1 for an example), (iv) a sketch of the device sequence (if applicable) as well as (v) the operational conditions.

Optimisation of the multi-component SIA systems is done in the same way as for single component analysis. It is, however, sometimes necessary to optimise more than one response peak or value. Chemical parameters need more attention than physical parameters since most of the reactions employed is dependant on pH. The sample frequency is also lower for multi-component systems, because longer and more complex flow paths are followed. The fact that two or more analytes are determined in one cycle compromise for the longer analysis time.

1.4 Aim of this study

Process monitoring in the chemical and pharmaceutical industries has moved towards more automated and computer controlled systems. The need for information about processes, process components and the changes in component concentrations has increased in pace. Unfortunately, most SIA methods are designed to deliver analytical results for just one analyte at a time. Literature surveys showed that 72% of all articles published describe single component analysis, while only 28% contain information about multi-component analysis[1]. Multiple determinations are feasible, not only because it is more cost effective, but also because it reduces or eliminates interferences of species which are closely related to the analyte. With multi-component analysis it is not necessary to separate the interfering specie(s) from the analyte, since they can be determinated at the same time. This results in less sample preparation and eliminates loss of analyte due to long and sometimes ineffective separation methods.

---

1 Literature used to calculate the statistical data are the same as the references cited in Chapter 2.
Speciation studies were included as multi-component analysis.

Cobalt is invariably associated with nickel, and often also with copper and lead, and it is usually obtained as a byproduct or coproduct of the recovery of these metals [46]. Since cobalt and nickel both have dual importance (biological as the metal complexes from certain enzymes and as toxic components in higher concentrations), sequential injection analysis was used to determine cobalt and nickel in natural waters as well as in soil extracts, using a differential kinetic method (Chapter 7). SIA is ideally suited for kinetic determinations due to its discontinuous nature. Longer stop-flow periods can be included into the method to allow longer reaction time for slower reactions.

As in the case of cobalt and nickel, iron, zinc and copper also have important biological as well as industrial roles to play. Contrary to their importance they also become very toxic to humans, animals and plants in high concentrations. Lead and mercury are the only elements in this study which do not have any essential biochemical role to play. Lead is generally considered to be a non-essential toxic element which accumulates in the organism, while all forms of mercury are considered to be poisonous. Due to *(i)* the toxicity of mercury, *(ii)* the fact that organo-mercury compounds can be formed in nature (methyl-mercury and probably dimethyl-mercury), and *(iii)* the bio-accumulation of methyl-mercury [47], there is a great need for the accurate determination of mercury. These determinations are not only needed to locate polluted areas, but definitely to prevent mercury pollutants to enter the environmental chain by controlling industrial and research effluents. Since the determination of organo-mercury is complicated by the different species that can be formed, this study concentrate more on prevention than cure. Aqueous samples as well as extracts of inorganic mercury from soil and urine spikes were analysed.

Mercury was determined together with cobalt using a simplified sequential injection extraction method (Chapter 8) and together with cadmium using a sequential injection extraction which involved a pH gradient (Chapter 9). Mercury was also determined along with six other elements using sequential injection extraction and a diode array spectrophotometer as detection system (Chapter 10). The other elements were: Lead, copper, cobalt, cadmium, zinc and iron. The extractions all involved Dithiozone as extractant and chromophore. Different solvents were used. The solvents were chosen

for their ability to form thin organic layers on the walls of the tubing, into which the analytes could be extracted. Film thickness depends on the ratio between the viscosity and surface tension of the organic solvent used as well as the affinity of the solvent for the tubing material (Teflon).

The kinetic determination as well as the different extractions involved complex programming and mathematical calculations to get the systems running and to evaluate the data obtained in these systems. Compared to these complicated systems, a very simple sequential injection system was also evaluated. A cation, Fe(III), and an anion, SO_4^{2-}, were determined using a tandem SIA system (Chapter 6). The reaction between Fe(III) and tiron (4,5-dihydroxy-1,3-benzene-disulfonic acid) was monitored spectrophotometrically at 667 nm, while the sulphate was determined at the same wavelength using a turbidimetric determination. This system was able to do either sequential or simultaneous determinations of the two analytes in the same or different samples. The same analytes are used to evaluate the sandwich technique proposed by Estela *et al.* [33].

1.5 References

1. J. Růžička and G. D. Marshall, **Anal. Chim. Acta.**, **273** (1990) 329.
2. J. Růžička, G. D. Marshall and G. D. Christian, **Anal. Chem.**, **62** (1990) 1861.
3. T. Gübeli, G. D. Christian and J. Růžička, **Anal. Chem.**, **63** (1991) 2407.
4. J. L. Zable, **Operational Parameters of Sequential Injection Analysis and the Fundamentals of Calculating the Dispersion at the Maximum Zone Overlap,** PhD-Thesis, University of Washington, 1996.
5. G. D. Marshall and J. F. van Staden, **Anal. Instrum.**, **20** (1992) 79.
6. G. D. Marshall and J. F. van Staden, **Process Control Qual.**, **3** (1992) 251.
7. G. D. Marshall, **Sequential Injection Analysis**, PhD-Thesis, University of Pretoria, 1994.
8. R. E. Taljaard, **Application of Sequential Injection Analysis as Process Analyzers,** MSc-Thesis, University of Pretoria, 1996.
9. A. Botha, **Sequential Injection Analysis: Evaluation of Operational Parameters and Application to Process Analytical Systems,** MSc-Thesis, University of Pretoria, 1999.
10. A. Cladera, E. Gomez, J. M. Estela and V. Cerdà, **Talanta**, **43** (1996) 1667.
11. S. D. Chung, G. D. Christian and J. Růžička, **Process Control Qual.**, **3** (1992) 115.
12. E. Gomez, C. Tomas, A. Cladera, J. M. Estela and V. Cerdà, **Analyst**, **120** (1995) 1181.
13. J. F. van Staden and R. E. Taljaard, **Anal. Chim. Acta**, **323** (1996) 75.
14. J. C. Masini, P. J. Baxter, K. R. Detwiler and G. D. Christian, **Analyst**, **120** (1995) 1583.
15. E. Rubi, R. Forteza and V. Cerdà, **Lab. Rob. Autom.**, **8** (1996) 149.
16. J. F. van Staden and R. E. Taljaard, **Anal. Chim. Acta**, **331** (1996) 271.
17. J. F. van Staden and H. du Plessis, **Anal. Commun.**, **34** (1997) 147.
18. J. F. van Staden and R. E. Taljaard, **Anal. Chim. Acta**, **344** (1997) 281.
19. A. Ivaska and W. W. Kubiak, **Talanta**, **44** (1997) 713.
20. J. Růžička, **Analyst**, **119** (1994) 1925.
21. A. Ruis, M. P. Callao, J. Feere and F. X. Ruis, **Anal. Chim. Acta**, **337** (1997)

287.

22. M. Guzman, C. Pollema, G. D. Christian and J. Růžička, **Talanta, 40** (1993) 81.
23. M. Valcarcel and M. D. Luque de Castro, **Flow Injection Analysis - Principles and Applications**, Horwood, Chichester, 1987.
24. J. F. van Staden, H. du Plessis and R. E. Taljaard, **Anal. Chim. Acta, 357** (1997) 141.
25. P. Ek, S. Hulden and A. Ivaska, **J. Anal. At. Spectrom., 10** (1995) 121.
26. M. D. Luque de Castro and M. Valcarcel, **Analyst, 109** (1984) 413.
27. D. Betteridge and B. Fields, **Anal. Chim. Acta, 132** (1981) 139.
28. D. Betteridge and B. Fields, **Fresenius Z. Anal. Chem., 314** (1983) 386.
29. T. Yamane and C. Ishimizu, **Mikrochim. Acta (Wien), I** (1991) 121.
30. A. O. S. S. Rangel and I. V. Toth, **Port. Anal. Sci., 12** (1996) 887.
31. J. Alpizar, A. Crespi, A. Cladera, R. Forteza and V. Cerdà, **Electroanalysis, 8** (1996) 1051.
32. J. Alpizar, A. Crespi, A. Cladera, R. Forteza and V. Cerdà, **Lab. Rob. Autom., 8** (1996) 165.
33. J. M. Estela, A. Cladera, A. Munoz and V. Cerdà, **Int. J. Environ. Anal. Chem., 64** (1996) 205.
34. H. M. Al-Swaidan, **Talanta, 43** (1996) 1313.
35. R. W. Min, J. Nielsen and J. Villadsen, **Anal. Chim. Acta, 320** (1996) 199.
36. M. R. Wei, J. Nielsen and J. Villadsen, **Anal. Chim. Acta, 312** (1995)149.
37. I. Lukkari, K. Irgum, P. lindgren and J. Liden, **Process Control Qual., 7** (1995) 185.
38. K. L. Peterson, B. K. Logan, G. D. Christian and J. Růžička, **Anal. Chim. Acta, 337** (1997) 99.
39. A. Ruis, M. Callao and F. X. Ruis, **Anal. Chim. Acta, 316** (1995) 27.
40. P. J. Baxter, G. D. Christian and J. Růžička, **Chem. Anal., 40** (1994) 455.
41. M. T. Oms, A. Cerdà and V. Cerdà, **Anal. Chim. Acta, 315** (1995) 321.
42. E. Gomez, C. Tomas, A. Cladera, J. M. Estela and V. Cerdà, **Analyst, 120** (1995) 1181.
43. A. N. Araujo, R. C. C. Costa, J. L. F. C. Lima and B. F. Reis, **Anal. Chim. Acta, 358** (1998) 111.

44. G. C. Luca, B. F. Reis, E. A. G. Zagatto, M. Conceicao, B. S. M. Montenegro, A. N. Araujo and J. L. F. C. Lima, **Anal. Chim. Acta**, **366** (1998) 193.

45. S. V. Karmarkar, **Am. Environ. Lab.**, **10** (1998) 6.

46. N. N. Greenwood and A. Earnshaw, **Chemistry of the Elements**, Pergamon Press, Oxford, 1984.

47. I. Drabæk and Å. Iverfeldt in Quevauviller, Maier and Griepink (eds.), **Quality Assurance for Environmental Analysis**, Elsevier Sciences B. V., 1995, p 305.

CHAPTER 2

Sequential Injection Analysis

2.1 Introduction

The use of process control strategies represent a significant shift in the thinking of many process control engineers. Increasing pressure on the chemical manufacturing industry to produce higher quality products in an economically viable and environmentally acceptable manner, increases the requirements to maintain strict control of plant conditions throughout the production process.

The sophisticated instrumentation of laboratory facilities are unlikely to be suitable for manufacturing environments, and hence, dedicated systems offering long-term dependability must be developed. The demand for mechanically simple and robust flow-injection methodology has been the driving force behind the development of the sequential injection technique. The simplicity of the sequential injection (SI) manifold and its low need for maintenance makes it an ideal tool in process analysis. As miniaturization and reduction of reagent consumption are also ultimate goals in chemical sensing, it is useful to review the use of combined injection and programmed flow as a central issue in designing chemical sensors and structurally simplified chemical analysers.

Extraction, separation, pre-concentration, dialysis (matrix removal), titrations and dilution methods were adapted for use in sequential injection manifolds. Colorimetric, electrochemical and other detectors, equipped with suitable flow-through cells, were also incorporated into these manifolds. A new scope of SIA manifolds were developed for use in both industrial applications as well as in the laboratory.

2.2 Historical background

Sequential injection analysis (SIA), introduced in 1990 [1, 2], is a simple and convenient concept of flow analysis. Although this technique is a mere nine years old today, its roots can be traced back as far as 1974 [3]. To understand where sequential injection fits in and why Růžička refers to it as "a new look at a familiar landscape" [3], it is best to start at the very beginning.

Flow injection analysis (FIA) is an analytical technique that is based on the injection of a known volume of sample, with a geometrically well-defined shape, into a moving, unidirectional carrier or reagent stream. In this moving stream, the sample undergoes physical and chemical transformation until a detectable specie causes a detector response downstream of the injection point. If all critical parameters (reproducible injection, controlled reaction time and controlled dispersion) are held within certain tolerance levels, the result will be reproducible [4]. The instrumentation needed for an FIA system are a multichannel pump, an injection valve, a flow-through detector and a recorder. Except for the last component, which was replaced when computers invaded laboratories some ten years later, this basic flow scheme remained essentially unchanged [5].

When FIA research became orientated towards the exploitation of concentration gradients formed by the dispersion process [6], new techniques using stopped-flow, reversed flow, sinusoidal flow, reagent injection, sequential injection and single solution calibration were developed. Transformation of FIA into SIA signifies recognition of the tremendous versatility of this method, originally designed as a mere tool for automation of serial assays [7]. Much work has been done to assess the basic parameters of flow injection systems [8]. With the introduction of sequential injection analysis the basic parameters for flow injection were assumed to be applicable, because the same basic components (with minor changes) were used. Sequential injection (SI) is mechanically simpler than flow injection for it uses only a single pump, a single valve and a single channel. SI uses a selection (rather than an injection) valve, through which precisely

measured volumes of sample and reagent solutions are aspirated into a holding coil by means of a pump that is capable of a precise, controlled stop-go-forward-reverse movement [9 - 12]. A basic sequential injection analysis manifold is shown in Fig. 2.1.

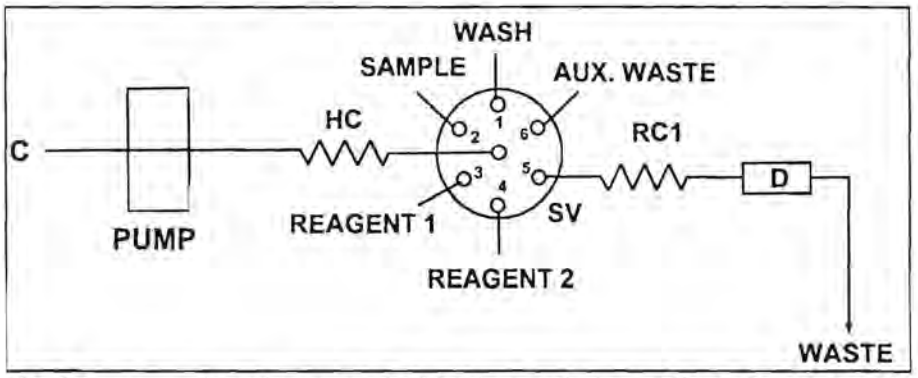

Fig. 2.1 A basic sequential injection analysis manifold. C - carrier, HC - holding coil, RC - reaction coil, SV - selection valve and D - detector.

Mainly four different liquid drivers were used in sequential injection analysis. Papers dealing with its applications used a sinusoidal flow piston pump specially designed for SIA [11, 13 - 16]. With this pump, the flow rate is dependent on the rotation angle, the radius of the pump, the cam, and the frequency of the pump. Repeatability and reproducibility are good, but it is difficult to maintain a constant flow rate during an analysis. The performance of peristaltic pumps to be used in SIA has been investigated by Ivaska and Růžička [17]. These pumps are suitable for SIA applications, especially when used with Neoprene tubing. Automatic burettes that are computer programmable and have variable speed are mainly used by the Spanish group [18 - 20]. A drawback of these liquid drivers is that it is impossible to use flow rates lower than 2 mℓ/min. A field-decoupled electro-osmotic pump is described by Liu and Dasgupta [21, 22] as an ideal pumping system for SIA, because the flow direction is readily and reproducibly reversed and the flow rate can be maintained with a high degree of reproducibility.

Full exploitation of these flow techniques in automated modes of operation necessitates computer control. Specialized software packages were designed to

control both the movement of the apparatus (pumps and valves) and to handle data acquisition and storage. The FlowTEK package (obtainable from MINTEK, Randburg, South Africa) was designed by Marshall and coworkers [9, 23] and is widely used. The Spanish group uses the program DARRAY, obtainable from SCIWARE, Palma de Mollorca, Spain [20]. Růžička's group [24] uses a program called FIALab for control and data acquisition.

The advantages of SIA have been discussed in detail by Růžička and Gübeli [13] and in comprehensive reviews and congresses [3, 9, 10, 12, 15, 25 - 28]. A valuable contribution by the group at the University of Washington was the exploitation of new sensor systems which broadened the scope of sequential injection analysis tremendously and opened new horizons in the field of flow analysis. First, Scudder *et al.* [29] developed a fountain cell for use in fluorescence microscopy. A chemiluminescence system that combines the simplicity and reproducibility of SIA with the unique radial flow properties of the fountain cell was then successfully employed for the chemiluminescence determination of hydrogen peroxide and glucose [30]. The fountain cell design was further used as basis for a perfusion chamber to perform the characterization of planar concentration gradients in a sequential injection system for cell perfusion studies [31]. The group [32, 33] also innovated and designed a novel jet ring cell which was incorporated into a sequential injection system for automated immunoassays and for preconcentration of analytes on sorbents with *in situ* spectroscopic detection. The jet ring cell with a renewable solid support was connected to a sequential injection system to determine glucose amperometrically [34]. A renewable gas sampling interface (liquid droplet) coupled with a SIA analyser was used to determine ammonia [35].

SIA was also applied for the determination of total ammonium nitrogen and free ammonia in a fermentation medium [16], nitrites and nitrates [36 - 38], D-lactic acid in pork [39], glucose using sensor injection and amperometric detection [40] and cyanide using ion-selective electrodes [41]. Wine [42] and sugar [43] analysis were done using sequential injection (SI)-FTIR spectrometry. Sequential injection manifolds were also

used to handle reagents for fluorescence microscopic measurements [3].

Coupling of sequential injection analysis with inductively-coupled plasma mass spectrometry as an analytical tool for trace element detection was used by Al-Swaidan [44]. The technique was applied for the determination of lead, nickel and vanadium at the part per billion level in sample solutions of Saudi Arabian crude oils. Hydride-forming elements were determined by direct current plasma atomic emission spectrometry based on a modified version of the sequential injection technique [45].

SIA was also employed as a sample preparation device for especially high-performance liquid chromatography [46, 47]. Lukkari *et al.* [46] used solid-phase extraction on Al oxide in a sequential injection system to purify pyrocatechol, protocatechuic acid, pyrogallol and gallic acid in black liquor. Sequential injection systems for the determination of mercury by cold-vapour atomic absorption spectroscopy [48, 49] used special gas-liquid separation units for effective analysis.

Application of the SIA technique to anodic stripping voltammetry (ASV) allowed the on-line plating of the mercury film and therefore substantially reduced the generation of mercury waste [50]. Other potentiometric applications include the determination of glycerol and 2,3-butanediol in wine [51]. Primary explosive azides in environmental samples were determined amperometrically using a SIA system [52]. A sequential injection system used in speciation studies employed two detectors in series, namely a potassium ion-selective electrode and a flame emission spectrometer [53].

SIA was also extensively used for the monitoring of bioprocesses [14, 54 - 56], enzyme activity [57, 58] and fermentation processes [59, 60]. Immobilized enzyme reactors played a great part in sequential injection analysis [39, 61 - 65] as well as systems for medical and pharmaceutical use [66 - 72]. Other SIA methods were also used for medical and pharmaceutical uses [73, 74]. Vitamin C was monitored photometrically in a kinetic application involving an iron(II)-iron(III) reaction [75], while morphine was determined with a SIA system employing chemiluminescence detection [76]. Van

Staden and McCormack [77] used a SIA system to determine amino acids spectrophotometrically. Chemiluminescence detection was employed in the preliminary analytical evaluation of novel reagents using a SIA system [78]. A method for determining the bromine (Br) number by coulometric flow-injection titrations, using sequential injection with sinusoidal flow is described by Taylor [79]. SIA was even applied to determine 90Sr in nuclear waste [80].

2.3 Basic principles

Following the first step of zone sequencing, during which the sample and reagent zones are stacked in the holding coil conduit adjacent to each other, the valve is switched to the detector position (Fig. 2 A). In the next step, the flow is reversed so that the stacked zones are propelled through the valve and the reactor to the detector (Fig. 2 B). As the central streamline moves at a rate twice the speed of the mean flow velocity, whereas the elements of fluid more adjacent to the walls move at lesser rates, the cores of the sequenced zones penetrate each other [8]. During this movement the flow reversal creates a complex region within which the analyte is transformed into a detectable specie (Fig. 2 C). The fundamental requirement for SI to succeed is to achieve maximum zone penetration through a deliberate increase in axial dispersion, obtained by means of the flow reversal and channel design [1, 13, 81].

Reproducible dispersion is the basis for analysis by flow injection methods. Dispersion is the result of all the physical forces acting on the injected zones. It is the process by which the zones transform from homogeneous, geometrically well defined zones at the moment of injection to the final zone that is detected downstream. The dispersion coefficient is the ratio of the detector response of the injected solution in the absence of these forces to that of the solution due to these forces. Růžička and Hansen [8] defined the conceptually simple and practically useful dispersion coefficient, $D = C^0/C$, where C^0 is the detector response of the undispersed solution zone and C is the detector response of the dispersed element of fluid that yields the analytical readout. Because there is generally a direct relationship between the property used for

detection, the magnitude of the transduced signal recorded and the concentration of the sample or its reaction product, the dispersion coefficient can be taken as the signal height ratio [8, 9]. The random walk model was also used by Růžička and Marshall [1] to describe dispersion in the SIA analyser channel.

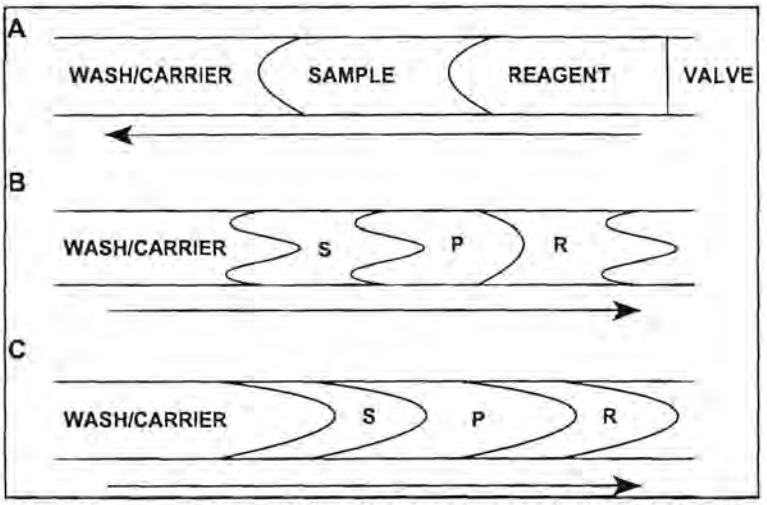

Fig. 2.2 Flow profiles of the sequenced (A) and injected zones (B - immediately after flow reversal and C - in reaction coil 2). S - sample, R - reagent and P - formed product zone.

Although Růžička and Gübeli [13] stated that "for a rational design of the sequential injection analyser, the degree of sample dispersion must be considered as main design guideline", zone penetration (related to dispersion) is found to be the key parameter, the control of which is essential to the successful execution of sequential injection [14]. The importance of zone penetration can be ascribed to the fact that this influence has a dramatic impact on the surface area over which a concentration gradient exists and therefore over which axial mixing takes place. It follows from the foregoing that, for reagent-based chemistries, a region of mutually interdispersed sample and reagent zones must be identified, within which D_s is larger than 2 and where at the same time sufficient excess of reagent is present.

Analogous to the definition of resolution, zone penetration is defined as

$$P = 2W_0/(W_s + W_r) \tag{2.1}$$

Complete overlap is obtained for P = 1, zero overlap for P = 0 and for values in between partial overlap will be obtained. This approach yields useful results although it is difficult to determine the value automatically [11]. An isodispersion point, I_D, is observed in cases where 1 > P > 0 (Fig. 2.3). At this point the dispersion of the sample and reagent zones are identical and the ratio of sample and reagent concentrations is the same as their ratio prior to injection ($C_s/C_r = C_s^0/C_r^0$).

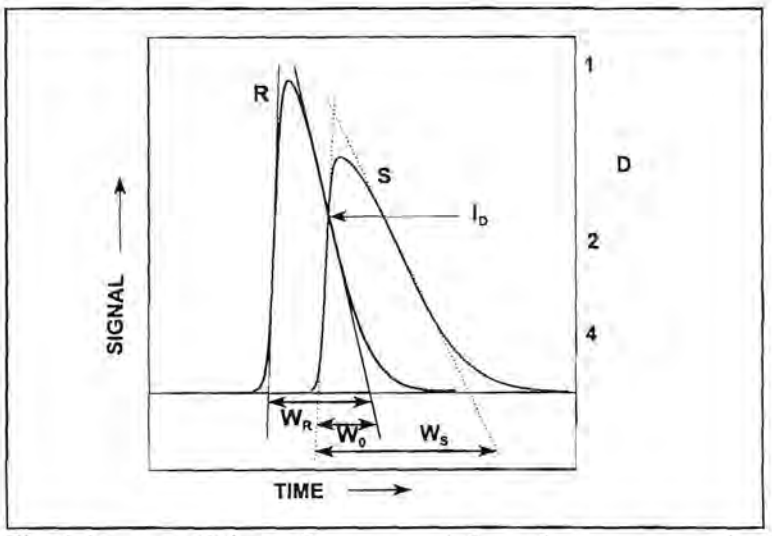

Fig. 2.3 Schematic representation of zone penetration showing the isodispersion point (I_D). R - reagent zone, S - sample zone, D - dispersion coefficient, W_R - baseline width of reagent zone, W_S - baseline width of sample zone and W_O - baseline of the overlap.

The isodispersion point is independent of concentration, but studies done by van Staden *et al.* [82] illustrate the shift of the isodispersion point due to the difference in concentration gradients when different volume ratios of sample and reagent were employed. These studies also showed that the position of penetration and the sequence of introduction of samples and reagents for different sample and reagent volume ratios in a total constant volume has a major influence on the response of the

final peak profile. This is illustrated in Figs. 2.4 and 2.5, where Fig. 2.4 represents the injection order of first the metal followed by the ligand and Fig. 2.5 represents the reversed injection order. The response of the final peak profile depends largely on the kinetics involved in both the ascending and tailing parts of the sample and reagent zones at the isodispersion point. Zable [4] found mathematical equations to calculate the maximum zone overlap. Marshall and van Staden [11] measured zone penetration by integrating the area of overlap. The larger this number, the greater the degree of zone penetration. This approach too suffers from certain limitations as it does not indicate the sensitivity of the measurement, because it does not take the concentration of the sample and reagent into account.

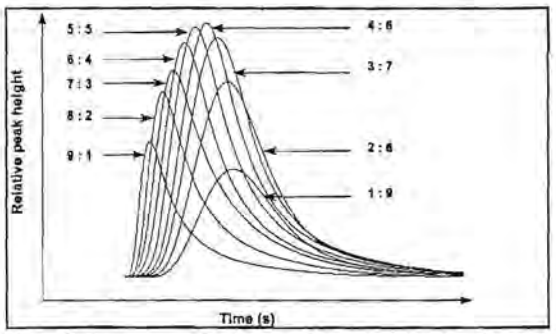

Fig. 2.4 Schematic representation of the influence of different sample : reagent ratios in a total constant volume. The figure represents the injection order of first the metal followed by the ligand.

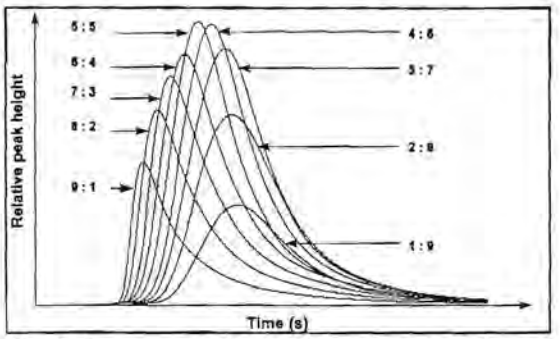

Fig. 2.5 Schematic representation of the influence of different sample : reagent ratios in a total constant volume. The figure represents the injection order of first the ligand followed by the metal (reversed order).

2.4 Operational parameters

Although some would argue that SIA is simply a variation of FIA, there are certain fundamental differences in the use and control of the operational parameters used in SIA. Many researchers generally set up a system without regard to the dispersion of the individual components or some of the general rules for optimising the system. There are a number of publications describing different techniques of optimisation [83 - 86] and standardization [87] as well as systems able to diagnose multivariate

responses, with the aim of detecting faulty responses [88, 89]. The greatest challenge is the theory of flow dynamics, which will lead to optimisation of flow systems based on flow stopping and reversal. When applying the sequential injection technique, it is imperative to understand the principles on which it is based in order to do subsequent analysis. The extent of dispersion that the product peak will undergo is essentially influenced by the operational parameters that govern the SIA flow conduit.

A number of papers were published that described the most important parameters to be optimised [4, 9, 11, 14, 90, 91]. Almost without exception the following parameters had been shown to have a marked effect on zone dispersion in an SIA system: the volumetric flow rate, tube diameter, length of flow path from injection to detection, sample and reagent volumes, order of sample and reagent injection, flow reversal and to a lesser extent reactor geometry. The use of mixing chambers in the flow conduit and their influence on dispersion was studied by van Staden and Botha [90]. To evaluate the influence of every parameter, a non-reactive dye was used as sample and reagent zone respectively in a series of experiments.

The *volumetric flow rate* includes both the loading and forward flow rates and is also referred to as the combined effect of pump speed and the internal diameter of the pump tubing when using a peristaltic pump [4, 9, 90]. In correlation with the Vanderslice expression, $D = k'q$, where q is the flow rate in mℓ/min, the dispersion of the different zones decreases as the flow rate is increased [92]. The dispersion coefficient decreases with increasing flow rate because the residence time decreases, in a nonlinear fashion, with increasing flow rate [9]. A linear relationship consists between the pump speed and flow rate; therefore the flow rate can be altered by changing the pump speed [9, 11, 90]. At high flow rates a deterioration in sensitivity and reproducibility is experienced due to the higher back-pressure [9, 93]. It is preferred that the loading flow rate should be faster than the forward flow rate to ensure higher sample throughput, provided that the pump will allow this [11].

The *length of the tubing* is dictated by the experimental requirements [9]. Longer tubing leads to longer residence times and therefore larger dispersion. Zable [4] stated that the dispersion must be proportional to the square root of the tube length, but experimental data had shown that there was a linear relationship between dispersion and path length. The mixing height (number of plates or tanks) is defined as the average length of tubing used for each mixing stage [8].

In SIA the manifold tubing is divided into two parts: the holding coil which is the tubing between the liquid device (pump) and the selection valve and the reaction coil which is the part connecting the selection valve with the detector. The holding coil primarily acts as a reservoir and should be large enough to prevent the sample and reagents from entering the pump conduit. The reaction coils should not exceed one-third of the volume of the washing solution, thereby ensuring that they are adequately flushed during every experiment [11]. Reaction coils are usually kept as short as possible to avoid excessive dilution of the formed product zone. The length is governed by the physical distance between the valve and the detector [9, 13].

A knowledge of the reaction rate is of particular value when adapting a method to sequential injection analysis, because the time spent in the manifold can be too short to ensure complete colour development. Due to the discontinuous nature of SIA, stopped-flow periods can easily be incorporated to enlarge reaction times [94 - 96]. Van Staden and Taljaard [94] used a stopped-flow period of 80 seconds to ensure adequate formation of indophenol during the determination of ammonia.

Related to the Dean number the *tubing diameter* had a dramatic influence on the dispersion of the different zones [4]. The dispersion is found to be proportional to the fourth root of the coil diameter. Several factors should come to mind when considering the optimum tube diameter. These include the resultant back-pressure in a length of tubing, the vulnerability to blockage and the degree of radial dispersion attainable [9, 11]. Wider tubing is usually used for the holding coil, because of its promotion of axial dispersion and, therefore, zone penetration. Narrower tubing is used for the reaction

coils to prevent excessive dilution of the formed product zone. Wider tubing is used for the uptake tubes to prevent any back-pressure.

Gübeli *et al.* [14] have conducted an in depth study on the effect of *sample and reagent volume* on zone penetration and sensitivity. Their conclusions can be summarized in three rules:

1. Changing of the sample zone volume is an effective way of changing the sensitivity of the measurement. Dilution of concentrated samples is best achieved by reducing the injected sample volume.
2. Injecting at least twice as large reagent zone volume as sample zone volume, while keeping the volume of the sample zone less or equal to 0.5 $S_{1/2}$, allows the optimum conditions for single based chemistries to be met. ($S_{1/2}$ is defined as the sample volume required to yield a dispersion factor of two in the manifold).
3. Two reagent chemistries can be accommodated provided that the sample volume is kept below the $S_{1/2}$ value, so that the sample zone is surrounded by the reagent zones and that the concentration of the injected reagents are sufficiently high.

Van Staden *et al.* [82] found that the best sensitivity was obtained when a 1:1 sample to reagent ratio was used. At this ratio, the two zones experienced almost the same axial dispersion and penetration occurred almost at the maximum of the descending sample zone as well as the maximum of the ascending reagent zones. Gübeli *et al.* [14] found that increasing zone volumes at equal volume ratios caused zone overlap to decrease from nearly complete overlap (with small equal volumes) to a partial one (with relatively large equal volumes). While keeping the reagent volume constant, the authors [14] also varied the zone volume ratios by increasing the sample volume from less than the reagent volume to one where the sample volume was in excess of the reagent zone. This also resulted in a decrease in zone overlap.

Optimum sample and reagent zone volumes can be determined by plotting log [1 - (A_{max}/A_0)] versus sample volume ($\mu\ell$), where A_0 is the absorbance corresponding to the

case where the element of fluid undergoes no dispersion. The $S_{1/2}$ value can be determined from the slope of the linear relationship. Experimental results gave good correlation with calculated values [90]. $S_{1/2}$ values are, however, influenced by a number of experimental parameters. Cladera *et al.* [97] and Araujo *et al.* [98] showed that the ionic strength or electrolyte concentration of the medium influenced the $S_{1/2}$ value. The flow rate (slower flow rates result in higher $S_{1/2}$ values), the number of flow reversals and the dimensions of the reactor loop also influence the value [97].

A simple and convenient method for the determination of injection volumes in sequential injection analysis is presented by van Staden and Malan [99]. It is based on comparing the dilution of the injected dye with a standard calibration curve. The proposed colour method gave the volume of the whole injection device more accurately than methods where the inner dimensions of the injection device are not precisely known. The colour method is within the 95% confidence level with an RSD of 0.8%. Sampling strategies in sequential injection analysis were also investigated by Vieira *et al.* [100]. These techniques were exploited using a monosegmented-flow approach.

In a publication of Mas-Torres *et al.* [101], the authors discussed a new approach to sequential injection analysis. This approach involved the use of the sample as carrier stream. Although this technique may render good results, it takes away one of the main advantages of sequential injection analysis - the fact that it uses minimized amounts of sample [9].

The importance of the correct *order of* sample and reagent *injection* is highlighted in a number of publications [11, 82, 94, 102 - 104]. The order in which the different sequences of reagents are drawn up are very dependent on the reactions involved. The residence time of a specific zone also depends on its position in the reagent sequence. The zone that is drawn up first reaches the detector last due to the flow reversal. This zone has the longest residence time of all the zones and is therefore more dispersed [4, 9, 11]. The following must be considered: when sensitivity is important, the reagent, at a sufficiently high concentration, should be introduced first

and allowed to penetrate the sample zone, which will experience minimal dispersion. If buffering of the sample by the wash solution is required, the order must be reversed. If solubility considerations prevent the reagent concentration from being increased, sandwiching of the sample between two reagent zones is an option to be considered [11].

Although it is the first *flow reversal* and its duration that is the most effective in providing mutual zone penetration [11, 14], more than one flow reversal was needed in the determination of ammonia, due to insufficient mixing of the adjacent zones (because of their different viscosities). The stack of zones was subjected to three flow reversals before the product zone was propelled to the detector. Multiple flow reversals were also used to better the transfer of ammonia over the membrane in a coupled gas-diffusion-SIA system [18] as well as to improve iron dialysis through the membrane during the determination of iron(III) [93].

Various reactors have been described in the literature on FIA manifolds [8]. Where the reactor consists of a length of tubing, various *geometries* have been proposed. Three were evaluated to establish the effect of reactor geometry on zone penetration and geometry. Studies done by Taljaard [9] and Marshall and van Staden [11] showed that reactor geometry does not have a marked effect on sensitivity or precision. Straight tubes are, however, preferred in SIA manifolds due to the better axial dispersion obtained.

It should be noted that only the physical dispersion of all of the above mentioned parameters were highlighted. The influence of a chemical reaction on dispersion is not even mentioned. The optimum values for each parameter will to a large extent depend on the specific reaction conditions and do not only depend on maximum sensitivity, but also on the reproducibility of measurements (%RSD). A set of parameters resulting in high sensitivity can be rejected if the relative standard deviation is too high, as shown by van Staden and du Plessis [105] and by Nakano *et al.* [106]. It is however surprising that such good precision is attained in SIA systems, because the reaction

takes place at an interface with steep concentration gradients [11].

2.5 Single zone sequential injection analysis

The analysis of chemical species that can be measured directly, such as those that have a high molar absorptivity of light at a specific wavelength (e.g. concentrated hexavalent chromium) can be analysed using single zone sequential injection analysis [4]. The technique can also be used for pH determinations or methods where detection is done using ion-selective electrodes or chemical sensors. In these types of analysis the sample is the only zone injected.

2.6 Two zone sequential injection analysis

Double zone sequential injection analysis depends on the addition of a single reagent. In this type of analysis, the sample and the reagent solution are the only two zones injected. Reaction stoichiometries of different complexes can easily be determined when using a two zone system [85, 102]. Van Staden *et al.* [102] described a system to determine the reaction stoichiometries of both the Fe(III)/Tyron complex (1:1) and the Fe(II)/1,10-phenanthroline (1:3) using the Yoe-Jones' Method and Job's Method. The main advantage of these methods above their FIA counterparts is that the tedious and time-consuming process of changing the sample loops for every different ligand : metal ratio, is eliminated. Sultan and Desai also described a SIA method for the concentration, stoichiometry and formation constant studies when promethazine hydrochloride complexed with palladium(II) in hydrochloric acid [107].

The turbidimetric determination of sulphate also employs in principle a two zone sequence. Due to the build up of barium sulphate in the manifold an alkaline buffer-EDTA solution was introduced to clean the tubing. This zone was separated from the acidified barium chloride reagent by means of a water zone, resulting in a sequence of a stack of four zones [108]. Two zone sequential injection analysis was also used by van Staden and Botha [139, 140] in the determination of Cu(II) with DDTC.

2.7 Three zone SIA systems

The order in which the different sequences of reagents are drawn up depends very much on the reactions involved. In the determination of ammonia using the indophenol blue method [94], a three zone sequence of sample, phenol reagent and hypochlorite reagent was used. This sequence is in contrast with the manual and flow injection methods [109], where the hypochlorite reagent is first added to the sample. The importance of the correct zone sequence is also highlighted in the determination of phosphate [103], where the sample had to be drawn up first to ensure minimum reaction time between the molybdenum and ascorbic acid reagents. This was done because of the rapid reduction of the molybdenum by the ascorbic acid prior to reaction with the phosphate in the aqueous samples. When the molybdenum reagent was sequenced between the sample and ascorbic acid zones, the phosphate already started to react with the molybdenum while the ascorbic acid was being drawn up. Munoz *et al.* [110] did an evaluation of spectrophotometric methods for the determination of orthophosphates using sequential injection analysis. Three zone SIA was also applied to determine calcium in water, urine and pharmaceutical samples using CPC [104] as well as in paper machine white water [111, 112].

2.8 More than three zone systems

Although it is stated that three zones were the maximum to ensure effective mixing [3, 9, 13], Guzman and Compton [113] published an article where six zones were used in the determination of rhFXIII fluorometric activity. The SI method simulated to a large extent the chronology of the manual procedure and a mixing chamber was incorporated into the manifold to ensure efficient mixing of the different zones.

2.9 Multi-component techniques in SIA

Only a limited number of papers considering multi-component techniques were published [19, 114 - 119]. A multi-linear regression program for the simultaneous

determination of calcium and magnesium in mixtures, was introduced by Gómez *et al.* [19]. Also using the chromogenic reagent 4-(2-pyridylazo)resorcinol, Taljaard and van Staden [114] described a procedure for the simultaneous kinetic determination of nickel and cobalt in water and soil extracts. The feasibility of large sample volumes in sequential injection analysis, in order to determine various analytical parameters in an unique sample injection, was investigated by Estela *et al.* [115]. This technique employs two reagents sandwiched around a large sample volume and allows the determination of two different parameters in the sample. The accuracy of the resolution of each resulting reaction peak and the linear working ranges are dependent on injected sample volumes, reagents and their concentrations.

A sequential flow injection method for the simultaneous determination chloride and fluoride in water with potentiometric detection using two ion selective electrodes in two serial flow through cells is described by Alpizar *et al.* [116]. The authors [120] also described the simultaneous determination of chloride and pH in waste waters by sequential injection analysis. This method uses a separate flow cell to measure pH by stopping the flow during the chloride determination. Simultaneous determination of calcium and magnesium in mineral waters was also done by Araujo *et al.* [118]. In this case, the sequential injection system was used as a sample preparation step and the analysis was done via flame atomic absorption spectrometry. Another simultaneous determination, these of phosphate and silicate in waste waters, using SIA is described by Mas-Torres *et al.* [119].

2.10 More complicated systems

2.10.1 Calibration

Baron *et al.* [40] described a single standard calibration technique using the same manifold as for dilution with a dilution coil. Through variations of the volume parameter sizes, conditions were found that generate four 'slices' from the tail of the gradient in the dilution conduit. This gave increasing responses at the detector. These values

were used for generating data required for system calibration. The response with the dilution conduit was compared with a volumetric calibration using the steady-state responses of four BTB standards. By using the previously calculated dispersion coefficients, the actual concentration at the SIA peak maximum for the four aliquots (slices) was calculated and plotted as concentration versus absorbance together with the responses for the volumetric standards. These values agree within 5%, which is sufficiently close to confirm the validity of the SIA method. It is also possible to cluster standards around the multi-position valve so that the system might be automatically recalibrated as required [12]. A multivariate statistical process control procedure, for sequential injection analysis systems, is developed by Rius *et al.* [89]. This multivariate calibration technique was evaluated for sulphate analysis.

2.10.2 Dialysis

Dialysis is a valuable tool that fulfils a very important role for on-line separations as part of segmented auto analysers, flow injection and sequential injection systems [121]. Iron(III) was separated from a sample matrix by dialysis in a sequential injection system [93]. The dialysed iron was complexed with Tyron and the resulting complex was monitored spectrophotometrically at 667 nm. In this work, the influence of various parameters, including pump speed of both donor and recipient streams, sample volume, reagent volume, dialysis time and the effect of multiple flow reversals, on dialysis efficiency was studied. A sample frequency of 8 samples per hour and a detection limit of 45 mg/ℓ Fe(III) were obtained.

To ensure different flow rates for the donor and recipient streams respectively, two pumps were used in the application [93]. A slower flow rate was used for the donor stream, because of the longer dialysis time needed and a faster flow rate for the recipient stream, resulting in better penetration of the zones and shorter rinsing times. The dialyser unit used consisted of a 160 x 30 x 25 mm single dialyser. The path length of both the donor and recipient streams was 300 mm. The grooves of the dialyser had an inner diameter of 0.5 mm. A Technicon type C membrane was used.

The coil connecting the outlet of the recipient stream to the carrier container must be kept as short as possible to avoid the introduction of bubbles via the inlet of the dialyser.

With the incorporation of a passive neutral semi-permeable dialysis membrane into the conduits of the sequential injection system, the contact time of the sample zone with the membrane had a marked influence on the quantity of iron dialysed through the membrane. Using the feature of multiple flow reversals, the percentage dialysis was improved to 4.5%, which compares well with the 4% obtained with conventional flow analysis [122]. In the optimized system a dialysis time of 180 seconds was used.

Dialysis was also used in the spectrophotometric determination of L(+)-lactate in wines [123]. For the determination of total ammonium-nitrogen and free ammonia in a fermentation medium, a two channel sequential injection system was used [16]. The streams were propelled by an Alitea S2-V two channel piston sinusoidal flow pump equipped with two cam driven parallel syringes. Two electrically actuated multi-position valves, a six port valve on the donor line and an eight port valve on the acceptor line, were used to direct the flow streams. A Celgard 2400 hydrophobic membrane was used in the combined gas diffusion unit/flow cell. Luo *et al.* [124] described the determination of gaseous ammonia using a glass diffusion denuder in a sequential injection system.

Coupling of gas-diffusion separation and sequential injection analysis is applied to determine ammonia in aqueous environmental samples [18]. The sample and an alkaline solution are sequentially aspirated using an automatic burette and mixed by flow reversal while being propelled to a gas-diffusion unit. Here the ammonia formed diffuses through a hydrophobic membrane into an acid-base indicator solution used as acceptor stream. The dispersion (broadening of the zones) is dependent on the travelled length (l) and on the number of flow reversals (N). This effect can be favourable in GD-SIA because zone broadening will result in longer residence times for the sample in the diffusion unit, without changing the flow rate, which could favour

ammonium diffusion.

Differences in pressure between both sides of the membrane reduced the gas transfer efficiency and caused large sample dispersion and long-tailed, undefined peaks. Maximum preconcentration was achieved when both the inlet and outlet of the acceptor channels were closed during the preconcentration step. Placing an injection valve in the manifold ensured that the pressure at both sides of the membrane almost stayed the same. Increased travel distance (l) meant larger washing volumes and longer rinsing times and that reduced the sample frequency. It was therefore concluded that longer travel times was not an effective way of increasing sensitivity.

The inclusion of a second holding coil, providing a reservoir of a ready-to-use indicator solution, allowed the minimization of the dispersion of the indicator acceptor zone. This limited the sample frequency, because the holding coil had to be refilled after every measuring cycle. To ensure limited dispersion and dilution of the indicator zone, an air segment was inserted between the indicator zone and the water carrier in the holding coil. The sensitivity improved about three times for N = 3 - 5. The limit of detection was 2 mg/ℓ and the transfer efficiency of ammonia through the membrane was calculated to be 15%.

2.10.3 Titrations

Van Staden and du Plessis [105] described a sequential injection titration system for the titration of a strong acid with a strong base. The concept is based on the sequential injection of a base titrant, acid analyte and a second base titrant zone into a distilled water carrier stream. Using this zone sequence close resemblance with flow-injection titrations was obtained. The stack of zones is swept by flow reversal through a reaction coil to the detector. The base zones contain Bromothymol Blue as indicator and the endpoint is monitored spectrophotometrically at 620 nm. A straight reactor with a length of 90 cm and a diameter of 0.51 mm was used as gradient device (instead of a mixing chamber) for the creation of the concentration profile of the acid

sample. This was done because the use of a mixing chamber resulted in excessive dilution of all the zones and a dramatic decrease in sample throughput.

A linear relationship between peak width and logarithm of acid concentration is obtained in the range 0.01 to 0.1 mol/ℓ of HCl with 1 x 10^{-3} mol/ℓ NaOH as titrant. Other linear ranges are possible at different titrant concentrations. The results obtained for the sequential injection titration compare excellently with those obtained with standard potentiometric titrations with an RSD < 0.30%.

A titration method without mixing or dilution is described by Holman *et al.* [125]. This method also involves the use of chemical sensing membranes. A method for determining the bromine (Br) number by coulometric flow-injection titrations, using sequential injection with sinusoidal flow is described by Taylor [79].

2.10.4 Dilution

On-line dilution with sequential injection analysis has been evaluated using a dilution coil in the conduits of the manifold system and a dilution step as part of the timing sequence [9, 40, 126, 127]. The manifold of the SIA system with the dilution coil is more complicated than the system including the dilution step. The former method needs more complicated programming as well. Control over the magnitude and range of dilution is effected by three volume parameters: Sample volume, V_S, transfer volume, V_T, and analysis volume, V_A [40]. The sample volume is the amount of sample or standard which is drawn into the holding coil via the sample port. The transfer volume describes the volume of sample plus accompanying wash solution in the holding coil and tubing which is transferred into the dilution conduit from the holding coil. The analysis volume is the volume of the aliquot taken from the dilution conduit to the holding coil and then pushed through the detector.

Shorter analysis time favours the dilution with the dilution step, but the limited linear range of this method is a large drawback. Dilution is obtained by introducing a well-

defined water zone between the barium chloride reagent zone and the sample zone. The degree of dilution obtained depended on the timing sequence allowed for the dilution step. Timing sequences between 0 and 15 seconds were evaluated and the calibration curves associated with the different linear regions are illustrated in Fig. 2.6. It is clear from the curves that a linear calibration curve (Fig. 2.6 D) was obtained between 750 and 5000 mg/ℓ sulphate with a timing sequence of 15 seconds.

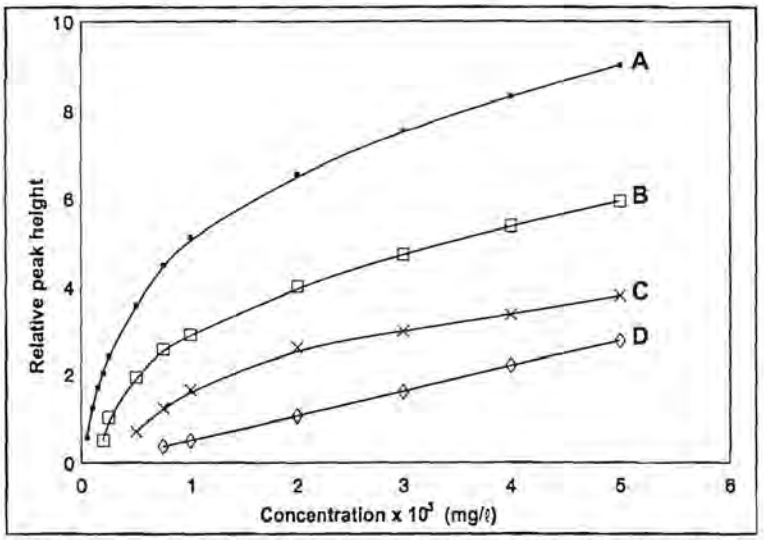

Fig. 2.6 Calibration curves for standard sulphate solutions using a dilution step between the sample and reagent zones. (A) The range 50 - 5 000 mg/ℓ using a dilution step of 6.5 s, (B) the range 150 - 5 000 mg/ℓ using a dilution step of 10 s, (C) the range 500 - 5 000 mg/ℓ using a dilution step of 12.5 s and (D) the range 750 - 5 000 mg/ℓ using a dilution step of 15 s.

In the determination of phosphate in bioprocesses, dilution (when required) was performed in a mixing chamber connected to the selector valve [128]. In the spectrophotometric catalytic determination of iodide in nutrition salts, Lima *et al.* [127] used a SIA system with mixing chamber for handling high concentrated solutions.

2.10.5 Extraction

Peterson *et al.* [129] described a flow-based extraction method where an aqueous sample and organic solvent were sequentially injected into an extraction coil, mixed and separated due to the differential flow velocities of the aqueous and organic phases. A 500 $\mu\ell$ aqueous sample is propelled through a 50 $\mu\ell$ segment of organic solvent whose flow is impeded due to hydrophobic interactions with the walls of a Teflon extraction coil. This wall drag allows the faster moving aqueous sample to penetrate through and ultimately separated from the slower organic solvent. These steps are repeated with a back extraction into a second aqueous segment (100 $\mu\ell$) that is collected and analysed with high-pressure liquid chromatography (HPLC).

Barbiturates (phenobarbital, amobarbital, pentobarbital and secobarbital) and serontonin re-uptake inhibitors (SRIs) - venlafaxine, paroxetine, sentraline and norsertraline - were extracted as model acidic and basic compounds from urine into a 1 : 4 (v : v) mixture of 1-octanol and butyl chloride and back extracted into 0.45 mol/ℓ NaOH (acidic sample) and 0.18 mol/ℓ H_3PO_4 (basic sample), respectively. The sample throughput, including extraction and back extraction, was 20 samples per hour. This extraction procedure was mainly used for sample preparation and air instead of water was used as propellant. A volume of 400 $\mu\ell$ acetonitrile, loaded initially, washed the organic film to waste - leaving the extraction coil ready for the next extraction cycle. The solvent composition was found to be a critical parameter for successful application of SIE (sequential injection extraction), because it determined the difference in flow velocity between the organic and aqueous phases, the chemical selectivity and extraction efficiency.

Nakano *et al.* [106] combined wetting film extraction with colorimetry to determine nanogram amounts of molybdenum(VI). Using a very simple manifold and almost the same procedure as described earlier a highly sensitive and selective sequential injection system was developed. Molybdenum (which reacted with thiocyanate) was extracted in the first step into a toluene film as an ion paired complex. The thiocyanate

ligands were displaced by 1,5-diphenylcarbazone (DPC) to form an intensely coloured product which was measured at 540 nm. Wetting film extraction was also used in the photometric determination of vanadium(IV) and vanadium(V) [130] and chromium(VI) and chromium(III) in water [131].

Grate and Taylor [132] described an on-line soil extraction procedure employing SIA. On-line soil extraction was performed with the soil placed in an open-ended column attached to the sample line.

2.10.6 Preconcentration and separation

Rubi *et al.* [133, 134] described a sequential injection assembly for the determination of Fe(II) in natural waters. Fe was preconcentrated on a microcolumn packed with a chelating resin (Chelex 100) that was inserted into the manifold. The sample was passed through the column and the Fe, retained by the resin was subsequently eluted with 2 mol/ℓ HNO_3. The SIA system offers automatic preconcentration, elution, detection and data acquisition. Using a simple sequential injection method, ammonium was determined with conductometric detection. NH_3 permeated through a gas permeable membrane and was collected (preconcentrated) in a static acceptor stream [135].

In the determination of 90Sr, the 90Sr was separated from other radionuclides using a sorbent minicolumn containing a resin that selectively binds 90Sr as a crown ether under acidic conditions [80]. The isolated 90Sr was then detected on-line with a flow-through liquid scintillation counter.

2.10.7 Mixing chambers

Despite the fact that mixing chambers have certain undesired properties such as large dead volumes and that it causes a hold up effect, it offers some distinct advantages, for example, in the use of mixing of liquids with different viscosities [136]. Mixing

chambers were initially used in sequential injection analysis to dilute highly concentrated samples [40, 127, 128] or to ensure adequate mixing when three or more zones were involved [81, 113, 114, 137]. Accordingly, in an SI process control application, a mixing chamber connected to a fibre optic detector has proven to be successful for the determination of total biomass [24, 138]. This mixing chamber or cell was used both as a dilution chamber and detection cell. Recently, mixing chambers were used to improve the degree of mixing - even for cases where only two zones were used [102].

Depending on the application of the mixing chamber, it can be placed either between the holding coil and the valve or between the valve and the reaction coil. When placing the mixing chamber between the holding coil and valve, the zones will be drawn up through the mixing chamber into the holding coil and then propelled through the mixing chamber to the detector after flow reversal took place. For the mixing chamber positioned between the valve and the reaction coil, the zones will be drawn into the holding coil and then propelled through the mixing chamber. A lot more dispersion is expected for the former situation, because the zones enter the mixing chamber twice and because of the increased mixing, an increase in dispersion is experienced [90, 140].

The volume of the mixing chamber is also an important parameter which could be used to control the amount of dispersion needed. Larger volumes resulted in larger dispersion, which is not always desirable [90, 114, 140]. In the simultaneous determination of cobalt and nickel, a mixing chamber with a volume of 500 $\mu\ell$ was used to ensure adequate mixing of the reagents before splitting the product zone in two [114].

2.11 Conclusion

Although the sample throughput frequency of an SIA system is normally less than that of the conventional FIA system [13, 14], the major advantage of SIA is the more cost effective use of reagents. SIA methodology has important advantages over conventional FIA as it is simple in equipment and the manifold does not have to be changed if flow parameters or injection volumes are modified. It is also a very versatile approach as a single SIA configuration can be adapted for multi-reagent techniques and multi-detection systems without the need of reconfiguring the manifold.

Different sample-handling techniques were successfully adapted to sequential injection analysis. Calibration using a dilution conduit is particularly suited to sensor injection in a situation where the sensor is susceptible to fouling or degradation over time. Flow detector fouling does not occur in SIA manifolds as the detector is in contact with water between analysis [103, 128]. The use of a dilution conduit in the SIA mode allows for simple and precise dilution of analytes and for easy and rapid generation of a set of calibration samples from a single standard solution. It is also possible to cluster standards around the multi-position valve so that the system might be automatically recalibrated as required.

Sequential injection analysis has reached the point where a manifold that does not need changing can be designed. Further developments concentrate on using versatile controlling software to manipulate sample and reagents in novel ways to achieve desired sample-handling procedures. In comparison with flow injection analysis it is more flexible for applying stopped-flow and reversed-flow operations [138]. Although this does not mean that sequential injection analysis will replace flow injection analysis, SIA surely has a very useful future laying ahead.

2.12 References

1. J. Růžička and G. D. Marshall, **Anal. Chim. Acta.**, **237** (1990) 329.
2. J. Růžička, G. D. Marshall and G. D. Christian, **Anal. Chem.**, **62** (1990) 1861.
3. J. Růžička, **Analyst**, **119** (1994) 1925.
4. J. L. Zable, **Operational Parameters of Sequential Injection Analysis and the Fundamentals of Calculating the Dispersion at the Maximum Zone Overlap**, PhD-Thesis, University of Washington, 1996.
5. J. Růžička and E. H. Hansen, **Trends Anal. Chem.**, **17** (1998) 69.
6. J. Růžička, **Anal. Chem.**, **55** (1983) 1040A.
7. J. Růžička, **Anal. Sci.**, **7** (1991) 635.
8. J. Růžička and E. H. Hansen, **Flow Injection Analysis**, 2nd ed.; Wiley, New York, 1988.
9. R. E. Taljaard, **Application of Sequential Injection Analysis as Process Analyzers**, MSc-Thesis, University of Pretoria, 1996.
10. G. D. Marshall, **Sequential-Injection Analysis**, PhD-Thesis, University of Pretoria, 1994.
11. G. D. Marshall and J. F. van Staden, **Process Control and Quality**, **3** (1992) 251.
12. J. Růžička, **Anal. Chim. Acta**, **261** (1992) 3.
13. J. Růžička and T. Gübeli, **Anal. Chem.**, **63** (1991) 1680.
14. T. Gübeli, G. D. Christian and J. Růžička, **Anal. Chem.**, **63** (1991) 2407.
15. G. D. Christian and J. Růžička, **Anal. Chim. Acta**, **261** (1992) 11.
16. I. Lukkari, J. Růžička and G. D. Christian, **Fresenius J. Anal. Chem.**, **346** (1993) 813.
17. A. Ivaska and J. Růžička, **Analyst**, **118** (1993) 885.
18. M. T. Ohms, A. Cerdà, A. Cladera, V. Cerdà and R. Forteza, **Anal. Chim. Acta**, **318** (1996) 251.
19. E. Gómez, C. Tomás, A. Cladera, J. M. Estela and V. Cerdà, **Analyst**, **120** (1995) 1181.
20. A. Cladera, C. Tomàs, E. Gómez, J. M. Estela and V. Cerdà, **Anal. Chim. Acta**,

302 (1995) 297.

21. S. Liu and P. K. Dasgupta, **Talanta**, **41** (1994) 1903.
22. S. Liu and P. K. Dasgupta, **Anal. Chim. Acta**, **308** (1995) 281.
23. G. D. Marshall and J. F. van Staden, **Anal. Instrum.**, **20** (1992) 79.
24. P. J. Baxter, G. D. Christian and J. Růžička, **Analyst**, **119** (1994) 1807.
25. G. D. Christian, **Biol. Prospect.**, **8** (1993) 7.
26. D. A. Joelsson and A. Ivaska, **Kemi**, **20** (1993) 591.
27. G. D. Christian, **J. Flow Injection Anal.**, **11** (1994) 2.
28. G. D. Christian, **Analyst**, **119** (1994) 2309.
29. K. M. Scudder, C. H. Pollema and J. Růžička, **Anal. Chem.**, **64** (1992) 2657.
30. D. J. Tucker, B. Toivola, C. H. Pollema, J. Růžička and G. D. Christian, **Analyst**, **119** (1994) 975.
31. C. H. Pollema and J. Růžička, **Analyst**, **118** (1993) 1235.
32. J. Růžička, C. H. Pollema and K. M. Scudder, **Anal. Chem.**, **65** (1993) 3566.
33. C. H. Pollema and J. Růžička, **Anal. Chem.**, **66** (1994) 1825.
34. T. Lindfors, I. Lahdesmaki and A. Ivaska, **Anal. Lett.**, **29** (1996) 2257.
35. S. Liu and P. K. Dasgupta, **Anal. Chem.**, **67** (1995) 2042.
36. M. T. Ohms, A. Cerdà and V. Cerdà, **Anal. Chim. Acta**, **315** (1995) 321.
37. J. F. van Staden and T. A. van der Merwe, **S. Afr. J. Chem.**, **51** (1998) 109.
38. S. V. Karmarkar, **Am. Environ. Lab.**, **10** (1998) 6.
39. H. Shu, H. Håkanson, and B Mattiasson, **Anal. Chim. Acta**, **283** (1993) 727.
40. A. Baron, M. Guzman, J. Růžička and G. D. Christian, **Analyst**, **117** (1992) 1839.
41. M. J. C. Taylor, D. E. Barnes, G. D. Marshall, D. R. Groot and S. J. S. Williams, **Process Control Qual.**, **3** (1992) 173.
42. R. Schindler, R. Vonach, B. Lendl and R. Kellner, **Fresenius J. Anal. Chem.**, **362** (1998) 130.
43. R. Schindler, M. Watkins, R. Vonach, B. Lendl, R. Kellner and R. Sara, **Anal. Chem.**, **70** (1998) 226.
44. H. M. Al-Swaidan, **Talanta**, **43** (1996) 1313.
45. P. Ek, S. G. Hulden and A. Ivaska, **J. Anal. Atom. Spectrom.**, **10** (1995) 121.

46. I. Lukkari, K. Irgum, P. Lindgren and J. Liden, **Process Control Qual.**, **7** (1995) 185.

47. J. Emneus and G. Marko-Varga, **J. Chromatogr. A**, **703** (1995) 191.

48. F. M. B. Mirabo, A. C. Thomas, E. Rubi, R. Forteza and V. Cerdà, **Anal. Chim. Acta**, **355** (1997) 203.

49. I. D. Brindle and S. Zheng, **Spectrochim. Acta. Part B**, **51** (1996) 1777.

50. A. Ivaska and W. W. Kubiak, **Talanta**, **44** (1997) 713.

51. G. C. Luca, B. F. Reis, E. A. G. Zagatto, M. Conceicao, B. S. M. Montenegro, A. N. Araujo and J. L. F. C. Lima, **Anal. Chim. Acta**, **366** (1998) 193.

52. R. T. Echols, R. R. James and J. H. Aldstadt, **Analyst**, **122** (1997) 315.

53. A. O. S. S. Rangel and I. V. Toth, **Port. Anal. Sci.**, **12** (1996) 887.

54. P. J. Baxter and G. D. Christian, **Chem. Res.**, **29** (1996) 515.

55. L. H. Christensen, J. Marcher, U. Schultz, M. Carlson, R. W. Min, J. Nielsen and J. Villaden, **Den. Biotechnol. Bioeng.**, **52** (1996) 237.

56. E. H. Hansen, B. Willumsen, S. K. Winther and H. Drabøl, **Talanta**, **41** (1994) 1881.

57. R. W. Min, M. Carlsen, J. Nielsen and J. Villadsen, **Biotechnol. Tech.**, **9** (1995) 763.

58. S. C. Chung, G. D. Christian and J. Růžička, **Process Control Qual.**, **3** (1992) 115.

59. H. C. Shu, H. Håkanson and B. Mattiasson, **Anal. Chim. Acta**, **300** (1995) 277.

60. C. Garcia de Maria and A. Townshed, **Anal. Chim. Acta**, **261** (1992) 137.

61. M. Hedenfalk and B. Mattiasson, **Anal. Lett.**, **29** (1996) 1109.

62. X. Liu and E. H. Hansen, **Anal. Chim. Acta**, **326** (1996) 1.

63. C. H. Pollema, J. Růžička, G. D. Christian and Å. Lernmark, **Anal. Chem.**, **64** (1992) 1356.

64. N. W. Barnett, S. W. Lewis and D. Tucker, **Fresenius' J. Anal. Chem.**, **355** (1996) 937.

65. J. L. F. C. Lima, T. I. M. S. Lopes and A. O. S. S. Rangel, **Anal. Chim. Acta**, **366** (1998) 187.

66. S. M. Sultan and F. E. O. Suliman, **Analyst**, **121** (1996) 617.

67. R. W. Min, J. Nielsen and J. Villadsen, **Anal. Chim. Acta**, **320** (1996) 199.

68. G. D. Christian, **J. Pharm. Biomed. Anal.**, **10** (1992) 769.

69. S. M. Sultan, F. E. O. Suliman and B. B. Saad, **Analyst**, **120** (1995) 561.

70. P. J. Baxter, G. D. Christian and J. Růžička, **Anal. Chem.**, **40** (1994) 455.

71. L. X. Tang and F. J. Rowell, **Anal. Lett.**, **31** (1998) 891.

72. M. R. Wei, J. Nielsen and J. Villadsen, **Anal. Chim. Acta**, **312** (1995) 312.

73. S. Parab, B. J. van Wie, I. Byrnes, E. J. Robles, B. Weyrauch and T. O. Tiffany, **Anal. Chim. Acta**, **359** (1998) 157.

74. F. E. O. Suliman and S. M. Sultan, **Microchem. Jour.**, **57** (1997) 320.

75. S. M. Sultan and N. I. Desai, **Talanta**, **45** (1998) 1061.

76. N. W. Barnett, C. E. Lenehan, S. W. Lewis, D. J. Tucker and K. M. Essery, **Analyst**, **123** (1998) 601.

77. J. F. van Staden and T. McCormack, **Anal. Chim. Acta**, **369** (1998) 163.

78. N. W. Barnett, R. Bos, S. W. Russel and R. A. Russel, **Analyst**, **123** (1998) 1239.

79. R. H. Taylor, C. Winbo, G. D. Christian and J. Růžička, **Talanta**, **39** (1992) 789.

80. J. W. Grate, R. Strebin, J. Janata, O. Egorov and J. Růžička, **Anal. Chem.**, **68** (1996) 333.

81. M. Guzman, C. Pollema, J. Růžička and G. D. Christian, **Talanta**, **40** (1993) 81.

82. J. F. van Staden, H. du Plessis, S. M. Linsky, R. E. Taljaard and B. Kremer, **Anal. Chim. Acta**, **354** (1997) 59.

83. J. de Gracia, M. L. M. F. S. Saravia, N. J. Araujo, J. L. F. C. Lima, M. del Valle and M. Poch, **Anal. Chim. Acta**, **348** (1997) 143.

84. A. Rius, M. P. Callao, J. Ferre and F. X. Rius, **Anal. Chim. Acta**, **337** (1997) 287.

85. F. E. O. Suliman and S. M. Sultan, **Talanta**, **43** (1996) 559.

86. A. Rius, M. P. Callao and F. X. Rius, **Anal. Chim Acta**, **316** (1995) 27.

87. F. Sales, M. P. Callao and F. X. Ruis, **Chemom. Syst.**, **38** (1997) 63.

88. I. Ruisanchez, J. Lozano, M. S. Larrechi, F. X. Rius and J. Zupan, **Anal. Chim. Acta**, **348** (1997) 113.

89. A. Rius, M. P. Callao and F. X. Rius, **Analyst**, **122** (1997) 737.

90. J. F. van Staden and A. Botha, **S. Afr. Jour. Chem.**, **51** (1998) 100.

91. A. Joelsson and A. Ivaska, **Kem. Tidskr.**, **105** (1993) 20.

92. M. Valcarcel and M. D. Luque de Castro, **Flow Injection Analysis. Principles and Applications**, Horwood, Chichester, 1987.

93. J. F. van Staden, H. du Plessis and R. E. Taljaard, **Anal. Chim. Acta**, **357** (1997) 141.

94. J. F. van Staden and R. E. Taljaard, **Anal. Chim. Acta**, **344** (1997) 281.

95. C. Zang, Y. Naruzawa and S. Kitahama, **Chem. Lett.**, **5** (1993) 877.

96. C. Zang, Y. Naruzawa and S. Kitahama, **J. Flow Injection Anal.**, **10** (1993) 79.

97. A. Cladera, E. Gómez, J. M. Estela, and V. Cerdà, **Talanta**, **43** (1996) 1667.

98. A. N. Araujo, J. Gracia, J. L. F. C. Lima, M. Poch, M. Lucia and M. F. S. Saraiva, **Fresenius' J. Anal. Chem.**, **357** (1997) 1153.

99. J. F. van Staden and D. Malan, **Anal. Commun.**,**33** (1996) 339.

100. J. A. Vieira, I. M. Jr. Raimundu, B. Reis, E. A. G. Zagatto and J. L. F. C. Lima, **Anal. Chim. Acta**, **366** (1998) 257.

101. F. Mas-Torres, A. Cladera, J. M. Estela and V. Cerdà, **Analyst**, **123** (1998) 1541.

102. J. F. van Staden, H. du Plessis and R. E. Taljaard, **Instrum. Science Technol.**, **27** (1999) 1.

103. J. F. van Staden and R. E. Taljaard, **Mikrochim. Acta**, **128** (1998) 297.

104. J. F. van Staden and R. E. Taljaard, **Anal. Chim. Acta**, **323** (1996) 75.

105. J. F. van Staden and H. du Plessis, **Anal. Comm.**, **34** (1997) 174.

106. S. Nakano, Y. Luo, D. Holman, J. Růžička and G. D. Christian, **Microchem. Jour.**, **55**, (1997) 392.

107. S. M. Sultan and N. I. Desai, **Analyst**, **122** (1997) 911.

108. J. F. van Staden and R. E. Taljaard, **Anal. Chim. Acta**, **331** (1996) 271.

109. J. J. Pauer, **The Flow-Injection Analysis of Certain Determinants in Surface and Ground Water**, MSc-Thesis, University of Pretoria, 1989.

110. A. Munoz, F. Mas-Torres, J. M. Estela and V. Cerdà, **Anal. Chim. Acta**, **350** (1997) 21.

111. J. Nyman and A. Ivaska, **Anal. Chim. Acta**, **308** (1995) 286.

112. J. Nyman and A. Ivaska, **Pap. Puu**, **78** (1996) 513.

113. M. Guzman and B. J. Compton, **Talanta**, **40** (1993) 1943.

114. R. E. Taljaard and J. F. van Staden, **Anal. Chim. Acta**, **366** (1998) 177.

115. J. M. Estela, A. Cladera, A. Munoz and V. Cerdà, **Int. J. Environ. Anal. Chem.**, **64** (1996) 205.

116. J. Alpizar, A. Crespi, A. Cladera, R. Forteza and V. Cerdà, **Electroanalysis**, **8** (1996) 1051.

117. E. Gomez, C. Tomas, A. Cladera, J. M. Estela and V. Cerdà, **Analyst**, **120** (1995) 1181.

118. A. N. Araujo, R. C. C. Costa, J. L. F. C. Lima and B. F. Reis, **Anal. Chim. Acta**, **358** (1998) 111.

119. F. Mas-Torres, A. Munoz, J. M. Estela and V. Cerdà, **Analyst**, **122** (1997) 1033.

120. J. Alpizar, A. Crespi, A. Cladera, R. Forteza and V. Cerdà, **Lab. Rob. Autom.**, **8** (1996) 165.

121. J. F. van Staden, **Fresenius J. Anal. Chem.**, **352** (1995) 271.

122. C. J. Hattingh, **Membraanskeidings met behulp van Dialise in Vloeisisteme**, MSc-Thesis, University of Pretoria, 1994.

123. A. N. Araujo, J. L. F. C. Lima, M. L. M. F. S. Saraiva and A. E. G. Zagatto, **Am. Jour. Enol. Viticul.**, **48** (1997) 428.

124. Y. Luo, R. Al-Othman, G. D. Christian and J. Růžička, **Talanta**, **42** (1995) 1545.

125. D. A Holman, G. D. Christian and J. Růžička, **Anal. Chem.**, **69** (1997) 1763.

126. J. F. van Staden and R. E. Taljaard, **Fresenius J. Anal. Chem.**, **357** (1997) 577.

127. A. N. Araujo, J. L. F. C. Lima, M. L. M. F. S. Saraiva, R. P. Sartini and E. A. G. Zagatto, **J. Flow Injection Anal.**, **14** (1997) 151.

128. J. C. Masini, P. J. Baxter, K. R. Detwiler and G. D. Christian, **Analyst**, **120** (1995) 1583.

129. K. L. Peterson, B. K. Logan, G. D. Christian and J. Růžička, **Anal. Chim. Acta**, **337** (1997) 99.

130. S. Nakano, Y. Luo, D. A. Holman, J. Růžička and G. D. Christian, **J. Flow Injection Anal.**, **13** (1996) 148.

131. Y. Luo, S. Nakano, D. A. Holman, J. Růžička and G. D. Christian, **Talanta**, **44** (1997) 1563.

132. J. W. Grate, and R. H. Taylor, **Field Anal. Chem. Technol.**, **1** (1996) 39.

133. E. Rubi, M. S. Jimenez, F. B. de Mirabo, R. Forteza and V. Cerdà, **Talanta**, **44** (1997) 553.

134. E. Rubi, R. Forteza and V. Cerdà, **Lab. Rob. Autom.**, **8** (1996) 149.

135. M. T. Ohms, A. Cerdà and V. Cerdà, **Electroanalysis**, **8** (1996) 387.

136. E. Purgor, Z. Fehér, G. Nagy, K. Toth, G. Horvai and M. Gratzll, **Anal. Chim. Acta**, **109** (1979) 1.

137. A. R. Crespi, R. Forteza and V. Cerdà, **Lab. Rob. Autom.**, **7** (1995) 245.

138. H. C. Shu and Y. C. Lin, **Huaxue**, **53** (1995) 424.

139. J. F. van Staden and A. Botha, **Talanta**, **49** (1999) 1099.

140. A. Botha, **Sequential Injection Analysis: Evaluation of Operational Parameters and Application to Process Analytical Systems**, MSc-Thesis, University of Pretoria, 1999.

CHAPTER 3

Simultaneous Determinations

3.1 Introduction

When choosing an analytical method, three factors should be considered in the selection process: Cost, Speed and Accuracy. The ideal method will count the last atom in no time and cost nothing. In practice, higher speed reduces accuracy, and higher speed and accuracy cost more. The best compromise should be adequately accurate, at the highest affordable speed.

One of the simplest ways of increasing speed without increasing cost or compromising accuracy is to do simultaneous determinations. Simultaneous determinations are defined as the determination of the concentration of two or more chemical species in a single sample using only a single set of sample preparation steps and a single presentation of the sample to the instrument.

The need to measure several parameters rapidly in the same sample in areas such as clinical chemistry, environmental pollution and industrial control has urged the development of automated methods of analysis which in both the continuous and discrete modes offer the possibility of carrying out simultaneous determinations [1]. In the discrete mode, the same sample must be present in as many locations as there are parameters that are going to be determined, there being a single detection system. In the continuous mode, the sample is split up into as many channels as there are parameters that are going to be determined. Reaction and detection units exist for each of them.

The most elementary classification of simultaneous methods of analysis can be made on the basis of taking the correlation between the detection unit and the species to be

determined. Thus, there is one group of methods in which a detector for each species to be analysed exists, while another group consists of methods in which the number of detectors is lower than the number of species to be determined.

Although simultaneous determinations are quite common in flow injection analysis, only a few articles were published which described these techniques in sequential injection systems (refer to Chapter 2). Since sequential injection analysis developed from the mother technique, flow injection analysis, techniques used in FIA are adopted for use in SIA systems. It is therefore appropriate to highlight a few of these techniques employed in flow injection analysis.

3.2 Simultaneous determinations in FIA

Despite the obvious importance of developing FIA manifolds for simultaneous determinations, only two reviews [1, 2] on this subject have appeared since the inception of FIA. The main simultaneous determinations developed for FIA are summarised in Table 3.1.

TABLE 3.1 Simultaneous determinations using flow injection analysis [1]

	Detection systems		Injection system	Principle
Conventional FIA methods	With several detectors	In series	Single injection	Several ion-selective electrodes with a single reference electrode.
		In parallel	Single injection	With splitting of the flow after the injection.
		Single multi-detector	Multi-injection	With a valve for each parameter and a multi-channel detector.
			Zone sampling	Collection of part of the injected bolus that is directed to another detector.
	With a single detector		Sequential injection	Use of different reagents for different samples according to the parameter to be determined.
			Single injection	Splitting up of the flow with two flow cells aligned in the same optical path. pH gradient Ion-exchange

TABLE 3.1 continues Simultaneous determinations by flow injection analysis [1]

	Detection systems		Injection system	Principle
FIA methods based on differential kinetics	With several detectors	In series	Single injection	Measurements at different times in each detector. Combination of conventional FIA and stopped-flow.
	With a single detector		Single injection	Splitting up of a sample with a double path cell. Splitting up the flow into two different reactors and subsequent confluence. Different measurement times in the two bolus-reagent inter-phases.
			Multi-injection	Double injection of two aliquots of sample that pass through different reactors and merge before the detector.

Luque de Castro and Valcárcel [1] stated that the word "simultaneous" in analytical terms means measurements of several species in the same sample or in different portions of the same samples carried out at the same time. Other methods that employ measurements of samples at different times were referred to as sequential measurements. Sequential measurements are included into this discussion, since it also allow multi-component detection.

The review of Kubáň [2] also highlights the difficulties in the classification of multi-component FIA systems. This is because of the wide selection of methods and tricks involved and the inconsistent nomenclature used by different research groups. It is, therefore, also important to understand the difference between multi-detection and multi-determination [1].

Multi-detection:

Two or more signals are obtained from a single injected sample. It can be performed with a single detector at different times, at different instrumental conditions (wavelength, potential applied, etc.) or with several detection points located in series or parallel. It may be,

(i) *Sequential*, using one or several detection points to obtain several signals at different times per injected sample; or

(ii) *Simultaneous*, using a single detection point performing simultaneous measurements at different instrumental conditions.

Multi-determination:

Determination of two or more analytes in a sample. It can be,

(i) *Sequential*, determining *n* analytes from *n* injections of the same sample.

(ii) *Simultaneous*, determining several analytes from a single sample injection.

It must be noted that multi-detection does not always involve multi-determination, since multi-detection can be applied to measure physical constants such as diffusion constants.

3.2.1 Simultaneous determinations with several detectors

The relative location of the detectors in simultaneous FIA systems permits a sub-classification according to whether their configuration is in series or in parallel. Their characteristics differ considerably.

3.2.1.1 Detectors in series

Fig. 3.1 shows a typical manifold where detectors are arranged in series. The most common examples are the use of ion-selective electrodes placed sequentially in the manifold. Other non-destructive detection methods can also be applied, provided that the manifold configurations prevent excessive dilution of formed products.

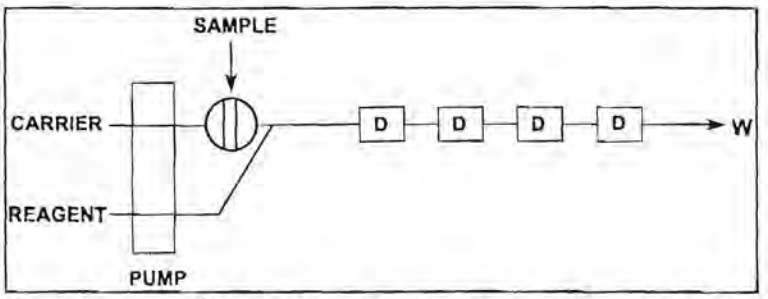

Fig. 3.1 Schematic diagram of a FIA manifold for simultaneous determinations employing several (multi) detectors (D). (W - waste).

3.2.1.2 Detectors in parallel

It is possible to distinguish between the FIA manifolds by comparing the manner in which the sample reaches each detector. The most common division is where the sample is split up in a regular and reproducible manner, sending each part of the sample to a different detector (Fig. 3.2) [3]. The length of the reactors of each sub-system is a function of the intrinsic characteristic of the employed reactions. Suitable diameter and length of tubing used, are also needed to compensate for the resulted decrease in pressure in the sub-systems. This is done to ensure that homogeneous division of the sample is obtained.

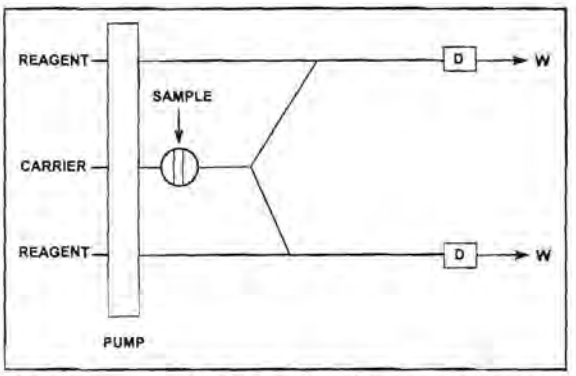

Fig. 3.2 Schematic diagram of a FIA manifold where detectors in parallel are used. (D - detector and W - waste)

Samples can also be propelled to different detectors by using several valves operating simultaneously (simultaneous multi-injection). Fig. 3.3 shows a typical FIA manifold employing multiple valves. Each valve injects the corresponding sample into an aqueous stream that merges with a reagent suitable for the determination of the species to be analysed in the sub-system.

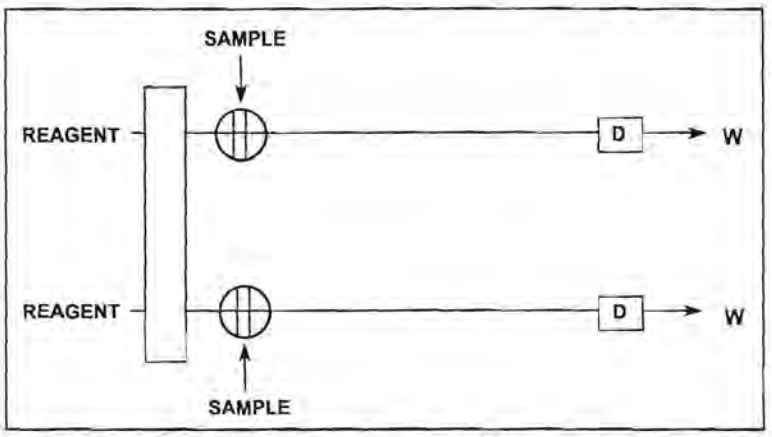

Fig. 3.3 Schematic diagram of a FIA system where multi-injection is used. (D - detector and W - waste)

Less usual is the technique of zone sampling where a part of the original injected sample is extracted and send to one detector, while the rest of the sample is send to another detector. This technique is used in simultaneous determinations where the parameters (or species) being analysed require different degrees of sample dispersion [4].

An advantage of having detectors in parallel arrangement is the fact that destructive detection systems can be used, since the same sample does not need to pass through a series of detectors. These destructive detectors include atomic-absorption spectrophotometers, flame photometers, ICP and ETA.

3.2.2 Simultaneous determinations with a single detector

FIA manifolds utilizing only one detector usually make use of photometric detection, where the two (or more) analytes absorb at the same wavelength after being reacted with a suitable reagent. Single multi-detectors, like ICP and AAS are also included under this heading. These detectors are unfortunately very expensive. Figs. 3.4 to 3.6 show FIA systems for multi-component analysis utilising only one detector.

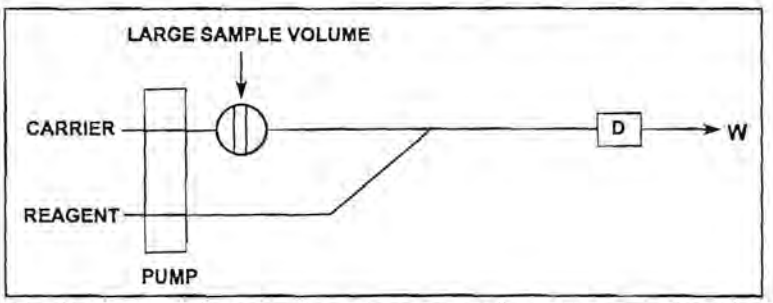

Fig. 3.4 Schematic diagrams of a FIA manifold for simultaneous determinations with a single detector. This manifold is based on the establishment of a concentration gradient. (D - detector and W - waste).

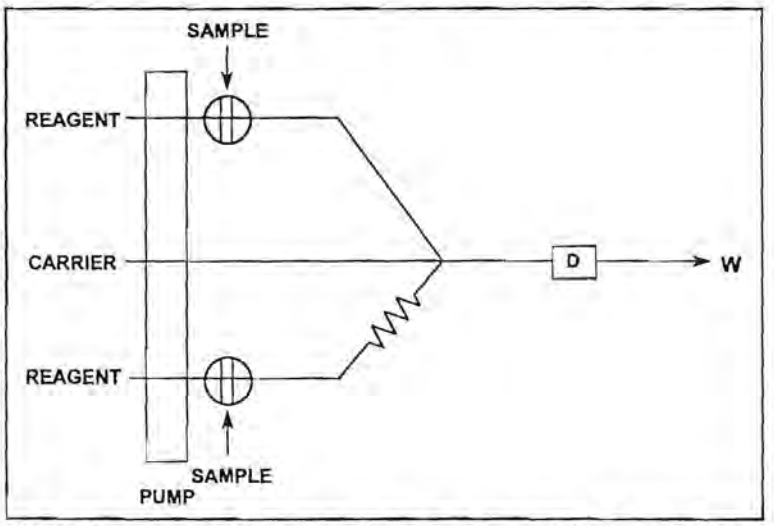

Fig. 3.5 Schematic diagram of a FIA manifold with simultaneous double injection and a asymmetric merging configuration. (D - detector and W - waste).

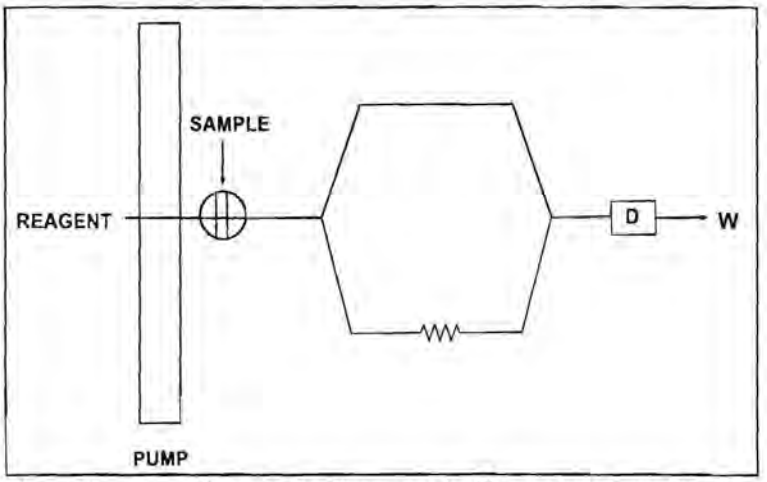

Fig. 3.6 Schematic diagram of a FIA system based on the splitting up of the sample channel into two reactors, which merge in front of the detector (D). (W - waste).

3.2.2.1 Two flow cells

A FIA manifold designed by Steward and Růžička [5] allow the detection of two compounds using two flow-through cells aligned in the same optical path. After injection the sample is split into two channels and allow to merge with the appropriate reagents, where after it is propelled through the two flow-through cells. A longer transmission line (tubing) is used to delay the one part of the sample, ensuring that the peaks corresponding to the two species do not overlap. The flow cells used must be carefully constructed, since the background value depends on the type of material as well as the thickness of the walls of the cell. Too high background values lead to small linear ranges and low sensitivity.

3.2.2.2 pH gradients

This method involves a single detector and a single injection and is based on the use of a carrier with a pH value that is different to that of the sample. If the volume of the latter is sufficiently large, two zones of different characteristics exist that are close to the interfaces with pH values different of that of the central zone plug. The characteristics of these regions can be used to determine several species in the same

sample. Since this technique was used in Chapter 9, it will be discussed in greater detail in the following paragraph.

The complexation of metal ions with most spectrophotometric reagents, and especially with those ligands that might be protonated, is dependant on the pH of the reaction medium as well as the nature and the concentration of the ligand considered. Plots of pH versus absorbance are characteristic for any given metal ion - reagent combination and they are additive if the reagent is in large excess [6]. The shape of a curve obtained for a mixture of metal ions takes the form of a series of stepwise increases in absorbance towards higher pH, as each metal reaches the pH at which complexation took place. Provided that the pH regions of increasing absorbance do not overlap, the concentration of each metal may be determined from the absorbance change at each step and each element may be identified by the pH at the point of inflection [6].

3.2.2.2.1 Establishment of pH gradients [6]

The pH at any point along the tube when a sample of strong acid has been injected into a carrier stream of weak base will be governed by the extent of chemical reaction which has taken place between the acid and the base, and by the physical distribution of the acid and base along the tube. The effect of the chemical reaction follows from elementary acid-base theory. If an acid of concentration C_A and acidity constant K_a reacts with a base of concentration C_B, and the fraction of acid present after the reaction, f_A, is defined as $C_A/(C_A + C_B)$, then

$$pH = pK_a - \log [f_A/(1 - f_A)]. \qquad (3.1)$$

Within the limits of buffering action, $0.1 < f_A < 0.9$, there is an approximately linear relationship between f_A and pH.

In a flowing system the physical distribution of the injected acid will follow a dispersion pattern, which in its most general form is described by

$$C_\theta = [2(\pi D/uL)^{1/2}]^{-1} \exp [-(1 - \theta)^2(4D/uL)^{-1}] \qquad (3.2)$$

where C is the concentration, $\theta = t/\bar{t}$ (t is the time of the measurement and $\bar{t}$ is the

mean residence time), D is the diffusion coefficient, u is the flow rate and L is the length of the tube. Fig. 3.7 outlines such a dispersion profile.

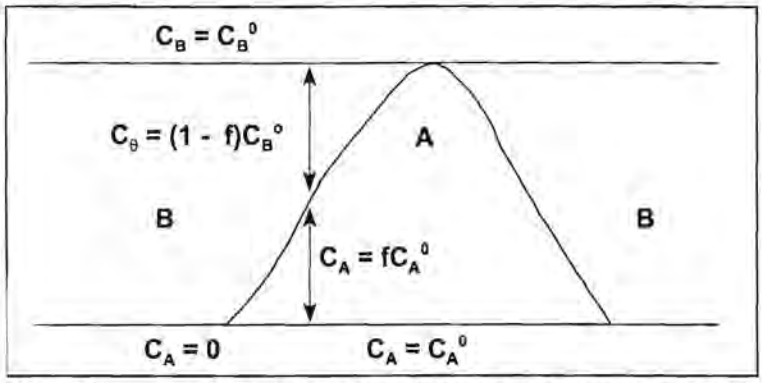

Fig. 3.7 Schematic radial distribution of a sample of acid (A) in an alkaline (basic) carrier stream (B). C_A^0 and C_B^0 are the initial concentrations and C_A and C_B the concentrations after dispersion.

These considerations do not take in account the mode of mixing, which is of course crucial. In narrow tubes at low flow rates, radial molecular transport plays an important role in bringing about mixing of sample and carrier and indeed may predominate at very low flow velocities. If the tube was considered as a series of segments, in any one of which the concentration of acid and base were given by equation 3.2 and if mixing was by radial diffusion, a pH gradient would be established across the sample plug, the gradient being alkaline at the circumference and acidic at the centre. Whatever the mechanism of mixing, the process is efficient and the net effect of physical dispersion and chemical reaction is that the predicted pH gradient follows the line described by equation 3.2, with the pH at the points of inflection corresponding to the pK_a of the weak base if C_A^0 and C_B^0 are equal.

Insofar as the physical dispersion is easy to control and vary, and is reproducible, it is a straight forward matter to alter the pH gradient to suit requirements. The range of pH over the gradient is governed by the choice of weak base. A simple buffer is used if the pH range is to be narrow, but an universal buffer is used if the pH range is to be great. The argument is the same for a strong base injected into a weak acid or series of weak acids.

Care must be taken that the injected acid (or base) zone undergoes sufficient dispersion to allow gradual pH changes. Acid-base boundaries that are too steep resulted in overlapping of peaks.

3.2.2.3 Ion exchange

FIA and ion exchange association provide the possibility of carrying out simultaneous determinations. These reactions are usually indirect methods of determinations and are based on inhibitory effects on metal catalysed reactions [1].

3.3 Commutation in flow injection analysis

The application of intermittent and alternating streams without stopping the peristaltic pump, the sequential injection process and the concept of mono segmented flow injection systems have all been achieved successfully with manual commutation. Time controlled commutation greatly expanded the possibilities of FIA, allowing the development of new processes such as zone sampling, zone trapping and time based injection [7].

A commutator is usually made of perspex and consists of two fixed external plates with a movable central bar, all held tightly together by two screws with springs. Holes (1 mm bore) are made through the pieces of the commutator in accordance with the related flow diagram. For insertion of the polyethylene connecting tubes, either Tygon bushings were used or the holes were drilled so as to be slightly conical near the surface. Silicone rubber sheets with holes corresponding to those of the external plates were placed between the commutator pieces to avoid leakage. A metal lever, which can be operated manually or electronically, is used to move the central bar of the commutator between the two resting positions associated with the two (or more) states of the manifold. A simple commutator is illustrated in Figs. 3.8 A and B.

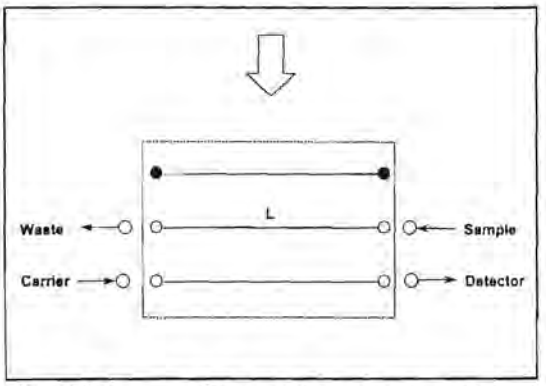

Fig. 3.8A Schematic representation of the movable part of a commutator in the LOAD position.

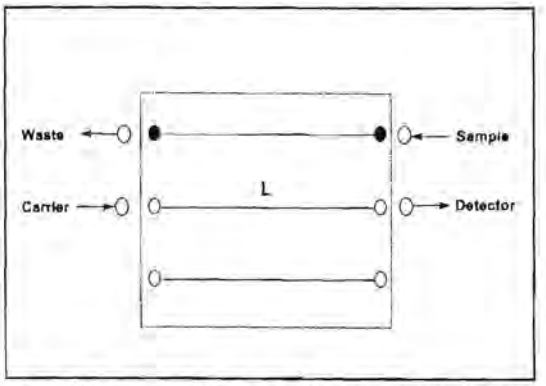

Fig. 3.8B Schematic representation of the movable part of a commutator in the flow through position.

In Fig. 3.8 A the sample flow through the commutator to waste. In this way the loop (L) inside the commutator is filled with a precise volume of sample. The movable part of the commutator is now moved downwards (Fig. 3.8 B). This result in the insertion of the sample loop into the flowing carrier stream. The 'injected' sample is now propelled to the detector, while the flow of the sample stream is either stopped or is still flowing to waste through the third channel in the commutator. When the movable part of the commutator is moved back to the original position, the sample loop is filled for the next analytical cycle.

Commutators with more channels can allow the sequential or time-based 'injection' of different samples and reagents. It can also allow stopped-flow periods by blocking the flow in through a certain channel, without actually stopping the peristaltic pump. In this way sequential or simultaneous determinations can be performed.

3.4 Methods based on differential kinetics

One of the advantages of kinetic analysis methods over equilibrium methods is the possibility of carrying out simultaneous determinations based on the different rates of their reactions with a common reagent. In spite of this being a promising aspect, it has

several important limitations that restricts its applicability. Firstly, it should be emphasised that it is not easy to find chemical systems in which significantly important differences can be established in the experimental conditions between two or more reaction rates. On the other hand, the differential kinetic methods described do not have a very high level of accuracy and/or reproducibility, because slight disturbances produced by the diversity of samples or by slight changes in the working conditions lead to a low precision in comparison with other manual or kinetic techniques [1].

The principle of the kinetic methods is that for pseudo-first order reactions of different rates straight line calibration curves may be obtained for samples for any time *t* after injection for various metal concentrations. For different metals (analytes) which have different rates, the calibration curve will have different slopes, slower reaction components having lower slopes [9].

Few differential kinetic methods have been developed for FIA. For a description of the most significant contributions the systematisation in Table 3.1 has been adopted, according to the number of detectors that the system contains.

3.4.1 Systems with two detectors

This consists of a differential kinetic mode with a simple principle. The signal produced by the reacting species is measured at two different times, t_1 and t_2, in each detector [1]. The FIA manifold employs the two detectors in series (Fig. 3.1), which means that no splitting of zones take place. The detectors are situated sufficiently apart to allow ample time for the slower reaction to develop.

3.4.2 Systems with multi-detection

Hooley and Dessy [8] described a kinetic determination based on multiple measurements. The multiple detection system consists of a quarts reactor tube with a series of independent detection units with a LED (light emitting diode) and a

photodetector. Its signal is monitored by an electronic data-processing system. A plug of reactant sample passes successively through each measurement point at different times in such a matter that it is possible to process as many types of kinetic data as there are detectors. The relative locations of these detectors depends on the flow and the rate of the reactions considered. It is an ideal system for kinetic determinations and very useful for the simple determination of rate constants.

3.4.3 Systems with a single detector

Employing these manifolds, the detector must provide two different signals, or a signal increase, or both, at two times (or at a time increase) that coincide(s) with different reaction times. Several different manifold configurations for carrying out these determinations exist. Distinction can be made between systems with double and single injection.

3.4.3.1 Single injection

3.4.3.1.1 Combination of conventional FIA and stopped flow

These determinations depend on the fact that the first analyte complex is completely formed when it reached the detector, while the slower reaction develop during the delay time (stopped flow period) in the flow cell. These methods are only successful if the reaction of the more reactive component is essentially complete before the reaction of the less reactive component reaches one half-life [9].

3.4.3.1.2 Splitting of the flow

Fig. 3.6 shows a typical manifold where the sample stream is split into two parts and propelled through reactors with different lengths and diameters. The different geometrical and hydrodynamic properties of the two channels provide different residence times for each of them and two analyte peaks are obtained. The one part

of the sample travels through a shorter reactor and reaches the detector first (time = t_1), allowing the detection of mainly the more reactive component, while the second peak (at t_2) allow detection of the less reactive compound. Adaption of this method to SIA is described in Chapter 7.

Detection is done either by using a double path flow cell [9, 11] or by stopping the flow when the zone reaches the flow cell. Data collection is done by monitoring of the change in absorbance as the reaction develops [10]. The ratio in which the sample is split is an important aspect when accuracy, sensitivity and reproducibility are concerned. The variables influencing the splitting are thoroughly described by Fernandez *et al.* [11].

3.4.3.2 Double injection

The principle of this method is that two zones of different composition are simultaneously injected and are propelled through tubing of different lengths (which coincide prior to detection) so that they reach the detector sequentially, resulting in two analyte peaks [1].

3.4.3.3 Adaptation to SIA systems

Since sequential injection analysis has the advantage that stopped flow periods can be easily incorporated, adaption of kinetic determination to SIA has many positive features. Unfortunately, it also has a few disadvantages. Because of the discontinuous nature of SIA, splitting of the sample zone can not be done by simply propelling the zone through two reactors with different geometrical and hydrodynamic properties. The zone is split by pumping the first part of the reacting sequence of zones into a second holding coil and leave it there to allow time for the less reactive compound to form. The rest of the zone which is still inside the first holding coil is then propelled through the detector and measured. The selection valve is then turned in such a way to select the second holding coil again. The portion of the zone "stored"

there is then drawn back into the first holding coil where after it is propelled through the detector to be measured. Fig. 3.9 shows the SIA manifold used for the kinetic determination of Ni(II) and Co(II) in Chapter 7.

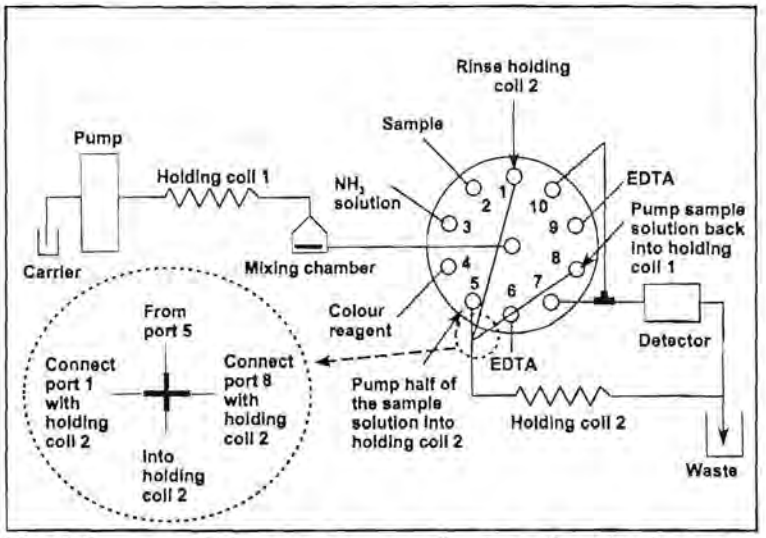

Fig. 3.9 SIA system used for the simultaneous determination of Ni(II) and Co(II).

The system can be largely simplified if the selection valve could move in both directions, *viz.* clockwise and counter-clockwise. If this is, however, not the case, different procedures are needed. In the manifold used in Chapter 7, the VICI selection valve was able to move only in the counter-clockwise direction. Since the port in the middle of the valve is connected to only one other port at a time, it was needed to connect the second holding coil to ports 5, 8 and 1 by means of a perspex connector. When the first holding coil (port in the middle of the valve) was connected to port 5 (second holding coil) half of the stack of zones was pumped into the second holding coil. The remainder of the zones in the first holding coil was reacted with EDTA (port 6) and propelled through the detector (port 7).

Since it was impossible to move back to port 5 to collect the part of the zones in the second holding coil, the second holding coil was connected via the perspex connecter to port 8. Because port 8 was connected to the first holding coil via the port in the middle of the valve, this connection allowed the movement of the zones from the

second holding coil back into the first holding coil. The zone was then reacted with EDTA (port 9) and propelled through the detector (port 10 was connected to the detector line via a T-piece perspex connector). To avoid any sample carry-over, it was needed to rinse the second holding coil prior to the next analysis. To do this, port 1 (which was connected to the first holding coil via the port in the middle of the valve) was connected with a short piece of Tygon tubing to the perspex connector and doing so it was connected to the second holding coil. Forward movement of the pump ensured effective rinsing of the second holding coil.

3.5 Multi-component techniques in sequential injection analysis

When excluding the articles published in speciation analysis, multi-component analysis in sequential injection analysis is virtually a novelty. The first publication on multi-component techniques in SIA was, however, published in 1995 [12]. A multi-linear regression program for the simultaneous determination of calcium and magnesium in mixtures was described. The assay relied on the formation of the Ca and Mg complexes with the chromogenic reagent 4-(2-pyridylazo)resorcinol (PAR); the complex mixture could be readily resolved, notwithstanding the extensive spectral overlap involved. Data were recorded with a diode array spectrophotometer and spectra were corrected in order to avoid the effect of changes in the refractive index inside the sensing microcell.

Estela *et al.* [13] described the simultaneous determination of ionic species by SIA using a sandwich technique with large sample volumes. Iron(II) and nitrite were determined using a large sample volume (2 mℓ) with different reagents at each end of the plug. Minimum zone overlap (good resolution between the two analyte peaks) was obtained with this large sample zone, which lead to minimum mutual interference. The optimisation of the method is slightly more difficult than for others and the sample and reagent consumption are much higher, since higher concentration and bigger reagent zones were needed to obtain the desired sensitivity. This technique was also evaluated in Chapter 6 together with a tandem SIA application.

Multi-component techniques involving detectors such as HPLC [14, 15], ion-selective electrodes [16, 17], ICP [18], immobilized enzymes [19] and hydride generation direct plasma AAS [20] are also described.

3.6 Other techniques that can do simultaneous determinations [21]

Separational (chromatographic) techniques are inherently simultaneous. The components of a sample are separated and the same attribute of every component measured. If this technique is combined with a scanning spectrometric technique, identification and quantification can be done simultaneously.

All techniques that involves scanning (monitoring the effects of varying levels of energy on the sample) are in principle capable of simultaneous determinations. The main problem with this is the great number of possible interferences, that require complex calibration procedures.

Thermal techniques are capable of simultaneous determinations, but in general resolution is poor. It is the only family of non-spectroscopic techniques that can analyse solid samples.

Of the electrochemical techniques, the scanning voltammetric techniques are the main candidates for simultaneous determinations. Non-scanning electrochemical techniques are not inherently simultaneous.

The usefulness of instruments that are in principle capable of simultaneous determinations is often limited by the time it takes to gather the information. Slow scans and lengthy separations are usually the culprits. This is why the development of new instrumentation that gather information faster are often used in simultaneous determinations. Examples of these, mostly expensive, detectors are diode-array spectrophotometers, FT-IR and ED-XRF.

Several simultaneous determinations also involve the use of a dialyser to separate the analytes from interferences as well as to isolate them from the matrix [22 - 25]. Although most speciation studies are also in effect simultaneous determinations, they were not discussed, since they do not really fit the term multi-component analysis.

3.7 Concepts in simultaneous determinations

A problem that arises in simultaneous determinations, not found in single determinations, is that of *mutual interference*. Chemical interference takes place when a species other than the analyte present in the sample changes the response of the instrument to a value different from the one when only the analyte is present. This is a problem in any kind of analysis. *Mutual interference* takes place when the concentration of two or more species are to be determined, and the instrumental response to at least one of them is influenced by of one or more of the other species to be determined. The higher the *selectivity*, the smaller the problem of interference.

In separational techniques, the problem of mutual interferences is overcome by increasing the separation (number of plates).

Ordinary interferences can be eliminated; mutual interferences cannot, because to do so would destroy information. If the action of the interferences is well understood, measuring both interfering and interfered analytes can give enough information to separate the mutual effects. From this, the concentration of the analytes can be determined. A simple example of this is the simultaneous spectrophotometric determination of titanium, vanadium, and molybdenum in steel [26].

The absorbance (A) at a certain wavelength and light path length depends on the molar absorptivity (ϵ) and the concentration (c) of a chemical species. According to "Beer's law" [27] the dependence is linear:

$$A = \epsilon c$$

If two species (x and y) absorb at the same wavelength, the total absorbance is equal to the sum of the individual absorbances:

$$A = \epsilon_x c_x + \epsilon_y c_y$$

When the absorbances at two wavelengths (λ_1 and λ_2) are measured and the molar absorptivities are known, a system of two simultaneous equations in two unknowns is generated:

$$A^{\lambda_1} = \epsilon_x^{\lambda_1} c_x + \epsilon_y^{\lambda_1} c_y$$

$$A^{\lambda_2} = \epsilon_x^{\lambda_2} c_x + \epsilon_y^{\lambda_2} c_y$$

The two unknowns can be determined by simple algebra, or (preferably) by multiple linear regression. In principle, measuring at *n* wavelengths make determinations of *n* analytes possible.

Another example is the use of the Nikolskii-Eisenman equation to separate the effects of mutually interfering ions on an array of electrodes [21].

$$E_{ij} = E_i^{o} + S_j \log(a_{ik} + \sum_{n} K_{ij} a_{il}^{z_i/z_j})$$

The potentials E of j electrodes are measured in i samples. Using the known activities a_{ik} of the primary ions and the interfering ions (a_{il}), the slope S_j, the standard potentials $E°_i$ and the selectivity coefficients K_{jk} of the electrodes are determined by non-linear curve fitting. Knowing the parameters of the electrodes, predictions of activity can be made from the measured potentials of unknown samples.

In his review on simultaneous determinations in FIA, Kubáň [2] mentions another problem of simultaneous determinations: *redundant information*. More data are collected than is needed for the determination of the analytes in question. Storage space (physical and/or electronic) costs makes this an expensive excercise.

3.8 Conclusion

Simultaneous analysis are of great value in the fields of clinical analysis, environmental analysis and also in control laboratories. Multi-component SIA (and FIA) systems have the advantage that automation lead to less errors due to human imperfectness and that precise timing, splitting of samples and multiple measurements can be accomplished. Although it is true that increasing the number of detectors increases the overall cost of the manifold, there are several relatively inexpensive detectors that can perform the detection just as well. In a world where efficiency needs to be high, while cost needs to stay low, development of multi-component techniques employing only one detector will be the road to the future.

3.9 References

1. M. D. Luque de Castro and M. Valcárcel Cases, **Analyst**, **109** (1984) 413.
2. V. Kubâñ, **Crit. Reviews Anal. Chem.**, **23** (1992) 15.
3. W. D. Basson and J. F. van Staden, **Water Res.**, **15** (1981) 333.
4. B. F. Reis, A. O. Jachintho, J. Moratti, F. J. Krug, E. A. G. Zagatto, F. H. Bergamin and L. C. R. Pessendal, **Anal. Chim. Acta**, **123** (1981) 221.
5. J. W. B. Steward and J. Růžička, **Anal. Chim. Acta**, **82** (1976) 137.
6. D. Betteridge and B. Fields, **Anal. Chim. Acta**, **132** (1981) 139.
7. F. J. Krug, H. Bergamin and E. A. G. Zagatto, **Anal. Chim. Acta**, **179** (1986) 103.
8. D. J. Hooley and R. E. Dessy, **Anal. Chem.**, **55** (1983) 313.
9. D. Betteridge and B. Fields, **Fresenius Z. Anal. Chem.**, **314** (1983) 386.
10. T. Yamane and C. Ishimizu, **Mikrochim. Acta**, **1** (1991) 121.
11. A. Fernandez, M. D. Luque de Castro and M. Valcárcel, **Anal. Chem.**, **56** (1984) 1146.
12. E. Gómez, C. Tomás, A. Cladera, J. M. Estela and V. Cerdà, **Analyst**, **120** (1995) 1181.
13. J. M. Estela, A. Cladera, A. Muñoz and V. Cerdà, **Intern. J. Environ. Anal. Chem.**, **64** (1996) 205.
14. K. L. Peterson, B. K. Logan, G. D. Christian and J. Růžička, **Anal. Chim. Acta**, **337** (1997) 99.
15. I. Lukkari, K. Irgum, P. Lingren and J. Linden, **Swed. Process Control Qual.**, **7** (1995) 185.
16. J. Alpizar, A. Crespi, A. Cladera, R. Forteza and V. Cerdà, **Electroanalysis**, **8** (1996) 1051.
17. J. Alpizar, A. Crespi, A. Cladera, R. Forteza and V. Cerdà, **Lab. Rob. Autom.**, **8** (1996) 149.
18. H. M. Al-Swaidan, **Talanta**, **43** (1996) 1313.
19. R. Wei Min, J. Nielsen and J. Villadsen, **Den. Anal. Chim. Acta**, **312** (1995) 149.

20. P. Ek, S. Hulden and A. Ivaska, **J. Anal. At. Spectrom.**, **10** (1995) 121.

21. D. Malan, **Arrays of Crystalline Membrane Ion-Selective Electrodes in Flow Injection Potentiometry**, MSc-Thesis, University of Pretoria, 1998.

22. J. L. F. C. Lima, A. O. S. S. Rangel and M. M. S. Roque da Silva, **Atom. Spectros.**, **12** (1991) 204.

23. J. L. F. C. Lima, A. O. S. S. Rangel and M. M. S. Roque da Silva, **Cienca e Technica Vitivinicola**, **9** (1990) 121.

24. J. L. F. C. Lima, A. O. S. S. Rangel and M. M. S. Roque da Silva, **Journal International des Sciences de la Vigne et du Vin**, **24** (1990) 167.

25. J. F. van Staden, **Anal. Chim. Acta**, **261** (1992) 453.

26. A. Weissler, **Industrial and Engineering Chemistry**, **17** (1945) 695.

27. G. D. Christian and J. E. O'Reilly, **Instrumental Analysis** 2nd ed., Allyn and Bacon, Boston, 1986.

CHAPTER 4

Extractions

4.1 Introduction

Liquid-liquid extraction is among the most frequently used conventional methods for sample pretreatment preceding measurements of the analyte concentration. It offers a potential for selectivity and sensitivity improvement in a large number of determinations. By use of partitioning between an organic and an aqueous phase, an analyte can be separated from an interfering matrix, or interfering matrix components can be removed from the sample in order to increase the selectivity of the determination of the analyte. Furthermore, an analyte can be concentrated by extracting it from a large volume of an aqueous sample into a small volume of an organic phase, thus improving the detection limits.

Manual liquid-liquid extraction procedures are usually very tedious, involving a large consumption of solvents and chemicals and are subjected to potential contaminants from the atmosphere and chemical glassware. In addition, the conventional liquid-liquid extraction process requires manipulation with significant volumes of hazardous and/or toxic organic solvents. The handling of a large number of samples and the introduction of bias and errors associated with the various requisite manipulations must also be taken into account.

The rapid development of automated liquid-liquid extraction is perhaps due to the broad use and importance of the liquid-liquid extraction process. One of the most effective ways to shorten the duration of this process has been the construction of dynamic "on-line" liquid-liquid extraction systems applying the principles of continuous flow analysis.

Regardless of the way in which the liquid-liquid extraction step is performed - via a manual batch procedure or by use of some kind of mechanised or automated system - three basic operations are usually necessary [1]:

(1) the organic and aqueous immiscible phases must be dispersed in defined volumes;

(2) the phases must be brought into intensive contact with each other for the extraction to take place; and

(3) the phases must be physically separated from each other after the extraction event in order to make the chemical separation meaningful.

4.2 Extraction in conventional FIA systems [1]

In classical FIA extraction, aqueous sample solutions are usually introduced continuously or in definite volumes (< 100 to 200$\mu\ell$) into a continuous aqueous stream. This stream serves as both a reagent and a carrier stream in the simplest single-line FIA version. The aqueous sample solution can also be merged and mixed with another, separate aqueous stream containing an organic analytical reagent, spectral buffer or others. In this way, appropriate chemical reactions as well as solution homogenisation take place in a reaction-and-mixing coil before entering a phase segmenter.

The resultant aqueous stream (ideally pulse-less) of an extractable component is then segmented with an organic immiscible solvent stream at the segmenter mixing point, where more or less reproducible droplets of one phase in the other are formed. The size of the droplets is regulated by a combination of gravity, density and interfacial and hydrodynamic forces. The geometry of the inner capillary system of the segmenter and the quality of the surface also play a role.

The droplets move into the outflow channel after having been formed and tend to minimize their interfacial area with the other phase and to maximize the contact surface area with the wall material of the outflow tubing, thereby wetting it. The process results

in the formation of independent, more or less regular segments of both phases in a single moving stream which them enter the extraction coil.

Depending on the outflow channel material and on the material of the extraction capillary coil, the solvent that has the greater affinity for the tubing material coats the tubing walls with a very thin film, representing a relatively stationary phase. The film of one solvent surrounds the deformed spherical, ellipsoidal or tubular segments of the other solvent. Organic solvents wet Teflon and are repelled by glass. Conversely, aqueous phases prefer glass and metal to Teflon [1, 2]. The former case is more frequently used in liquid-liquid extraction FIA; the latter plays an important role in the re-extraction (back extraction) step of two-step liquid-liquid extraction FIA.

The extraction process occurs principally in the extraction coil and to a lesser extent in the segmenter and the phase separator. During extraction the extractable sample components are transported from a relatively homogeneous aqueous solution of higher analyte concentration into segments of the immiscible organic phase through the segment interface. The interfacial area available for the extraction consists of menisci between the two phases and a film surrounding the segments. An analyte diffuses to the interface between the two phases and extraction equilibrium is reached, the attainment of which depends on a number of factors.

Naturally, the degree of extraction is a function of the residence time of the analyte in the extraction coil, which is affected by the coil length and the flow rate. Extraction efficiency in the extraction coil is usually high and often virtually complete in several seconds.

The influence of the flow rate and system manifold parameters on the extraction efficiency depends on the kinetics of the extraction process and the mass transport processes involved. The extraction rate increases with decreasing segment size and decreasing inner diameter of the extraction tube; hence, the use of a narrower extraction tube and small/short segments enhance extraction. The choice of material

used for the extraction coil indirectly influences the extraction efficiency; the efficiency is high for stripping an analyte from the aqueous to the organic phase for PTFE coils, while it is very low for glass or metal coils. In contrast, the efficiency of analyte stripping from organic to aqueous phase is higher for glass and metal coils than for PTFE coils.

The segments of the aqueous and organic phases are subsequently separated in a phase separator into individual streams. The extractable analyte in the receiving phase is determined using a flow-through detection system. The analytical signals are treated in a conventional manner, with the analyte concentration calculated from the peak height, the peak width or the peak area. In principle, the other separated phase is directed to waste through a restriction coil (which also controls the separation efficiency of the phase separator).

Since reactions needed extraction differ in degree of difficulty, various types of system manifold arrangements of different complexity are available. These arrangements or operational modes include:

(1) *Without phase separation*: This is the simplest mode, the aqueous solution of the sample being injected into a single-channel manifold together with the organic phase stream (or an extractable substance in the organic phase injected into the organic or aqueous phase stream).

(2) *Single extraction*: The segmentation system is located prior to or following the injection valve.

(3) *Multiple extraction*: The separation process is repeated several times by using the same or a different extractant in successive steps.

(4) *Back extraction*: A multistage extraction mode in which the aqueous sample is first extracted into an organic medium and then back-extracted into another aqueous phase, where measurements are performed.

(5) *Special techniques*: These included techniques such as closed-loop systems, systems with non-segmented streams, systems without phase separation units

or systems with liquid separation membranes.

4.3 Basic components of FIA extraction manifolds

Several fundamental considerations must be taken into account when designing a liquid-liquid extraction system. These are connected to reproducible segmentation of the two miscible phases; optimisation of the geometry of the complete liquid-liquid extraction system; the selection of proper construction materials for all individual system components and a highly efficient and fast separation of the phases after reaching the separation equilibria [1].

4.3.1 Transport units

A stable pumping system is usually required in liquid-liquid extraction FIA. The aqueous stream can be propelled using a standard peristaltic pump with ordinary PVC tubing. In contrast with this, the flow of the organic solvent is usually created by use of [1, 2]:

(1) A peristaltic pump with pumping tubes comprised of inert material (such as modified PVC (Tygon), silicone rubber, flexible polyurethane (Tygotane) or fluoroplastics (Acidflex or Viton)) since the flexible tubes commonly used in FIA are useless.

(2) A liquid chromatographic pump (piston or syringe) with pulse dampers and pressure indicators.

(3) A displacement technique, involving pumping an aqueous stream into a closed container (usually a thick-walled bottle) by using a peristaltic pump with ordinary pumping tubes; the container is completely filled with an organic solvent, which is replaced at a constant aqueous flow rate and forced into the FIA system.

(4) A constant gas overpressure (using pressurised inert gas), forcing the organic phase through the FIA system from a closed container.

4.3.2 Segmenters

Phase segmentation involves dividing the continuous flow of the organic and aqueous phase into one uniform stream with alternating segments. The immiscible phases are brought together in a narrow tube in a controlled manner so that defined segments of each phase are formed. Segmentation and separation of the two immiscible phases are of crucial importance to the quality of the results obtained.

There are two major variables to consider in connection with segmentation: Segmentation reproducibility and segment size. While segment size may not effect the extraction efficiency of a fast extraction process or when large sample volumes are introduced into the system, it could theoretically affect the efficiency of slower systems. The maximum segment size is determined by the interfacial tension of the organic and aqueous phases, both between each other and between a phase and the tubing material, such that the maximum segment size decreases with decreasing values of interfacial tension $\gamma_{0/a}$. The choice of tubing material, tubing dimensions and geometry of the mixing chamber also is critically important.

Several segmenters of varying efficiency are available. These segmenters can generally be divided into two groups, depending on their principle of segmentation (postsegmenter introduction of the sample being a special case):

(1) Continuous flow segmenters (including those which operate on the basis of differences in gravity and density.
(2) Mechanical types of segmenters.

4.3.3 Extraction coils

In the extraction coil mass transfer takes place between the segments of the two phases. When the coil is made of Teflon, the aqueous phase, which is repelled by it, circulates as bubbles, whereas if the coil is made of glass, the aqueous phase wets the

walls and the organic phase flows as bubbles or plugs. In both cases the bubbles are completely enveloped by the other solvent. Three criteria for the selection of the type of coil to be used, have been established [2]:

(1) the material chosen for the coil should such that the analyte is initially present in the bubble phase in order the limit cross-contamination between successive samples.
(2) The ratio of the interfacial area to the initial volume of the phase containing the analyte should be as high as possible.
(3) The analyte should be capable of moving rapidly from one point in the original solution to the interface between the phases.

The last two criteria also require the analyte to be present in the bubble phase, since in this way the interfacial area-to-volume ratio is higher and the movements of the analyte towards the interface are clearly shorter and faster than in the opposite situation. Taking these two criteria into account, it can be deduced that,

(1) if the analyte is initially present in the organic phase, the extraction coil should be made of glass in order to achieve higher extraction efficiency than would be the case with another Teflon coil of the same length and diameter;
(2) it is preferable to use a Teflon coil to extract from the aqueous into the organic phase.

In most cases the transfer yields achieved ranges between 70 and 90% and is linked to the variables in the system, which should, therefore, be rigorously controlled in order to obtain reproducible results. An unusually long coil, although highly efficient, would result in a greater extent of analyte dispersion in the phase of interest. The ideal diameter of the extraction tube ranges between 0.5 and 1.0 mm. Auxiliary methods intended to increase transfer efficiency, such as including inert beads in the coil, immersion in a thermostatic bath or subjection of the coil to vibrations or an ultrasonic field, should be applied cautiously since any resulting emulsions may significantly alter

the function of the phase separator.

Extraction coils have been use in various configurations, but the simplest and most frequently used coils have a symmetrical of helical shape. The horizontal position of the main axis of the coil forces the mixing process and introduces a secondary flow rate perpendicularly orientated to the axial, which increases mass transport.

The secondary flow patterns are established in response to the centrifugal force in coiled extraction capillaries. They bisect the capillary profile, reducing the diffusion distance by half. The radial secondary flow causes effective mass transport, interchanging material in a slower moving streamline with material in the faster one. Hence, mass transport is forced by intrasegmental movement due to the viscous drag of the two immiscible fluids. Curved and coiled extraction coils should, therefore, give better internal radial mixing in the segment and would result in more effective extraction.

The viscosity difference between the two immiscible solvents manifests itself in the extraction process as an inhibitor of diffusion. With increasing viscosity, the rate of mass transfer decreases, thereby decreasing radial mixing and increasing the residence time of the sample component(s).

The enrichment factor (the ratio between the flow of the aqueous phase containing the sample and the organic phase) is influenced by the segmentation process. The enrichment factor rarely exceeds 20 in commonly used manifolds. The length of the organic (and the aqueous) segments cannot be reduced indefinitely; the lower limit of organic phase segments has experimentally been estimated to be about 1.5 times the internal diameter of the extraction coil tube [3]. The extraction efficiency decreases markedly if the organic phase droplets become too small to form a continuous film on the tubing wall. Also, the segmentation may be unstable due to coalescence of very small segments during transport through the extraction coil.

4.3.4 Phase separators

The phase separation process involves a partitioning of the segmented phases after the extraction has been completed in the extraction coil, in such a manner that the unwanted phase is directed to waste while the other phase(s) is resampled or pumped through the detection system. In most practical separators, the two-phase system cannot be desegmented totally into two pure individual phases. Typically, phase separation efficiency is 80 to 100%.

The phase separator is designed to handle small volume segments of the two immiscible phases, received from the extraction coil in the form of a segmented flow stream. The objectives of the phase separator are to:

(1) Continuously separate the phases carrying the extracted analyte and to continuously split them into two or three individual streams in such a manner that one or two of them may be used for determination of the analyte concentration.

(2) Work properly over a wide range of flow rate ratios Q_a/Q_o (Q_a - flow rate of the aqueous phase and Q_o - flow rate of the organic phase) and total flow rate Q_t.

(3) Recover as much as possible of the desired phase (approaching 100%).

(4) Maintain the concentration profile of the analyte and prevent deterioration of the original concentration gradient of the sample.

(5) Prevent any further sample dispersion and dilution during the separation process (band broadening).

(6) Handle very small segment volumes of both phases (usually 1 to 30 $\mu\ell$).

(7) Handle different types of solvents.

The phase separator must also be made of materials that are chemically inert (glass, stainless steel or fluoroplastics) to attack by solvents and chemicals. The long-term stability of the phase separator should be good and it should be easy to operate. Preferably, no adsorption should occur and the volume of the cavities or grooves in the

separator should be kept as small as possible.

Current phase separators for liquid-liquid extraction flow injection analysis systems can be divided into three groups:

(1) Density (chamber) separators, working on the principle of the density difference between the two phases.

(2) Affinity (heterogeneous material) separators that are constructed from a lipophilic (usually PTFE) and a hydrophilic (e.g. glass or stainless steel) material, working on the principle of the affinity difference between the phases and the separator materials (as well as the density difference between the two phases).

(3) Membrane phase separators that use a lipophilic (and/or hydrophilic) membrane to exclude one or both phases from the segmented stream.

4.4 Extraction processes using SIA manifolds

Sequential injection extraction was, not surprisingly, introduced by Růžička's research group. Peterson *et al.* [4] report on a flow based extraction method where an aqueous sample and organic solvent are injected sequentially into an extraction coil, then mixed and separated due to the differential flow velocities of the aqueous and organic phases. The sequential injection extraction manifolds are much simpler than the ones used for FIA extractions, since no segmenters or phase separators were needed.

Contrary to FIA extractions where continuous separation takes place, a critical parameter, zone inversion length, was established in SIA extractions. Zone inversion length represent the distance travelled by the aqueous solution from the loading position until it has moved completely through the organic phase. At this stage the organic phase coated the walls of the Teflon tubing, allowing the extraction of the analyte into the organic layer.

Fig. 4.1 shows the basic protocol of a sequential injection extraction procedure. The phases involved in the extraction method are as follow:

(1) Organic wash solution is loaded into the extraction coil, followed by an air segment, the organic phase and the aqueous phase containing the analyte. The organic wash solution is only loaded when the carrier stream is unable to remove the remainder of the thin film.

(2) As the pump moves in reverse, the organic phase coats the tubing wall as it is followed by the aqueous phase (AQ). The aqueous phase pushes through the organic phase (ORG) as it moves through the extraction coil.

(3) Air is pumped into the coil, propelling AQ further through the organic layer, until all the organic solvent has been deposited on the tubing, ensuring complete contact of the two phases during this step.

(4) After this step, the pump changes direction, pushing AQ back through ORG.

(5) The aqueous phase is pushed out through the valve to waste with the analytes extracted into the organic phase.

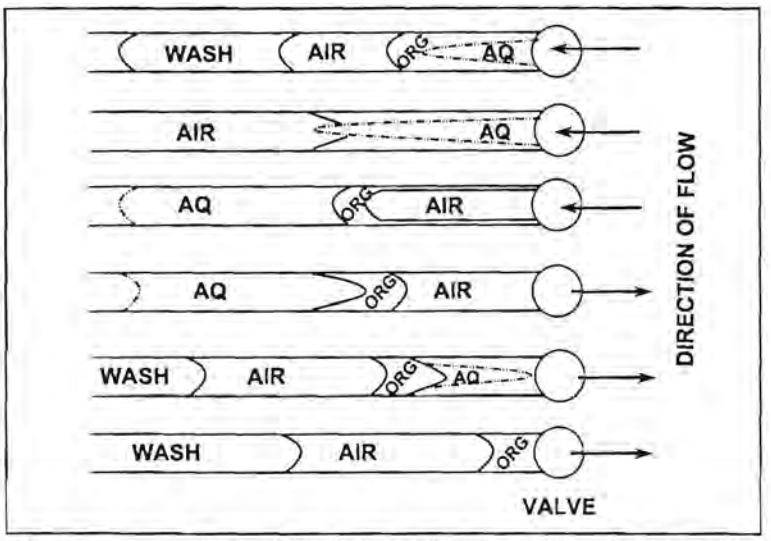

Fig. 4.1 Experimental protocol used in sequential injection wetting film extraction. AQ 1 and AQ 2 refer to the order in which the aqueous zones were drawn into the extraction coil and ORG represent the organic phase.

(6) On account of the difference in air and liquid movement, a fraction of the organic phase remains coated on the tubing, while the rest forms a segment that is aligned next to the valve head.

When a back-extraction step is needed, a second aqueous segment, buffered to an optimal pH, is aspirated into the extraction coil and passes through the organic phase as described above and the same sequence is repeated. During the second cycle, analytes are extracted out of the organic phase into the aqueous segment, which is collected through a collection port and analysed. Finally, the wash solvent, initially introduced, washes the organic layer of the tubing to waste, leaving the tubing ready for the next extraction.

As in the case with FIA extractions, the extraction efficiency was dependant on the residence time of the aqueous phase in the extraction coil. The length of the extraction coil has, therefore, a major role to play in allowing sufficient tubing to accommodate the distance needed for the zone inversion length. The volume of the organic phase as well as the flow rate will influence the zone inversion length and therefore also the length of the extraction coil [5, 6].

4.5 Theory on liquid-liquid extractions [7]

In analytical applications the liquid-liquid partition equilibria, which are commonly called extraction equilibria, usually take place between an aqueous solution (phase I, subscript aq) and an organic solvent (phase II, subscript org) which is immiscible with water. Such a partition equilibrium can be characterized (for a constant temperature and pressure) by the thermodynamic equilibrium constant $(K_{D,A})_a$ as defined in equation 4.1.

$$(\mu_A^0)_{aq} - (\mu_A^0)_{org} = -\Delta G_{D,A}^0 = RTln\frac{(a_A)_{org}}{(a_A)_{aq}} = RTln(K_{D,A})_a \qquad (4.1)$$

Where the quantities $(\mu_A^0)_{aq}$ and $(\mu_A^0)_{org}$ are the standard chemical potentials and $(a_A)_{aq}$ and $(a_A)_{org}$ the activities of substance A in the aqueous and organic phases, respectively. The standard chemical potentials of the substance A for the two phases as well as the values of ΔG_D^0 and $(K_{D,A})_a$ remain constant only for ideal behaviour of the system; this implies that the mutual solubility of the two liquids is negligible and that the solvation and the activity coefficients of the substances are not changed over a wide range of concentration.

For practical applications it is necessary to convert the thermodynamic constant $(K_{D,A})_a$ into the concentration partition constant $K_{D,A}$ (called the distribution constant).

$$K_{D,A} = \frac{[A]_{org}}{[A]_{aq}} = (K_{D,A})_a \frac{(y_A)_{aq}}{(y_A)_{org}} \qquad (4.2)$$

where $[A]_{org}$ and $[A]_{aq}$ represent the equilibrium molar concentrations of the substance A in the particular case. As shown by equation 4.2, the distribution constant is a true constant either for a dilute solution where the activity coefficients approach unity or for systems where the activity coefficients are controlled by the addition of an inert electrolyte. The change in the distribution constant due to variations in activity coefficients does not usually exceed one order of magnitude.

4.6 Extraction of metals

If a metal is extracted from an aqueous solution into an organic non-polar solvent, the metal ion is transferred across the liquid-liquid boundary as an uncharged particle which can be either an electroneutral complex (or chelate) formed with the organic reagent or an ion-association complex. Various types of ion-association complexes can be distinguished: (1) a large complex metal ion is associated with a large ion of opposite charge (e.g. $[(2,9\text{-dimethyl-1,10-phenanthroline})_2Cu]^+ . ClO_4^-$ or $[(C_6H_5)_4P]^+ . ReO_4^-$); (2) at least one of the ions is solvated with solvent molecules which are oxygen-donors (oxonium system); (3) metal salts of organic acids with large

molecules [(copper(II)caprate]).

In general, it is necessary to consider that the complexation equilibria in both phases involve formation of polynuclear mixed complexes. In these equalibria other ions and molecules can participate besides the metal ion and the ligand: the ions H^+ or OH^-, molecules of the organic extractant (denoted as HL), molecules of water and the organic solvent, S. The composition of the species formed can be expressed by a general formula

$$M_m(HL)_xH_{-y}(H_2O)_zS_s \qquad (4.3)$$

where coefficient *x* represents the number of molecules of the extracting reagent taking part in the formation of the complex. The coefficient *y* denotes the number of H^+ ions liberated from molecules of HL and H_2O by the formation of the complex species.

The average degree of hydration of complexes in the aqueous phase remains constant at a given temperature and ionic strength even when their equilibrium concentrations are changed. Generally unhydrated complex species are extracted into organic solvents of low permittivity. In some cases the formation of solvates with the organic solvent contributes favourably to the extraction (synergistic effect). The existence of polynuclear complexes of the type M_mL_n is shown by the dependance of the extraction on the total concentration of the metal in the aqueous solution. For most chelates the presence of polynuclear complexes has not been observed at all whereas for the ion-association systems it becomes apparent for $c_M > 10^{-3}$ mol/ℓ.

4.7 Dithizone as extractant

Pure diphenylthiocarbazone (Dithizone) (Fig. 4.2) is a blank or blackish-brown crystalline powder. It is insoluble in water and dilute acids and sparingly soluble in ethanol and ether. Dithiozone is soluble in hexane and carbon tetrachloride, freely soluble in chloroform, carbon disulphide and bases [8].

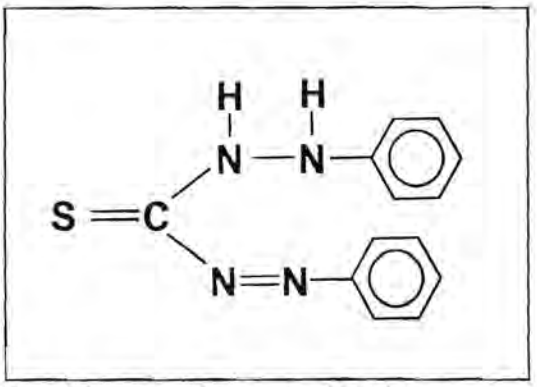

Fig. 4.2 Structure of Dithizone.

Dithizone reacts with a number of heavy metal ions to form intensely coloured complex compounds (dithizonates). Such heavy metals are known generally as "Dithizone metals". They are close to one another in the periodic table and form sulphides which are only slightly soluble in water. The Dithizone metals are listed in Table 4.1 (The metals printed in bold are used in this study).

TABLE 4.1 The different Dithizone metals as they appear on the periodic table.

Group	VII b	VIII	I b	II b	III a	IV a	V a	VI a
Dithizone metals	Mn	**Fe Co Ni**	**Cu**	**Zn**				
		Pd	Ag	**Cd**	In	Sn		Te
		Pt	Au	**Hg**	Tl	**Pb**	Bi	Po

Distinction is made between primary and secondary dithizonates, according to whether the metal ion reacting with Dithizone only replaces the imide hydrogen and forms the so-called keto-complex (I) or also react with the hydrogen of the thiol compound and forms the so-called enol complex (II). Most of the metals form secondary complexes, while mercury, cobalt and copper can form both primary and secondary complexes. This will be described in full in the appropriate chapters.

4.7.1 Disadvantages of Dithizone

Since Dithizone is such a sensitive reagent it necessitates the use of specially purified reagents and organic solvents with especially clean glassware. This high sensitivity

also imposes the need for unusually high standards of laboratory cleanliness. The latter is overcome by the fact that sequential injection systems are closed systems with minimum contact between the reagents, samples and products and the laboratory environment.

Dithizone is also not a very selective reagent, since it formed intensely coloured product with all Dithizone metals. Changing the pH values improve the selectivity of the reagent [8 - 11].

4.8 Choice of solvent

The organic liquid used in Dithizone should strictly speaking be termed the *diluent* for the active *extractant* Dithizone [9]. It is relevant to enquire what effect a change in diluent will have upon the value of the extraction constant, K_{eq}, for a given metal-Dithizone system and whether a change in organic solvent could improve the separability of two metals. It was, however, found that a change in diluent could not achieve any worthwhile improvement in separability of two metals [9].

There are, however, many other factors which influence the choice of diluent, even though when considering small-scale laboratory operations where purified solvents could be use, because economic factors are of secondary importance. The mechanical aspects of extraction involve properties such as surface tension, interfacial tension, viscosity and density, which affect the formation of droplets and hence the mass transference of dissolved constituents and the physical, as opposed to the purely chemical, aspects of the overall kinetics.

These factors also control the separation of droplets when agitation ceases and hence the speed of completeness of phase separation. With less dense solvents this consideration of phase separation may present problems, although there may be special cases where the use of a diluent not much less dense than water (e.g. cyclohexane or methyl isobutyl ketone) has special advantages [9].

Both carbon tetrachloride and chloroform are satisfactory for Dithizone extractions (and are most commonly used), for they do not readily form emulsions under normal conditions and the phases separate well. The toxicity of the vapours demands the use of a well-ventilated laboratory or the regular use of a fume chamber. Neither solvent is inflammable although contact of the vapours with bunsen burners operating in the vicinity may generate phosgene [9].

At room temperature both diluents are pretty resistant to hydrolysis and the action of acids, alkalis and other reagents involved in the Dithizone extractions. While carbon tetrachloride is preferred for purifying Dithizone and for the extractive titrations of Ag, Bi, Cu, Hg, Pd, Pt and Zn, for monocolour procedures and qualitative tests, chloroform has some advantages for the extractive titration of Au, Cd, In, Pb and Tl, for handling larger amounts of metals and for separations at high pH values.

Several solvent are suitable to dissolve Dithizone [9, 17]. These solvents as well as the solubility of Dithizone therein are listed in Table 4.2. A knowledge of the solubility of Dithizone in organic solvents is important when discussing its behaviour in two-phase extraction systems of analytical importance. The data show that the solubility in paraffinic and alicyclic solvent is low, as is the case with alcohols and ketones. Higher solubilities are reached in aromatic hydrocarbons and the highest values are found with the chlorinated paraffins, such as CCl_4, $CHCl_3$ and $C_2H_4Cl_2$.

Since solutions of Dithizone of any but the lowest concentration are deeply coloured, and often almost opaque, it is quite difficult to be certain whether excess solid is present in contact with a saturated solution. Special care is needed to ensure that metallic impurities are not introduced by the filtering medium, especially when the concentration is to be calculated afterwards from the absorbance of a suitably diluted aliquot and a knowledge of the molar (decadic) absorption coefficient, ϵ [9].

TABLE 4.2 Solubility of Dithizone in organic solvents

No.	Solvent	Solubility (g/ℓ)			
		0°C	20°C	30°C	35°C
1	Dichloroethane	-	21.66	-	-
2	Chloroform	1.7	16.9	20.3	19.0
3	Dichloromethane	-	-	12.6	-
4	Nitromethane	-	-	-	-
5	α-Bomonaphthalene	-	2.97	-	-
6	Carbon disulphide	1.62	2.83	-	3.60
7	Nitrobenzene	-	-	-	-
8	o-Dichlorobenzene	1.19	1.74	-	3.68
9	Chlorobenzene	0.894	1.43	2.5	3.15
10	Benzene	-	1.24	4.24	-
11	Acetonitrile	-	1.0	-	-
12	Toluene	0.35	0.95	-	1.87
13	Acetone	-	0.93	-	-
14	Methyl isobutyl ketone	-	0.805	-	-
15	Isopentyl formate	-	0.80	-	-
16	Isopentyl ethanoate	-	0.65	24.3	-
17	Carbon tetrachloride	0.272	0.512	0.74	1.27
18	Dioxan	-	0.349	-	-
19	Diethyl ether	-	0.4	-	-
20	Ethanol	-	0.3	-	-
21	n-Pentanol	-	0.054	-	-
22	Cyclohexane	-	0.014	-	-
23	Methylcyclohexane	-	0.01	-	-
24	n-Hexane	-	0.04	-	-
25	Water, pH < 7	-	5×10^{-5}	-	-
	Mixed solvents (v/v)				
26	2% $CHCl_3$-98% C_6H_{14}	-	0.0225	-	-
27	10% $CHCl_3$-90% C_6H_{14}	-	0.0964	-	-
28	20% $CHCl_3$-80% C_6H_{14}	-	0.295	-	-
29	50% $CHCl_3$-50% C_6H_{14}	-	2.56	-	-
30	70% $CHCl_3$-30% C_6H_{14}	-	6.93	-	-

Initially carbon tetrachloride was chosen as organic solvent for Dithizone (Chapter 9), but it was ruled out for further applications due to its toxicity and ozone depleting properties. A non-toxic solvent, ethanol, was used as solvent in all other extractions done (Chapters 8 and 10), due to its good film forming capacity.

The visible absorption spectrum of Dithizone is, however, very sensitive to the organic solvent in which it is dissolved [11]. Table 4.3 lists the visible absorption spectra of Dithizone in different solvents. The spectra obtained for Dithizone in CCl_4, hexane and ethanol are shown in Fig. 4.3.

TABLE 4.3 The visible absorption spectra of Dithizone in different solvents [11]

Solvent	λ_{max} (nm)	
	Peak 1	Peak 2
n-Hexane	617	447
Cyclohexane	623	452
Diethylether	615	440
Carbon disulphide	640	462
Ethanol	596	440
Toluene	622	450
Acetone	610	445
Carbon tetrachloride	620	450
Dioxan	617	446
Benzene	622	453
Chlorobenzene	622	452
Nitrobenzene	627	454
Dioxan-water [1:1 (v/v)]	602	446
Nitromethane	607	440
Chloroform	605	440
Tetrachloroethane	607	445

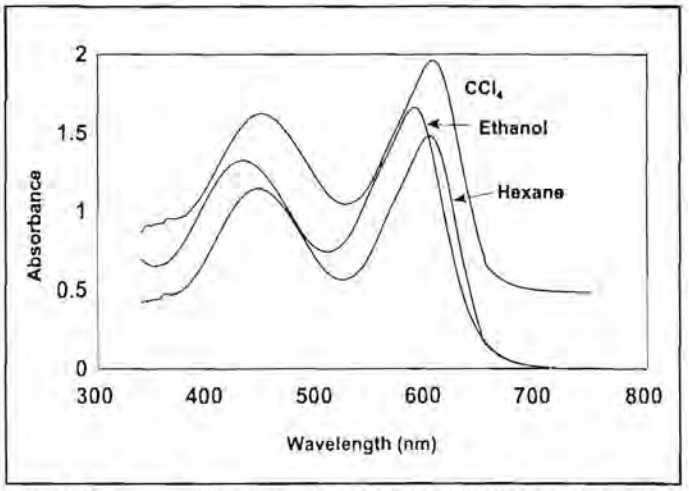

Fig. 4.3 Spectra obtained for Dithizone in carbon tetrachloride, ethanol and hexane.

The spectra of the different metal dithizonates determined in this study were obtained and are listed in Tables 4.4 to 4.6. Table 4.4 lists the dithizonates dissolved in carbon tetrachloride, Table 4.5 the dithizonates in hexane and Table 4.6 the dithizonates in ethanol.

TABLE 4.4 λ_{max} and the corresponding absorbance values for the extractions of metal ions with Dithizone in CCl_4

Metal ion	λ_{max} (nm)	Absorbance (AU)	λ_{max} (literature [8, 12, 18])	pH range
Dithizone	616 446	1.32 0.86	620 450	-
Cu^{2+}	441	0.75	450 550	7 - 14 2 - 5
Ni^{2+}	529	0.87	665	6 - 9
Co^{2+}	432 546	0.63 0.54	465 542	13 - 14.5 6.5 - 10.5
Pb^{2+}	508	0.73	520	6.5 - 10.5
Zn^{2+}	479	1.14	538	6.5 - 9.5
Fe^{3+}	540	1.20	-	7.5 - 8.5
Hg^{2+}	518	0.87	515 485	7 - 14 1 - 4
Cd^{2+}	520	0.68	520	6 - 14

These extractions were all perform at a pH between 6 and 7. Higher pH values were also evaluated, but some of the metal ions formed complexes with the NaOH and the results were inaccurate. Some of the formed dithizonates were not very stable - especially nickel changed from a dark red colour (λ_{max} = 529 nm) to a violet-brown colour (λ_{max} = 435 nm).

TABLE 4.5 λ_{max} and the corresponding absorbance values for the extractions of metal ions with dithiozone in hexane.

Metal ion	λ_{max} (nm)	Absorbance (AU)	λ_{max} (literature [12])	$pH_{½}$
Dithizone	426 619	1.015 0.721	447 617	-
Cu^{2+}	403 544	0.885 0.600	-	7 - 14 2 - 5
Ni^{2+}	404 528	0.559 0.444	-	6 - 9
Co^{2+}	401 531	0.636 0.685	-	13 - 14.5 6.5 - 10.5
Pb^{2+}	403	0.645	-	6.5 - 10.5
Zn^{2+}	425 625	1.267 0.939	-	6.5 - 9.5
Fe^{3+}	458	1.080	-	7.5 - 8.5
Hg^{2+}	488 521	0.541 0.545	-	7 - 14 1 - 4
Cd^{2+}	405	0.754	-	6 - 14

It was interesting to observe that except for three metal ions (lead, iron and cadmium), all the metal dithizonates gave spectra with two absorption maxima. Only for zinc the second λ_{max} corresponds with the peak for the reagent, Dithizone. The other metal dithizonates' second peaks all fall in the interval 401 - 405 nm. Unfortunately, hexane is not a reagent commonly used for extractions with Dithizone and no literature data could be found to verify these interesting results.

TABLE 4.6 λ_{max} and the corresponding absorbance values for the extractions of metal ions with Dithizone in ethanol.

Metal ion	λ_{max} (nm)	Absorbance (AU)	λ_{max} (literature [12])	$pH_{½}$
Cu^{2+}	447 -	0.812 -	-	7 - 14 2 - 5
Ni^{2+}	469	0.423	-	6 - 9
Co^{2+}	519 -	0.743 -	-	13 - 14.5 6.5 - 10.5
Pb^{2+}	500	1.37	-	6.5 - 10.5
Zn^{2+}	571	0.863	-	6.5 - 9.5
Fe^{3+}	425	1.92	-	7.5 - 8.5
Hg^{2+}	519 -	1.024 -	-	7 - 14 1 - 4
Cd^{2+}	436	0.934	-	6 - 14

Extractions with Dithizone in ethanol gave high intensity peaks. Since the extractions were all done at pH 6 - 7, the primary dithizonates of copper, cobalt and mercury did not form and no absorption peaks were observed. As in the case with hexane, it was impossible to obtain any literature values to verify these results.

4.9 Factors influencing film formation and thickness

When an organic solvent zone is injected into a flow system (FIA or SIA), the resulting segment shape depends primarily on the ratio between the segment volume and the inner radius of the tube, the total flow rate, the interfacial tension of the solvents, the surface tension of the solvents, the tubing material and a few other factors [1].

Depending on the material of the extraction capillary coil, the solvent displaying greater affinity to the tubing material will cover its inner walls with a very thin film of relatively stationary nature. The film of organic solvent will surround the deformed spherical, ellipsoidal or tubular aqueous segment(s) in fluoropolymer tubing, whereas the segment(s) of organic phase will be surrounded by an aqueous film in glass or metal

tubing.

As stated earlier, the driving force for the film formation is the minimization of the interfacial energy of the solid/liquid interface, which is determined by the relative magnitudes of the surface tension of the inner wall surface of the tubing to the liquids (wetting ability) and the interfacial tension in the liquids. The film thickness is related to the nature of the film-forming phase in such a way that higher viscosity and/or lower interfacial tension result in a thicker film [1, 6].

Another factor influencing the formation of the wetting film is the hydrodynamic forces connected with mass transport due to the velocity distribution of the laminar flow across the tube profile, as the segment of non-wetting solvent forms a compressible bolus flowing through the stream of the other solvent. Besides other factors influencing the segment shape, the mean value of the film thickness of one liquid behind a single plug of another, evidently depends on the linear velocity, u, of the flowing stream.

The linear velocities in FIA and SIA are generally low and the prevailing flow pattern is laminar. Consequently, the flow velocity near the tubing wall is zero, while in the centre of the tube it is twice the mean value taken along the radius. The film forms a relatively stationary phase along the wall, forcing a secondary internal flow to circulate within each segment [1].

The film formed by one phase on the tubing as a result of a linear velocity distribution across the tubing diameter or due to the wetting properties of the solvent, causes changes in the segment geometry. Assuming a constant volume, V_s, of the segment(s) of one immiscible phase in the continuous stream of the other phase, the lengthening of the aqueous phase segment caused by the wall film can be predicted.

The segment length, L_s, can be expressed as a function of the segment volume, V_s, and the outer radius of the cylindrical segment, r_s, which depends on the inner radius of the tubing, r_0, and the mean value of the film thickness, d_f ($r_s = r_0 - d_f$), in the form

$$L_s = V^s/(\pi r_s^2) = V_s/[\pi(r_0 - d_f)^2] \quad (4.4)$$

Here, the segment length, L_s, is inversely proportional to the second power of the outer radius of the segment, r_s. With increasing film thickness, d_f, L_s will decrease as a result of the decreasing outer radius of the segment at higher flow rate or linear velocity. The relative segment lengthening decreases with increasing tube inner radius [1]. Thickness of the wetting film is directly proportional to the inner diameter of the extraction coil. As a result, the extraction capacity is larger for wider and longer extraction coils [6].

The solvent composition, therefore, is a critical parameter for the successful application of sequential injection extraction, determining the difference in flow velocity between the organic and aqueous phases and the chemical selectivity and efficiency of the extraction. Due to hydrophobic interactions with the Teflon walls of the tubing, a fraction of the organic solvent, V_{org}, forms a stationary film, V_f, whose volume determines the overall flow velocity of the organic solvent, u_{org} [12].

$$u_{org} = \frac{(V_{org} - V_f)}{V_{org}} \times u_{aq} \quad (4.5)$$

Therefore, in a continuous pumping segmented stream of aqueous and organic phases, the flow velocity of the analytes in the organic phase is slower than that of analytes travelling in the aqueous phase. Sequential injection extraction, however, uses discrete zones of immiscible phases, not a continuous carrier stream. By loading the faster moving aqueous sample behind a slower moving organic solvent plug, the differential migration serves as a mechanism for both contacting and separating immiscible phases. A separated phase may be collected for subsequent operations and measurements [4].

The thickness of the organic film influences extraction by affecting the mass transfer of analytes in and out of the film. The film thickness, d_f, can be calculated using the formula

$$d_f = kd_t(u\eta/\gamma)^a \quad (4.6)$$

where u represents the flow velocity in m/s, d_t the tube diameter in m, η the viscosity of the solvent in cP (kg/ms) and γ the surface tension of the organic solvent in mN/m, with k approximately equal to ½ and a approximately equal to $^2/_3$ [4]. Although the flow rate, u, and the interior diameter of the tubing play a role in the calculation of the film thickness, the critical parameter in choosing an organic solvent is the value $^\eta/_\gamma$, called the film thickness parameter. The film thickness parameters for some selected organic solvents are given in Table 4.7.

TABLE 4.7 Film thickness parameter for some organic solvents

Solvent	Surface tension (γ) (mN/m) [13, 14]	Viscosity (η) (cP) [13, 14]	Film thickness parameter (η/γ)
Benzene	28.88	0.601	2.08×10^{-2}
Carbon tetrachloride	27.00	0.88	3.26×10^{-2}
Ethanol	22.80	1.06	4.64×10^{-2}
Hexane	18.40	0.31	1.68×10^{-2}
Methanol	22.60	0.553	2.45×10^{-2}

From this parameter it is observed that film thickness is directly proportional to viscosity and inversely proportional to surface tension. The performance of the film is especially sensitive to viscosity [6].

There is a trade off between the capacity of the film for the analyte and the ease with which the film can be eluted to a detector. Both these characteristics depend, predictably, on the thickness or viscosity of the film - thick films have high capacity, but are difficult to elute. As a lower limit, the film must be thick enough that it does not

break up during sample perfusion. As an upper limit, it must be possible to remove the quantitatively. Between these two limits, one should compromise between sensitivity and dynamic range. Lower capacity results in higher sensitivity, because a smaller volume of extractant solvent yields higher enrichment factors. Higher capacity allows for a higher breakthrough concentration [6, 19]. For a quantitatively extracted component, the breakthrough volume of an extraction coil is described by

$$V_1(breakthrough) = fV_{coil}\left(\frac{\Theta_{aq/org}}{1 + \Theta_{aq/org}}\right) \qquad (4.7)$$

where f is the dilution factor resulting in the aqueous solution, V_{coil} is the total volume of the extraction coil and $\Theta_{aq/org}$ is the ratio of aqueous phase to organic phase [19].

4.10 Verification of extraction results

Irrespective of the extraction method used, the extraction recoveries should be verified. This can be done by spiking a sample of similar composition to the sample analysed with a known content of the analyte. The main drawback is that the spike is not always bound in the same way as the naturally occurring analyte. It is therefore recommended to let the spike equilibrate at least overnight [15].

4.11 Conclusion

Liquid-liquid extractions represents one of the most progressive techniques of analytical flow systems since it is very applicable to important problems related to selectivity and sensitivity improvement in many branches of analytical chemistry. Liquid-liquid extraction flow systems has contributed to the solution of analytical problems in a great variety of areas, especially in clinical biochemistry, pharmaceutical chemistry and environmental chemistry, which require the separation and preconcentration of analytes from very complexed matrices.

Sequential injection extraction SIE provides more economical use of reagent and sample solutions as well as simplified manifolds compared to those of flow injection analysis. SIE manifolds do not need phase segmenters and separators which not only simplify the manifolds, but also exclude excessive dilution and other problems associated with these devices [16]. Despite the use of toxic organic solvents, the role of liquid-liquid extraction SIA in some areas will become indisputable.

4.12 References

1. V. Kubáň, **Crit. Rev. Anal. Chem., 22** (1991) 477.
2. M. Valcárcel and M. D. Luque de Castro, **Flow Injection Analysis. Principles and Applications**, John Wiley & sons, Chichester, 1988.
3. L. Nord and B. Karlberg, **Anal. Chim. Acta, 164** (1984) 233.
4. K. L. Peterson, B. K. Logan, G. D. Christian and J. Růžička, **Anal. Chim. Acta, 337** (1997) 99.
5. S. Nakano, Y. Luo, D. A. Holman, J. Růžička and G. D. Christian, **Microchem. Jour., 55** (1997) 392.
6. Y. Luo, S. Nakano, D. A. Holman, J. Růžička and G. D. Christian, **Talanta, 44** (1997) 1563.
7. Z. Holzbecher, L. Diviš, M. Král. L. Šůcha and F. Vláčil, **Handbook of Organic Reagents in Inorganic Analysis**, Ellis Horwood Limited, Chichester, 1976.
8. J. Fries and H. Getrost, **Organic Reagents for Trace Analysis**, E. Merck, Darmstadt, 1977.
9. H. M. N. H. Irving, **Dithizone**, The Chemical Society, London, 1977.
10. G. Iwantscheff, **Das Dithizon und seine Andwendung in der Mikro- und Spurenanlyse**, Verlag Chemie, Weinheim, 1958.
11. A. T. Hutton, **Polyhedron, 6** (1987) 13.
12. C. A. Lucy and K. K. Yeung, **Anal. Chem., 66** (1994) 2220.
13. P. W. Atkins, **Physical Chemistry**, fourth ed., Oxford University Press, Oxford, 1990, pp 293 - 969.
14. G. W. C. Laye and T. H. Laby (eds.), **Tables of Physical and Chemical Constants**, Longman, London, 1973.
15. A. M. Ure, C. M. Davidson and R. P. Thomas in Quevauviller, Maier and Griepink (eds.), **Quality Assurance for Environmental Analysis**, Elsevier Sciences, 1995, pp 505 - 521.
16. I. Facchin, J. J. R. Rothwedder and C. Pasquini, **Jour. Autom. Chem., 19** (1997) 33.
17. A. M. Kiwan, **Talanta, 44** (1997) 947.

18. B. Romberg and H. Müller, **Anal. Chim. Acta, 353** (1997) 165.

19. C. A. Lucy and S. Varkey, **Anal. Chem., 67** (1995) 3036.

CHAPTER 5

Analysis of Aqueous, Biological and Soil Samples

5.1 Introduction

The massive array of analytical techniques nowadays at one's disposal and the speed with which vast quantities of results can be generated are obliging the analyst to look 'downstream'. That is, they need to know exactly the use to which their results are to be put. This is to ensure that appropriate protocols can be designed for the use envisaged. A further development which is linked to the increasing skills of the analyst is an increasing move towards the determination of one or more components in *many* samples rather than the *total* analysis of a smaller number of samples.

Chemical analysis should be seen as a *whole process* stretching from collection, through pre-treatment, acquisition of results (the traditional view of analysis) to data processing and evaluation.

Once the field sample has been collected and transported to the laboratory, the analyst is usually faced with another group of activities prior to the actual acquisition of results. These may involve such activities as drying, measuring of weights or volumes, dissolution in solvents, separation from interfering materials and preconcentration of the analyte. Even drying a sample, which is often thought of as a trivial process, is not as straightforward as it seems.

A very important aspect of many analyses are the need to obtain the analyte in the form of a solution, either in water or in an organic solvent. However, there are many situations where it is undesirable to dissolve the sample completely. In these cases only certain soluble components of the sample will be extracted, leaving the rest of the sample in the solid state. This process is termed 'leaching' and describe the

procedure whereby one or more components are taken into solution, perhaps accompanied by a chemical reaction. The solution is then separated from the solid phase, perhaps by filtration [3] and analysed.

Soil analysis is traditionally carried out in soil laboratories for identification of potential soil deficiency or toxicity status of different soil types. This was done mostly for the prediction of likely effects on the food chain, functionally defined as the bioavailability of the different species to plants. This bioavailability is determined by the analysis of chemical extracts of soils by reagents, often empirically derived, that extract element concentrations which correlate with plant uptake, or with plant growth, yield or health. It must be kept in mind that total soil content is often a poor indicator of its bioavailability.

Clinical analysis of biological samples are a major part of analytical chemistry. These analysis need to be done at high frequencies and speed and the results must be accurate and reliable, since peoples lives are at stake. Quality control and pollution monitoring of natural waters, especially in a water scare country like South Africa, also became a large industry in the last few years.

5.2 Soil samples

5.2.1 Soil sampling

There is strictly speaking no right or wrong way to obtain a sample, provided that the sample taken is representative of the lot of which it originates. When sampling soil it is probably best to treat it as a particulate material containing a variety of sizes of particles. Provided none of the particles is very large, then some form of thief device (e.g. of the concentric-tube type) might prove useful. When the thief device proved to be inadequate, then it will be necessary to remove the soil sample by digging. This way a fairly large quantity of soil (usually in the range of 1 m^3) are removed. It would be necessary to break down the larger particles and sub-sample it by using the coning

and quartering technique [4].

The soil samples used throughout this study was obtained on a maize farm in the Northern Free State. Sampling was done by digging. A sample of 50 cm x 50 cm x 15 cm was dug out and sub-sampled after thorough mixing. The sub-samples varied in mass according to the inner volume of the mixing chamber used for extraction.

5.2.2 Sample pretreatment

Many solid samples, like soil samples, contain a potentially large, variable and indeterminate amount of water with them. This water content may vary on storage either through evaporation or through absorption of water vapour from the atmosphere. It would be impossible to analyse such samples quantitatively unless the water content was standardised between samples. This is normally done by drying the sample before analysis by some standard procedure, normally in an oven at temperatures close to 100°C [3].

For example, when pretreating a soil sample with the primary goal to determine bioavailable metal ions, the following procedure might be used [3]:

(1) Dry the sample at 105°C to constant weight.

(2) Pass the sample through a coarse sieve (low mesh-number) to remove large stones and other material. There is now need to grind the sample, since no complete dissolution is necessary. (This step would be included when determination of total metal content was required. When grinding a sample care must be taken that the process does not contaminate the sample [6]).

The sample is now ready to be weighed and purified. Purification (separation) of the analyte is done by either removing the analyte from the matrix or by removing the matrix. Several procedures are available, such as extraction (leaching) with a suitable extractant at a suitable pH, precipitation of interferents as insoluble salts or masking

of interferents with suitable masking agents [6].

The soil samples used for experiments was dried at 100°C for about 12 hours (overnight) and then left to cool to room temperature in a desiccator.

5.2.3 Soil extraction (leaching)

Most of the early studies of soil have been concerned with deficiency problems in plants or animals and successful extraction procedures have been validated by field experimental correlation between plant response and extract content over several seasons [1]. Soils are usually extracted with solutions containing chelating agents, such as DTPA or EDTA. Some of the soil extractants used to assess bioavailability of metals are summarised in Table 5.1.

TABLE 5.1 Extraction reagents for bioavailable heavy metal species in soils.

Extractant	Elements
Water	Cd, Cu, Zn
Sodium nitrate (0.1 mol/ℓ)	Cd, Pb
Ammonium nitrate (1 mol/ℓ)	Cd, Pb
Calcium chloride (0.05 - 0.1 mol/ℓ)	Cd, Cu, Mn, Ni, Pb
Ammonium acetate (1 mol/ℓ, pH 7)	Mo, Ni, Pb, Zn
Ammonium acetate/EDTA (0.5 mol/ℓ : 0.02 mol/ℓ)	Cu, Fe, Mn, Zn
EDTA* (0.05 mol/ℓ, pH 7)	Cd, Cu, Ni, Pb, Zn, Mo
DTPA* (0.005 mol/ℓ DTPA + 0.1 mol/ℓ TO* + 0.01 mol/ℓ $CaCl_2$)	Cd, Cu, Fe, Mn, Ni, Zn
2.5% HOAc	Cd, Co, Cr, Cu, Pb, Ni, Zn

* EDTA - Ethylenediaminetetraacetic acid
* DTPA - Diethylenetriaminepentaacetic acid
* TO - Triethanolamine

Extraction processes are not without problems. Calcium and magnesium usually interfere in the determinations of transition metals, because they compete against the metals for the chelating agents, especially when the pH is larger than 7. Fe(II)/Fe(III) and Zn(II) are usually interferents in determinations of other transition metals [2].

Extractions done in this study used 2.5% acetic acid as extractant, since all the analytes of interest could be leached therewith. These extractions were first tried on-line. This was done by placing the extraction unit (mixing chamber) in the sample uptake tube.

Several mixing chambers were built to use in the extractions. A schematic representation of a mixing chamber is given in Fig. 5.1. The dimensions used as well as the volumes that correspond to the different dimensions are given in Table 5.2.

TABLE 5.2 Measurements of the different mixing chambers used for extraction and mixing.

Diameter = 13 mm		Height = 8 mm	
Height (mm)	Volume (mℓ)	Diameter (mm)	Volume (mℓ)
4	0.642	18	2.714
6	0.907	23	4.431
8	1.172	-	-
10	1.438	-	-

Unfortunately, the soil particles were too finely divided and this led to extremely high back pressures - even with the largest mixing chamber used. The small soil particles also eventually blocked the SIA system. All extractions were therefore done off-line.

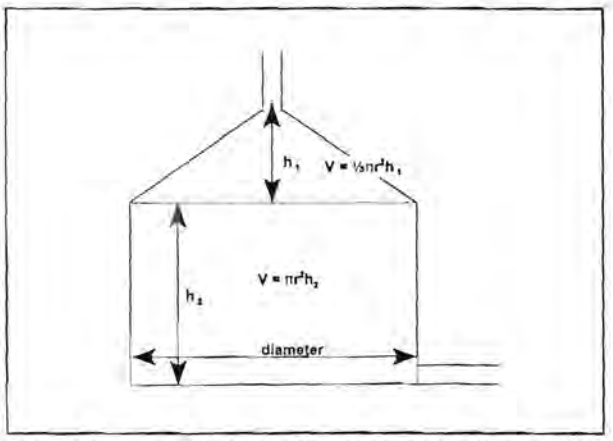

Fig. 5.1 Schematic representation of the mixing chambers used for extraction.

The extractions were done as follow: Sub-samples of 5.00 ± 0.02 g were weighed into 250 mℓ glass beakers and 50 mℓ aliquots of a 2.5% acetic acid solution were added. These mixtures were stirred for various periods, where after the pH was corrected to the reaction pH and the samples were analysed. The results obtained for the different stirring periods are summarised in Table 5.3. The soil samples were spiked with known amounts of both analytes, because the amount of nickel and cobalt in the samples were very low. Spiking the samples also allow the calculation of the percentage recovery or the extraction efficiency.

TABLE 5.3 Influence of various stirring periods on extraction efficiency

Time (min)	Known concentration in mg/ℓ		Concentration obtained with SIA in mg/ℓ		% Recovery	
	$[Co^{2+}]$	$[Ni^{2+}]$	$[Co^{2+}]$	$[Ni^{2+}]$	$[Co^{2+}]$	$[Ni^{2+}]$
10	3.50	3.00	2.79	2.09	79.7	69.7
20	3.50	3.00	3.05	2.58	87.14	86.0
30	3.50	3.00	3.21	2.63	91.7	87.7
40	3.50	3.00	3.23	2.65	92.3	88.3
50	3.50	3.00	3.25	2.64	92.9	88.0
60	3.50	3.00	3.24	2.68	92.6	89.3
120	3.50	3.00	3.25	2.70	92.9	90.0
360	3.50	3.00	3.26	2.74	93.1	91.3
720	3.50	3.00	3.30	2.70	94.3	90.0

Although most of the 'bioavailable' nickel and cobalt were extracted after a stirring period of 30 minutes, longer times were evaluated to improve the recovery of the analytes. This was clearly not successful. The results of a stirring period of 30 minutes compared to a stirring period of 12 hours are virtually the same. A extraction period of 30 minutes would therefore be sufficient to determine the soluble metal ions in the soil sample. Most of the samples were, however, stirred for 12 hours, since it was convenient to have the sample ready the next morning. Phase separation was done by simple decantation of the liquid phase. After pH corrections, the samples were analysed using the kinetic method described in Chapter 7.

5.3 Biological samples

Clinical analysis involve numerous determinations of analytes in matrices like blood and urine. In this study, urine was chosen as clinical matrix to verify the sequential injection analysis systems' applicability to clinical analysis.

5.3.1 Sampling and preservation of urine

The urine was sampled and stored in polyethylene bottles, which was thoroughly rinse with diluted hydrochloric acid. These samples were immediately frozen. Prior to analysis it was allowed to come to room temperature and then diluted.

When urine is allowed to stand about, particularly in a warm place, it usually acts as a culture medium for miscellaneous organisms. Commonly urea-splitting bacteria multiply and convert urea into ammonia. This causes the urine to be alkaline with consequent loss of ammonia. A secondary result is the precipitation of substances that are insoluble in alkaline media, particularly calcium phosphate, so that the specimen is unsuitable for analysis of these constituents. Much of the difficulty can be avoided if reasonable cleanliness is observed in taking and keeping the specimen and if it is kept cold, preferably refrigerated. If this is impossible, it may be necessary to use a preservative, particularly in the case of 24-hour collections [5].

The following preservatives are available [5]:

(1) *Hydrochloric acid.* Acidification of the specimen is a very satisfactory method of preservation and is suitable for nitrogen, ammonia, calcium and phosphorus determination. It is not suitable for uric acid, which is precipitated.
It is safer to use the diluted acid rather than the concentrated acid, which is sometimes recommended, particularly as the bottles are frequently sent to wards and clinics.

(2) *Toluene.* This is commonly used but of doubtful efficiency. It is convenient for sodium and potassium, uric acid and protein analyses.

(3) *Hibitane.* For urine glucose determination, a preservative is required which is neither a reducing agent (as is chloroform or thymol) nor an enzyme inhibitor (such as formalin or mercuric salts), but will, nevertheless, prevent destruction of glucose.

(4) *Glacial acetic acid.* This is used for ascorbic acid and 5-hydroxy-indolylacetic acid determinations.

5.3.2 Sample pretreatment

Most of the urine samples underwent only a dilution step as sample pretreatment. Filtering of samples might be necessary if suspended solids are present. Frozen samples must first be brought to room temperature, shaken thoroughly and then analysed.

5.3.3 Extraction of samples

To extract or separate the analyte from the matrix, liquid-liquid extractions were employed. For the systems described in this study, the diluted urine was introduced directly into the sequential injection system and the metal ions were extracted into the thin film of organic solvent (containing dithizone) coating the Teflon walls of the extraction coil tubing. The metal dithizonates in the organic phase are intensely coloured and provide sensitive determination of the various metal ions.

5.4 Aqueous solutions

5.4.1 Sampling of liquids

At the outset, liquids appear to present less of a problem to the sampler than for instance particulate solids. However this is true only when [4]:

(1) the quantity of the liquid to be sampled is small and thus can be homogenised by shaking it;
(2) the liquid is composed of only one phase.

Great care must be taken and attention paid when sampling larger quantities of liquid. Liquids for sampling in bulk may be divided into four categories [4]:

(1) those flowing in open systems (e.g. rivers, canals or industrial effluents),
(2) those flowing within closed systems (e.g. in pipelines),
(3) those stored in closed containers (e.g. tanks, drums or carboys),
(4) liquids in open bodies (e.g. lakes or reservoirs).

5.4.1.1 Liquids flowing in open systems

Since environmental monitoring and control include the study of the quality of water, it is not only necessary to determine substances in natural water, but also to control the amount of polluting substances that are added to natural water systems by means of industrial effluents.

The chemical composition of flowing water may vary according to changes in a number of parameters such as temperature, flow rate, distance from source, depth, pollution and sources of water. None of these parameters could be controlled by the sampler. Because of this large number of factors, it is difficult to draw accurate conclusions as a result of a single sample being taken. The full information may be available only after

a large number of samples have been analysed.

The samples are commonly collected by using wide-necked bottles or canisters, which are immersed at a suitable point in a flowing stream. For sampling at various depths, a weighted glass bottle with removable stopper is a simple but effective device. From the surface of the river, the bottle is lowered into the water to the required depth, as measured by the length of rope or chain holding the basket. The stopper is then removed and the sample taken. The device is then hauled back to the surface and the sample is transferred to a suitable container for storage.

5.4.1.2 Liquids flowing within closed systems

Taking samples flowing in pipelines are an important way to ensure quality control in industries. When sampling liquids flowing within closed systems, it is important that the flow rate of the liquid is taken into account. At low flow rates laminar flow predominates. This results in the liquid flowing at a velocity maximal at the centre of the pipe and decreasing to zero to the wall. In order to ensure homogeneity, it is preferable that turbulent flow is created just before the point where the sample is taken. Liquids flowing at higher rates already flow turbulently and thus no further action is needed prior to sampling.

The sample is removed, where possible, from the direction opposite to that of the flow. This is to avoid the sample being forced out of the sampling tube by the flow of the liquid. The diameter of the sampling nozzle must be chosen in such a way to ensure the correct sample flow rate into either the collection vessel or the analyser [4].

5.4.1.3 Liquids stored in closed containers

Products that are stored in containers might deteriorate with time or become contaminated. Any liquid stored in a tank is liable to stratification due to the differing densities of liquids held in the tank. Therefore, if it is impossible to homogenise the lot

prior to sampling it, increments of samples must be taken at different depths. The same devices can be used as described in section 5.3.1.1. Once a sample has been received by the laboratory, any further sub-sampling can be carried out after shaking the sample to ensure that it is homogeneous [4].

5.4.1.4 Liquids in open bodies

'Open bodies of liquids' signifies large volumes of liquids in essentially static conditions. In order to obtain a representative sample of for instance a lake, it will be necessary to sample the liquid at various depths. However, if the lake is not too deep and the sampling is to be carried out on a regular basis, then it is worthwhile constructing a permanent sampling device at specific points in the lake [4].

5.4.2 Storing of samples

Ideally samples should be analysed immediately. If this is, however, impossible, samples must be stored in cool places (preferably refrigerated) and be analysed as soon as possible. If the analyte concentration in the sample is very low, acidification of the sample is advised. This would prevent the adsorption of the analyte to the sides of the container.

5.4.3 Pretreatment of samples

Pretreatment of aqueous samples involve one of the following operations: dilution, preconcentration, filtering, decolourising or pH corrections. Dilution is the simplest of these methods, since it only involve the addition of a known amount of solvent (water) to a known aliquot of the sample. pH corrections are done by adding an appropriate amount of acid, base or suitable buffer to the sample. Coloured sample may interfere in photometric determinations. Decolourisation can be brought about by passing the sample through a column of deactivated carbon or to use dialysis to remove the coloured matrix.

Preconcentration is done mainly by passing the sample through a column with a suitable resin, such as an ion-exchange resin. The analyte is removed from the matrix, usually containing excess solvent, and eluted with a small volume of elutant to increase its concentration. Suitable ion-exchange resins to preconcentrate metal ions are: 8-hydroxyquinoline-formaldehyde-resorcinol (HOQFR), 8-hydroxyquinoline-formaldehyde-hydroxyquinone (HOQFHQ), 8-hydroxyquinoline-furaldehyde-resorcinol (HOQFuR), 8-hydroxyquinoline-furaldehyde-hydroquinone (HOQFuHQ) and 8-hydroxyquinoline-bensaldehyde-resorcinol (HOQBR) [7]. Other resins include: Amberlite IRA-400 (chloride form) [8] and 8-quinolinol [9]. Recently, algae and other organisms such as yeast have been exploited as analytical reagents to preconcentrate trace metals [10, 11]

When analysing samples that are liquids or solutions, the suspended solid particles therein may interfere with the determination. If so it may be necessary to separate the suspended solids from the bulk of the sample. This would normally be done by conventional filtering techniques, although centrifugation may also be used. The most inexpensive way of filtration is the use of filtering paper. A number of porosities are available. Coarse papers filter solutions quite quickly, while fine papers require a great deal of time and patience. The largest porosity that will still retain the precipitate must be chosen. Care must be taken that the sample is not contaminated during filtration.

5.4.4 Separation techniques used for aqueous samples

Either the analyte or the matrix could be removed, when removing interfering species. These separation techniques include precipitation of the interferent with a suitable complexing agent, or simply by masking the interferent using a suitable masking (complexing) agent. Liquid-liquid extractions are also frequently used. In this study, the metal ions were extracted into the thin organic film formed against the Teflon walls of the extraction coil tubing.

5.5 Conclusion

All analytical methods involve sampling and virtually every method involves some sort of sample pretreatment. This pretreatment step often is a significant and major part of the overall procedure. When evaluating an analytical method, deciding whether its performance is suitable for the purpose intended to, or when comparing two methods, it is important that the pretreatment stages are considered very carefully. What happens at the pretreatment stage may well govern: (1) the overall accuracy and reliability of the results obtained, and/or (2) the total time and effort involved in performing the analysis. Usually, a method involving minimum sample pretreatment is favoured, provided that it is capable of delivering results of acceptable accuracy and reliability.

5.6 References

1. A. M. Ure, C. M. Davidson and R. P. Thomas in Quevauviller, Maier and Griepink (eds.), **Quality Assurance for Environmental Analysis**, Elsevier Sciences, 1995, pp 505 - 521.
2. H. L. Bohn, B. L. McNeal and G. A. O'Conner, **Soil Chemistry**, second edition, John Wiley & sons, Inc., New York, 1985.
3. R. Anderson, **Sample Pretreatment and Separation. Analytical Chemistry by Open Learning**, John Wiley & Sons, Chichester, 1987.
4. B. W. Woodget and D. Cooper, **Samples and Standards. Analytical Chemistry by Open Learning**, John Wiley & Sons, Chichester, 1986
5. A. S. Prasad and D. Oberleas, **Trace Metals in Human Health and Disease: Volume 1, Zinc and Copper**, Academic Press, New York, 1976.
6. L. W. Potts, **Quantitative Analysis. Theory and Practice**, Harper & Row, New York, 1987.
7. R. Purohit and S. Devi, **Analyst**, **120** (1995) 555.
8. J. L. Burguera and M. Burguera, **Anal. Chim. Acta**, **127** (1981) 199.
9. F. Malamas, M. Bengtsson and G. Johansson, **Anal. Chim. Acta**, **160** (1984) 1.
10. H. A. M. Elmahadi and G. M. Greenway, **Jour. Anal. Atom. Spectros.**, **9** (1994) 549.

CHAPTER 6

Tandem Sequential Injection Analysis: Determination of Iron and Sulphate

6.1 Introduction

Iron has been known since prehistoric times and no other element has played a more important role in man's material progress. Iron beads dating from around 4 000 BC were without doubt of meteoric origin and later samples, produced by reducing iron ore with charcoal, were not cast because temperatures were not attainable without the use of some form of bellows. Instead, the spongy material produced by low-temperature reduction would have had to be shaped by prolonged hammering. It seems that iron was first smelted by the Hittites in Asia Minor sometime in the third millennium BC, but the value of the process was so great that its secret was carefully guarded and it was only with the eventual fall of the Hittite empire around 1 200 BC that the knowledge was dispersed and the "Iron Age" began. In more recent times the introduction of coke as the reductant had far-reaching effects and was one of the major factors in the initiation of the Industrial Revolution. The name "iron" is Anglo-Saxon in origin (*iren*, cf. German *Eisen*). The symbol Fe and words such as "ferrous" were derived from the Latin *ferrum*, iron [1].

Iron is thought to be the main constituent of the earth's core as well as being the major component of "siderite" meteorites. In the earth's crustal rocks it is the fourth most abundant element (after oxygen, silicon and aluminium) and the second most abundant metal. It is also widely distributed, as oxides and carbonates, of which the chief ores are: haematite (Fe_2O_3), magnetite (Fe_3O_4), limonite ($\sim 2Fe_2O_3.3H_2O$) and sederite ($FeCO_3$). Iron pyrite (FeS_2) is also common, but it is not used as a source of iron because of the difficulty in eliminating the sulphur. The distribution of iron has been

considerably influenced by weathering. Leaching from sulphide and silicate deposits occurs readily as $FeSO_4$ and $Fe(HCO_3)_2$, respectively. In solution, these are quickly oxidised and even mildly alkaline conditions cause the precipitation of iron(III) oxide [1].

Sulphur is widely distributed in nature, but it is seldom concentrated enough to justify economic mining. Its ubiquitity is probably related to its occurrence in nature in both inorganic and organic compounds and to the fact that it can occur in at least five oxidation states: -2 (sulphides, H_2S and organosulphur compounds), -1 (disulphides, S_2^{2-}), 0 (elemental sulphur), +4 (SO_2) and +6 (sulphates). Elemental sulphur in the caprock of salt domes was almost certainly produced by the anaerobic bacterial reduction of sedimentary sulphate deposits (mainly anhydride or gypsum). An interesting discovery recently made is that sulphur, together with sulphuric acid, forms a major component of the atmosphere of the planet Venus [1].

Sulphur occurs in many localities as the sulphates of electropositive elements and to a lesser extent as sulphates of Al, Fe, Cu and Pb. Gypsum ($CaSO_4.2H_2O$) and anhydride ($CaSO_4$) are particularly notable. Similarly, by far the largest untapped source of sulphur is in the oceans as the dissolved sulphates of Mg, Ca and K. It has been calculated that there are some 1.5×10^9 cubic km of water in the oceans of the world and that 1 cubic km of sea-water contains approximately 1 million tonnes of sulphur combined as sulphate [1].

6.2 Biological and industrial importance of iron and sulphate

Biologically, iron plays crucial roles in the transport and storage of oxygen and also in electron transport and it is safe to say that, with only a few possible exceptions in the bacterial world, there would be no life without iron [1]. Iron is the most important transition element involved in living systems, being vital to both plants and animals. The stunted growth of the former is well known on soils which are either themselves deficient in iron, or in which high alkalinity renders the iron too insoluble to be accessible to the plants. In case of man, iron was the first minor element to be

recognised as being essential when, in 1681, it was used to treat anaemia. The adult human body contains about 4 g of iron of which about 3 g are in the form of haemoglobin and this level is maintained by absorbing a mere 1 mg of iron per day - a remarkably economical utilization [1].

Industrially, iron is as important. It is used as iron nails, iron boats and ships, iron aqueducts and iron-framed buildings. However, it is not in the pure state, but in the form of an enormous variety of steels that iron finds its most widespread uses, the world's annual production being of the order of 700 million tonnes [1].

Pollution of fresh water sources is a main concern as it will determine the quality of the final water product. Industrial effluents and leaching of pollutants due to agricultural activities are the main reasons for the need of water purification. Water purification and recycling is nowadays a major industry. The method of treatment depends upon the source of the water, the use envisaged and the volume required. Since an excess of any element in water can be considered to be pollution, the World Health Organization's drinking water standards are listed in Table 6.1.

TABLE 6.1. World Health Organization drinking-water standards

Material	Maximum desirable [ ] in mg/ℓ	Maximum permissible [ ] in mg/ℓ
Total dissolved solids	500	1500
Mg	30	150
Ca	75	200
Chlorides	20	60
Sulphates	200	400

Although soil sulphur tends to be associated with the soil's organic fraction and plant and microbial uptake of sulphate and incorporation into organic compounds tend to maintain the sulphur content of soil [2], sulphates are potentially easily leached from soils. These sulphates increase the concentration of sulphates in water which are meant to become drinking water.

Highly weathered soil contain high amounts of iron, but because the low solubility of iron hydroxide (iron polarize its associated water molecules and repel H^+ ions) Fe is leached only very slowly from soil, resulting in low concentrations of iron in drinking water. Unfortunately, highly acidic conditions can arise from exposure to air of mine spoils containing iron pyrite [2]. The pyrite oxidises to sulphuric acid and $Fe(OH)_3$, leaving acidities of pH 2 or lower. It seems therefore needed that iron and sulphate may be determined simultaneously in the same sample. Together iron and sulphate can also deliver a positive contribution to the environment. Sulphate is the cheapest salt of Fe^{3+} and forms no less than six different hydrates (12, 10, 9, 7, 6 and 3 mols of water of which $9H_2O$ is the most common); it is widely used as a coagulant in the treatment not only of potable water but also sewage and industrial effluents. Addition of $Fe_2(SO_4)_3$ produces flakes of $Fe(OH)_3$ that can be filtered off [1].

Other industrial applications of sulphate include the paper industry where 'salt cake' (Na_2SO_4) is a key chemical in the kraft process for making brown wrapping paper and corrugated boxes [1]. Smaller amounts of Na_2SO_4 are used in glass manufacturing and detergents. Gypsum, $CaSO_4.2H_2O$, is a major industrial mineral. Most of the gypsum is for Portland cement or agricultural purposes.

Sulphur dioxide is made commercially on a large scale, either by combustion of sulphur or H_2S or by roasting sulphide ores (particularly pyrite, FeS_2) in air. It is also produced as a noxious and undesirable byproduct during the combustion of coal and fuel oil. The ensuing environmental problems and the urgent need to control this pollution are matters of considerable concern and activity. The detection of SO_2 in the atmosphere has become a refined analytical procedure. Several techniques are available. Some of these are based on sulphate determinations [1].

6.3 Choice of analytical method

Several approaches have already been described for the determination of sulphate ions in various materials. The existing manual methods, for example the standard

gravimetric method [3] and the titrimetric methods [4 - 6], including the potentiometric methods with ion-selective electrodes, which usually involve precipitation titrations with lead(II) solution and a lead sensitive electrode [5 - 11], are all cumbersome, tedious and time-consuming. Accordingly, a number of spectrophotometric methods for determining sulphate have been developed. The three methods that appear to be used most frequently are the barium chloroanilate method [6, 12, 13], the methylthymol blue method [14] and the barium sulphate turbidimetric procedure [15]. A number of methods have also been adapted to flow-injection analysis for the determination of sulphate. The spectrophotometric methods include the methylthymol blue method [16], the dimethylsulphonazo-III-(sulhonazo-III) procedure [17, 18], the barium chloroanilate method [19] and the barium sulphate turbidimetric method [20 - 22].

Madsen and Murphy [16] reported a FIA procedure for the determination of sulphate in rain water using the automated methylthymol blue (MTB) method. Samples were drawn through a cation-exchange column in the sample line in order to eliminate interferences from some cations. The procedure is sensitive with a detection limit of 0.1 mg/ℓ, but has a narrow linear range (0.1 to 6.0 mg/ℓ) and samples with higher sulphate values had to be diluted manually before analysis. The method is not very precise (RSD of 4.1%) and with a rate of 20 samples h^{-1}, the throughput is rather low, when compared with a normal sample capacity for FIA of about 40 to 60 samples h^{-1}. Kondo *et al.* [23] report on the sensitive determination of sulphate in river water. This method suffers from a relatively low sample throughput (30 samples h^{-1}) and also has a limited calibration range (0 to 30 mg/ℓ).

The method that appears to be used almost universally is the barium sulphate turbidimetric procedure. Krug *et al.* [24] first adapted the turbidimetric sulphate procedure to FIA, using various types of flow systems with more than one reagent or carrier stream. A sampling rate of 180 samples h^{-1} was achieved, the concentration range was extended to 140 mg/ℓ with a good precision (0.85%). Basson and van Staden [23] improved on the 40 samples h^{-1} for the segmented barium sulphate turbidimetric procedure. The sampling rate was increased to about 200 samples h^{-1} and

the flow diagram simplified to a single carrier reagent stream. The precision was however unacceptable (3.9%).

As in the case of sulphate, there are ample techniques available to determine iron in different matrixes. Manual methods include gravimetric analysis using 8-hydroxyquinoline or cupferron [6], photometric titrations [26] or potentiometric determination [26]. A number of reagents are also used in the photometric determination of iron and most of the methods employing these reagents are adapted to FIA and SIA systems.

Zolotov *et al.* [27] used xylenol orange to determine iron(III) in a FIA system that also include on-line preconcentration of the analyte, while Kang *et al.* [28] described a photometric determination of iron using 2-(5-bromo-2-pyridylazo)-5-(N-propyl-N-sulphopropylamino)aniline. Reagents that are being used extensively in flow injection analysis, and now also in SIA, are 1,10-phenantroline [26, 29 - 31], thiocyanate [32 - 35] and tiron (4,5-dihydroxy-1,3-benzenedisulfonic acid) [36 - 38].

The reactions chosen for this tandem determination were the turbidimetric determination of sulphate together with the photometric detection of iron employing tiron. Reasons for this decision included the fact that both systems were already adapted (to a certain extent) to SIA [36, 39], which made the instrumental setup easier and the two reactions took place at approximately the same pH (2 - 2.5) The main reason was, however, that since the absorbance of a suspension was measured in the case of sulphate, the absorbency could be measured at the same wavelength as the iron-tiron complex. This made the use of a single detector possible, which resulted in a more cost-effective system.

6.4 Principle of the reactions chosen for the tandem-SIA system

6.4.1 Principle of the turbidimetric determination

The turbidimetric determination of sulphate is based on the following reaction:

$$SO_4^{2-}{}_{(aq)} + BaCl_{2(aq)} \rightarrow BaSO_4\downarrow + 2\ Cl^-{}_{(aq)}$$

A colloidal barium sulphate suspension, which is pH dependant, is formed. The accuracy and precision, therefore, depend critically on the crystalline form and size distribution of the light-scattering particles in the suspension. The degree of suspension is controlled by several factors and therefore the concentrations related to reagents and precautions preparing the reagents must be strictly followed.

Polyvinyl alcohol [24] and gelatine [25] have been used to stabilise the barium sulphate suspension in order to obtain a relatively good precision. Thymol is added to the reagent to prevent bacterial growth [40].

6.4.1.1 Colloidal suspensions

A colloidal state exists when particles with sizes in the range of 1 - 250 nm are dispersed in a medium [26]. Because turbidimetric determinations rely on the formation of stable colloids, it is essential to find conditions favouring the formation of colloidal suspensions. To produce this type of suspension it is necessary that a large number of small nuclei must form immediately when the reagents are mixed together.

Although the exact mechanism by which nuclei form depends on the characteristics of each particular system, there are two models which are appealing in their simplicity. According to the first, nuclei can form "homogeneously" within the liquid phase. Local concentration fluctuations in solutions bring together aggregates of ion pairs. Crystals form around these aggregates. According to the second model, nuclei are formed

"heterogeneously" around foreign particles, such as dust, present in the solution.

Once a nucleus has been formed, a crystal can grow by a two-step process involving *diffusion* of solute ions to the nucleus surface and their subsequent *deposition*. The rate of growth can be limited by either process. The rate of diffusion depends on the concentration of the ions near the surface and in the bulk of the solution and the temperature, whereas the rate of deposition depends on the nature of the surface and the pattern of crystal growth [26].

Because a large number of small nuclei is needed for a colloidal suspension, nuclei formation is accelerated by addition of gelatine as 'seed crystals'. When a large number of nuclei form very fast the dissolved solute is used up so quickly that the nuclei cannot grow very large, resulting in the large number of small nuclei needed for a colloidal suspension.

The turbidimetric determination is based on the optical properties of the colloidal suspension. A true solution of ions is said to be "optically empty", because when a beam of light is shone through the solution no light is scattered at right angles to the light path. If, however, particles larger than about 10 nm are dispersed in a solvent, light is scattered at right angles at high intensities (the Tyndall effect) [26].

6.4.2 Principle of the iron-tiron reaction

Since total iron was determined with this system, it was important to ensure that all the iron are in the 3+ oxidation state. This was done by adding $K_2Cr_2O_7$ to each sample to ensure complete oxidation of all iron(II) to iron(III). To ensure that the iron(III) was not reduced to iron(II) again the reagent as well as the standards were dissolved in $HClO_4$ solution. Iron(III) reacts with tiron (Fig. 6.1) on a 1:1 basis, yielding a blue iron-tiron complex. This complex is pH dependant. At pH 9.8 a red to yellow colour develops on addition of iron, while a blue colour develops at pH values in the acidic range (2 - 4) [6]. For this application a pH of 2.5 was used, because the pH needed

for the sulphate determination was 2.5.

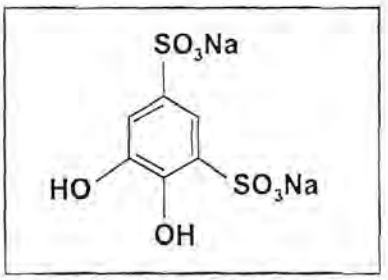

Fig. 6.1 Structural formula of tiron.

6.5 Determination of iron and sulphate with sequential injection analysis

6.5.1 Experimental

6.5.1.1 Reagents and solutions

All reagents were prepared from analytical-reagent grade unless specified otherwise. All aqueous solutions were prepared with doubly distilled deionised water. All solutions were degassed before measurements.

Standard sulphate solutions: A stock solution containing 5 000 mg/ℓ of sulphate was prepared by dissolving 16.7715 g $Na_2SO_4.10H_2O$ (Merck) in distilled water and diluting it to 1 ℓ. Working solutions in the range of 1 - 500 mg/ℓ were prepared by suitable dilution of the stock solution.

Buffer solution: 40 g of EDTA (disodium salt) (Merck), 7 g of ammonium chloride (Merck) and 57 mℓ concentrated ammonia (sp. gr. 0,88) (Riedel-de-Haën) were dissolved in 500 mℓ distilled water and diluted to 1 ℓ.

Barium chloride solution: A potassium hydrogen phthalate - hydrochloric acid buffer at pH 2.5 was prepared by adding 388 mℓ of a 0.1 mol/ℓ HCl solution to 500 mℓ of a 0.1 mol/ℓ potassium hydrogen phthalate solution. 15 g of $BaCl_2.2H_2O$ (Merck), 1.0 g thymol and 0.62 g gelatine were dissolved in this buffer and the solution was diluted to 1 ℓ. The reagent was filtered through a Millipore membrane (type HA) (45 µm).

Standard iron solutions: A 1 000 mg/ℓ iron(III) stock solution was prepared by dissolving 72.34 g $Fe(NO_3)_3.9H_2O$ (Merck) in 1 ℓ of a 0.01 mol/ℓ $HClO_4$ solution. Working solutions in the range of 1 - 500 mg/ℓ were prepared by suitable dilution of the stock solution with 0.01 mol/ℓ $HClO_4$ solution.

A 0.1 mol/ℓ tiron (4,5-dihydroxy-1,3-benzenedisulfonic acid) (Aldrich) stock solution was prepared by dissolving 3.142 g tiron in 100 mℓ 0.01 mol/ℓ $HClO_4$. A working solution of 500 mg/ℓ (1.6×10^{-3} mol/ℓ) tiron was prepared by suitable dilution of the stock solution with 0.01 mol/ℓ $HClO_4$. A 0.01 mol/ℓ $HClO_4$ solution was used as carrier solution.

6.5.1.2 Apparatus

The sequential injection system depicted in Figure 6.2 were constructed from the following components: a Gilson Minipuls peristaltic pump (operating at 10 rpm); a 10-port electrically actuated selection valve (Model ECSD10P; Valco Instruments, Houston, TX, USA) and a Unicam 8625 UV-visible spectrophotometer equipped with a 10-mm Hellma type flow-through cell (volume: 80 µl) for absorbance measurements. The barium sulphate suspension as well as the iron-tiron complex formed, were monitored by measuring the absorbance at 667 nm. Data acquisition and device control were achieved using a PC30-B interface board (Eagle Electric, Cape Town, South Africa) and an assembled distribution board (MINTEK, Randburg, South Africa). The *FlowTEK* [41] software package (obtainable from MINTEK, Randburg, South Africa) for computer-aided flow-analysis was used throughout for device control and data acquisition.

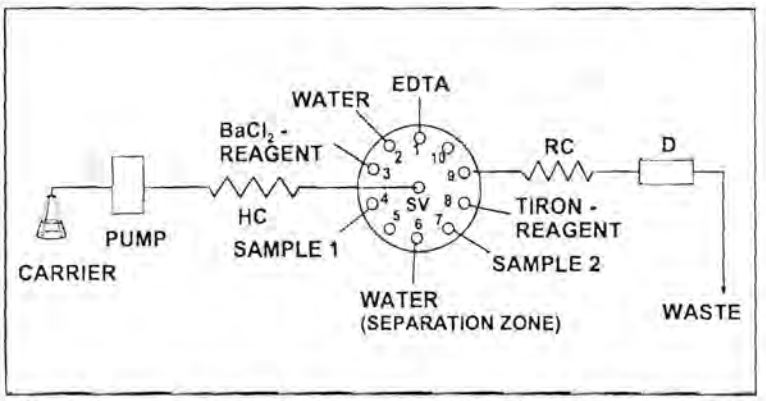

Fig. 6.2 A schematic diagram of the SIA system used for the simultaneous determination of iron and sulphate. HC - holding coil, RC - reaction coil, SV - selection valve and D - detector.

6.5.1.3 Manifold

The components of the SIA system were arranged as illustrated in Fig. 6.2. The holding coil was made of 6.5 m x 1.02 mm i.d. coiled Tygon tubing (tubing was coiled around a perspex rod with diameter 10 mm) and the reactor coil of 1.0 m x 0.65 mm i.d. straight Tygon tubing. All uptake tubing had lengths of 45 cm and inner diameters of 1.02 mm to ensure minimal back pressure. The flow rate used was 5.0 mℓ/min.

6.5.1.4 Procedure

The seven zones: EDTA, water, barium chloride-reagent, sample 1, spacer zone (water), sample 2 and the tiron-reagent, were all drawn up successively. Thereafter the flow direction was changed and the stack of zones was pumped through the detector. Since *FlowTEK* [41] only measured the peak height of the larger peak, data acquisition was done using two different device sequences. The first device sequence included the introduction of the seven zones into the holding coil, as well as the recording of the first peak, the iron-tiron complex. The second device sequence was only used for recording of the second peak, the barium sulphate suspension. The two methods (sequences) followed one another without any delay and were therefore grouped together in a procedure. The device sequences (methods) for the determination of iron and sulphate are given in Tables 6.2 and 6.3.

In the method postulated in Tables 6.2 and 6.3, sample 1 and sample 2 could be either the same sample or two different samples, which gave the method a little more flexibility. A sandwich technique, as described by Estela *et al.* [31], was also evaluated. The method used was basically the same as for the tandem determination. The second water and sample zones were omitted in this application and a bigger volume of sample 1 was used. Details of the device sequence used are given in Table 6.4.

TABLE 6.2 First device sequence of the tandem sequential injection system.

Time (s)	Pump	Valve	Description
0	Off	EDTA ①	Pump off, select EDTA stream
4	Reverse		Draw up EDTA solution
9	Off		Pump stops
10		Water ②	Select water stream
11	Reverse		Draw up water
26	Off		Pump stops
27		$BaCl_2$ ③	Select $BaCl_2$ stream
28	Reverse		Draw up $BaCl_2$-solution
33	Off		Pump stops
34		Sample 1 ④	Select first sample line
35	Reverse		Draw up sample/standard solutions
44	Off		Pump stops
45		Water ⑤	Select water line
46	Reverse		Draw up water
61	Off		Pump stops
62		Sample 2 ⑥	Select second sample line
63	Reverse		Draw up sample/standard solutions
67	Off		Pump stops
68		Tiron-reagent ⑦	Select tiron-reagent stream
69	Reverse		Draw up tiron-reagent
72	Off		Pump stops
73		Detector ⑧	Select detector line
74	Forward	Detector ⑧	Pump first part of stack of zones through detector.
122	Off		Pump stops, switch to next method.

TABLE 6.3 Second device sequence of the tandem sequential injection system

Time (s)	Pump	Valve	Description
0	Forward	Detector ⑧	Pump rest of the stack of zones through the detector.
85	Off		Pump stops, end of procedure.

TABLE 6.4 Device sequence of the sequential injection system using the sandwich technique.

Time (s)	Pump	Valve	Description
0	Off	EDTA ①	Pump off, select EDTA stream
4	Reverse		Draw up EDTA solution
9	Off		Pump stops
10		Water ②	Select water stream
11	Reverse		Draw up water
26	Off		Pump stops
27		$BaCl_2$ ③	Select $BaCl_2$ stream
28	Reverse		Draw up $BaCl_2$-solution
37	Off		Pump stops
38		Sample 1 ④	Select first sample line
39	Reverse		Draw up sample/standard solutions
63	Off		Pump stops
64		Water (step)	Step past inlet for water stream
65		Sample 2 (step)	Step past inlet for sample 2 stream
66		Tiron-reagent ⑦	Select tiron-reagent stream
67	Reverse		Draw up tiron-reagent
69	Off		Pump stops
70		Detector ⑧	Select detector line
71	Forward		Pump stack of zones through detector
191	Off		Pump stops, end of method

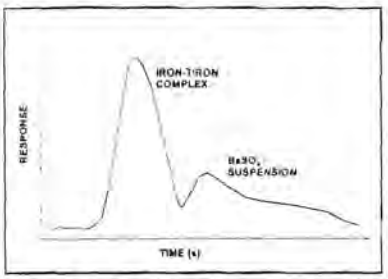

Fig. 6.3 Profile of a sample with high iron concentration and low sulphate concentration.

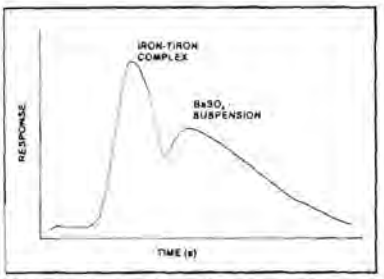

Fig. 6.4 Profile of a sample with approximately the same concentration of both analytes.

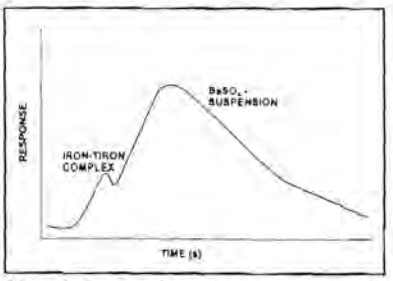

Fig. 6.5 Profile of a sample with low iron concentration and high sulphate concentration.

For this last method double peaks arose. The first peak was due to the iron-tiron complex and the second due to the barium sulphate suspension. Depending on the concentration of the respective analytes, the peak profiles showed the patterns represented in Figs. 6.3, 6.4 and 6.5. Because *FlowTEK* [41] measures only the larger peak, mathematical and statistical manipulation of the data files were done using the Quadro Pro-program of the Perfect Office package.

Fig. 6.3 represents the profile of a sample with high iron concentration and low sulphate concentration. Fig. 6.4 represents a sample with approximately equal concentrations of the two analytes, while Fig. 6.5 represent a sample with high sulphate concentration and low iron concentration.

6.5.2 Method optimisation

6.5.2.1 Order of reactions

The formation of the barium sulphate suspension to the correct measurable conditions from Ba^{2+} and SO_4^{2-} is a relatively slow process, while the reaction between iron and tiron is considered to be relatively fast. To ensure adequate time for the sulphate suspension to form, the reagents and sample for this reaction are drawn up first. The longer residence time in the holding coil would be suitable for the slower reaction, while the faster reaction's (iron with tiron) reagents are introduced last into the holding coil resulting in shorter residence times [50, 51].

6.5.2.2 Physical parameters

The conditions for the simultaneous determination of iron and sulphate were optimised by studying the influence of various parameters such as flow rate and the dimensions of the different coils (tube diameter and tube length). The response, given by the degree of zone penetration, and precision, given by the reproducibility of zone penetration, were used as indicators in the optimisation of the sequential injection system.

6.5.2.2.1 Flow rate

The formation of the barium sulphate suspension to the correct measurable conditions from Ba^{2+} and SO_4^{2-} is a relatively slow process. The flow rate during the different sequences is therefore a very important parameter to be optimised because it regulates the volume of the sample and reagent zones, and the flow of the zones through the system. The most important aspect dealt within this section was the residence time for the two reactions in the holding coil. As stated earlier, longer residence time led to better reaction development which was especially needed for the sulphate determination. The fact that the reagents for the turbidimetric determination were introduced first took care of the residence time. The reagents for the iron-tiron reaction were introduced last, allowing shorter residence time for the faster reaction.

Faster flow rates shorten residence time - even for the zones introduced first. It was therefore necessary to find a flow rate that fulfill all the requirements needed for the two reactions. Fig. 6.6 shows the results obtained for the two different reaction peaks at different flow rates. It is clear that the optimum flow rate for both reactions was 5 mℓ/min. The relative standard deviation for both reactions at the optimum flow rate revealed good results. Slower flow rates led to bigger dispersion and therefore inferior sensitivity, while at faster flow rates zone penetration was hindered due to insufficient axial dispersion.

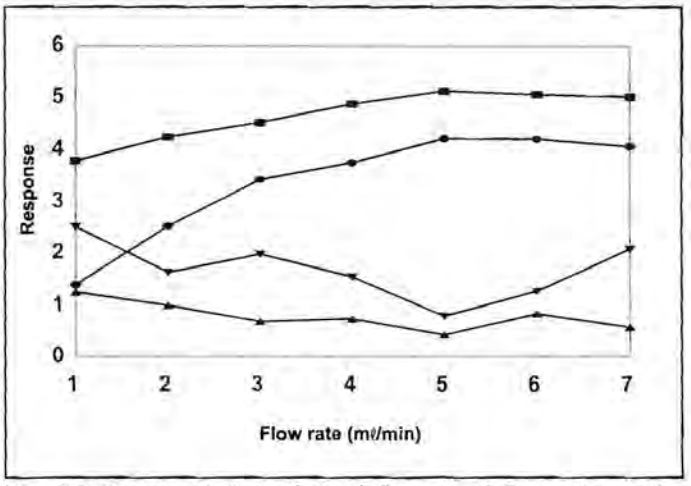

Fig. 6.6 Representation of the influence of flow rate on the sensitivity and reproducibility of the measured response of the two analyte peaks. ■ = relative peak height (iron-Tiron complex), ● = relative peak height (sulphate suspension), ▲ = %RSD(iron-Tiron complex) and ▼ = %RSD (sulphate suspension).

The same flow rate (5 mℓ/min) was used for the sandwich technique. The results of the influence of flow rate on sensitivity and precision are given in Table 6.5. As in the case of the tandem system, slower flow rates led to low sensitivities and peak tailing, which increased the rinsing time. At higher flow rates the %RSD became very high due to the insufficient zone penetration. This was especially true for the iron-Tiron complex, which zones were drawn up last.

TABLE 6.5 Effect of flow rate (pump speed) on sensitivity and precision using the sandwich technique

Flow rates (mℓ/min)	Mean relative peak height		% RSD	
	Iron-Tiron complex	Sulphate suspension	Iron-Tiron complex	Sulphate suspension
1.0	3.74	2.24	1.89	2.51
2.0	4.05	2.95	0.98	1.63
3.0	4.53	3.43	0.78	2.08
4.0	4.78	3.75	0.85	0.95
5.0	5.21	3.97	0.45	0.79
6.0	5.16	4.17	0.34	1.02
7.0	5.01	4.06	0.54	3.08

The results showed an increase in the mean relative peak height (sensitivity), for the iron-Tiron complex, from a value of 3.7 at a flow rate of 1.0 mℓ/min to a value of 5.2 at a flow rate of 5.0 mℓ/min due to an increase in zone penetration with increasing flow rate. The same trend can be observed for the sulphate determination - an increase in relative peak height from 2.2 to 4.2 when the flow rate was increased between 1.0 and 6.0 mℓ/min. Optimum precision in zone penetration resulted with a flow rate of 5.0 mℓ/min, where RSD values of 0.45% for iron and 0.79% for sulphate were obtained.

6.5.2.2.2 Holding coil

The main function of the holding coil is to serve as a reservoir [42], preventing the stack of zones from entering the conduit of the pump tubing of the peristaltic pump where deformation could take place. As zone movement into the holding coil takes place, axial dispersion and, therefore, zone penetration occurs. The dimensions (tube diameter and length) of the holding coil contribute to the dispersion needed for optimum zone overlap.

Tube diameter is responsible for the distance travelled by a zone. The tube inner diameter is normally an inverse of the zone length for a specific zone volume. The smaller the tube diameter the longer the zone length. The effect of holding coil tube diameter on sensitivity and precision was studied by several groups [39, 42 - 46] and the conclusion made was that it is mainly the tube diameter that influences the axial dispersion, not the tube length. To ensure maximum axial dispersion, wider tubing must be used and the geometry of the holding coil must be preferably straight.

In this study a holding coil with length of 6.5 m and inner diameter of 1.02 mm were used. The length of the holding coil might seem to be a bit too long, but since such a large number of zones were drawn up, it was extremely important that the zones could fit into the holding coil without reaching the pump conduit.

6.5.2.2.3 Reaction coil

In the final stage of the sequential injection analyser merging zones from the holding coil are propelled forward, by the peristaltic pump, through the reaction coil to the flow-cell of the detector. Maximum peak response and precision are obtained when the dimensions of the reaction coil are well defined. Tube diameter, length and geometry of the reaction coil needed, therefore, to be appropriate for the system.

Previous results [39] showed that the reaction coil should be as short and narrow as possible to avoid excess dilution of the formed product peak. Since the length of the reaction coil is usually dictated by the physical distance between the valve and the detector, the optimum length is taken as the piece of tubing just long enough to connect the two devices.

Narrower tubing resulted in sharper, less-dispersed peaks. Because it is known that the sulphate suspension tends to block narrow tubing, this parameter was optimise with respect to sensitivity and reproducibility for both analyte peaks. A number of tube diameters (0.51 - 1.59 mm) were evaluated. There was a general tendency for the formed product zones to disperse more in the tubing when the diameter increases from 0.51 to 1.59 mm, resulting in a decrease in peak height (Fig. 6.7). Reproducibility of the product zones also decreased for wider diameters. Narrower tube diameters gave better results for the iron determination, while it was clear that the sulphate peak reached a maximum response value at a diameter of 0.64 mm. This value was chosen as optimum for the proposed system.

The holding coil and reaction coil dimensions for the application of the sandwich technique were the same as described in the two sections above.

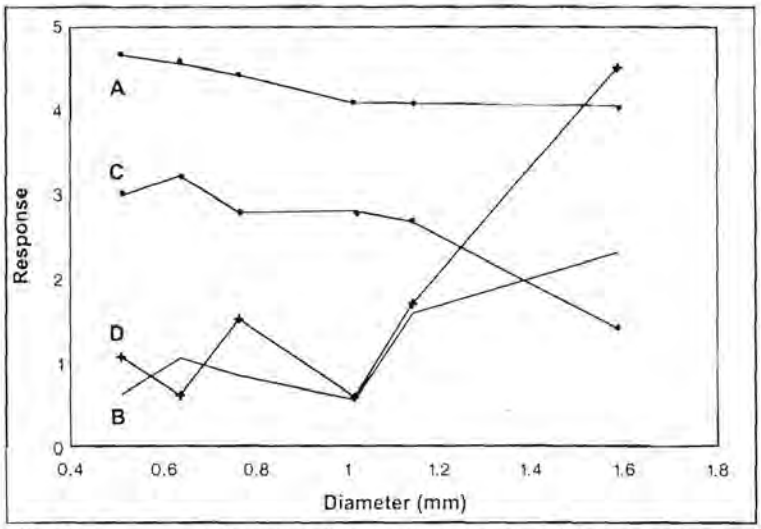

Fig. 6.7 Influence of the tube diameter of the reaction coil on relative peak height of the iron-Tiron complex (A) and the sulphate suspension (B) and precision (%RSD) of the iron-Tiron complex (C) and the sulphate suspension (D).

6.5.2.3 Chemical parameters

6.5.2.3.1 Optimisation of the barium chloride reagent

The formation of the correct barium sulphate suspension in the conduits of the sequential injection system was of critical importance to produce reproducible results with the proposed process analyser. This was achieved by the optimization of the barium chloride reagent solution. Preliminary results showed that the formation of the sulphate suspension was pH dependant [39]. A solution containing 10 g of $BaCl_2.2H_2O$ dissolved in 1 ℓ distilled water was therefore used to evaluate the effect of pH on the sensitivity and precision. The results obtained with a 200 mg/ℓ sulphate solution are listed in Table 6.6.

TABLE 6.6 Effect of pH on the absorbance of a 200 mg/ℓ standard sulphate solution

Sample pH	Abs. of $BaSO_4$	%RSD
1	0.521	1.02
2	0.522	0.98
2.5	0.966	0.75
3	0.659	0.72
4	0.524	0.81
5	0.458	0.95
7.69	0.378	1.14

It is obvious from Table 6.6 that a pH of 2.5 gave the best sensitivity. As the pH of real samples varied, and to prevent tedious sample preparation steps, it was necessary to use a buffer of pH 2.5 to prepare the reagent. A barium chloride solution containing a potassium hydrogen phthalate - hydrochloric acid buffer at pH 2.5 was therefore prepared by adding 388 mℓ of a 0.1 mol/ℓ HCl solution to 500 mℓ of a 0.1 mol/ℓ potassium hydrogen phthalate solution. $BaCl_2.2H_2O$ (10 g) was dissolved in this buffer and the solution was diluted to 1 ℓ. Results obtained with this reagent showed good sensitivity, but the precision still remained poor with an RSD of 7.7%. Another problem experienced was that the potassium hydrogen phthalate precipitated when it was left overnight and had to be redissolved every morning. Addition of 0.062 g gelatine per 100 mℓ solution improved both the sensitivity and the reproducibility remarkably. The problem with the overnight precipitation of potassium hydrogen phthalate was also solved, as it seemed that the gelatine stabilised the solution. The addition of gelatine however gave rise to a background value (due to sulphate impurities in the gelatine), but this value was very small compared to the analyte peak and the reproducibility was very good. When the reagent was filtered through a Millipore membrane (type HA) (45 µm), the background value was eliminated completely. This reagent solution was stable for up to six months. To prevent bacterial growth, 0.1 g thymol per 100 mℓ solution was added.

The high concentration of barium chloride was needed to compensate for the loss in sensitivity due to the longer residence time experienced by the zones involved in the sulphate determination. The high concentration also ensured that the linear span of the determination covers sulphate concentration ranges between 10 and 200 mg/ℓ.

6.5.2.3.2 Optimisation of the Tiron reagent

The Tiron reagent was dissolved in a 0.01 mol/ℓ $HClO_4$ solution. This was done for two reasons. Firstly, the reaction between iron(III) and Tiron is pH dependant, in such a way that different pH values resulted in different complex colours. To ensure the formation of the blue iron-Tiron complex a pH of 2 - 2.5 was needed. Secondly, since iron(III) was determined, addition of $HClO_4$ eliminated any possibility of the sample being reduced to Fe(II). The pH needed for both the iron-Tiron and the sulphate reactions was 2.5, which was especially useful when applying the sandwich technique.

For the reaction between iron(III) and Tiron a ratio of 1:1 between sample and reagent was needed [47]. The higher the reagent concentration, the larger the linear span of the determination. A concentration of 500 mg/ℓ was chosen for this application and resulted in the determination of iron(III) in samples at concentrations between 5 and 500 mg/ℓ.

6.5.2.3.3 Sequence of sample and reagents

Employing the tandem determination of the two analytes, seven zones were stacked in the holding coil *viz.* an alkaline buffer-EDTA zone, water (spacer zone 1), barium chloride reagent, sample 1, another water zone (spacer zone 2), sample 2 and the Tiron reagent. The order in which the different sequences of reagents and sample are drawn up and propelled into the detector is very important in SIA. The results obtained, revealed that the alkaline buffer-EDTA solution had to be separated from the acidified barium chloride reagent solution by a water zone to prevent the formation of a Ba-

EDTA complex (log K_f = 7.8 [37]). There were therefore only two zones that need to be properly mixed for the sulphate determination, which was separated from the iron determination by means of a second water zone. The sample zone was initially placed between the water and barium chloride reagent zones. That configuration gave a mean relative peak height of 4.13 with an RSD of 0.92%. When the zones were changed and the barium chloride reagent zone was placed between the water and the sample, better results were obtained, with a mean relative peak height of 4.93 and RSD of 0.89%.

Experiments showed that the zones for the iron determination gave optimum results when the sample was introduced first followed by the reagent (relative peak height = 6.78 and %RSD = 0.57 compared to a relative peak height of 5.83 and %RSD of 0.62 for the reversed sequence). This arrangement was also preferred to ensure no overlap between sample 1 (sulphate determination) and the Tiron reagent.

For the sandwich technique, the sequence of zones was as follows: the buffer-EDTA solution, water zone, barium chloride reagent, the sample zone and the Tiron reagent.

6.5.2.3.4 Volume of the barium chloride reagent solution

The volume of the barium chloride reagent solution is a function of both the flow rate as well as the period the reagent is drawn up. The influence of a number of reagent volumes on sensitivity and precision were evaluated by changing the period which the reagent was drawn up. The results obtained, are summarised in Table 6.7.

TABLE 6.7 Effect of barium chloride reagent volume on sensitivity and precision

Volume (µl)	Mean relative peak height	% RSD
83.3	4.46	2.47
166.7	4.83	2.62
250	4.94	1.43
333.3	4.85	1.45
416.7	4.92	2.07
500	4.84	4.02

A reagent volume of 250 µl gave the best sensitivity and precision and was chosen for the proposed SI analyser. Larger volumes underwent smaller dispersion, which compensated for the fact that the residence time of this zone in the holding coil was much longer than for any other zone (excluding the EDTA wash solution).

6.5.2.3.5 Volume of sample 1

The sample volume also depends on the flow rate as well as the period the sample is drawn up. Various volumes were examined and the results are summarised in Fig. 6.8. A sample volume of 750 µl was selected for the proposed system due to the best sensitivity and precision. It seemed that larger volumes (> 750 µl) would result in better sensitivity. This was however not the case. When the sample zone became too large, a decrease in zone overlap was observed.

It seemed strange that the volume of sample 1 was so much bigger than for the reagent. The high concentration of the barium chloride solution used as well as the fact that the reaction stiochiometry favoured a 1:1 reaction, gave a reasonable good explanation for this observation.

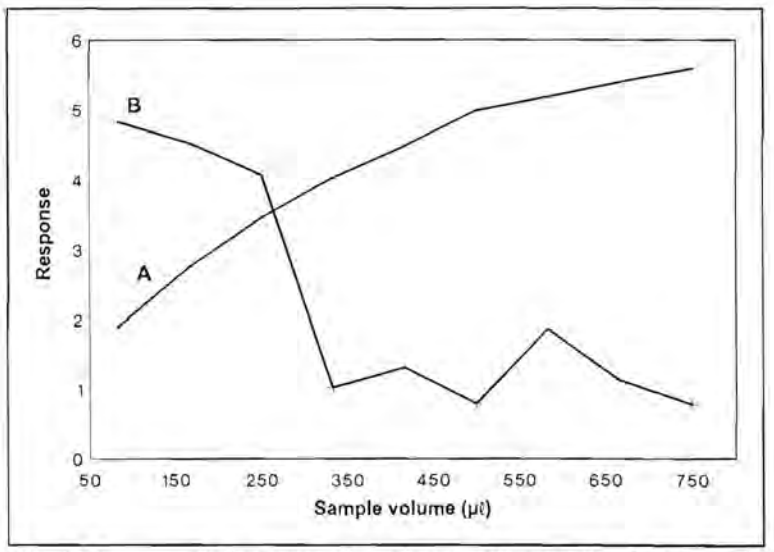

Fig. 6.8 Influence of volume of sample 1 (sulphate determination) on zone penetration (A) and precision (B - %RSD).

6.5.2.3.6 Volume of sample 2

Shorter residence time in the holding coil would lead to smaller dispersion [52, 53]. To achieve the necessary axial dispersion, smaller sample volumes (which underwent bigger dispersion) were introduced for the iron determination. The results of the evaluated volumes are represented in Fig. 6.9.

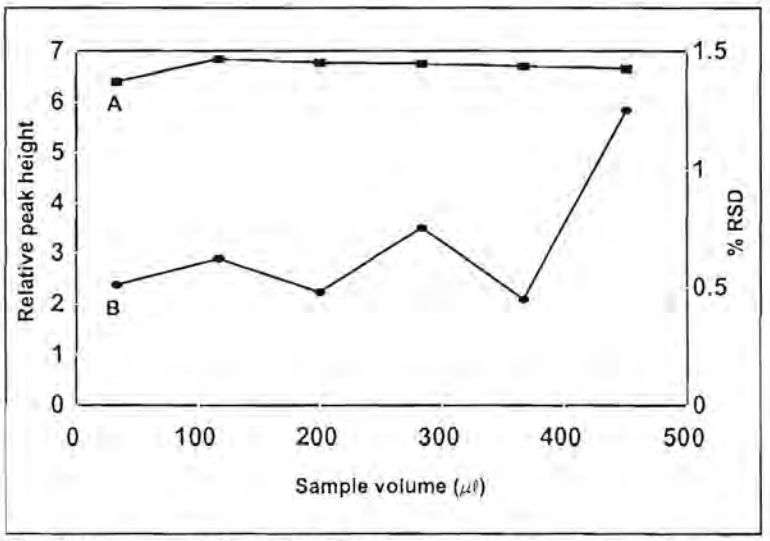

Fig. 6.9 Influence of the second sample volume (iron determination) on sensitivity and precision. A - relative peak height and B - %RSD.

The sensitivity increased slightly with increased sample volume until a plateau was reached. The optimum volume for the second sample was chosen to be 120 $\mu\ell$.

6.5.2.3.7 Volume of the Tiron reagent solution

Since the Tiron reagent was drawn up last, it was expected that the dispersion experienced would be very small, due to the short residence time. To compensate for that, a small volume of reagent was introduced into the system. To ensure that all the iron(III) would be converted to the iron-Tiron complex, an excess of reagent was used. Since the reaction between the iron and Tiron took place on a 1:1 basis, the volume should need to be a little bigger than that of the sample. From the results, represented in Fig. 6.10, it was, however, clear that the volume of the reagent does not really influence the sensitivity. Smaller reagent volumes gave slightly better sensitivity, probably due to better zone overlap which resulted from a better axial dispersion of the reagent zone. An optimum reagent volume of 150 $\mu\ell$ was selected to ensure an excess of reagent, especially when more concentrated samples had to be determined.

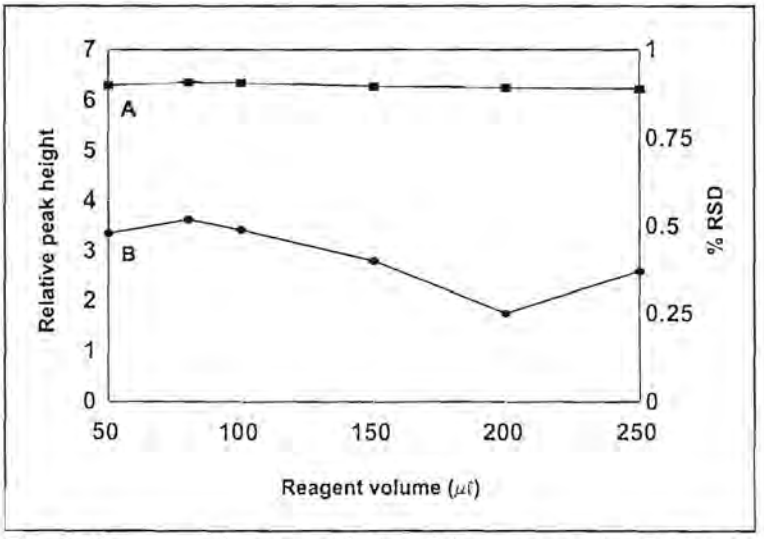

Fig. 6.10 Influence of the Tiron reagent volume on sensitivity and precision (iron determination). A - relative peak height and B - %RSD.

6.5.2.3.8 Sample and reagent volumes used in the sandwich technique

One of the advantages of SIA is the low sample and reagent consumption [39]. According to previous studies [31, 39, 48], the recommended volumes for both sample and reagent in SIA systems are between 0.5 $V_{½}$ and $V_{½}$. $V_{½}$ is the injected volume that resulted in an extent of dispersion such that the product concentration was half of its original concentration. The aim of this sandwich technique was to determine two analytes in one sample using two reagents. It would be obvious that the volumes used in this application were going to be rather different from those routinely employed for other purposes.

The dispersion of the first reagent (the barium chloride reagent, referred to as R_1) increased due to the longer residence time in the SIA manifold. The volume of this zone needed to be bigger and to compensate for this problem. Since the sample zone acted like a spacer zone between the two reagents, it had to be of sufficient volume to eliminate any possible interference between the two reactions that took place. The second reagent (the Tiron reagent, referred to as R_2) underwent smaller dispersion, due to its shorter residence time in the manifold. Smaller volumes would therefore be necessary for this reagent in relation to the first reagent. The same optimum volumes and reagent concentrations used in the tandem system were initially use to evaluate the sandwich technique.

Preliminary experience in the on-line dilution of sulphate [39], showed that the spacer zone volume must be much bigger than the volumes of both reagents. In the sulphate analysis a spacer zone of 15 s (1.25 mℓ) were used and zone overlap still took place. The bigger the sample zone, the better resolution between the two reaction peaks were expected. Volumes between 1.25 mℓ and 2.10 mℓ were evaluated. The shapes of the peaks obtained for different concentrations are given in Figs. 6.3 to 6.5. For the evaluation, analytes of the same concentration (100 mg/ℓ) were used. Evaluation was done by calculating the resolution between the two peaks employing the formula used in chromatography [26]. Resolution is the difference in retention times (or volumes) of

two peaks, divided by their baseline widths (Fig. 6.11). The equation used is

$$R = (t_A - t_B)/[(W_A + W_B)/2] \qquad 6.1$$

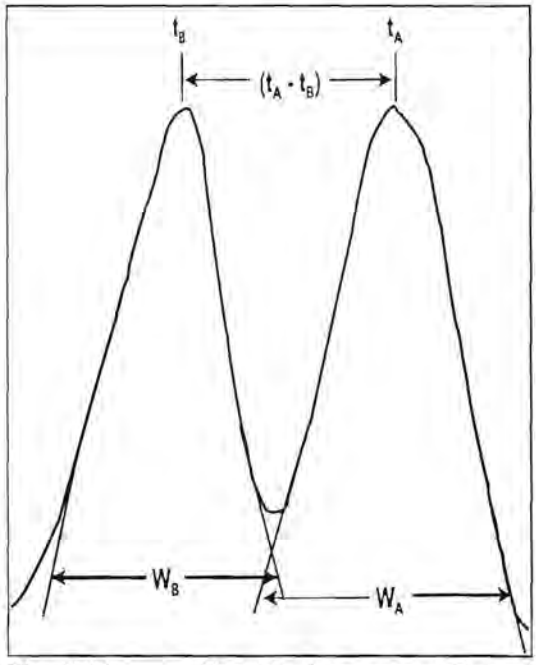

Fig. 6.11 Graphical representation of peak resolution.

Using equation 6.1, the following results were obtained for the different sample volumes evaluated (Table 6.8). The time (in s) was taken as the time where the peak maximum appear and the baseline widths as the distance (in mm) between the tangents drawn to the ascending and descending parts of the peaks. The experimental results confirmed the expectations. Resolution between the two peaks increased with increased sample volume, but was never totally complete. Complete resolution between the two peaks might be possible, but that would need extremely large sample volumes. Sample volumes greater than 1.5 mℓ gave resolution values that produced acceptable separation between the two peaks. Optimum sample volume was therefore chosen to be 2.0 mℓ.

TABLE 6.8 Influence of different sample volumes on the resolution of the two reaction peaks used in the sandwich technique.

Sample volume (mℓ)	Resolution
1.25	15
1.35	34
1.40	57
1.50	84
1.60	115
1.65	150
1.75	189
1.85	232
1.90	270
2.00	294.5
2.10	314.8

The volumes of the two reagents were evaluated again after the optimum sample volume was obtained. The results were very similar to the ones obtained with the tandem application and the optimum reagent volumes were therefore taken as 150 $\mu\ell$ for the Tiron reagent and 250 $\mu\ell$ for the barium chloride reagent.

6.5.3 Method evaluation

The proposed sequential injection analyser was evaluated with regard to linearity, accuracy, precision, detection limit, sample interaction (carry-over), interferences and sampling rate.

6.5.3.1 Linearity

The linearity of the proposed SIA system for the tandem determination of iron and sulphate was evaluated under optimum running conditions. The relationships obtained for relative peak height versus iron(III) and sulphate ion concentration were

respectively:

$$y = 0.57x_{(Fe)} + 0.214;\ r^2 = 0.9997$$
$$y = 0.0278x + 0.5195;\ r^2 = 0.9982$$

where y = relative peak height for the two peaks, respectively, $x_{(Fe)}$ = iron(III) concentration in mg/ℓ and x = sulphate ion concentration in mg/ℓ. The correlation coefficient (r^2) indicated that the method was linear for an iron concentration ranging between 5 and 500 mg/ℓ and for a sulphate concentration between 10 and 200 mg/ℓ.

The linear ranges for the individual analytes were the same for the sandwich technique, but the sensitivities (and therefore the slope of the graphs) were slightly smaller. The corresponding equations for iron(III) and sulphate were:

$$y = 0.285x_{(Fe)} + 0.324;\ r^2 = 0.9962$$
$$y = 0.048x + 0.425;\ r^2 = 0.9892$$

respectively. The high concentrations used for the reagents allowed for the wider analytical ranges of the two reactions. The linear range in both cases were therefore dependant on both the concentration of reagents as well as their respective volumes.

6.5.3.2 Accuracy

The accuracy of the proposed SIA analyser was evaluated by calculating the percentage recovery of the two analytes after being analysed with the SIA system. Seven synthetic aqueous samples were analysed this way. Iron and sulphate were also determined in real aqueous samples by standard addition. Tap water from three different locations were evaluated. These locations include the laboratory, an outside tap used for watering plants and a flat in the Sunnyside (Pretoria, South Africa) vicinity. The results as shown in Tables 6.9, 6.10 and 6.11 revealed acceptable accuracy with the lowest percentage recovery in the region of 93% for both the tandem and sandwich techniques. The tap water analysed showed similar concentrations for sulphate and

the concentrations found were well below the levels listed in Table 6.1. The iron concentration in the outside tap's water was higher, probably due to the material the tap was constructed of.

TABLE 6.9 Evaluation of the accuracy of the proposed tandem SIA system

Sample	Known concentration ([ ] in mg/ℓ)		SIA ([ ] in mg/ℓ)		% Recovery	
	SO_4^{2-}	Fe^{3+}	SO_4^{2-}	Fe^{3+}	SO_4^{2-}	Fe^{3+}
Sample A	14.6	5.0	15.1	5.03	103.42	100.6
Sample B	46.4	35.0	46.7	33.9	100.65	96.86
Sample C	19.1	20.0	18.6	19.2	97.38	96.0
Sample D	121.6	140.0	125.1	145.8	102.89	104.14
Sample E	34.4	155.0	32.0	152.5	93.02	98.39
Sample F	35.2	45.0	33.6	45.2	95.45	100.44
Sample G	189.5	190	202	188.9	106.60	99.42

TABLE 6.10 Evaluation of the accuracy of the proposed sandwich SIA system

Sample	Known concentration ([ ] in mg/ℓ)		SIA ([ ] in mg/ℓ)		% Recovery	
	SO_4^{2-}	Fe^{3+}	SO_4^{2-}	Fe^{3+}	SO_4^{2-}	Fe^{3+}
Sample A	14.6	5.0	15.9	5.1	108.90	102.0
Sample B	46.4	35.0	47.5	36.9	102.37	105.42
Sample C	19.1	20.0	19.6	21.3	102.58	106.5
Sample D	121.6	140.0	125.1	145.8	102.89	104.14
Sample E	34.4	155.0	34.0	153.9	98.83	99.29
Sample F	35.2	45.0	36.6	45.2	103.98	100.44
Sample G	189.5	190	192.2	188.9	101.42	99.42

TABLE 6.11 Comparison of results obtained for the analysis of tap water samples with the tandem and sandwich SIA techniques using standard addition.

Sample	Sulphate concentration ([ ] in mg/ℓ)		Iron(III) concentration ([ ] in mg/ℓ)	
	Tandem technique	Sandwich technique	Tandem technique	Sandwich technique
Tap water (lab)	31.9	35.9	50.5	52.3
Tap water (flat)	30.0	34.4	53.4	55.4
Tap water (outside)	46.6	49.6	76.5	79.8

6.5.3.3 Precision

The precision of the method was determined by 10 repetitions of each standard solution in the linear range of the specific method as well as 10 repetitions of each sample within the range. The results of these repetitions, for both the tandem and sandwich techniques, are listed in Tables 6.12 and 6.13.

TABLE 6.12 Precision of the proposed tandem and sandwich SIA systems

Standard ([ ] in mg/ℓ)	% RSD			
	Tandem technique		Sandwich technique	
	SO_4^{2-}	Fe^{3+}	SO_4^{2-}	Fe^{3+}
10	1.22	0.98	2.51	1.03
20	2.81	1.02	2.03	0.99
50	2.57	0.95	1.95	0.92
100	1.10	1.85	1.82	0.89
150	2.44	0.74	1.54	0.73
200	1.43	0.81	1.37	0.51
300	-	0.65	-	0.53
400	-	0.54	-	0.42
500	-	0.23	-	0.57

TABLE 6.13 Precision of the proposed tandem and sandwich SIA systems

Sample	% RSD			
	Tandem technique		Sandwich technique	
	SO_4^{2-}	Fe^{3+}	SO_4^{2-}	Fe^{3+}
Sample A	1.34	0.65	2.15	0.89
Sample B	1.79	0.31	2.23	0.75
Sample C	1.21	1.05	1.52	0.53
Sample D	1.02	0.57	1.73	0.68
Sample E	0.95	0.74	1.91	0.73
Sample F	1.14	1.24	1.07	0.58
Sample G	0.53	0.25	0.91	0.73
Tap water (lab)	1.05	0.74	0.82	0.37
Tap water (flat)	0.81	0.54	0.76	0.45
Tap water (outside)	1.83	1.03	1.46	0.85

A precision of less than 2.9% RSD was obtained for both SIA systems.

6.5.3.4 Detection limits

The detection limit is both a function of sensitivity and noise. The lowest concentration, that could be determined without doubt, would be considered the detection limit of the system. The detection limits for both the iron and sulphate determinations were calculated as follow: The relative peak height for a blank solution was measured at the times where the peak maxima of iron and sulphate appeared, respectively. These values were multiplied by three to generate a peak height value that could be measured with certainty. The concentration values of the corresponding peak height values were read from the individual calibration curves and then used as detection limits. Using this technique, the detection limits for the tandem SIA systems were 10 mg/ℓ and 5.4 mg/ℓ for sulphate and iron respectively. The detection limits calculated for the sandwich technique were 15.7 mg/ℓ for sulphate and 7.8 mg/ℓ for iron.

The calculated values are in good agreement with Madsen and Murphy's [16] statement that barium sulphate turbidimetric methods have been successful only when sulphate concentrations in the sample of interest are above 10 mg/ℓ. The detection limit is instrument dependant below 10 mg/ℓ sulphate [49]. It is suggested that if concentrations of below 10 mg/ℓ need to be determined, either another method (e.g. methylthymol blue method) or sample preconcentration should be used depending on the instrumental design. Determination of lower iron concentrations will also feature preconcentration steps which may include cation exchange columns.

6.5.3.5 Sample interaction

One of the problems associated with the sulphate turbidimetric procedure, is the built-up of barium sulphate precipitate in the flow system which tends to settle in the flow-cell. This leads to low precision and ultimately blocks the manifold. The addition of an alkaline buffer-EDTA solution to redissolve the accumulated barium sulphate precipitate is one way of overcoming the problem.

Baban *et al.* [48] used a carrier solution of barium(II) ions with an excess of EDTA in alkaline medium (pH 10) to dissolve any accumulated precipitate. Precipitation occurs under the very acidic conditions of the well-defined zone (pH 1.5 - 2.5) in the analytical manifold where a pH-gradient in the sampling zone is established. The precipitate is, however, redissolved outside this zone by the self-cleansing action of the excess alkaline-EDTA carrier solution. By using pH-gradients and alkaline-EDTA a sufficiently stable barium sulphate suspension is obtained, which obviates the use of protective colloids such as polyvinyl alcohol or thymol gelatine.

Van Staden [20] used a different approach by utilising 60 μℓ water samples from one loop of a two position sampling valve alternating with an alkaline buffer-EDTA solution (100 μℓ) from the second loop which was injected into a barium sulphate-thymol-gelatine single line carrier stream. This ensures that the residual precipitate, coating the walls of the flow-cell, is redissolved and the system kept clean.

The EDTA-buffer solution did not only took care of the build up of barium sulphate in the system, it also ensured that no iron residue was left in the SIA manifold once an analytical cycle was completed.

Sample interaction was determined using the equation:

$$Interaction = \frac{(A_3 - A_1)}{A_2} \times 100$$

where

A_1 = the true peak height of a sample with a low analyte concentration (10 mg/ℓ),

A_2 = the true peak height of a sample containing ten times more analyte (100 mg/ℓ), and

A_3 = the peak height for an interacted sample containing the same amount of analyte as A_1.

The relative peak heights of A_1, A_2 and A_3 were respectively 0.45, 3.57 and 0.47 for sulphate and 1.24, 5.78 and 1.24 for iron when employing the tandem method. The sample interaction between samples as calculated was 0.56% for sulphate and 0% for iron, which is negligible. Sample interaction is reduced effectively by the EDTA-solution that rinse the system after every experiment.

For the application of the sandwich technique, a negative interference was experienced. The relative peak heights of A_1, A_2 and A_3 were respectively 0.37, 3.48 and 0.36 for sulphate and 1.22, 5.69 and 1.20 for iron. These values corresponded to sample interactions of -2.78% for sulphate and -1.64% for iron. This interference was however not because of sample carry-over, but because of the formation of slightly insoluble $Fe_2(SO_4)_3$ (log K_f = 4.0 [26]).

6.5.3.6 Sample frequency

The sampling rate is calculated by dividing 3600 s (1 h) through the time (in seconds) needed to complete one experiment. It took 207 seconds to complete one analytical

cycle when using the tandem SIA system, which gave a sample frequency of about 17 samples per hour. The total time needed to complete one analytical cycle when employing the sandwich technique, was 191 seconds, which gave a sample frequency of almost 19 samples per hour.

6.5.3.7 Interferences

There are a number of ions that might be possible interferences in the samples analysed and these interferences were evaluated. A number of cations, as well as anions, interfered in the determination of sulphate. The addition of the cations to the sulphate standard seemed to change the ionic environment. This resulted in a change in the conditions affecting particle formation. This effect is called a salt error, where high concentrations of ions not common to a reaction increase the overall ionic strength of the solution and so change the solubility of salts and equilibria of complex formation. Most of the complexes formed between the cations and sulphate were soluble in water and were not suppose to interfere by forming a precipitate.

The main interfering substances, bicarbonate, carbonate (alkalinity) and chloride, were all present at levels not usually found in raw and potable waters. The interferences, apart of that of carbonate, were probably due to physical rather than chemical effects. Since viscosity and refractive index differences between sample and carrier could cause mixing boundaries. The alkalinity interference was probably due to consumption of the acid in the reagent.

Calcium, bismuth, iron, cerium, manganese, antimony, selenium, tin, tellurium, thorium and vanadium interfered in the determination of sulphate. Nakashima *et al.* [18] stated that the 'calcium ion in river water severely interferes with the determination of sulphate'. The interferences due to cations could be eliminated by cation exchange. Interferences due to fluoride and phosphate could be removed by pretreatment with magnesium oxide [49]. Hydrochloric acid was added to the barium chloride solution to prevent the formation of precipitates of carbonate, chromate, sulphite, phosphate

and oxalate of barium which might interfere [22]. Nakashima *et al.* [18] found however that Mg^{2+} and NH_4^+ (30 mg/ℓ), Na^+ (50 mg/ℓ), K^+ (80 mg/ℓ) and Cl^-, NO_3^-, PO_4^{3-}, HCO_3^- and SiO_3^{2-} (100 mg/ℓ) do not interfere with the sulphate determination at levels which are normally present in natural waters. Jones [49] found that amounts of sodium up to a maximum concentration of 4 g/ℓ had no effect on the recovery of sulphate. At low pH levels $Fe_2(SO_4)_3$ hydrates precipitate and interfere in the determination of sulphate [1]. This was especially a problem when the sandwich technique was used. In the tandem system a cation exchange column could be incorporated in the inlet line of the sample used for sulphate determination. This was impossible when using the sandwich technique, since only one sample was utilized.

Copper, zinc and calcium were tested as possible interferences in the iron determination. Zinc and calcium were found to be slight interferents, causing only small (< 6%) enhancement of the analyte signal when present in a 1:1 ratio with iron. Copper compete with iron for the Tiron reagent and forms a yellowish-green complex. Fluorides, citrates and tartrates do not interfere in the determination, while thiocyanate interfere seriously in all ratios.

6.6 Conclusion

A sequential injection analyser was developed to monitor iron and sulphate concentrations in aqueous solutions. These aqueous solutions include effluents of chemical process industries as well as natural waters. Incorporation of an alkaline buffer-EDTA solution in the correct sequence of the system redissolved accumulated barium sulphate precipitate and iron residues to give a high degree of sensitivity, accuracy and precision. The tandem SIA system proved to be slightly more complicated in terms of programming and needed more ports on the selection valve. Its sample frequency is also lower than that of the sandwich technique. Advantages of this technique include, however, higher sensitivity and better handling of interferences. The tandem technique also has the feature that it can determine sulphate and iron in a single sample or it can be employed to determine sulphate and

iron separately in two or more individual samples.

Both systems are fully computerised and are able to monitor sulphate and iron in samples at a frequency of 17 (tandem) and 19 (sandwich) samples per hour with a relative standard deviation of less than 2.9% for both techniques. The calibration curve is linear between 10 and 200 mg/ℓ for sulphate and between 5 and 500 mg/ℓ for iron. The linear ranges are dependant on reagent concentration and reagent volume and can comfortably be adapted to handle more concentrated solutions.

6.7 References

1. N. N. Greenwood and A. Earnshaw, **Chemistry of the Elements**, Pergamon Press, 1986.
2. H. L. Bohn, B. L. McNeal and G. A. O'Connor, **Soil Chemistry**, John Wiley & Sons, Inc., New York, 1985.
3. American Society for Testing and Materials, **1973 Book of ASTM Standards. Part 23. Water: Atmospheric Analysis**, ASTM. Philadelphia, 1973, pp. 425 - 431.
4. W. C. Schroeder, **Ind. Eng. Chem.**, **5** (1933) 403.
5. J. W. Ross and M. S. Frant, **Anal. Chem.**, **41** (1969) 967.
6. J. Fries and H. Getrost, **Organic Reagents for Trace Analysis**, E. Merck, Darmstadt, 1977.
7. **Orion Res. Newsl.**, **2** (1970) 21.
8. A. Hulanicki, R. Lewandowski and A. Lewenstam, **Analyst**, **101** (1976) 939.
9. E. P. Scheide and R. A. Durst, **Anal. Lett.**, **10** (1977) 55.
10. M. Trojanowics and A. Hulanicki, **Chem. Anal.** (Warsaw), **22** (1977) 615.
11. J. Vesely, **Collect. Czech. Chem. Commun.**, **46** (1977) 368.
12. R. J. Bertolacini and J. E. Barney, **Anal. Chem.**, **29** (1957) 281.
13. J. Agterdenbos and N. Martnius, **Talanta**, **11** (1964) 875.
14. A. L. Lazrus, K. C. Hill and J. P. Lodge, **A New Colorimetric Microdetermination of Sulphate Ion**, Technicon Symposia 1965, Automation in Analytical Chemistry, Mediad Inc., New York, 1966, p. 291.
15. R. T. Sheen, H. L. Kahler, E. M. Ross, W. H. Betz and L. D. Betz, **Chem. Anal. Ed.**, **7** (1935) 262.
16. B. C. Madsen and R. J. Murphy, **Anal. Chem.**, **53** (1981) 1924.
17. H. F. R. Reijnders, J. J. van Staden and B. Griepink, **Fresenius' Z. Anal. Chem.**, **295** (1979) 410.
18. S. Nakashima, M. Yagi, M. Zenki, M. Doi and K. Toei, **Fresenius' Z. Anal. Chem.**, **317** (1984) 29.
19. K. Yakata, F. Sagara, I. Yoshida and K. Ueno, **Anal. Sciences**, **6** (1990) 711.

20. J. F. van Staden, **Fresenius' Z. Anal. Chem.**, **310** (1982) 239.

21. J. F. van Staden, **Fresenius' Z. Anal. Chem.**, **312** (1982) 438.

22. J. F. van Staden, **Water S A**, **12** (1986) 43.

23. O. Kondo, H. Miyata and K. Tóei, **Anal. Chim. Acta.**, **134** (1982) 353.

24. F. J. Krug, F. H. Bergamin, E. A. G. Zagatto and S. S. Jorgensen, **Analyst**, **102** (1977) 503.

25. W. D. Basson and J. F. van Staden, **Lab. Practice**, **25** (1978) 863.

26. L. W. Potts, **Quantitative Analysis. Theory and Practice**, Harper and Row, New York, 1987.

27. Y. A. Zolotov, I. M. Maksimova, E. I. Morosanova and A. A. Velikorodny, **Anal. Chim. Acta**, **308** (1995) 378.

28. S. W. Kang, T. Sakai, N. Ohno and K. Ida, **Anal. Chim. Acta**, **261** (1992) 197.

29. K. Tsunoda, H. Itabashi and H. Akaiwa, **Anal. Chim. Acta**, **229** (1995) 327.

30. N. Clarke and L. G. Danielsson, **Anal. Chim. Acta**, **306** (1995) 5.

31. J. M. Estela, A. Cladera, A. Munoz and V. Cerdà, **Int. J. Environ. Anal. Chem.**, **64** (1996) 205.

32. J. de Gracia, M. L. M. F. S. Saravia, A. N. Araujo, J. L. F. C. Lima, M. del Valle and M. Poch, **Anal. Chim. Acta**, **348** (1997) 143.

33. A. N. Araujo, J. Gracia, J. L. F. C. Lima, M. Poch, M. Lucia and M. F. S. Saraiva, **Fresenius J. Anal. Chem.**, **357** (1997) 1153.

34. E. Rubi, R. Forteza and V. Cerdà, **Lab. Rob. Autom.**, **8** (1996) 165.

35. J. F. van Staden, C. Saling, D. Malan and R. E. Taljaard, **Anal. Chim. Acta**, **350** (1997) 37.

36. J. F. van Staden, H. du Plessis and R. E. Taljaard, **Anal. Chim. Acta**, **357** (1997) 141.

37. M. Endo and S. Abe, **Fresenius J. Anal. Chem.**, **358** (1997) 546.

38. K. Oguma, S. Kozuka, K. Kitada and R. Kuroda, **Fresenius J. Anal. Chem.**, **341** (1991) 545.

39. R. E. Taljaard, **Application of Sequential Injection Analysis as Process Analyzers**, MSc-Thesis, University of Pretoria, 1996.

40. W. D. Basson and J. F. van Staden, **Water Research**, **15** (1981) 333.

41. G. D. Marshall, **Analytical Instrumentation**, **20**(1) (1992) 79.

42. G. D. Marshall, **Sequential-Injection Analysis**, PhD-Thesis, University of Pretoria, 1994.

43. A. Botha, **Sequential Injection Analysis: Evaluation of Operational Parameters and Application to Process Analytical Systems**, MSc-Thesis, University of Pretoria, 1999.

44. J. L. Zable, **Operational Parameters of Sequential Injection Analysis and the Fundamentals of Calculating the Dispersion at Maximum Zone Overlap**, PhD-Thesis, University of Washington, 1996.

45. G. D. Marshall and J. F. van Staden, **Process control and Quality**, **3** (1992) 251.

46. T. Gübeli, G. D. Christian and J. Růžička, **Anal. Chem.**, **63** (1991) 2407.

47. J. F. van Staden, H. du Plessis and R. E. Taljaard, **Instrum. Science Technol.**, **27** (1999) 1.

48. J. Růžička and G. D. Marshall, **Anal. Chim. Acta**, **237** (1990) 329.

49. **Sulphate in Waters, Effluents and Solids.** Methods for the Examination of Waters and Associated Materials, 2nd ed, London, HMSO, 1988.

50. S. Baban, D. Beetlestone, D. Betteridge and P. Sweet, **Anal. Chim. Acta.**, **114** (1980) 319.

51. E. A. Jones, **MINTEK report M111**, 1983, pp 7 - 10.

52. M. Valcarcel and M. D. Luque de Castro, **Flow Injection Analysis. Principles and Applications**, Ellis Horwood, Chichester, 1987.

53. J. Růžička and E. H. Hansen, **Flow Injection analysis**, 2nd ed, John Wiley & Sons, New York, 1988.

CHAPTER 7

Simultaneous Kinetic Determination of Nickel(II) and Cobalt(II) using Sequential Injection Analysis

7.1 Introduction

Although hardly any metallic cobalt was used until the twentieth century, its ores have been used for thousands of years to impart a blue colour to glass and pottery. It is present in Egyptian pottery dated at around 2 600 BC and Iranian glass beads of 2250 BC. "Smalt", produced by fusing potash, silica and cobalt oxide, can be used for colouring glass or for glazing pottery. The secret of making this brilliant blue pigment was apparently lost, to be rediscovered in the fifteenth century. Leonardo da Vinci was one of the first to use powered smalt as a 'new' pigment when painting his famous "The Madonna of the Rocks" [1].

The source of the blue colour was recognised in 1735 by the Swedish chemist G. Brandt, who isolated a very impure metal, or "regulus", which he named "cobalt rex". In 1870 T. O. Bergman showed this to be a new element. Its name has some resemblance to the Greek word for "mine", but it is almost certainly derived from the German word *Kobalt* for "goblin" or "evil spirit". The miners of northen European countries thought that the spitefulness of such spirits was responsible for ores which, on smelting, not only failed unexpectedly to yield the anticipated metal, but also produced highly toxic fumes [1].

More than 200 ores are known to contain cobalt but only a few are of commercial value. The more important ores are arsenides and sulphides such as smalltite, $CoAs_2$, cobaltite (or cobalt glance), CoAsS, and linnaetite, Co_3S_4. These are invariably associated with nickel, and often also with copper and lead, and it is usually obtained

as a byproduct or coproduct of the recovery of these metals. The world's major sources of cobalt are the African continent and Canada with smaller reserves in Australia and the USSR [1].

An alloy of nickel was known in China over 2 000 years ago, and Saxton miners were familiar with the reddish coloured ore, NiAs, which superficially resembles Cu_2O. These miners attributed their inability to extract copper from this source to the work of the devil and name the ore "Kupfernickel" (Old Nick's copper). In 1751 A. F. Cronstedt isolated an impure metal from some Swedish ores and, identifying it with the metallic component of Kupfernickel, named the new metal "nickel". In 1804 J. B. Richter produced a much purer sample and so was able to determine its physical properties more accurately [1].

Nickel is the seventh most abundant transition metal and the twenty-second most abundant element in the earth's crust (99 ppm). Its commercially important ores are of two types [1]:

(1) *Laterites*, which are oxide/silicate ores such as garnierite $(Ni,Mg)_6Si_4O_{10}(OH)_8$, and nickeliferous limonite, $(Fe,Ni)O(OH).nH_2O$, which have been concentrated by weathering in tropical rainbelt areas, such as New Caledonia, Cuba and Queensland.

(2) *Sulfides* such as pentlandite, $(Ni,Fe)_9S_8$, associated with copper, cobalt and precious metals so that the ore typically contain about 1,5% Ni. These are found in more temperate regions such as Canada, the USSR and South Africa.

7.2 Atomic and physical properties of the elements

Cobalt is lustrous and silvery with a bluish tinge, while nickel is silvery-white. Nickel is both malleable and ductile so that it is readily worked. It is also readily obtained in finely divided forms which are catalytically very active. Table 7.1 lists some properties of cobalt and nickel. When comparing the data given it is clear why these two

elements can be determined simultaneously using the same reagent.

TABLE 7.1. Properties of the elements cobalt and nickel [1].

Property	Co	Ni
Atomic number	27	28
Number of naturally occurring isotopes	1	5
Atomic weight	58.9332	58.69
Electronic configuration	$[Ar]3d^7\ 4s^2$	$[Ar]3d^8\ 4s^2$
Electronegativity	1.8	1.8
Melting point (°C)	1 495	1 455
Boiling point (°C)	3 100	2 920
ΔH_{fus}/kJ.mol^{-1}	16.3	17.2
ΔH_{vap}/kJ.mol^{-1}	382	375
Density (20 °C)/g.cm^{-3}	8.90	8.908
Electrical resistivity (20°C)/μohm cm	6.24	6.84
Magnetism	Ferro	Ferro

7.3 Uses of Co and Ni

About 30% of the total worldwide cobalt production is devoted to the production of chemicals for the ceramic and paint industries. In ceramics the main use is now not to provide a blue colour, but rather white by counterbalancing the yellow tint arising from iron impurities. Blue pigments are, however, used in paints and inks, and cobalt compounds are used to hasten the oxidation and hence the drying of oil-based paints [1].

The bulk of nickel is used in the production of alloys both ferrous and non-ferrous. Smaller amounts of nickel are used as catalysts in the hydrogenation of unsaturated vegetable oils and in storage batteries such as the Ni/Fe batteries. Nickel is used in

apparatus for the production of NaOH due to its resistance to attack by aqueous caustic alkalis [1].

7.4 Biological importance of cobalt and nickel

The determination of trace amounts of cobalt in natural waters is of great interest because cobalt is important for living species as complexed vitamin B_{12}. Vitamin B_{12} is present in human and animal cells in the forms of adenosylcobalamin(III) and methylcobalamin(IV). The deficiency of cobalt in ruminants usually results in different types of anaemia [2]. The wasting disease in sheep and cattle known variously as "pine" (Britain), "bush sickness" (New Zealand), "coast disease" (Australia), and "salt sick" (Florida) has been recognised since the late eighteenth century. Iron treatment to this anaemic condition had mixed success, till it was found that the efficacious principle in the iron treatment was actually the impurity, cobalt [1].

Despite of its essential biological role, high concentrations of cobalt can be very dangerous. In moderate concentrations, such as 3 mg/gallon, cobalt may be hazardous to man. Toxicological effects of large amounts of cobalt include vasodilation, flushing and cardiomyopathy in humans and animals. The importance of cobalt in human and ruminant nutrition has led to work on the determination of cobalt in soils, plants, feedstuffs, herbage, natural waters and fertilizers. Investigations have been extended to the biochemistry of cobalt in animals, humans, microorganisms and enzymes [2]. Cobalt is essential for microorganisms fixing molecular N_2 and thus for higher plants relying on symbiotic nitrogen assimilation [3]. There is, however, still very little information available concerning the distribution and speciation of cobalt in the environment owing to analytical difficulties.

Nickel is the metal component of the enzyme urease and as such considered to be essential to plants. Evidence has also been presented that nickel being essential to some domestic animals. Essentiality of nickel to man does not yet seem to have been demonstrated. More attention has been focussed on the toxicity of nickel in low

concentrations, such as the fact that nickel can cause allergic reactions and that certain nickel compounds are carcinogenic [3].

The maximum recommended concentration of toxic ions such as nickel and cobalt in drinking water for livestock is: Co - 1.0 mg/ℓ and Ni - 2.5 mg/ℓ [4]. For drinking water for human consumption the upper limits are even less. Soil containing the following concentration ranges of cobalt and nickel is seen as natural and generally harmless: Co: 1 - 40 mg/kg and Ni: 10 - 1 000 mg/kg. Typical values found in soil (total determination) are 8 mg/kg and 40 mg/kg of Co and Ni respectively.

Defining the amount toxic to plants, or to animals subsisting on those plants, is very difficult. Plant concentrations indicative of toxicity are unknown for most plants and vary with growth conditions. The amount in the solid soil phase is a poor indicator of an ion's availability to plants. The concentration of ions dissolved in the ground water gives better estimates of ion concentrations that are immediately available to plants. Recommended maxima for livestock drinking water are conservative guides to the desirable maxima in ground water, because plants are much more tolerant of high trace metal concentrations than are animals. Fortunately, soil retention, exclusion by plant roots and limited translocation to the plant top, all exclude trace metal ions from the animal food chain [4].

7.5 Choice of analytical method

Various techniques are employed to determine cobalt and nickel. These techniques include IGP-AES, ETA, XRF, AAS (and f-AAS) [5], chromatography [5, 6] and potentiometry [7]. Although these techniques deliver accurate results and have low detection limits, the apparatus are very expensive and not suitable for on-site, on-line routine analysis. Spectrophotometric methods coupled with flow injection analysis proved to be a better alternative, but due to its high sample and reagent consumption, were ruled out in favour of the sequential injection systems. For this study, kinetic determinations of Co and Ni was chosen. Sequential injection analysis is, due to its

discontinuous nature, ideally suited for kinetic determinations where longer waiting times can be incorporated into the method to allow longer reaction times. Kinetic determinations rely on the precise and consistent timing and mixing conditions which take place between the time the sample is introduce into the system and the time the product passes through the detector. SIA systems are completely computer-driven and accurate and precise timing is one of its biggest advantages. The kinetic determination was also chosen because it proved to be the most cost-effective method. Since the products formed during the reactions are measured at the same wavelength, only one detector was needed.

A list of possible reagents to determine cobalt and nickel is given in Table 7.2.

TABLE 7.2 Possible reagents and methods for the detection and determination of cobalt and nickel.

Reagent	Method	Analyte	Wavelength
Nitroso-R-salt (disodium-1-nitroso-2-hydoxy-naphtalene-3,6-disulfonate) [8, 12]	Photometry	Co	516 nm
2-(5-bromo-2-pyridylazo)-5-(N-propyl-N-sulphopropylamino) aniline [9]	Photometry	Co	570 nm
Pyridylazoresorcinol (PAR) [10, 15]	Photometry, kinetic	Co, Ni	640 nm
Dithiozone (diphenylthiocarbazone) [11]	Extraction, photometry	Co	519 nm*
1-(2-pyridylazo)-2-naphtol (PAN) [11, 13]	Extraction, photometry	Co, Ni	640 nm
Dimethylglyoxime (2,3-butanedione dioxime) [11]	Gravimetry, titrimetric analysis, extraction, photometry	Ni and large amounts of Co	450 nm
Sodium diethyldithiocarbamate [11]	Extraction, photometry	Ni, Co, Cu, Fe	325 nm
p-acetylarsenazo [14]	Photometry	Ni	630 nm
2-(5-bromo-2-pyridylazo)-5-(N-propyl-N-sulfopropylamino)aniline (PSAA) [16]	Photometry, kinetic	Ni, Co	580 nm
2-hydroxybenzaldehyde thiosemicarbazone [17]	Photometry, kinetic	Ni, Co	400 nm

* Wavelength was determined experimentally with ethanol as solvent.

7.6 Principle of the kinetic determination of cobalt and nickel using PAR

The different rates of the dissociation of the citrate complexes of cobalt(II) and nickel(II) at pH 8 are used as a base for the kinetic assay of these two ions at mg/ℓ level in a sequential injection system. The first step in the determination is the formation of cobalt and nickel citrate complexes. The formation constants for the metal ion complexes are as follow: log K_f = 12.5 for cobalt and log K_f = 14.3 for nickel [18]. The values were obtained for solutions with an ionic strength of 0.5 mol/ℓ.

The dissociation is followed by the formation of the PAR complexes (which is fast compared to the dissociation). The reactions are indicated as follow:

$$M(cit)^- \rightarrow M^{2+} + cit^{3-}$$

$$M^{2+} + 2PAR \rightarrow M(PAR)_2^{2-n} + nH^+$$

where cit is the citrate anion and *n* indicates that the number of protons released depends on the pH of the system. The rate constants of the dissociation reactions are sufficiently different to enable cobalt and nickel to be determined with reasonable precision.

PAR, the scavenger in the reactions, is not selective and forms complexes with copper(II), iron(II) and (III), manganese(II), zinc(II), lead(II) and many other metal ions. Yotsuyangani *et al.* [19] have reported a method for the selective determination of iron, cobalt and nickel using PAR as a spectrophotometric reagent in a masking medium of EDTA. This is achieved by adding first PAR and then EDTA to the sample. For all tested ions except iron(III), cobalt(II), nickel(II), uranyl and palladium(II) the substitution reaction

$$M(PAR)_n + EDTA \rightarrow M(EDTA) + nPAR$$

proceeds rapidly at room temperature and masks such elements.

The method is successful only if the reaction of the more reactive component is essentially complete before the reaction of the less reactive component reaches one half-life [20] and depends on first order or pseudo-first order reaction kinetics. Theoretically the method may be used to determine more than two analytes by solving as many simultaneous equations for the absorbances as there are analytes and detectors. The number of analytes which may be determined with precision are however limited. Kinetic methods in general suffers from poor precision in one analyte if the other analyte has a much higher concentration [17].

The principle of the SIA method is that for the pseudo-first order reactions of different rates, straight line calibration curves may be obtained for samples at any time *t* after aspiration of various metal concentrations. For different metals which have different rates, the calibration curves will have different slopes, slower reacting components having lower slopes. The relative difference in the ratio of the slopes belonging to each metal give rise to equations which may be used for the determination of each metal.

7.7 The simultaneous kinetic determination of cobalt and nickel

7.7.1 Experimental

7.7.1.1 Reagents and solutions

All solutions are prepared from analytical grade reagents unless specified otherwise. Deionised water from a Modulab system (Continental Water Systems, San Antonio, TX, USA) was used to prepare all solutions and dilutions. The water used as carrier was degassed before use.

Citrate Complex Forming Reagent (CCFR): This reagent contains 0.08 mol/ℓ citrate (23.528 g $C_6O_7H_5Na_3.2H_2O$ in 1 ℓ) and 0.02 mol/ℓ borax (7.627 g $Na_2B_4O_7.10H_2O$ in 1 ℓ). The pH of the solution was adjusted to 8 using hydrochloric acid.

Colour Forming Reagent (CFR): 0.2552 g of 4-(2-pyridylazo)resorsinol monosodium monohydrate ($C_{11}H_8N_3NaO_2.H_2O$) was dissolved in 1 ℓ of CCFR, resulting in a 1 x 10^{-3} mol/ℓ PAR solution.

EDTA Masking Reagent (EMR): 18.612 g EDTA was dissolved in 1 ℓ distilled water.

Analyte stock solutions: A 100 mg/ℓ Ni(II) stock solution was prepared by dissolving 0.405 g $NiCl_2.6H_2O$ in 1 ℓ distilled water. A 100 mg/ℓ Co(II) stock solution was prepared by dissolving 0.404 g $CoCl_2.6H_2O$ in 1 ℓ distilled water. Working solutions were prepared by suitable dilution of the stock solutions.

For soil extractions a 0.43 mol/ℓ acetic acid solution was used as eluent and a 12% (v/v) ammonia solution was used to ensure the correct reaction pH.

7.7.1.2 Apparatus

The SIA system depicted in Fig. 7.1 was constructed of the following components: A Gilson Minipuls peristaltic pump (operating at 10 rpm), a magnetic stirrer, a stirrer chamber with internal volume of 500 μℓ, a 10-port electrically actuated Valco selection valve (Model ECSD10P) and a Unicam 8625 UV/visible spectrophotometer equipped with a 10 mm Hellma flow-through cell (volume 80 μℓ). The absorbance of both red coloured PAR complexes was measured at 510 nm. Data acquisition and device control were achieved using a PC30-B interface board (Eagle Electric, Cape Town, South Africa) and an assembled distribution board (MINTEK, Randburg, South Africa). The *FlowTEK* [21] software package (obtainable from MINTEK) was used throughout the procedure. The first holding coil was constructed of 3.5 m x 1.16 mm i.d. coiled Tygon tubing, the second holding coil of 1.5 m x 0.76 mm i.d. straight Tygon tubing and the reaction coil of 1.1 m x 0.76 mm straight Tygon tubing.

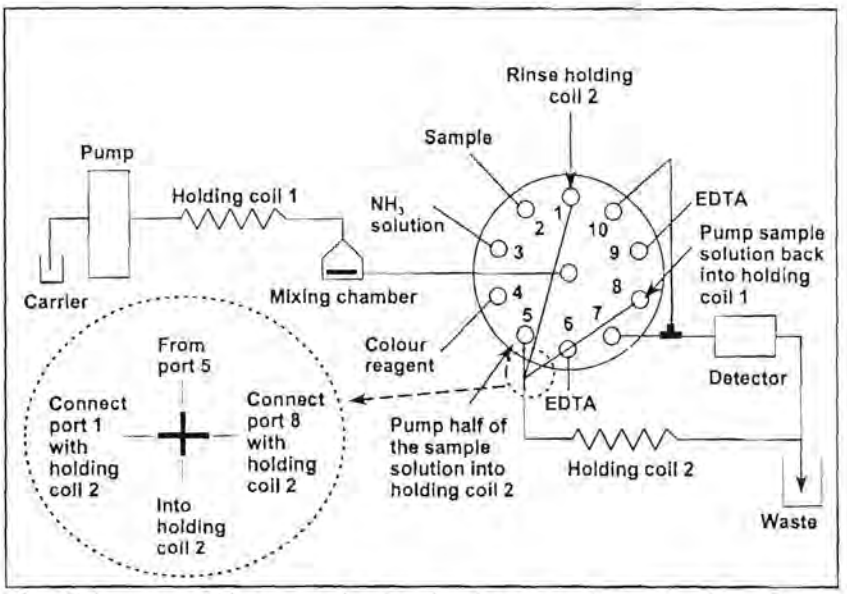

Fig. 7.1 SIA system for the simultaneous determination of trace amounts of nickel and cobalt.

7.7.1.3 Procedure

Since differential kinetic determinations dominate the simultaneous determination of two or more closely related species, like cobalt and nickel, in mixtures without prior separation, all ten ports of the valve were used to accommodate the two reactions that take place in the manifold (the faster reaction (Ni(II) with PAR and the slower reaction (Co(II) with PAR). The sample (port 2), ammonia solution (port 3) and colour reagent (port 4) were sequentially drawn up into the mixing chamber to allow thorough mixing thereof. Half of this complexed zone was pump into a second holding coil (port 5) to ensure the longer reaction time needed for the slower reaction, while the other half was reacted with EDTA (port 6) and propelled through the detector (port 7) for measurement (measuring time t_1). Since the VICI valve used in this application was able to move only in a counter-clockwise direction, it was impossible to move back to port 5 to collect the 'stored' half of the reacting zones. The second holding coil was therefore connected to port 8 via a perspex connector with four in- or outlets as shown in Fig. 7.1. When port 8 was connected to the first holding coil (occupying the port in the middle of the valve), the zone inside the second holding coil could be drawn back into holding coil 1. This zone was reacted with EDTA (port 9) and propelled through

the detector (port 10 was connected via a perspex T-piece connector to detector line) for measurement (measuring time t_2).

It must be noted that prior to each cycle the second holding coil was first rinsed to eliminate any possible sample carry-over. This was done via port 1 of the selection valve. Port 1 was connected to the second holding coil via the perspex connector (as shown in Fig. 7.1). Forward movement of the pump, allowed the movement of the wash (carrier) solution through holding coil 2.

Tables 7.3 and 7.4 give detailed representations of the procedure used. Since the FlowTEK software measures only the highest peak (peak height was used for measurements), two methods were programmed. The first was used to draw up the sample and reagents and for measurement of the first peak (measuring time t_1) and second was used for measurement of the second peak (measuring time t_2). These two methods were then combined in a procedure file to follow directly after one another without any delay.

TABLE 7.3 Device sequence of the sequential injection system used to draw up the different zones and for measurement of peak 1 (measuring time t_1).

Time (s)	Pump	Valve	Description
0	Off	Home	Pump off, valve was turned to select position 1. This position was connected via the perspex connector (with four inlets) to the second holding coil.
5	Forward	Holding coil 2	Forward movement of the pump resulted in the propulsion of the carrier (wash) solution through the second holding coil.
20	Off		Pump stopped - end of rinsing cycle.
20.5		Sample/ standard	Valve was turned to position 2 to select the sample (or standard) stream.
21.5	Reverse		The sample or standard solution was drawn up into the mixing chamber (holding coil 1).
35.5	Off		Pump stopped.
36		NH_3	Valve was turned to position 3 to select NH_3 stream.

TABLE 7.3 continue Device sequence of the sequential injection system used to draw up the different zones and for measurement of peak 1 (measuring time t_1).

Time (s)	Pump	Valve	Description
37	Reverse		NH_3 solution was drawn up into the mixing chamber.
38	Off		Pump stopped.
39		PAR	Valve was turned to position 4 to select the colour reagent stream.
40	Reverse		Colour reagent was drawn up into the mixing chamber.
46	Off		Pump stopped.
46.5		Holding coil 2	Valve was turned to position 5. This port was also connected to the second holding coil via the perspex connector (with four inlets).
47	Forward		Half of the product zone (in the mixing chamber) was pumped into the second holding coil to ensure longer reaction time.
64	Off		Pump stopped.
64.5		EDTA	Valve was turned to position 6 to select the EDTA stream.
66	Reverse		EDTA solution was drawn into holding coil 1 to react with the remaining half of the product zone.
67	Off		Pump stopped.
67.5		Detector	Valve was turned to position 7 to select the detector line.
68	Forward		The formed product zone was pumped through the detector (measuring time t_1).
192	Off		Pump stopped - end of measuring cycle 1.

TABLE 7.4. Device sequence of the sequential injection system used for measurement of peak 2 (measuring time t_2).

Time (s)	Pump	Valve	Description
0	Off	Holding coil 2	Valve was turned to select position 8. This port is also connected to the second holding coil via the four inlet perspex connector.
0.5	Reverse		The formed product zone 'stored' in holding coil 2 was drawn back into holding coil 1.
14.5	Off		Pump stopped.
15		EDTA	Valve was turned to position 9 ro select the EDTA stream.
16	Reverse		EDTA solution was drawn up into holding coil 1.
17	Off		Pump stopped.
18		Detector	Valve was turned to position 10 to select the detector line.
19	Forward		The second product zone was pumped through detector (measuring time t_2). Port 10 was connected with the detector line via a perspex T-piece connector.
135	Off		Pump stopped - end of analytical cycle.

7.7.1.4 Sample preparation

The samples analysed were aqueous samples and soil extracts. All water samples were analysed directly. Soil samples collected on a maize farm in the Northen Free State were used for analysis. Representative soil samples of 20.00 ± 0.05 g were dried at 30 °C for about 8 - 10 hours. 5.00 ±0.01 g of air-dried soil was weighed into a beaker and 50 mℓ of a 0.43 mol/ℓ CH_3COOH solution was added. The suspension was stirred for 30 minutes and then decantated or filtered. The filtrate was analysed directly (pH corrections were done on-line).

7.8 Method optimisation

Determinations involving chromogenic reagents in sequential injection analysis (SIA) are more complicated than their batch [22] and flow injection (FI) [23] counterparts, as direct acquisition of the sample spectrum can be hindered by two effects. One arises from changes in the refractive index when the injected products reach the detector. These changes give rise to a non-spectral, sample dependant variation of the signal, but can be readily corrected for by subtracting the absorbance at a wavelength at which neither the reagents nor the products absorb (using a diode array spectrophotometer [24]). The other effect originates from the absorbance of the chromogenic reagent and cannot be suppressed by instrumental zeroing (as in the case of FI) because the reagent is injected into a non-absorbing carrier and its absorption is variable.

Since PAR is a coloured reagent and absorbs in the same visible spectral region as its complexes with various metals, the peaks obtained will always be the summation of two contributions, *viz.*, that from the unreacted PAR and that from its complexes (Co-PAR and Ni-PAR in this case). Hence the actual peak height for each complex can be determined by subtracting the blank spectrum from that for an injected sample or standard. The amount of reacted PAR is assumed to be negligible relative to that of the unreacted reagent, which is plausible as the complexes formed are highly labile and a large excess of reagent is used.

7.8.1 Physical parameters

A number of physical parameters can influence the degree of dispersion and mixing in the manifold. To obtain the highest sensitivity and precision, but still maintain a sufficient sample throughput, it was necessary to optimise these parameters.

7.8.1.1 Pump speed

The pump speed does not only influence the volume of the different zones drawn up, but also the residence time of the zones in the manifold conduit. Since kinetic determinations need very precise timing, this parameter was optimise to get an optimum flow rate that suites the formation of both the cobalt and nickel complexes. Flow rates between 1.0 and 3.0 mℓ/min were evaluated. As seen from Fig. 7.2, the peak height increases with increasing flow rate to a maximum flow rate of 2.5 mℓ/min where after the peak height decreases. The % RSD improves with increasing flow rate in the same way as the sensitivity. This can be observed for both measuring times t_1 and t_2. An optimum flow rate of 2.5 mℓ/min was chosen due to its best precision and sensitivity. Care was taken that the volumes were adjusted to maintain constant values for all flow rates. This was done by altering the time the sample and reagents were being drawn up.

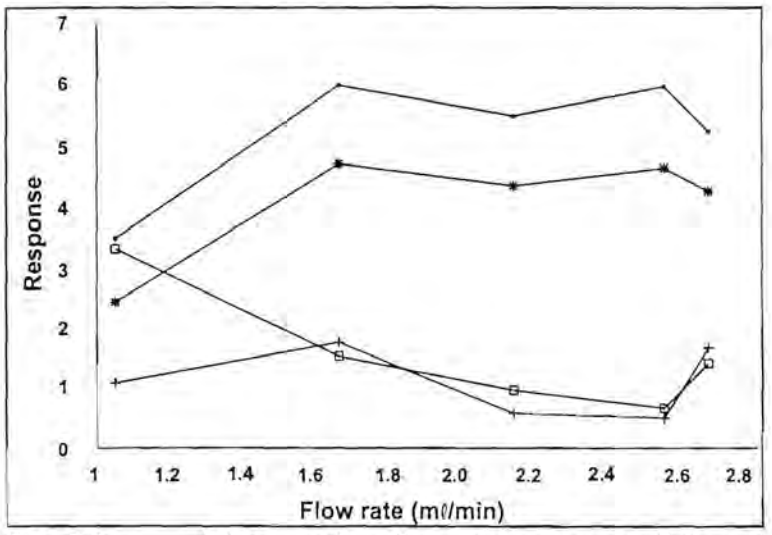

Fig. 7.2 Influence of the flow rate on the sensitivity and precision at both measuring times, t_1 and t_2. —●— = Peak height (t_1); —+— = %RSD (t_1); —✱— = Peak height (t_2) and —□— = %RSD (t_2).

7.8.1.2 Mixing chamber

Mixing chambers are used in SIA mainly to dilute highly concentrated samples [25] or to ensure adequate mixing of the zones when more than three zones are involved [26]. Because the formed product zone in this analysis was split into two, it was of utmost importance that thorough mixing took place. Three different systems were evaluated: In the first the mixing chamber was absent and in the second and third, mixing chambers with volumes of 1.2 and 0.5 mℓ respectively were incorporated into the first holding coil.

Evaluation of the first system was done by using a binary mixture of cobalt and nickel (10 mg/ℓ each). The relative peak height obtained with this system was 3.34 with a relative standard deviation (RSD) of 0.5% at t_1 and a relative peak height of 3.30 (RSD = 0.1%) at t_2.

Incorporation of the larger mixing chamber into the SIA system lead to excessive dilution, resulting in poor sensitivity especially at t_2 (relative peak height = 3.25 for t_1 (%RSD = 0.77) and 1.94 for t_2 (%RSD = 0.89%)). For the smaller mixing chamber the resulted dispersion was not so large and the contribution of the mixing chamber rendered very positive results. An increase in relative peak height at both measuring times was observed (peak height = 5.33 for t_1 (%RSD = 2.76) and 4.35 for t_2 (%RSD = 2.01)). The poor reproducibility was due to small air bubbles which accumulated in the upper part of the mixing chamber. This problem was solved after the in- and outlet of the mixing chamber were exchanged. Although the SI system containing the smaller mixing chamber needed longer rinsing times, due to the bigger dispersion in the mixing chamber, it was still chosen as the desirable system, because the better sensitivity outweighed the drawback of longer rinsing times.

It is important to keep the tubing connecting the mixing chamber with the valve as short as possible. This will ensure that major part of the stack of zones drawn up into the holding coil reaches the mixing chamber, which will result in better mixing.

7.8.1.3 Sample volume

As it is one of sequential injection analysis' advantages, the sample volume was altered by increasing or decreasing the time during which the sample was drawn up. The sensitivity increase as the sample volume increased for both measuring times. It is clear from Fig. 7.3 that volumes larger than 600 $\mu\ell$ should lead to even higher sensitivities at the two measuring times. The improvement when enlarging the volume from 550 to 600 $\mu\ell$ was, however, only 3.14% for t_1 and 9.81% for t_2. The good precision obtained at 600 $\mu\ell$ and the undesired longer rinsing times for larger volumes were both criteria which resulted in the choice of 600 $\mu\ell$ as optimum sample volume.

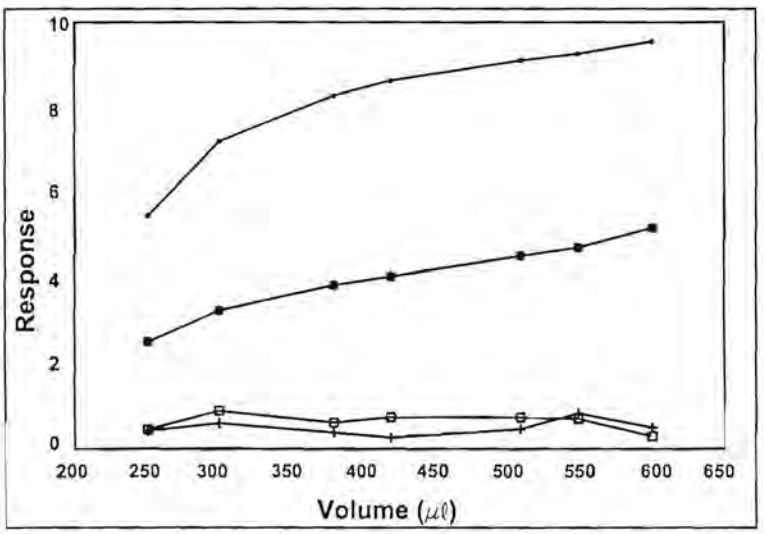

Fig. 7.3 Influence of the sample volume on peak height and reproducibility at t_1 and t_2. ◆ = Peak height (t_1); + = %RSD (t_1); ■ = Peak height (t_2) and □ = %RSD (t_2).

7.8.1.4 Colour reagent and complex forming agent volume

The citrate complex forming reagent agent was used to dissolve the PAR reagent, therefore the influence of the volume of both were evaluated at the same time. Different volumes ranging from 170 - 680 $\mu\ell$ were evaluated. The results, presented in Fig. 7.4, show that larger volumes resulted in better sensitivity and precision.

Unfortunately, larger volumes also lead to larger background values and therefore the signal-to-baseline ratio (S/B ratio) was used as criteria to obtain the optimum volume. The increase in relative peak height (response) for volumes between 170 - 680 $\mu\ell$ was from 6.76 to 7.53 for measuring time 1 (t_1) and from 6.43 to 7.09 for measuring time 2 (t_2). This resulted in a 11.39% increase for t_1 and 10.26% for t_2. The background signal for the same change in volume had increased with 48.15% for t_1 (0.81 to 1.20 units) and with 57.14% for t_2 (0.98 to 1.54 units). It was therefore clear that smaller reagent volumes resulted in better signal-to-background ratios. For both t_1 and t_2 the best precision and S/B ratio were obtained at 250 $\mu\ell$. The relative standard deviation were 0.52% and 0.37% respectively.

Additional complex forming agent was added to the sample before addition of the colour reagent to investigate the effect on the initial complex formation. Different volumes were evaluated. The results (Fig. 7.5) show a slight increase in sensitivity at t_1 and a decrease in peak height at t_2. The % RSD obtained is overall very good and only small variations are visible at the different volumes. The variation in peak height at the two different times are mainly due to the different ratios in which the product zone is divided. Care must, therefore, be taken that the zone is divided in the same ratio for each different analysis. It is clear from the results that it was unnecessary to add additional complex forming agent to the system. To remove the complex forming agent completely was however not advisable, since better results were obtained with the complex forming agent than without. The sensitivity as well as the reproducibility of the method were better when the complex forming agent were used.

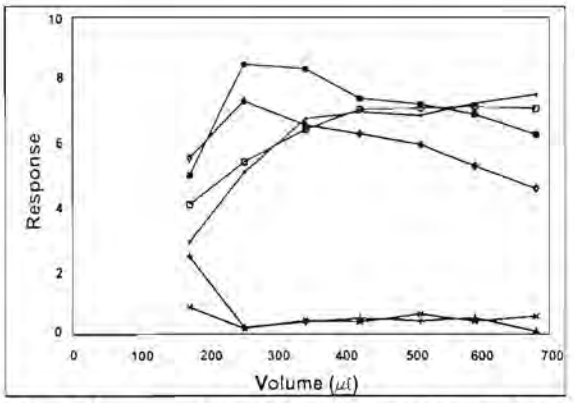

Fig. 7.4 Influence of the volume of the colour reagent and complex forming reagent mixture on sensitivity and reproducibility at t_1 and t_2. ◆ = Peak height (t_1); — = %RSD (t_1); ✱ = S/B ratio (t_1); ○ = Peak height (t_2); ◇ = %RSD (t_2) and ✕ = S/B ratio (t_2).

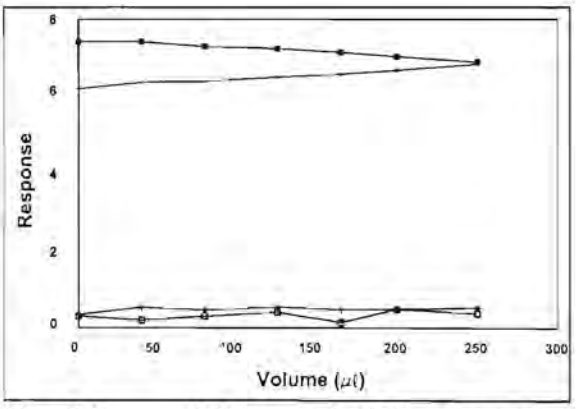

Fig. 7.5 Influence of additional complex forming agent on sensitivity and precision at both measuring times. ◆ = Peak height (t_1); — = %RSD (t_1); ✱ = Peak height (t_2) and ○ = %RSD (t_2).

7.8.1.5 Reagent concentration

Higher PAR concentrations led to better sensitivity, but also led to unacceptable high background values. Once again it was needed to take the signal-to-background ratio as determining criteria to obtain an optimal concentration for the colour reagent. A concentration of 1 x 10^{-3} mol/ℓ PAR was chosen as optimum, due to its good signal to background ratio and reproducibility. Table 7.5 illustrates the results obtained.

TABLE 7.5 Results obtained after evaluation of the PAR concentration.

Concentration (mol/ℓ)	Measuring time 1				Measuring time 2			
	RPH*	Back-ground	S/B ratio	%RSD	RPH	Back-ground	S/B ratio	%RSD
1 x 10^{-1}	7.53	1.20	6.28	0.09	7.09	1.54	4.60	0.57
1 x 10^{-2}	7.26	1.05	6.91	0.52	7.17	1.35	5.31	0.41
1 x 10^{-3}	5.10	0.60	8.5	0.22	5.42	0.74	7.32	0.18
1 x 10^{-4}	2.90	0.58	5	2.46	4.08	0.74	5.55	0.86

* RPH - relative peak height

7.8.1.6 EDTA volume

Several ions interfere in the simultaneous determination of Co(II) and Ni(II), as the colour reagent (PAR) is not selective. Addition of EDTA to the product zone allows the determination of the analytes in the presence of some interferences, because the conditional forming constants for the interferences with EDTA is larger than those of the interferences with PAR [18]. Addition of EDTA however also retarded the reaction rate of the colour forming reactions of nickel(II) and cobalt(II) with PAR to such an extend that it practically came to a standstill. EDTA was therefore added just prior to detection. Various different volumes were investigated. The results (Fig. 7.6) show that the peak height decreased as the volume increased. A optimum volume of 40 $\mu\ell$ was used to mask the major interferences.

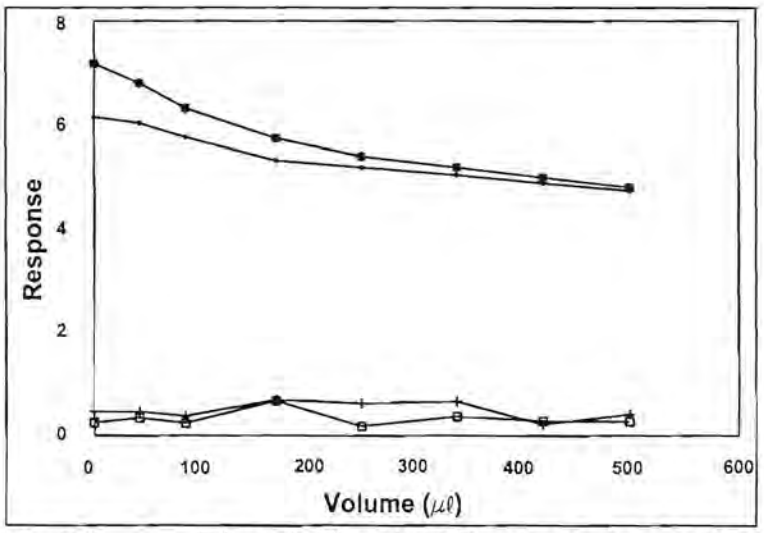

Fig. 7.6 Effect of different EDTA volumes on sensitivity and precision at t_1 and t_2. -●- = Peak height (t_1); -+- = %RSD (t_1); -■- = Peak height (t_2) and -□- = %RSD (t_2).

7.8.2 Chemical parameters

7.8.2.1 pH

The complexation of metal ions with most spectrophotometric reagents, and especially with those ligands that may be protonated, is dependant on the pH of the reaction medium as well as on the nature and concentration of the concerned ligand. Plots of pH versus absorbance, such as those obtained under static conditions with a number of metals and 4-(2-pyridylazo)resorcinol (PAR) are already established [27]. The influence of reaction pH was investigated and the results (Fig. 7.7) show that a pH of 8.00 gave the best precision and sensitivity. This pH was therefore chosen as optimum reaction pH. The pH of the sample influences the reaction as well. The pH of the water samples were in the order of 5.2 and for these pH values the added borax and citrate in the colour reagent were able to buffer the system to pH 8.00. For the soil samples, obtained by extraction, the pH was in the order of 1.10. Lower pH values promote the formation of the cobalt complex and interfere as a result seriously in the determination of nickel. To obviate this it was necessary to increase the pH of the sample to an extent that the added borax and citrate could buffer the reaction at pH 8.00.

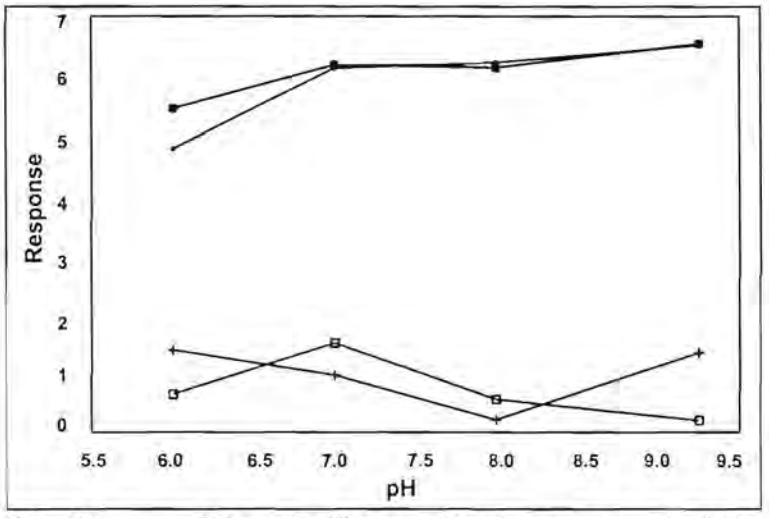

Fig. 7.7 Effect of different pH values on reproducibility and peak height at both measuring times. ◆ = Peak height (t_1); — = %RSD (t_1); ■ = Peak height (t_2) and □ = %RSD (t_2).

Addition of a 12% v/v NH_3 solution between the sample zone and the colour reagent zone led to an increase in pH and improved the sensitivity. NaOH was not added, because of the formation of less soluble $Ni(OH)_2$ (K_{sp} = 2.8 x 10^{-16}) and $Co(OH)_2$ (K_{sp} = 2.5 x 10^{-16}) [18]. Ammonia was seen to be more appropriate since the amine complexes of Co and Ni have very small formation constants (log K_f = 2.1 for Co and log K_f = 2.8 for Ni) [18]. The resulted amine complexes are also soluble.

The results (Fig. 7.8) show that the formation of the cobalt complex was definitely favoured at lower pH values. The addition of the NH_3 zone limited this advantage of Co and resulted in more appropriate peak heights for both measuring times. The obtained peak height values for samples of pH 5.20 were 6.35 (RSD = 0.89%) and 6.70 (RSD = 0.73%) for t_1 and t_2, respectively. Addition of 210 $\mu\ell$ NH_3 to samples with pH 1.10 resulted in peak height of 6.20 (RSD = 0.79%) and 6.80 (RSD = 1.06%) for t_1 and t_2, respectively.

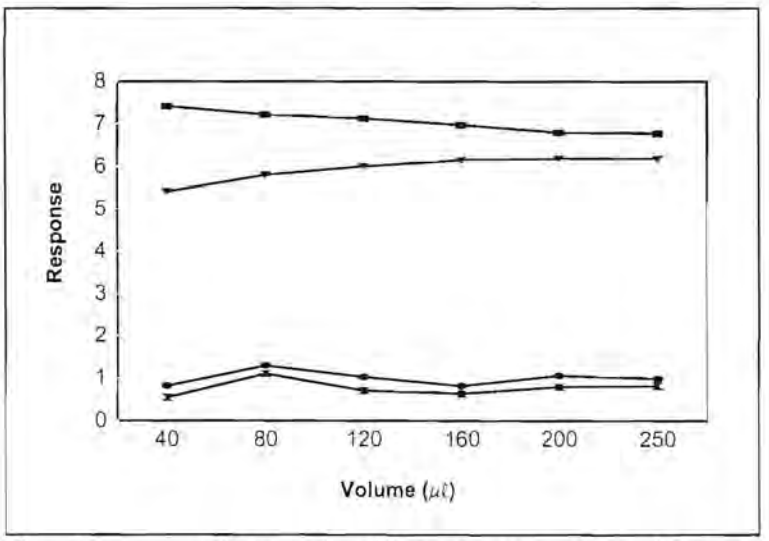

Fig. 7.8 Effect of different volumes of NH_3 on reproducibility and peak height at both measuring times for samples with pH 1.10. ▼ = Peak height (t_1); ● = %RSD (t_1); ■ = Peak height (t_2) and ▽ = %RSD (t_2).

7.8.2.2 Zone sequencing

Incorporation of the NH_3 zone in front of the sample zone resulted in an slight increase in sensitivity, but the precision became very poor (RSD > 12.1%). The optimum zone sequence was therefore sample, NH_3 and then the colour reagent. The NH_3 was not used when water samples were analysed.

7.9 Kinetic data and reaction order

7.9.1 Reaction rates

Chemical reactions rates cover a very wide range of velocities. Some reactions, such as the neutralization of a strong acid with a strong base, are so rapid that they appear to reach equilibrium instantaneously; whereas others, such as the (non-catalysed) reaction between oxygen and hydrogen at room temperature, are so slow that no reaction can be detected [29]. Reactions with half-lives larger than about ten seconds are considered to be *slow*, whereas those with half-lives shorter than ten seconds are considered to be *fast*. Since both complexes under discussion in this study proved to be moderate reactions, more attention will be given to the determination of reaction rates of slower reactions.

The rate of slow chemical reactions in solution can generally be studied by quite simple and conventional methods. The reactants are mixed in some vessel, and the progress of the reaction is followed by (i) titrating aliquots of the mixture or by (ii) measuring at known times, a physical property of the solution such as optical absorption or voltammetric diffusion current [29].

The speed of initial mixing of the components in the vessel, places a limit on the minimum half-live time that can be measured in this way. If the mixing is accomplished by simple stirring devices such as magnetic stirring bars, the mixing takes a few seconds, and reactions with half-live times shorter than 10 seconds are difficult to

measure with acceptable accuracy. On the other hand, the kinetics of reactions with long half-lives can be determined, but such determinations take a long time and are, therefore, undesirable for analytical purposes. Two hours are arbitrarily considered the longest acceptable time for routine analysis [29].

If the reaction is completed in more than two hours or less than ten seconds, several simple techniques can be used to adjust the rate so that the half-live lies within the desired range. These are: (a) changing the temperature of the reaction system, (b) changing the concentration of the reactants, and (c) changing the solvent medium or ionic strength of the solution.

The relationship between temperature and the rate constant k of a chemical reaction is given by the Arrhenius equation [29]

$$\frac{d(\ln k)}{dT} = \frac{E^*}{RT^2}$$

or in its integrated form $k = Ae^{-E^*/RT}$

where E* = activation energy

R = universal gas constant

and A = frequency factor.

For a large number of homogeneous reactions, the rate constant increase two or three times for each 10°C rise in temperature [29]. The temperature in the laboratory was kept at a constant 19°C to eliminate any possible fluctuations in results.

Reactions with very large rate constants can be measured simply by using low concentrations of reactants, provided that the methods sensitive enough to measure the small changes in concentration are available. High concentrations of the reacting species can be employed to speed up reactions with small rate constants, although

changes in the activity coefficients may hamper the calculation of initial concentration when high concentrations of reactants are used [29].

The PAR concentration used in this determination was restricted to 1 x 10^{-3} mol/ℓ since higher concentration led to higher background values and unacceptable low signal-to-background ratios (see Table 7.5).

Table 7.6 gives the kinetic data collected for the reaction between cobalt and PAR, while the data for the reaction between Ni(II) and PAR is given in Table 7.7. Solutions of 5 mg/ℓ Co(II) and 5 mg/ℓ Ni(II) were respectively used to determine the reaction rates. The same procedure was followed as for the determination of the analytes, but the flow was stopped just after the peak maximum were observed (for cobalt this was 91.6 s after the start of the analysis and for nickel 90.22 s). This time is taken as the starting time, t_0, for determining the rate constant. The time used to calculate the rate constant was calculated as the real time (from the start of the analysis) minus t_0. Since peak height is an indication of the absorbance of the specie at that moment, the absorbance (A) is calculated as peak height measured at a specific time (t) minus the peak height value (A_0) at the time the flow was stopped, t_0. Fig. 7.9 shows a plot of the response (A) versus time, while Fig. 7.10 shows a plot of $\ln(A - A_0)$ versus time for cobalt and Figs. 7.11 and 7.12 give the same plots for nickel.

TABLE 7.6 Kinetic data for the determination of the rate constant of the reaction between Co(II) and PAR.

Real time (s)	Absorbance (A)	Time (s)	$A - A_0$	$\ln(A - A_0)$
$91.64 = t_0$	$3.26 = A_0$	0	0	-
100.88	3.29	9.24	0.03	-3.51
110.82	3.33	18.18	0.07	-2.66
120.77	3.39	29.13	0.13	-2.04
130.72	3.44	39.08	0.18	-1.71
140.66	3.48	49.02	0.22	-1.51
150.61	3.55	58.97	0.29	-1.24
160.55	3.60	68.91	0.34	-1.08
170.50	3.65	78.86	0.39	-0.94
180.45	3.68	88.81	0.42	-0.87
190.39	3.70	98.75	0.44	-0.82
200.34	3.72	108.7	0.46	-0.78
210.28	3.75	119.64	0.49	-0.71
220.23	3.76	128.59	0.50	-0.69
230.18	3.78	138.54	0.52	-0.65
240.12	3.79	148.48	0.53	-0.63
250.07	3.80	158.43	0.54	-0.62

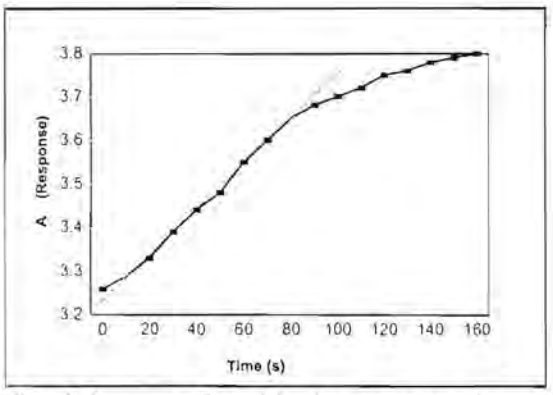

Fig. 7.9 Graphical representation of the measured peak height (response) versus time for Co.

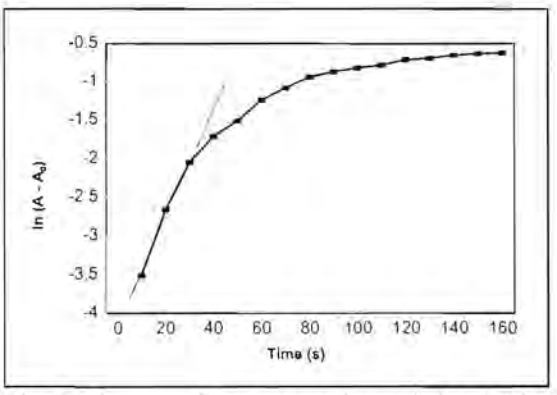

Fig. 7.10 Representation of the $\ln(A - A_0)$ versus time graph for Co.

TABLE 7.7 Kinetic data for the determination of the rate constant of the reaction between Ni(II) and PAR.

Real time (s)	Absorbance (A)	Time (s)	$A - A_0$	$\ln(A - A_0)$
$90.22 = t_0$	$2.46 = A_0$	0	0	-
100.17	2.55	9.95	0.09	-2.41
110.82	2.65	20.60	0.19	-1.66
120.77	2.75	30.55	0.29	-1.24
130.72	2.86	40.50	0.40	-1.29
140.66	2.96	50.44	0.50	-0.69
150.61	3.07	60.39	0.61	-0.49
160.55	3.16	70.33	0.70	-0.36
170.50	3.24	80.28	0.78	-0.25
180.45	3.30	90.23	0.84	-0.17
190.39	3.35	100.17	0.89	-0.12
200.34	3.40	110.12	0.94	-0.06
210.28	3.44	120.06	0.98	-0.02
220.23	3.47	130.01	1.01	0.01
230.18	3.50	139.96	1.04	0.04
240.12	3.53	149.90	1.07	0.07
249.36	3.55	159.14	1.09	0.09

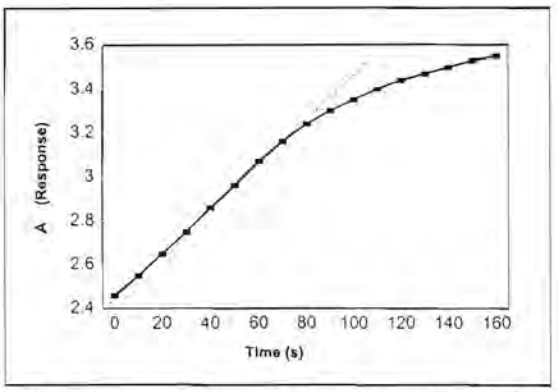

Fig. 7.11 Graphical representation of the measured peak height (response) versus time for Ni.

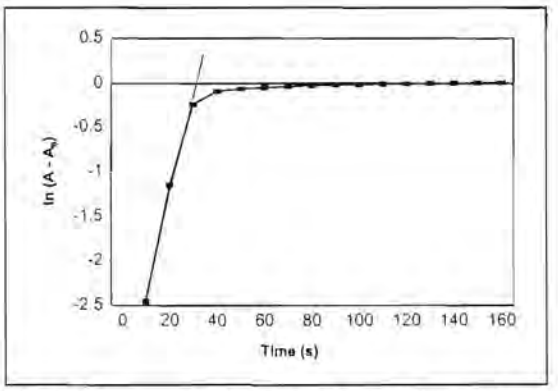

Fig. 7.12 Representation of the $\ln(A - A_0)$ versus time graph for Ni.

7.9.2 Reaction rate laws

The determination of the rate law is simplified by the isolation method in which the concentrations of all the reactants except one are in large excess. If reagent B is in large excess, it is a good approximation to take its concentration as constant throughout the reaction. Then, although the true rate law might be second-order overall, and

$$v = k[A][B]$$

[B] can be approximated by $[B]_0$ and the equation became

$$v = k'[A]$$

where $k' = k[B]_0$ which has the form of a first-order rate law. Since the true rate law has been forced into first-order form by assuming a constant B concentration, it is called a pseudo first-order rate law [28]. The PAR reagent was therefore added in 10-fold excess to ensure excess of reagent and thus a pseudo first-order reaction rate.

The kinetic determination is only successful, if the reaction of the more reactive component is essentially complete before the reaction of the less reactive component reach one half-life [20].

The order of the substitution reaction

$$ML^- + 2\ PAR \rightarrow M(PAR)_2^{2+} + L^{3-}$$

was established as pseudo-first order by standard kinetic methods using the optimised SIA system (see Figures 7.10 and 7.12). A linear least square regression analysis of ln ([A] - $[A]_0$) versus time gave, for nickel $K_{obs} = 0.050\ s^{-1}$ with a correlation coefficient of 0.9897 and for cobalt, $K_{obs} = 2.10\ s^{-1}$ with a correlation coefficient of 0.9919. The dotted lines in the figures indicated the region of the graphs used to determine reaction rates as well as to confirm the pseudo-first order reactions.

7.10 Evaluation of the SIA method

The proposed SIA method was evaluated under optimum running conditions with regard to linearity, sample frequency, reproducibility, sample interaction, detection limits, accuracy and major interferences.

7.10.1 Linearity

Calibration curves for the two metals were set up at both measuring times. Linear calibration curves were obtained for each individual metal ion at the two different measuring times. The graphs are linear between 0 and 10 mg/ℓ in each case (Table 7.8). For nickel: $r^2 = 0.9866$ at t_1 and 0.9918 at t_2 and for cobalt: $r^2 = 0.9964$ at t_1 and 0.9907 at t_2. The concentration range is limited by the fact that PAR absorbs at the measured wavelength and that the concentration of PAR needs to be kept significantly above that of the analyte to ensure rapid scavenging after the dissociation of the citrate complex.

TABLE 7.8. Calibration values for Co(II) and Ni(II) respectively.

Concen-tration	Cobalt(II)				Nickel(II)			
	Relative peak height		% RSD		Relative peak height		% RSD	
	t_1	t_2	t_1	t_2	t_1	t_2	t_1	t_2
Blank	0.55	0.75	1.4	1.8	0.46	0.65	1.4	1.4
1 mg/ℓ	1.67	1.44	0.5	0.7	0.94	1.19	1.1	0.6
2 mg/ℓ	3.11	2.40	0.4	0.4	1.46	1.77	1.0	1.5
5 mg/ℓ	5.81	4.37	0.5	0.4	2.77	3.35	1.1	0.9
10 mg/ℓ	9.61	8.42	0.3	0.3	4.25	5.25	0.7	0.6

7.10.2 Sample frequency and precision

Kinetic determinations have the disadvantage that it is slower than other analytical applications. Sufficient time need to elapsed to allow the slower reaction to take place to a desirable level. Since the total analysis time was 327 s, the proposed SIA method was able to monitor nickel and cobalt at a rate of 11 samples per hour with a relative standard deviation < 1.2% (Table 7.9).

TABLE 7.9. Precision of the proposed SIA method.

Composition of standards		% RSD	
$[Ni^{2+}]$ in mg/ℓ	$[Co^{2+}]$ in mg/ℓ	t_1	t_2
1.0	5.0	0.3	0.6
2.0	4.0	0.3	0.4
3.0	3.0	0.8	0.3
4.0	2.0	0.7	0.3
5.0	1.0	0.7	1.0
5.0	5.0	0.6	0.6
Soil extracts		% RSD	
$[Ni^{2+}]$ in mg/ℓ	$[Co^{2+}]$ in mg/ℓ	t_1	t_2
2.5	3.5	0.4	0.4
3.0	3.0	1.2	0.7
3.5	3.0	0.9	1.0

7.10.3 Sample interaction

Although the second holding coil was rinsed before each cycle, some carry-over between samples was experienced. The sample interaction between successive samples was calculated to be 0.53% for measuring time 1 and about 1.4% for measuring time 2. A sample with low analyte concentration (1 mg/ℓ) was analysed, followed by a sample with analyte concentration ten times higher than the first. To evaluate sample interaction the first sample was analysed again. Sample carry-over

was then calculated according to the difference between the two peak height values [30]. The percentage carry-over calculated was low enough to be ignored.

7.10.4 Accuracy

To evaluate the accuracy of the system two different protocols can be followed. The first and most common method is the construction of a calibration curve for each individual metal at both measuring times. Because absorbance is additive two equations (at t_1 and t_2) are obtained which should yield the required unknown concentrations when solved simultaneously [20]. The second calculation involved the use of matrixes [31]. The general equation can be written as follows:

$$Y = X\beta + \epsilon$$

where Y is a matrix of *p* responses measured from each individual metal (n), X is a matrix of *k* independent variables applicable on all responses of each individual (n). β is a matrix containing the unknown intercepts and regression coefficients and ϵ is a matrix containing residual terms to describe each element in Y exactly. The unknown regression coefficients can be obtained by the following equation:

$$X^TY = X^TX\beta$$

or

$$\beta + (X^TX)^{-1} X^TY$$

β can be used in the regression model to calculate the unknown concentrations. This method accounts for the interaction between the different analytes as well.

Five different aqueous mixtures of cobalt and nickel were analysed. Using the method involving matrix calculations the concentration values of the different analytes were obtained. The results are listed in Table 7.10. The calculated percentage recovery yielded satisfactory results in most cases. Four soil extracts were also analysed. The results and percentage recovery are given in Table 7.11. As can be seen from the last results, longer extraction times did not improve the extraction. The detection limits for the various analytes were also calculated using matrix calculations. The values used for X were $3\sigma + K$, where σ is the standard deviation of the baseline and K is the average peak height of the baseline. The calculated detection limits for nickel and cobalt were 0.14 mg/ℓ and 0.20 mg/ℓ, respectively.

The results (in Tables 7.10 and 7.11) was confirmed using the construction of two different calibration curves for each metal at the two measuring times. The absorbance A_t at time t for a chemical species M of molar absorbtivity ε_M in a cell length, l, forming with a first order rate constant, k, at temperature, T, is related to the initial concentration $[M']$ of a reacting species 'if the rate shows first order dependence on the species' by the equation

$$A_t = \varepsilon_M l[M'](1 - e^{-kTt}) + A' \qquad (7.1)$$

where A' is the initial absorbance of the system.

For measurements made on individual species, M, at fixed time (t), $\varepsilon_M l(1 - e^{-k}T')$ is a constant $K_{M,t}$. Therefore

$$A_t = K_{M,t}[M'] + A' \qquad (7.2)$$

This is true for a static system, but in the SIA system dispersion, D, of the sample zone occurs which is constant D_t for a fixed point down-stream, assuming constant flow rate, thus

$$A_t = D_t K_{M,t}[M'] + A' \qquad (7.3)$$

Therefore at measuring time 1 ($t = t_1$), for a sample

$$A_{t_1} = D_{t_1} K_{Co,t_1}[Co'] + D_{t_1} K_{Ni,t_1}[Ni'] + A' \qquad (7.4)$$

and at measuring time 2 ($t = t_2$)

$$A_{t_2} = D_{t_2} K_{Co,t_2}[Co'] + D_{t_2} K_{Ni,t_2}[Ni'] + A'' \qquad (7.5)$$

the terms $Dt\,K_{M,t}$ for each element (cobalt and nickel) at each measuring time (t_1 and t_2), and A' and A'' are obtained from calibration curves using solutions of the individual metals at each measuring time. They are the slopes and intercepts, respectively, of

these calibration curves. Then for each sample, A_{t1} and A_{t2} are obtained and equations (7.4) and (7.5) are then solved simultaneously for [Co'] and [Ni'].

For this system the following calibration curves were obtained:

At measuring time 1 (t_1) for Co: $A_{t1} = 1.28[Co] + 0.50$

At measuring time 1 (t_1) for Ni: $A_{t1} = 0.615[Ni] + 0.338$

Thus in terms of equation (7.4) these two calibration curves add up to give:

$$A_{t1} = 1.28[Co] + 0.615[Ni] + 0.838.$$

At measuring time 2 (t_2) for Co: $A_{t2} = 0.825[Co] + 0.705$

At measuring time 2 (t_2) for Ni: $A_{t2} = 0.56[Ni] + 0.643$

Thus in terms of equation (7.5) these two calibration curves add up to give:

$$A_{t2} = 0.825[Co] + 0.56[Ni] + 1.348.$$

The results obtained by solving the obtained equations were approximately the same as the results given in Tables 7.10 an 7.11. The percentage recovery for the different analysis were slightly lower than the values obtained in Tables 7.10 and 7.11. The reason therefore is possibly that the addition of the calibration curves, of the individual analytes, does not include the interaction between the two analytes as it is when using the matrix method.

TABLE 7.10 Accuracy of the proposed SIA system for the aqueous samples analysed using matrix calculations

Known concentration in mg/ℓ		Concentration obtained with SIA in mg/ℓ		% Recovery	
$[Co^{2+}]$	$[Ni^{2+}]$	$[Co^{2+}]$	$[Ni^{2+}]$	$[Co^{2+}]$	$[Ni^{2+}]$
1.0	5.0	0.87	5.13	87	102.6
2.0	4.0	2.21	3.79	110.5	94.8
3.0	3.0	2.93	3.07	97.7	102.3
4.0	2.0	4.10	1.90	102.5	95.0
5.0	1.0	4.89	1.11	97.8	111.0

TABLE 7.11 Accuracy of the proposed SIA system for the soil extracts analysed using matrix calculations

Known concentration in mg/ℓ		Concentration obtained with SIA in mg/ℓ		% Recovery	
Soil samples					
2.50	3.50	2.76	3.24	110.4	92.6
3.00	3.00	2.89	3.11	96.3	103.7
3.50[*]	3.00[*]	3.26	2.74	93.1	91.3
3.50[#]	3.00[#]	3.30	2.70	94.3	90.0

[*] Extraction time: 30 minutes
[#] Extraction time: 16 hours

7.10.5 Interferences

Several metal ions interfered in the determination, because the PAR reagent is not selective. Addition of an EDTA zone to the sample zone (5 mg/ℓ for both Co(II) and Ni(II)) allowed the system to tolerate Pb(II), V(V), Cr(III), Zn(II), Ca(II) and Mg(II) up to 10 mg/ℓ. This represented a 1 :1 ratio with the upper limit of detection of both Co and Ni of the proposed SIA method. Iron(III) interfered, however, seriously regardless the amount of EDTA added to the reaction mixture. Masking of the iron(III) with oxalate (log K_f = 8.0) or thiourea [18] made the determination of cobalt(II) and nickel(II) very selective.

7.11 Conclusion

The proposed method permits the resolution of binary mixtures of cobalt and nickel at low levels. No prior separation is necessary and simple and rapid determinations can be performed by employing coupled on-line complex formation and ligand substitution reactions in a sequential injection analyser. The method of differential kinetic analysis has proved to be effective in this analysis. Good precision and sensitivity were obtained with the method as well as satisfactory selectivity.

7.12 References

1. N. N. Greenwood and A. Earnshaw, **Chemistry of the Elements**, Pergamon Press, Oxford, 1984.
2. A. I. Yuzefovsky, R. F. Lonardo, M. Wang and R. G. Michel, **Jour. Anal. Atom. Spectr., 9** (1994) 1195.
3. H. A. McKenzie and L. E. Smythe, **Quantitative Trace Analysis of Biological Materials**, Elsevier, 1988, pp 421 - 435.
4. H. L. Bohn, B. L. McNeal and G. A. O'Connor, **Soil Chemistry**, 2nd edition, Wiley Interscience, Chichester, 1985, p 314.
5. **Cobalt in Potable Waters, Methods for the Examination of Waters and Associated Materials**, HMSO, 1981.
6. A. Ali, H. Shen and X. Yin, **Anal. Chim. Acta, 369** (1998) 215.
7. A. Economu and P. R. Fielden, **Talanta, 46** (1998) 1137.
8. M. Martinelli, H. B. Fo, M. A. Z. Arrunda and A. E. G. Zagatto, **Quim. Anal. (Barcelona), 8** (1989) 129.
9. T. Yamane and K. Koshino, **Anal. Chim. Acta, 261** (1992) 205.
10. M. A. Z. Arrunda, E. A. G. Zagatto and N. Maniasso, **Anal. Chim. Acta, 283** (1993) 476.
11. J. Fries and H. Getrost, **Organic Reagents for Trace Analysis**, E. Merck, Darmstadt, 1977.
12. Z. C. Zhu, **Fenix-Huaxue, 23** (1995) 1444.
13. P. Dolezel and V. Kuban, **Coll. Czech. Chem. Comm., 53** (1988) 1162.
14. S. L. Zhao, X. Q. Xia, H. R. Ma and H. J. Xi, **Talanta, 41** (1994) 1353.
15. R. E. Taljaard and J. F. van Staden, **Anal. Chim. Acta, 366** (1998) 177.
16. T. Yamane and C. Ishimizu, **Mikrochim. Acta (Wien), 1** (1991) 121.
17. A. Fernandez, M. D. Luque de Castro and M. Valcarcel, **Anal. Chem., 56** (1984) 1146.
18. L. W. Potts, **Quantitative Analysis. Theory and Practice**, Harper and Row Publishers, New York, 1987.
19. T. Yotsuyanagi, R. Yamashita and K. Aomura, **Anal. Chem., 44** (1972) 1091.

20. D. Betteridge and B. Fields, **Fresenius Z. Anal. Chem.**, **314** (1983) 386.

21. G. D. Marshall and J. F. van Staden, **Anal. Instrum.**, **20** (1992) 79.

22. E. Gómez, J. M. Estela and V. Cerdà, **Anal. Chim. Acta**, **249** (1991) 513.

23. A. Cladera, E. Gómez, J. M. Estela, V. Cerdà, A. Alvarez Ossorio, F. Rioncón and F. Salvà, **Int. J. Environ. Anal. Chem.**, **45** (1991) 143.

24. E. Gómez, C. Tomàs, A. Cladera, J. M. Estela and V. Cerdà, **Analyst**, **120** (1995) 1181.

25. A. Baron, M. Guzman, J. Růžička and G. D. Christian, **Analyst**, **117** (1992) 1839.

26. M. Guzman and B. J. Compton, **Talanta**, **40** (1993) 1943.

27. D. Betteridge and B. Fields, **Anal. Chim. Acta**, **132** (1981) 139.

28. P. W. Atkins, **Physical Chemistry**, fourth edition, Oxford University Press, Oxford, 1990, pp 782 - 784.

29. G. D. Christian and J. E. O'Reilly, **Instrumental Analysis**, second edition, Allyn and Bacon, Inc., Boston, 1986, pp 560 - 593.

30. R. E. Taljaard, **Sequential Injection Analysis as Process Analyzers**, MSc - Thesis, University of Pretoria, 1996.

31. K. R. Beebe and B. R. Kowalski, **Anal. Chem.**, **58** (1987) 1007A.

CHAPTER 8

Simultaneous Determination of Mercury(II) and Cobalt(II) in Aqueous, Soil and Biological Solutions using a Simple Sequential Injection Extraction Method

8.1 Introduction

Mercury was used in the Mediterranean world for extracting metals by amalgamation as early as 500 BC, possibly even earlier. Cinnabar, HgS, was widely used in the ancient world as a pigment (Vermilion). For more than a thousand years, up to AD 1500, alchemists regarded the metal as a key to the transmutation of base metals to gold and employed amalgams both for gilding and for producing imitation gold and silver. Because of its mobility, mercury is named after the messenger of the gods in Roman mythology and the symbol, Hg, is derived from *hydrargyrum* (Latin, liquid silver) [1].

Mercury makes up a very small part of the earth's crust (0.08 ppm) and is one of the elements called "chalcophiles". In the reducing atmosphere prevailing when the earth's crust solidified, these elements separated out in the sulphide phase and their most abundant ores are therefore sulphides. Cinnabar, HgS, is the only important ore and source of mercury and is found along lines of previous volcanic activity. The most famous and extensive deposits are at Almaden in Spain; these contain up to 6 - 7% Hg and have been worked since Roman times. Other deposits, usually containing < 1% Hg, are situated in the USSR, Algeria, Mexico, Yugoslavia and Italy [1].

Although hardly any metallic cobalt was used until the twentieth century, its ores have been used for thousands of years to impart a blue colour to glass and pottery. It is present in Egyptian pottery dated at around 2 600 BC and Iranian glass beads of 2250 BC. "Smalt", produced by fusing potash, silica and cobalt oxide, can be used for colouring glass or for glazing pottery. The secret of making this brilliant blue pigment was apparently lost, to be rediscovered in the fifteenth century. Leonardo da Vinci was one of the first to use powered smalt as a 'new' pigment when painting his famous "The Madonna of the Rocks" [1].

The source of the blue colour was recognised in 1735 by the Swedish chemist G. Brandt, who isolated a very impure metal, or "regulus", which he named "cobalt rex". In 1870 T. O. Bergman showed this to be a new element. Its name has some resemblance to the Greek word for "mine", but it is almost certainly derived from the German word *Kobalt* for "goblin" or "evil spirit". The miners of northen European countries thought that the spitefulness of such spirits was responsible for ores which, on smelting, not only failed unexpectedly to yield the anticipated metal, but also produced highly toxic fumes [1].

More than 200 ores are known to contain cobalt but only a few are of commercial value. The more important are arsenides and sulphides such as smalltite, $CoAs_2$, cobaltite (or cobalt glance), CoAsS, and linnaetite, Co_3S_4. These are invariably associated with nickel, and often also with copper and lead, and it is usually obtained as a byproduct or co-product of the recovery of these metals. The world's major sources of cobalt are the African continent and Canada with smaller reserves in Australia and the USSR [1].

8.2 Uses of mercury and cobalt

The use of mercury for extracting precious metals by amalgamation has a long history and was extensively used by Spain in the sixteenth century when her fleet carried mercury from Almaden to Mexico and returned with silver. Now, however, the greatest use is in the Castner-Kellner process for manufacturing chlorine and NaOH.

Increasing amounts are consumed in the electrical and electronic industries, as, for instance, in street lamps and AC rectifiers. The electrical resistivity of liquid mercury is exceptionally high for a metal and this facilitates its use as an electrical standard. Its small-scale use in thermometers, barometers and gauges of different kinds are familiar in many laboratories and hospitals. In the form of its compounds, it has widespread germicidal and fungicidal applications [1].

About 30% of the total worldwide cobalt production is devoted to the production of chemicals for the ceramic and paint industries. In ceramics the main use is now not to provide a blue colour, but rather white by counterbalancing the yellow tint arising from iron impurities. Blue pigments are, however, used in paints and inks, and cobalt compounds are used to hasten the oxidation and hence the drying of oil-based paints [1].

8.3 Why is it important to determine these elements?

The history of the toxic effects of mercury is long and all types of mercury compounds are considered toxic. The metal itself, having an appreciable vapour pressure, produces headaches, tremors, inflammation of the bladder and loss of memory. Mercury salts, such as $HgCl_2$, leads to the nervous disorder known as "hatter's shakes" and possibly also to the expression "mad as a hatter" [1].

Still more dangerous than metallic mercury or inorganic mercury compounds are organomercury compounds of which the methyl mercury ion ($HgMe^+$) is probably the ubiquitous. This and other organomercurials are more readily absorbed in the gastrointestinal tract than Hg(II) because of their greater permeability of biomembranes. They concentrate in the blood and have a more immediate and permanent effect on the brain and central nervous system, no doubt acting by binding to the -SH groups in proteins. The use of organomercurials as fungicidal seed dressings has also resulted in fatalities in many parts of the world when the seed was subsequently been eaten [1]. Public concern about mercury poisoning has led to more stringent regulations for the use of mercury. The added costs of conforming to still

higher standards, necessitate the use of cost effective analytical processes that are sensitive enough to detect trace amounts of mercury.

The determination of trace amounts of cobalt in natural waters is of great interest because cobalt is important for living species as complexed vitamin B_{12}. Vitamin B_{12} is present in human and animal cells in the forms of adenosylcobalamin(III) and methylcobalamin(IV). The deficiency of cobalt in ruminants usually results in different types of anaemia [2]. The wasting disease in sheep and cattle known variously as "pine" (Britain), "bush sickness" (New Zealand), "coast disease" (Australia), and "salt sick" (Florida) has been recognised since the late eighteenth century. Iron treatment to this anaemic condition had mixed success, till it was found that the efficacious principle in the iron treatment was actually the impurity, cobalt [1].

Despite of its essential biological role, high concentrations of cobalt can be very dangerous. In moderate concentrations, such as 3 mg/gallon, cobalt may be hazardous to man. Toxicological effects of large amounts of cobalt include vasodilation, flushing and cardiomyopathy in humans and animals. The importance of cobalt in human and ruminant nutrition has led to work on the determination of cobalt in soils, plants, feedstuffs, herbage, natural waters and fertilizers. Investigations have been extended to the biochemistry of cobalt in animals, humans, microorganisms and enzymes [2]. Cobalt is essential for microorganisms fixing molecular N_2 and thus for higher plants relying on symbiotic nitrogen assimilation [3]. There is, however, still very little information available concerning the distribution and speciation of cobalt in the environment owing to analytical difficulties.

8.4 Choice of analytical method

8.4.1 Different analytical techniques available for individual analysis

Mercury is usually determined using techniques such as IGP-AES [4], potentiometry [5, 6], cold vapour-AAS [7, 8], liquid chromatography [9], AAS [10] or coupling

between some of these techniques [11] as well as coupling some of these techniques with flow injection systems [11, 12]. Several reagents [6] are suitable to react with mercury to form coloured complexes that can be determined photometrically. Many of these photometric determinations were adapted to FIA systems - even those that needed an extraction step as part of the procedure. Photometric determinations include: kinetic methods [13] or indirect determinations where, for instance, the inhibitory effect of Hg(II) in the catalytic action of iodides on the As(III)-Ce(IV) reaction is measured [14]. Because Hg is considered to be a "Dithizone metal", determinations of mercury using extraction with diphenylthiocarbazone (Dithizone) are well known and widely used [6, 15 - 17]. With Dithizone it is also possible to determine organic forms of mercury, like the methylmercury species [17].

Various techniques are employed to determine cobalt. These techniques include IGP-AES, ETA, XRF, AAS (and f-AAS) [18], chromatography [9, 18] and potentiometry [19]. Although these techniques deliver accurate results and have low detection limits, the apparatus are very expensive and not suitable for on-site, on-line routine analysis. Spectrophotometric methods coupled with flow injection analysis proved to be a better alternative, but due to its high sample and reagent consumption, was ruled out in favour of the sequential injection systems. As in the case of mercury, several reagents [6] are suitable to react with cobalt to form coloured complexes that can be determined photometrically. These determinations include kinetic methods [20 - 23], pH gradient methods [24] and extractions [6, 17]. Being a "Dithizone metal" itself, cobalt can be quantitatively be determined by extraction with diphenylthiocarbazone (Dithizone) in the presence of other metals [6, 17].

To avoid the use of toxic organic solvents such as CCl_4 and $CHCl_3$ [25], ethanol was used as solvent for the Dithizone reagent. Since mercury is considered an interference in the determination of cobalt with Dithizone [26], the two metals were determined simultaneously. Dithizonates of both mercury and cobalt, when dissolved in ethanol at a pH of ~7.5, absorb at the same wavelength. This wavelength was experimentally determined to be 519 nm. For this reason, only one detector was needed to determine the two metals, leading to simplified, inexpensive apparatus.

8.4.2 Reactions with diphenylthiocarbazone

Depending on the reaction conditions, diphenylthiocarbazone (Dithizone) and mercury(II) ions form an orange-yellow dithizonate [$Hg(HDz)_2$] in the acidic range or a violet secondary dithizonate (HgDz) in the neutral to alkaline range [6]. Both complexes are insoluble in water, but readily soluble in some organic solvents. Unlike mercury, cobalt only form primary dithizonates. Cobalt dithizonate ($Co(HDz)_2$) has a violet colour and absorb at 519 nm when dissolved in ethanol. For this application the secondary dithizonate of mercury was used. This complex also absorbed at 519 nm when dissolved in ethanol.

The reaction between cobalt and Dithizone to form the primary dithizonate can be represented as follows [17]:

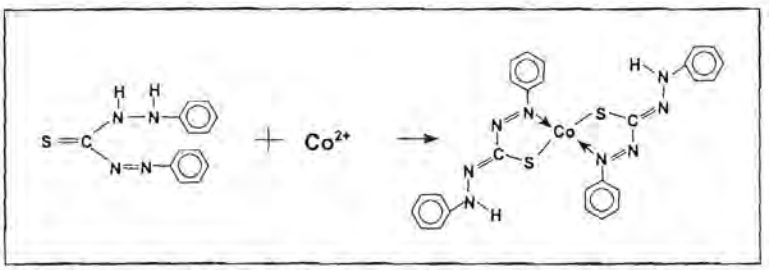

Fig. 8.1 Reaction scheme for the formation of primary dithizonates.

while the reaction between mercury and Dithizone to yield the secondary dithizonate is as follows [26]:

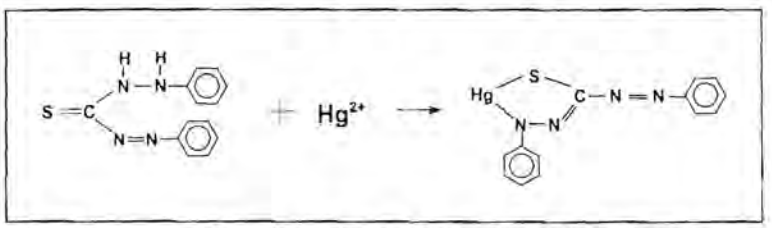

Fig. 8.2 Reaction scheme for the formation of secondary dithizonates.

8.5 Simultaneous determination of mercury and cobalt using sequential injection extraction

8.5.1 Experimental

8.5.1.1 Reagents and solutions

All solutions are prepared of analytical grade reagent unless specified otherwise. Deionised water from a Modulab system (Continental Water Systems, San Antonio, TX, USA) was used to prepare all aqueous solutions and dilutions. The water used as carrier was degassed before use.

Extractant: 0.05 g of Dithizone (Hopkins & Williams Ltd.) was dissolved in 250 mℓ ethanol to produce an emerald green stock solution. Stored in a cool place and protected from light this solution was stable for up to two weeks. Working solutions are obtained by suitable dilution of the stock solution with ethanol.

Mercury stock solution: A 100 mg/ℓ Hg^{2+} stock solution was prepared by dissolving 0.171 g $Hg(NO_3)_2.2H_2O$ (Merck) in 1ℓ of distilled water. Working solutions are obtained by suitable dilution of the stock solution.

Cobalt stock solution: A 100 mg/ℓ Co(II) stock solution was prepared by dissolving 0.404 g $CoCl_2.6H_2O$ (Riedel-de-Haën) in 1 ℓ distilled water. Working solutions were prepared by suitable dilution of the stock solutions.

Deionised water was used as carrier solution. A 0.43 mol/ℓ *acetic acid* solution was used as eluent during the soil extractions. For pH corrections either a 1 mol/ℓ NH_3 solution or a 0.5 mol/ℓ H_2SO_4 solution was used.

8.5.1.2 Instrumentation

The sequential injection extraction (SIE) manifold is illustrated in Fig. 8.1. It was constructed from two Gilson Minipuls peristaltic pumps (operating at 15 and 7 rpm respectively), a 4 m long extraction coil (1.02 mm i.d.) made of Teflon (PTFE) tubing (SUPELCO) and a 10-port electrically actuated VICI selection valve (Model ECSD10P) (Valco Instruments, Houston, Texas). Tygon pump tubing was used for both pumps.

The reaction coil was constructed using 30 cm of 0.75 mm i.d. porous silicon tubing together with an h-shaped glass debubbler (D3) (Dermo Tech). A 50 cm (0.8 mm i.d.) piece of Teflon tubing connected the debubbler to one of the peristaltic pumps, which operated at 0.4 mℓ/min to remove the air bubbles from the system. The holding coil was constructed of 1 m (0.8 mm i.d.) Teflon tubing. A third peristaltic pump was connected to the reaction coil by means of a T-piece. This pump was used during the optimisation of the flow rate as well as to rinse the flow cell when needed. This pump was operated manually and was not included when the device sequence was programmed with FlowTEK.

An Unicam 8652 UV-VIS spectrophotometer equipped with a 10 mm Hellma flow-through cell (volume 80 $\mu\ell$) was used to monitor the coloured product at 519 nm. Data acquisition and device control were achieved using a PC30-B interface board (Eagle Electric, Cape Town, South Africa) and an assembled distribution board (MINTEK, Randburg, South Africa). The FlowTEK [27] software package (obtainable from MINTEK) was used throughout the procedure.

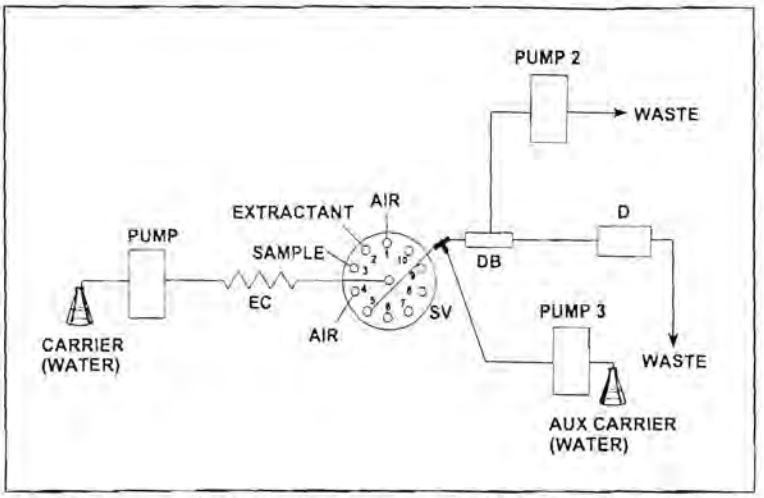

Fig. 8.3 Schematical representation of the sequential injection extraction manifold used for the simultaneous determination of cobalt(II) and mercury(II). EC - extraction coil, SV - selection valve, DB - debubbler and D - detector.

8.5.1.3 Procedure

A small air bubble was drawn up (through port 1 of the selection valve) to separate the extraction zones from the aqueous carrier solution. Thereafter the extractant zone (Dithizone in ethanol) (port 2) and the sample zone (port 3) were drawn up into the extraction coil. Another air bubble (port 4) was drawn up to separate these zones from the aqueous carrier, to avoid excess dilution of the formed extraction product. Since water and ethanol are miscible in all ratios, reversing of the flow resulted in mixing of the two zones. Extraction took place into the thin organic layer formed by the Dithizone zone whose flow was impeded due to the hydrophobic interactions with the walls of the Teflon coil. Because the two phases were mixed, no separation of phases was needed and the stack of zones was pumped directly to the detector (port 5). Pump 3 was manually switched on and off when considered necessary. This pump was connected to the detector line via a perspex T-piece connector.

Pump 2 was switched on (reverse) at the beginning of the analytical cycle to produce a sufficiently strong "sucking force" to remove both bubbles effectively prior to detection. Care was taken that the bubbles were removed effectively, but that not too much of the product zone was removed.

The instrumental procedure (as programmed in FlowTEK) is given in Table 8.1. The formed product peak was measured at 519 nm.

TABLE 8.1 Device sequence of the sequential injection system for determination of Hg and Co

Time (s)	Pump 1	Pump 2	Valve	Description
0	Off	Reverse	Air	Pump 1 off, pump 2 is switched on to produce a suction force in the debubbler, the valve is turned to position 1 to select the first air inlet.
4	Reverse			The air bubble is drawn up.
4.5	Off			Pump 1 stops.
5.5			Extractant	Valve is turned to position 2 to select the extractant line.
6.5	Reverse			The extractant solution is drawn up.
8.5	Off			Pump 1 stops.
9.5			Standard/sample	Valve is turned to position 3 to select the standard or sample line
10.5	Reverse			The standard or sample solution is drawn up.
13.5	Off			Pump 1 stops.
14.5			Air	Valve is turned to position 4 to select the second air inlet.
15.5	Reverse			The second air bubble is drawn up.
16	Off			Pump 1 stops.
17			Detector	Valve is turned to position 5 to select the detector line.
18	Reverse			Pump 1 is switched on in reverse. The extraction zones are drawn back into the extraction coil to ensure effective mixing and extraction.
26	Forward			Pump 1's pumping direction is now changed to forward. The stack of zones are pumped through the detector.
95	Off	Off		Both pumps are switched off. End of analytical cycle.

8.5.1.4 Sample preparation

Sample collection: Urine samples were collected in polypropylene flasks which had previously been cleaned by rinsing with dilute nitric acid and water. The samples were quickly frozen after collection with minimum air space above the urine. Soil samples were taken from a maize farm in the northern Free State and stored in polypropylene containers.

Before analysis, the frozen urine was allowed to come to room temperature and thoroughly mixed. Water samples with pH values of about 7 were analysed directly. Other samples were first pH corrected with either NH_3 or sulphuric acid. Representative soil samples of 20.00 ± 0.05 g were dried at 30°C for 8 - 10 hours. 5.00 ± 0.01 g of the air-dried soil was weighed into a beaker and 50 mℓ of a 0.43 mol/ℓ CH_3COOH solution was added. The suspension was stirred for 30 minutes and then decantated or filtered. The pH of the filtrate was adjust to 7.5 with NH_3 and the mixture was made up to 100 mℓ with distilled water.

8.5.2 Method optimisation

8.5.2.1 Physical parameters

A number of physical parameters can influence the degree of dispersion and extraction in the manifold. To obtain the highest sensitivity and precision it was necessary to optimise these parameters.

8.5.2.1.1 Introduction and removal of air bubbles

Air bubbles are highly undesirable in flow and sequential injection systems, not only because they led to spurious results, but also because it decreased the reproducibility of the procedure. Although it was feared that the introduction of air bubbles into a flow system would have led to irreproducible results, this was to a major extent not the

case. The bubbles separated the extraction zones from the surrounding carrier solution, preventing excessive dilution of the extraction zones. The bubbles were also pumped into the reaction coil and were removed by the debubbler prior to detection.

As important it was to introduce the air bubbles, it was even more important to remove them effectively prior to detection. A piece of porous silicon tubing (length 30 cm, i.d. 0.75 mm and o.d. 1.25 mm) was introduced as debubbler. This would be effective provided that there was ample back pressure on the air bubble, caused by the use of a flow restricter, or by simply elevating the outlet tube. The pressure placed on the bubble is then greater than atmospheric pressure and this difference force the air bubble through the porous tubing [28]. The pressure inside the SIA manifold was however not sufficiently high to push the air bubble through the pores. An h-shaped glass debubbler was then placed in the reaction coil. A 50 cm (0.8 mm i.d.) piece of Teflon tubing connected the debubbler to a pump operating at 0.4 mℓ/min to pump away the air bubbles. Care was taken that the bubbles were removed effectively, but that not too much of the product zone was removed. This debubbler proved to be the most effective and was incorporated into the SIA manifold.

8.5.2.1.2 Flow rate

Two different flow rates were used - a slower flow rate for the introduction of the zones into the extraction coil and for the extraction itself and a faster flow rate to propel the formed product zone through the detector. This parameter was optimise as follows: initially two pumps (1 and 3 (Fig 8.3)) were used to evaluate the influence of the flow rate on sensitivity and precision. Pump 3 was set on a constant pump rate of 4 mℓ/min, while the flow rate of the first pump was varied. The flow rate used to propel the zones through the detector was taken as the sum of the flow rates of pumps 1 and 3. Fig. 8.4 illustrates the results obtained for the various flow rates evaluated.

An optimum flow rate of 2.4 mℓ/min was chosen for pump 1, because of its sensitivity and good precision. Slower flow rates resulted in longer zone inversion times and

therefore thinner films. Faster flow rates, on the other hand, resulted in thick films with high extraction capacity [29]. Since the two phases are miscible in all ratios, faster flow rates resulted in better mixing of the zones. Flow rates higher than 2.4 mℓ/min gave less reproducible results, this was probably due to the decrease in axial dispersion because of the high flow rate [30, 31].

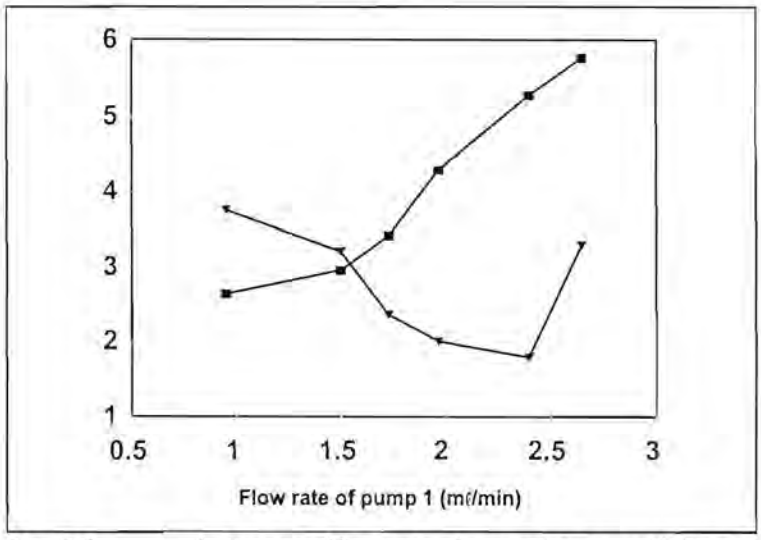

Fig. 8.4 Influence of flow rate of pump 1 on sensitivity and precision. -■- = relative peak height and -▼- = %RSD.

Faster flow rates in the reaction coil result in less dispersion of the extraction product [30, 31] and the pump rate of pump 2 was therefore optimised further. Fig. 8.5 shows the effect of the pump rate of pump 2 on sensitivity and reproducibility. Flow rates from 3.8 mℓ/min did not improve the sensitivity of the system and the optimum flow rate of pump 2 was set on 4 mℓ/min. The flow rate of the product zone through the detector was therefore 6.4 mℓ/min. The faster rinsing time also favoured shorter analysis time and therefore a higher sample throughput.

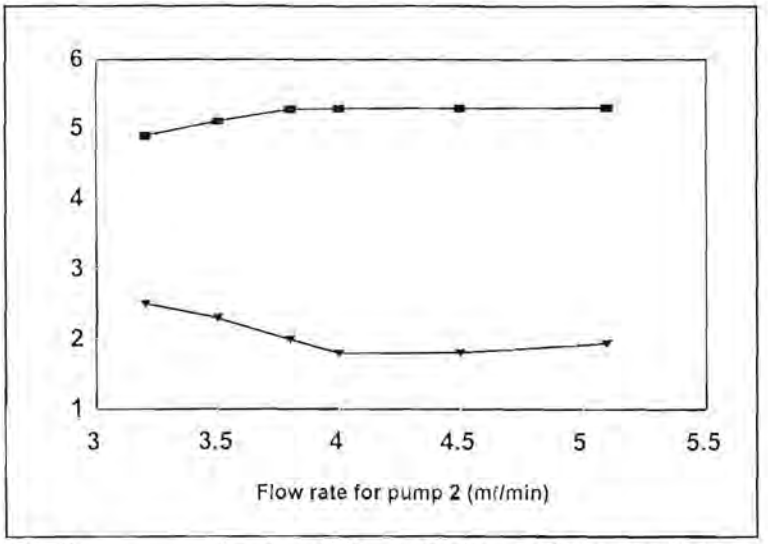

Fig. 8.5 Influence of flow rate of pump 2 on sensitivity and precision. ■ = relative peak height and ▼ = %RSD.

The pump rate used for pump 2 (debubbler) was also evaluated. The main criteria was that the bubbles had to be removed completely, while as small as possible part of the product peak was removed. The optimum flow rate was found to be 0.4 mℓ/min.

8.5.2.1.3 Sample volume

"Changing of the sample zone volume is an effective way of changing the sensitivity of the measurement. Dilution of concentrated samples is best achieved by reducing the injected sample volume", was the first of three rules listed by Gübeli *et al.* [32]. The sample volume was therefore carefully evaluated to obtain maximum sensitivity and reproducibility. Since a slower flow rate was used during the introduction of the sample and reagent volumes, the time needed to draw up the solution was longer than 1 second and led therefore to better precision. The results obtained in the evaluation is schematically represented in Fig. 8.6.

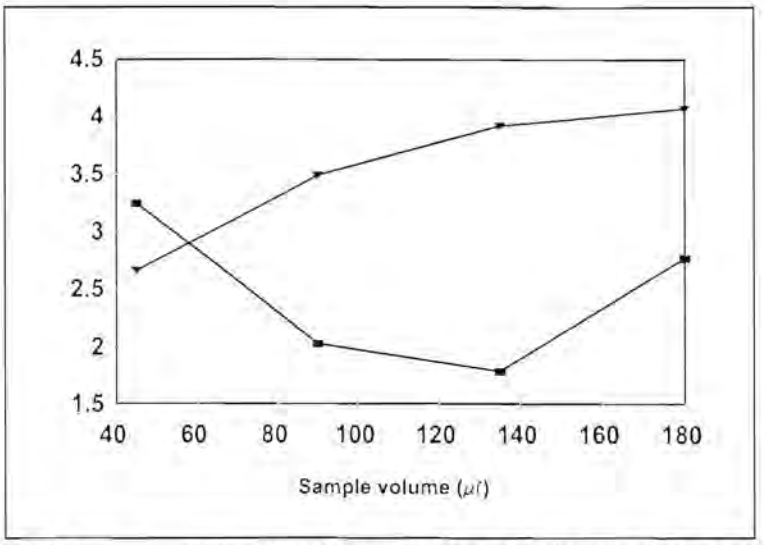

Fig. 8.6 Influence of sample volume on the sensitivity and reproducibility of the SIE method. ▼ = relative peak height and ■ = %RSD.

Although bigger sample volumes led to better sensitivity, the reproducibility of the method decreased with volumes bigger than 135 µℓ. Bigger volumes led to smaller axial dispersion and therefore insufficient overlap of the reacting zones [30, 31]. An optimum sample volume of 135 µℓ was thus chosen for the system.

8.5.2.1.4 Extractant volume and extraction time

Extractant volume is dependant on a critical parameter called the zone inversion length. Zone inversion length refers to the distance travelled by the zones from the load position (where the organic zone was situated in the extraction coil after aspiration), to the position where the aqueous phase has moved completely through the organic phase. At this point the organic zone has been deposited on the tubing as a film, allowing maximum contact between the two phases. The volume of the extractant zone influence both the time of the extraction as well as the length of the extraction coil.

Different extractant volumes were evaluated. The 50 µℓ used by Peterson *et al.* [29] was used as guideline in selecting an extractant volume. Volumes between 45 µℓ and

180 $\mu\ell$ were evaluated (Fig. 8.7). Smaller volumes gave very irreproducible results, because of the imperfect flow dynamics of the pump (start up and stopping are not instantaneous) [33], these small volumes were not aspirated reproducibly.

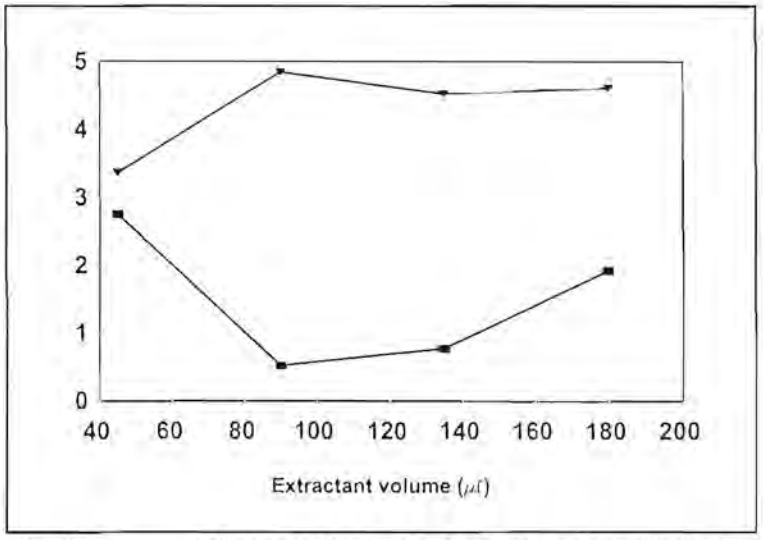

Fig. 8.7 Influence of extractant volume on sensitivity and precision. ▼ = relative peak height and ■ = %RSD.

A plateau is reached in peak height at volumes bigger than 90 $\mu\ell$. The optimum extractant volume was chosen to be 90 $\mu\ell$ due to the good precision and sensitivity it delivered.

Several extraction options were considered, since the two phases were mixed with one another. At first different zone inversion times were evaluated. Table 8.2 lists the results obtained. These extraction steps consisted of a reverse step, during which the aqueous phase moved through the organic phase, and a forward step, during which the aqueous phase moved back to its original position.

TABLE 8.2 Different extraction steps evaluated

Reverse step (s)	Forward step (s)	Total time (s)	Relative peak height	%RSD
4	5.5	9.5	2.78	1.02
6	7.5	13.5	3.04	0.94
8	9.5	17.5	3.41	0.76
10	11.5	21.5	3.39	0.78
12	13.5	25.5	3.36	0.89
14	15.5	29.5	3.28	2.0

Longer extraction times were also evaluated, but the peak shape changed when using them. The peaks appeared to have shoulders and in some cases it was difficult to measure the real peak height. An extraction step of 17.5 s was chosen as optimum. Since the two phases mixed completely, a range of flow reversals were introduced into the extraction step to investigate whether more effective mixing would improve the sensitivity. As can be seen from Table 8.3, the flow reversals did increase the sensitivity, but unfortunately the reproducibility deteriorated.

TABLE 8.3 Effect of multiple flow reversals on sensitivity and precision

Number of flow reversals	Size of reversal steps		Relative peak height	%RSD
	Reverse step (s)	Forward step (s)		
1	8	9.5	3.73	0.85
3	6	6	4.42	1.95
6	3	3	4.66	2.25
9	2	2	5.07	3.89

The same problem was experienced as in the case of longer extraction times. The peak deformed and was no longer representing the true concentration of the analyte. Since better mixing definitely increased the sensitivity of the measurements, a mixing chamber was placed into the reaction coil. The mixing was bettered, but the bigger dispersion due to the large dead volume of the mixing chamber, led to a decrease in

sensitivity. Incorporation of the mixing chamber also led to high back pressure and long rinsing times, which were undesired featured for the proposed system. An extraction step consisted of only one flow reversal was therefore chosen. This gave an optimum extraction time of 17.5 seconds and peaks with the desired Gaussian shapes.

8.5.2.1.5 Organic film thickness

Relative film thickness per unit length (d_f) can be predicted using the equation [29]

$$d_f = kd_t(u\eta/\gamma)^a$$

where u represents flow rate (velocity) and d_t tubing diameter. The solvent characteristics also play an important role and are included in the equation. Viscosity of the solvent is represented by η and surface tension by γ, k and a are constants between ~1/2 and ~ 2/3. From the equation it can be seen that film thickness is directly proportional to viscosity and inversely proportional to surface tension. As colligative properties, it is appropriate to consider either interfacial or surface tension to viscosity as a film thickness parameter, η/γ [29]. The film thickness parameter for ethanol was calculated to be 4.64×10^{-2} (η = 1.06 cP and γ = 21.80) [34]. The thickness of the organic film is very important since it influences extraction by affecting the mass transfer of analytes into the film [35]. Under optimum running conditions the relative film thickness was calculated to be 8.8 μm.

8.5.2.1.6 Diameter and length of tubing

Extraction coil: The length of the extraction coil depends on the zone inversion length. It was found that during the extraction step a reverse step of 8 seconds was used. This time multiplied with the flow rate 4.9 x cm/s (2.4 mℓ/min), resulted in a zone inversion length of 39,2 cm. Due to dispersion in the flow conduit, these zones occupy about nine times the inversion length. Thickness of the wetting film is directly proportional to the inner diameter of the coil [36]. As a result, the extraction capacity (volume of the

wetting film) is larger for wider and longer extraction coils. Using an extractant volume of 90 $\mu\ell$ an extraction coil of 3.6 m was needed. To ensure that none of the zones reached the pump conduit and became deformed, an extraction coil of 4 m was used. An inner diameter of 1.02 mm ensured good axial dispersion and zone overlap.

Reaction coil: Porous silicon tubing (30 cm, 0.75 mm i.d.) was used as reaction coil. This was done mainly to debubble the carrier stream prior to entering the flow cell. Unfortunately, this did not have the desired result and a glass debubbler was installed. The spectrophotometer should be positioned as close to the debubbler as possible. Longer distances between the debubbler and detector led to higher dispersion, longer rinsing times and ultimately lower sample throughput.

8.5.2.2 Chemical parameters

8.5.2.2.1 pH

The formation of both cobalt and mercury dithizonates is pH dependant. The pH range wherein primary cobalt dithizonates and secondary mercury dithizonates are formed, is 7 - 10.5 [6]. The pH of clean, drinkable water falls into this range. The pH of all samples that were analysed with this system were measured and corrected to pH 7.5 with 1 mol/ℓ ammonia solution or 0.5 mol/ℓ sulphuric acid solution. Ammonia was chosen, because its formation constants with the two analytes were low compared to those of sodium hydroxide [37]. The formation constants for the hydroxides are log K_f = 5.1 for Co and log K_f = 10.3 for mercury, compared to the constants for ammonia, which are log K_f = 1.6 for Co and log K_f = 8.7 for Hg.

8.5.2.2.2 Choice of organic solvent

The organic liquid used in Dithizone extractions should strictly speaking be termed the *diluent* for the active *extractant* Dithizone [17]. The choice of solvent or the solvent composition is a critical parameter for the successful application of sequential injection

extraction, determining the difference in flow velocity between the organic and aqueous phases, the chemical selectivity and efficiency of the extraction [29]. Solvents with low viscosities do not offer a sufficient difference in flow velocity when compared to water and make SIE less effective as it requires more time and longer extraction coils. On the other hand, highly viscous solvents are difficult to wash out of the tubing. With less dense solvents, phase separation may present problems, although there may be cases where the use of a diluent not much less dense than water has special advantages [17].

There are, of course, many other factors which influence the choice of diluent, even though in laboratories where purified solvents are used, economical factors are of secondary importance. Dithizone, as well as its metal dithizonates are all highly soluble in chlorinated solvents [17]. One disadvantage about CCl_4 is that it is highly carcinogenic and has ozone depleting properties [39]. To avoid the use of toxic organic solvents such as CCl_4 and $CHCl_3$ [25], ethanol was used as solvent for the Dithizone reagent.

Two major reasons were used to justify the use of ethanol as solvent. Firstly, since ethanol and water are miscible in all ratios, the use of phase separators were omitted and the mixture of aqueous and organic liquids containing the reaction product was determined. Secondly, according to the physical properties of ethanol, it was calculated that it would produce the thickest extraction film, when compared to a few other solvents. The film thickness parameters, as described in section 8.5.2.1.5, for ethanol and other organic solvents are given in Table 8.4.

TABLE 8.4 Film thickness parameter [29] for some organic solvents

Solvent	Surface tension (γ) (mN/m) [34, 40]	Viscosity (η) (cP) [34, 40]	Film thickness parameter (η/γ)
Benzene	28.88	0.601	2.08×10^{-2}
Carbon tetrachloride	27.00	0.88	3.26×10^{-2}
Ethanol	22.80	1.06	4.64×10^{-2}
Hexane	18.40	0.31	1.68×10^{-2}
Methanol	22.60	0.553	2.45×10^{-2}

The visible absorption spectrum of Dithizone is, however, very sensitive to the organic solvent in which it is dissolved [38]. It was found experimentally that the dithizonates of both cobalt and mercury had peak maxima at λ_{max} = 519 nm. Detection was therefore done at 519 nm.

8.5.2.2.3 Concentration of Dithizone

Dithizone is only sparingly soluble in ethanol, with a solubility of 0.3 g/ℓ at 20°C [17]. Since solutions of Dithizone of any but the lowest concentration are deeply coloured, and often almost opaque, it is quite difficult to be certain whether excess solid is present in contact with a saturated solution. Special care is needed to ensure that metallic impurities are not introduced by the filtering medium, especially when the concentration is to be calculated afterwards from the absorbance of a suitably diluted aliquot and a knowledge of the molar (decadic) absorption coefficient, ϵ [17].

A stock solution containing 0.05 g of Dithizone in 250 mℓ ethanol was prepared. Several dilutions, using ethanol, were made and evaluated. Most of these solutions could not been used due to the deep green colour of the unreacted Dithizone. A dilution factor of 5 was used to produce a solution with an absorbance in the range 0.6 - 1.0 (10 mm cell). This solution was used throughout the whole procedure as optimum Dithizone concentration. The solution had to be prepared daily, but the stock solution was stable for up to two weeks when stored in the refrigerator and protected from light.

8.5.3 Evaluation of the system

The proposed sequential extraction method was evaluated under optimum running conditions with regard to linearity of the two analytes respectively, sample frequency, reproducibility, sample interaction, detection limits, accuracy and major interferences.

8.5.3.1 Linearity

Evaluation under optimum running conditions delivered analytical curves for the extraction of Co(II) and Hg(II) with Dithizone as shown in Fig. 8.8. The curves for the individual metals are linear between 0.1 mg/ℓ and 50 mg/ℓ for both metals. For cobalt r^2 = 0.9914 and for mercury r^2 = 0.9875. Peak height was used to evaluate the analytical signal.

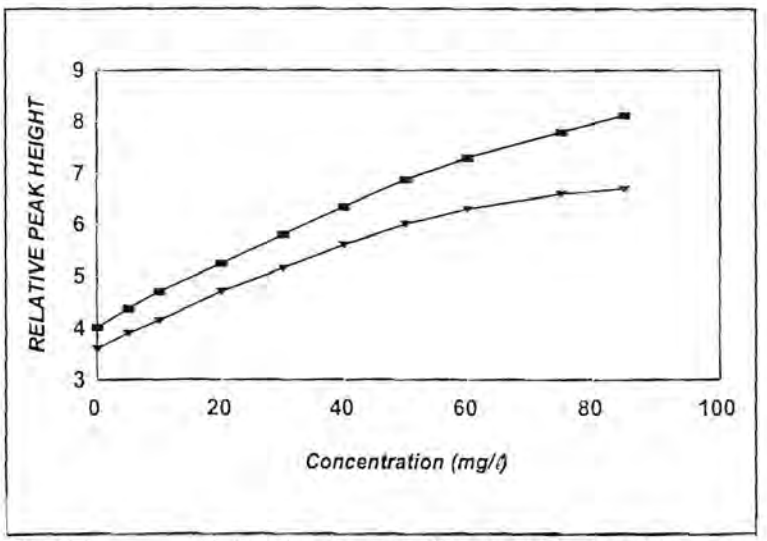

Fig. 8.8 Calibration curves of the individual metals. ■ = cobalt(II) and ▼ = mercury(II).

8.5.3.2 Accuracy

To investigate the accuracy of the SIE system a calibration curve for each individual metal was constructed. Because absorbance is additive, two equations can be obtained which should yield the required unknown concentrations when solved simultaneously [19]. The equations for the calibration curves obtained experimentally were:

Calibration curve for Hg(II): $A = 1.58[Hg] + 3.55$

Calibration curve for Co(II): $A = 1.87[Co] + 3.67$

Addition of the two equations gave:

$$A = 1.58[Hg] + 1.87[Co] + 7.22$$

To solve two equations two absorbance values are needed. The above data given represents the value of the peak maximum as determined by the FlowTEK program (refer to it as A). The other absorbance value was found by retrieving the data points of the specific peak profile into Quattro Pro and using the absorbance value recorded one second before the peak maximum was reached (refer to it as A'). The calibration data at this time were as follow:

For mercury: $A' = 1.14[Hg] + 2.98$; $r^2 = 0.9895$

For cobalt: $A' = 1.50[Co] + 3.67$; $r^2 = 0.9958$

Addition of the equations gave: $A' = 1.14[Hg] + 1.50[Co] + 6.65$

Solving these two equations (A and A') simultaneously give the desired concentrations.

Two different aqueous mixtures, two urine mixtures (one sample was spiked with 10 mg/ℓ Hg) and three soil extracts were analysed. The results are listed in Table 8.5. The percentage recovery was calculated for the aqueous samples and soil extracts, whilst standard addition to the urine samples showed that the urine did not contain Hg(II). The cobalt concentration in the urine sample was 1.3 mg/ℓ. The percentage recovery yielded satisfactory results in most cases.

TABLE 8.5 Evaluation of the accuracy of the proposed SIE method.

Sample	Known concentration in mg/ℓ		Concentration obtained with SIE in mg/ℓ		% Recovery	
	$[Co^{2+}]$	$[Hg^{2+}]$	$[Co^{2+}]$	$[Hg^{2+}]$	$[Co^{2+}]$	$[Hg^{2+}]$
Aqueous 1	0.1	5.0	0.13	4.91	130	98.2
Aqueous 2	40	20	40.8	19.7	102	98.5
Urine 1	-	10	1.34	9.84	-	98.4
Urine 2	-	-	1.3	0.05	-	-
Soil 1	15	0	14.6	0.07	97.3	-
Soil 2	10	25	10.0	25.1	100	100.4
Soil 3	0	30	0.3	29.39	-	97.97

8.5.3.3 Reproducibility

The results obtained when using the proposed system revealed surprisingly good reproducibility. It is expected when using air bubbles in the flow system, that the reproducibility will deteriorate due to the irregular stretching and compressing of the bubble. The slower flow rate used during the extraction step might contribute to the good results. The slower the flow rate, the more uniform the bubble can be stretched and compressed. Response values obtained for both metals, in the standard solutions as well as the samples analysed, show relative standard deviations lower than 1.9% for ten measurements at each concentration or sample (Table 8.6).

TABLE 8.6 Reproducibility of the proposed sequential injection extraction system

Standard/sample ([ ] in mg/ℓ)	%RSD
0.1	1.89
1.0	1.10
5.0	1.08
10.0	0.98
20.0	0.78
30.0	0.52
40.0	0.54
50.0	0.24
Aqueous 1	1.05
Aqueous 2	0.85
Urine 1	1.32
Urine 2	1.85
Soil 1	1.23
Soil 2	0.64
Soil 3	0.95

8.5.3.4 Sample frequency

To complete the whole analytical cycle, including the extraction and detection, took only 95 s. This resulted in a sample frequency of 38 samples per hour. When considering that two analytes were determined simultaneously, the sample frequency is quite remarkable for a sequential injection system.

8.5.3.5 Sample interaction

Negligible carry-over between samples was experienced when employing this system. A sample with low analyte concentration (1 mg/ℓ) was analysed, followed by a sample with analyte concentration ten times higher than the first. To evaluate sample

interaction the first sample was analysed again. Sample carry-over was then calculated according to the difference between the two peak height values [33]. The percentage carry-over calculated were low enough to be ignored. The sample interaction was calculated to be about 0.05%.

8.5.3.6 Detection limits

The detection limit is both a function of sensitivity and noise. The lowest concentration, that could be determined without doubt, would be considered the detection limit of the system. The detection limits of both Co(II) and Hg(II) were calculated as follows: The relative peak height for a blank solution was measured at the time where the peak maxima of the analyte peak usually appeared. This value was multiplied by three to generate a peak height value that could be measured with certainty. The concentration values of the corresponding peak height values were red from the individual calibration curves and then used as detection limits. Using this technique, the detection limits for the SIE system were calculated to be 0.15 mg/ℓ and 0.12 mg/ℓ for mercury and cobalt, respectively.

8.5.3.7 Interferences

Possible interferents were tested using a solution containing 1 mg/ℓ of both analytes. The following substances did not interfere with the determination of cadmium and mercury ions: 500 mg/ℓ SO_4^{2-}, 10 mg/ℓ PO_4^{3-}, 2 mg/ℓ Al^{3+} (Al do not react with Dithizone under neutral to alkaline conditions), 50 mg/ℓ Mg^{2+} and 400 mg/ℓ Ca^{2+}.

Chloride up to 14 g/ℓ (0.4 mol/ℓ) did not interfere in the mercury determination as long as the H_2SO_4 concentration did not exceed 2 mol/ℓ, while chloride concentrations of up to 100 g/ℓ could be tolerated in the cobalt analysis. Bromide, cyanide and thiocyanate interfere in the mercury determination, since they complex mercury more strongly than Dithizone. These anions could be tolerated up to 10 mg/ℓ. No interference was experienced in the cobalt determination by either bromide or chloride. Thiocyanate and

cyanate are usually used to mask interferences due to cobalt and interfered, therefore, seriously in the determination of cobalt. Anions could be removed by using anion exchange columns in the sample uptake tubes.

The metals normally present in urine, *viz.* Fe(II), Ni(II), Pb(II) and Zn(II), were also tested as possible interferents. The metals were individually added to two different urine samples which contained 1 mg/ℓ Co(II) and 1 mg/ℓ Hg(II) respectively. Although variation in pH usually is the most important way to eliminate interferences from metal cations, the cations still interfere at the optimum pH for the extractions. All the metals interfere in the determination. These interferences can however be masked by addition of a mixture of hydroxylamine (1 mol/ℓ), sodium potassium tartrate (0.75 mol/ℓ and potassium hexacyanoferrate(II) (1.5 mol/ℓ) [15]. 2 mℓ of this solution was added to 5 mℓ urine samples. These mixtures were then diluted to 10 mℓ with distilled water prior to introduction into the sequential injection extraction system.

8.6 Conclusion

A simplified, automated extraction system is described. Distilled water as carrier stream and small volumes of both sample and reagents are employed, ensuring a very cost effective system. Additional to the cost effect, is the use of a nontoxic solvent, ethanol, which make the technique much more environmental and operator friendly. It operates without phase separators or segmenters. This fact highlights the durability and robustness of the technique, since less maintenance will be needed. The sequential injection system is fully computerised and allow the determination of cobalt and mercury in the same sample without prior separation. A sample frequency of 38 samples per hour place it ahead of other SIA systems, where the main drawback usually is the low sample throughput. Miniaturisation of the manifold as well as suitable buffers to maintain pH levels, will make the sequential injection system very useful in many applications.

8.7 References

1. N. N. Greenwood and A. Earnshaw, **Chemistry of the Elements**, Pergamon Press, 1984.
2. T. W. Clarkson, J. C. Smith, D. O. March and M. D. Turner, in P. A. Krenkel (ed), **Heavy Metals in the Aquatic Environment**, Pergamon Press, Oxford, pp 1 - 12.
3. K. Nomiyama, in P. A. Krenkel (ed), **Heavy Metals in the Aquatic Environment**, Pergamon Press, Oxford, pp 15 - 23.
4. P. C. Rudner, A. G. de Torres, J. M. C. Pavon and E. R. Castellon, **Jour. Anal. Atom. Spec.**, **13** (1998) 243.
5. I. A. Gurév and N. V. Kuleshova, **Jour. Anal. Chem.**, **53** (1998) 15.
6. J. Fries and H. Getrost, **Organic Reagents for Trace Analysis**, E. Merck Darmstadt, 1977.
7. O. Haase, M. Klare, J. A. C. Broekært and K. Krengel-Rothensee, **Analyst**, **123** (1998) 1219.
8. G. Tao, S. N. Willie and R. E. Sturgeon, **Analyst**, **123** (1998) 1215.
9. A. Ali, H. Shen and X. Yin, **Anal. Chim. Acta**, **369** (1998) 215.
10. C. E. C. Malgalhaes, F. J. Krug, A. H. Fostier and H. Berndt, **Jour. Anal. Atom. Spec.**, **12** (1997) 1231.
11. X. Yin, W. Frech, E. Hoffmann, C. Ludke and J. Skole, **Fresenius J. Anal. Chem.**, **361** (1998) 761.
12. E. Janssen, **CANAS'95 Colloquium Analytsche Atomspektroskopie**, (1996) 257.
13. X. Peng, Q. Mao and J. Cheng, **Fresenius J. Anal. Chem.**, **348** (1994) 644.
14. M. D. Mateo, R. Forteza and V. Cerdà, **Int. Jour. Environ. Anal. Chem.**, **41** (1990) 39.
15. A. C. Rolfe, F. R. Russell and N. T. Wilkinson, **Analyst**, **80** (1955) 523.
16. D. J. S. Gray, **Analyst**, **77** (1952) 436.
17. H. M. N. H. Irving, **Dithizone**, The Chemical Society, London, 1977.
18. **Cobalt in Potable Waters**, Methods for the Examination of Waters and

Associated Materials, HMSO, 1981.

19. A. Economu and P. R. Fielden, **Talanta, 46** (1998) 1137.
20. A. Fernandez, M. D. Luque de Castro and M. Valcarcel, **Anal. Chem., 56** (1984) 1146.
21. T. Yamane and C. Ishimizu, **Mikrochim. Acta, 1** (1991) 121.
22. D. Betteridge and B. Fields, **Fresenius Z. Anal. Chem., 314** (1983) 386.
23. R. E. Taljaard and J. F. van Staden, **Anal. Chim. Acta, 366** (1998) 177.
24. D. Betteridge and B. Fields. **Anal. Chim. Acta, 132** (1981) 139.
25. M. P. San-Andres, M. L. Marina and S. Vera, **Analyst, 120** (1995) 255.
26. G. Iwantscheff, **Das Dithizon und seine Andwendung in der Mikro- und Spurenanlyse**, Verlag Chemie, Weinheim, 1958.
27. G. D. Marshall and J. F. van Staden, **Anal. Instrum., 20** (1992) 79.
28. G. B. Martin, H. K. Cho and M. E. Meyerhoff, **Anal. Chem., 56** (1984) 2612.
29. K. L. Peterson, B. K. Logan, G. D. Christian and J. Růžička, **Anal. Chim. Acta., 337** (1997) 99.
30. M. Valcarcel and M. D. Luque de Castro, **Flow Injection Analysis. Principles and Applications**, Ellis Horwood, Chichester, 1987.
31. J. Růžička and E. H. Hansen, **Flow Injection analysis**, 2nd ed, John Wiley & Sons, New York, 1988.
32. T. Gübeli, G. D. Christian and J. Růžička, **Anal. Chem., 63** (1991) 2407.
33. R. E. Taljaard, **Sequential Injection Analysis as Process Analyzers**, MSc-Thesis, University of Pretoria, 1996.
34. P. W. Atkins, **Physical Chemistry**, fourth ed., Oxford University Press, Oxford, 1990, pp 293 - 969.
35. C. A. Lucy, **Anal. Chem.**, 61 (1989) 101.
36. Y. Luo, S. Nakano, D. A. Holman, J. Růžička and G. D. Christian, **Talanta, 44** (1997) 1563.
37. L. W. Potts, **Quantitative Analysis. Theory and Practice**, Harper and Row, New York, 1987.
38. A. T. Hutton, **Polyhedron, 6** (1987) 13.
39. S. Nakano, Y. Luo, D. Holman, J. Růžička and G. D. Christian, **Microchemical**

Journal, **55** (1997) 392.

40. G. W. C. Laye and T. H. Laby (eds.), **Tables of Physical and Chemical Constants**, Longman, London, 1973.

CHAPTER 9

Simultaneous Determination of Cadmium(II) and Mercury(II) in Aqueous, Urine and Soil Samples using pH-gradient Sequential Injection Extraction

9.1 Introduction

When looking at Mendeleev's Periodic Table of Elements, zinc, cadmium and mercury all belong to the same group (II b), which make one thinks that their chemical behaviour will in some extent be similar. Their most noticeable features compared with other metals are their low melting and boiling points, mercury being unique as a metal which is a liquid at room temperature. It is, however, a remarkable contrast that, whereas Zn is biologically one of the most important metals and is apparently necessary to all forms of life, Cd and Hg have no known biological role and are amongst the most toxic off all elements [1].

Cadmium as well as mercury are adsorbed on ground particles. This adsorption usually occurs when the ground pH is in the pH range 4.5 to 5.5. Lower pH values increase the solubility of these two species in groundwater and make them more mobile and available for uptake by plant roots or micro-organisms. Under the influence of low pH values or high chloride concentrations, mercury is converted into toxic organic forms, like methyl mercury, which plays a major role in studies on the toxicity of mercury.

The so-called Minamata and itai-itai deceases are serious conditions caused apparently by heavy metals, such as mercury [2] and cadmium [3], in the aquatic environment. Most patients were middle-aged or elderly females, who suffered from severe pains all over the body and died in pain. The first symptom of the decease was usually lumbago,

followed by later development of pseudofractures and a waddling gait. The etiology of the itai-itai decease is related to dietary cadmium and malnutrition. Cadmium inhibit renal function, increased loss of calcium due to depression of proximal reabsorption and lead finally to osteomalacia [3]. Other symptoms due to cadmium poisoning are: (i) emphysema of the lungs, (ii) dysfunction of the kidneys and (iii) low molar mass proteinuria.

Cadmium in the aquatic environment is generally taken into the body via the gastrointestinal tract as drinking water and food; the absorption rate from the gastrointestinal tract has been demonstrated to be 3 - 6%, while uptake of cadmium through the lungs is said to be as high as 10 - 40%. One third of the cadmium taken up by the body is accumulated in the kidneys. The blood cadmium level probably indicates the present degree of cadmium exposure, and the total burden of cadmium is roughly proportional to urinary cadmium excretion [3].

To diagnose cadmium poisoning it is, however, necessary to know the degree of cadmium exposure and total body burden of cadmium [3]. Environmental cadmium should therefore be checked first of all. Techniques such as anodic stripping analysis and/or flameless atomic spectroscopy were mainly used to determine cadmium. This study concentrated on finding more cost-effective, rapid methodologies to determine cadmium in urine and aqueous solutions. A simple sequential injection extraction method was proposed to solve this problem.

In nature, mercury occurs in several forms, e. g. metallic mercury, inorganic mercury and organic mercury compounds. All forms of mercury are considered poisonous, but methylmercury is of particular concern since it is extremely toxic and is frequently found in the environment. Through a very effective biomagnification mechanism, methylmercury is enriched in food chains which results in high levels in top predators, like fish such as northern pike and tuna. In Japan, methylmercury contamination caused severe brain damage to twenty two infants whose mothers had ingested contaminated fish during pregnancy. In Iraq the intake of wheat flour from seeds

treated with organic mercury has also led to large scale poisoning. In general, exposure to organic mercury can cause brain damage to the developing foetus. Exposure is also considered more dangerous for young children because their nervous system is still developing and thus are more sensitive towards these compounds [4].

In normal persons who has not been subjected to any particular exposure, the total mercury levels in the blood and in the urine are less than 5 µg/ℓ. It is considered that there is a long term risk of intoxication above 30 µg/ℓ and 50 µgℓ in urine. A part of the mercury in the blood is in an organic form, primarily as methylmercury [5]. As in the case of cadmium, the urinary excretion of mercury is also a measure of the levels of total body burden.

Dickinson Burrows [6] wrote a review of the status of total mercury analysis, wherein the most important analytical techniques were reported. According to the review, flameless or cold-vapour atomic absorption spectrometry is the method of choice for most laboratories. Since most mercury poisoning comes from environmental mercury, usually in the form of methylmercury, and because urinary excretion gives an good indication of the level of poisoning, it was decided to determine mercury by a sensitive colorimetric method, using Dithizone. Because mercury and cadmium required monitoring in the same type of samples it was decided to determine them simultaneously.

9.2 Choice of analytical method

9.2.1 Methods of determination

Several analytical methods to determine mercury exist which include cold vapour AAS [7 - 10], chromatography (GC and HPLC) [11], potentiometric stripping analysis [12], enzymatic determination [13], ion-selective electrodes [14], ICP-AES [15,16] and spectrometry [17 - 24]. All of these methods, except for the last, have the disadvantage that it is relatively expensive and it could not be used for on-site field analysis.

Spectrophotometric determinations are therefore essential as inexpensive on-site measuring tools.

Several reagents [18] are suitable to react with mercury to form coloured complexes that can be determined photometrically. Many of these photometric determinations were adapted to FIA systems - even those that needed an extraction step as part of the procedure. Photometric determinations include: kinetic methods [25] or indirect determinations where, for instance, the inhibitory effect of Hg(II) in the catalytic action of iodides on the As(III)-Ce(IV) reaction is measured [23].

The extraction method for methylmercury, as developed by Gage [26], is still widely used. The extraction is based on the addition of acid (hydrochloric, hydrobromic or hydroiodic) to a homogenised sample, the extraction of the methylmercury halide into an organic solvent (benzene or toluene), purification by stripping with a thiol compound (cysteine or thiosulphate) and re-extracted into benzene. A problem with the extraction method is the formation of often persistent emulsions which can be avoided by the use of cysteine impregnated paper instead of cysteine solution [4]. Because Hg is considered to be a "Dithizone metal", determinations of mercury using extraction with diphenylthiocarbazone (Dithizone) are well-known and widely used [6, 17, 27]. With Dithizone it is also possible to determine organic forms of mercury, like the methylmercury species [27].

Cadmium is usually determined using flame-AAS [28] or cold vapour AAS [29] and ion-selective electrodes [30]. A number of colorimetric reactions are adapted to FIA, this include a number of applications where Dithizone is used as extractant [17, 20, 21]. Existing methods for the determination of cadmium involve preconcentration which is very time-consuming. The determination of cadmium at low concentrations which may be of toxicological significance requires a highly sensitive method. A flow injection system designed to determine lead and cadmium using liquid-liquid extraction with Dithizone in chloroform was used by Klinghoffer [21] and was refined by Burguera *et al.* [17] to increase the selectivity and sensitivity of this procedure.

Since both mercury and cadmium can be extracted with Dithizone and because of the extreme sensitivity of the reagent, this extraction was chosen as analytical method. According to Irving [27] and Fries and Getrost [18] carbon tetrachloride or chloroform were the best organic solvents for the dissolution of Dithizone. Carbon tetrachloride was chosen as organic solvent for this study, not only because of the solubility of Dithizone in CCl_4, but also because of the ability of CCl_4 to form a sufficiently thick thin-layer against the Teflon walls of the tubing. Carbon tetrachloride is also used as solvent, since it also enables the separation of Cd/Zn [18].

9.2.2 Reactions with diphenylthiocarbazone

Depending on the reaction conditions, diphenylthiocarbazone (Dithizone) and mercury(II) ions form an orange-yellow dithizonate [$Hg(HDz)_2$] in the acidic range or a violet secondary dithizonate (HgDz) in the neutral to alkaline range [18]. Both complexes are insoluble in water, but readily soluble in chloroform and carbon tetrachloride. The primary dithizonate is of analytical importance, because it is not only stable in 5 mol/ℓ sulfuric acid solution, but once formed it is also very stable in dilute alkaline solutions. It is however less stable in hydrochloric acid, and decomposes completely at higher HCl concentrations.

Dithizone is the preferred reagent for photometric determination of cadmium, although this reagent is not specific and numerous other heavy metals also form dithizonates. Cadmium determinations with Dithizone give optimum results when carried out at a pH of approximately 9. To ensure this pH an alkaline buffer made up from sodium potassium tartrate and NaOH (or KOH) of pH of 10.5 was used. The cadmium-Dithizone complex has a pinkish colour and is very stable in the strong alkaline range. Although Cd-dithizonate is easily decomposed by weak acids, it experiences no interference from HCl, H_2SO_4 and HNO_3 [18].

9.3 The simultaneous extraction of mercury(II) and cadmium(II) with Dithizone

9.3.1 Experimental

9.3.1.1 Reagents and solutions

All solutions are prepared of analytical grade reagent unless specified otherwise. Deionised water from a Modulab system (Continental Water Systems, San Antonio, TX, USA) was used to prepare all aqueous solutions and dilutions. The water used as carrier was degassed before use.

Extractant: 0.1 g of Dithizone (Hopkin & Williams Ltd.) was dissolved in 250 mℓ CCl_4 to produce an emerald green stock solution. This solution was stored in a dark bottle and overlaid with 10 mℓ water and 1 mℓ of a 0.5 mol/ℓ sulphuric acid solution. Stored in a cool place and protected from light this solution is stable for some months. Working solutions are obtained by suitable dilution of the stock solution with CCl_4. These solutions were saturated with water before use.

Mercury stock solution: A 100 mg/ℓ Hg^{2+} stock solution was prepared by dissolving 0.171 g $Hg(NO_3)_2.2H_2O$ (Merck) in 1ℓ of distilled water. Working solutions are obtained by suitable dilution of the stock solution.

Cadmium stock solution: A 100 mg/ℓ Cd^{2+} stock solution was prepared by dissolving 0.2744 g $Cd(NO_3)_2.4H_2O$ (Merck) in 1ℓ of distilled water. Working solutions are obtained by suitable dilution of the stock solution.

Alkaline buffer solution: A solution containing 5 g NaKtartrate and 2 g NaOH in 100 mℓ distilled water was used as buffer solution. This solution has an pH of ± 10.5.

H_2SO_4 solution: To ensure the correct pH for the Hg^{2+} extraction a 1 mol/ℓ H_2SO_4 solution was prepared by diluting 55.5 mℓ of concentrated acid (98%) to 1 ℓ with distilled water.

A 0.43 mol/ℓ *acetic acid* solution was used as eluent during the soil extractions.

9.3.1.2 Instrumentation

The sequential injection extraction (SIE) manifold is illustrated in Fig. 9.1. It was constructed from two Gilson Minipuls peristaltic pumps (both operating at 10 rpm), a 4 m long extraction coil (1.02 mm i.d.) made of Teflon (PTFE) tubing (SUPELCO) and a 10-port electrically actuated VICI selection valve (Model ECSD10P) (Valco Instruments, Houston, Texas). Acidflex pump tubing was used for both pumps. The reaction coil was constructed using 30 cm of 0.75 mm i.d. porous silicon tubing together with an h-shaped glass debubbler (D3) (Dermo Tech). A 50 cm (0.8 mm i.d.) piece of Teflon tubing connected the debubbler to pump 3 which was operating at 0.8 mℓ/min to pump away the air bubble. The holding coil was constructed of 1 m (0.8 mm i.d.) Teflon tubing. A Teflon pulsation coil of 6 m (0.25 mm i.d.), coiled around a 10 mm plastic rod, was used to eliminate pulsation of the CCl_4 carrier solution.

An Unicam 8652 UV-VIS spectrophotometer equipped with a 10 mm Hellma flow-through cell (volume 80 μℓ) was used to monitor the coloured product at 486 nm. Data acquisition and device control were achieved using a PC30-B interface board (Eagle Electric, Cape Town, South Africa) and an assembled distribution board (MINTEK, Randburg, South Africa). The FlowTEK [31] software package (obtainable from MINTEK) was used throughout the procedure.

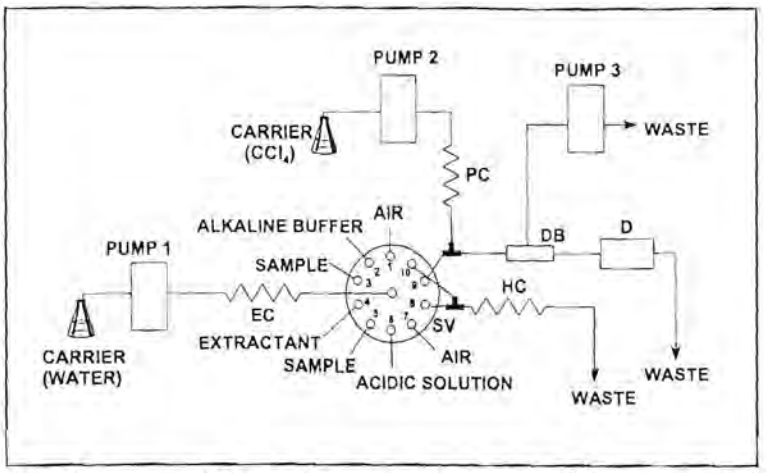

Fig. 9.1 Schematical representation of the sequential injection extraction manifold used for the simultaneous determination of cadmium(II) and mercury(II). EC - extraction coil, SV - selection valve, HC - holding coil, PC - pulsation coil, RC - reaction coil, DB - debubbler and D - detector.

9.3.1.3 Procedure

A small air bubble was drawn up (via port 1 of the selection valve) to separate the extraction zones from the aqueous carrier solution. Thereafter a zone containing alkaline buffer (port 2), a sample zone (containing both analytes) (port 3), the extractant zone (Dithizone in CCl_4) (port 4), a second sample zone (port 5) and a zone containing H_2SO_4 (port 6) were drawn up into the extraction coil. Another air bubble was drawn up (via port 7) to separate these zones from the aqueous carrier in the holding coil.

By switching pump 1 in the reverse direction, the H_2SO_4 and second sample zone mixed, ensuring the correct pH for the mercury extraction to take place. Extraction took place into the thin organic layer formed by the Dithizone zone, whose flow was impeded due to the hydrophobic interactions with the walls of the Teflon coil (Fig. 9.2). During this process an $Hg(HDz)_2$ complex was formed. This complex is stable in dilute alkaline solutions and therefore did not decompose when the flow was reversed to allow the alkaline extraction to take place in the same way as the acidic extraction.

The sequence of zones were propelled forward until the aqueous zones were pumped into the holding coil. The remaining cadmium and mercury dithizonates in the CCl_4, collected by the first bubble, was pumped into the reaction coil until the organic zone was just inside the reaction coil. The valve was switched to select port 10 which was connected via a T-piece to the holding coil. Pump 1 was then switched on (forward) to rinse the holding coil, while the product zone was propelled by the CCl_4 carrier solution using the forward motion of pump 2. The bubble was removed prior to detection using an h-shaped debubbler. Care was taken that the bubble was removed effectively, but that not too much of the product zone was removed.

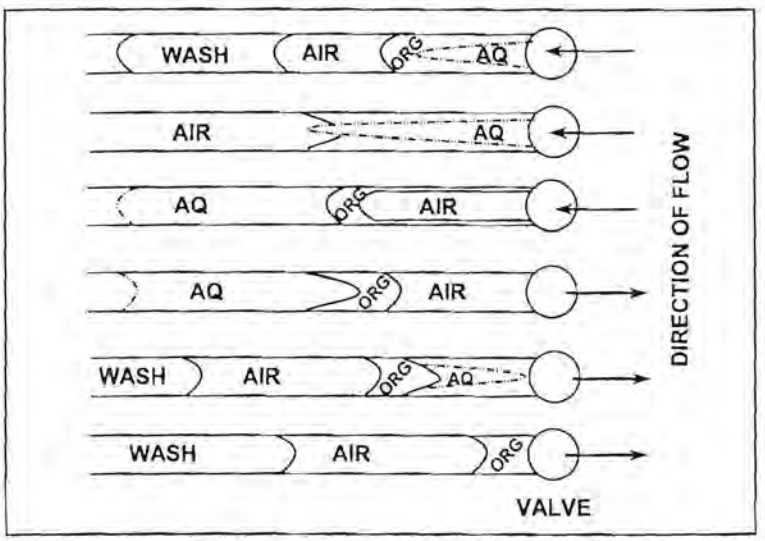

Fig. 9.2 Experimental protocol used in sequential injection wetting film extraction. AQ 1 and AQ 2 refer to the order in which the aqueous zones were drawn into the extraction coil and ORG represent the organic phase.

The instrumental procedure (as programmed in FlowTEK) is given in Table 9.1. The formed product peak was measured at 486 nm.

TABLE 9.1 Device sequence of the sequential injection system for determination of Hg and Cd.

Time (s)	Pump 1	Pump 2	Valve	Description
0	Off	Off	Air	Both pumps off, valve is turned to position 1 to select first air inlet.
4	Reverse			First air bubble is drawn up into the extraction coil.
5	Off			Pump 1 stops.
6			Alkaline buffer	Valve is turned to position 2 to select the alkaline buffer line.
7	Reverse			The alkaline buffer is drawn up into the extraction coil.
12	Off			Pump 1 stops.
13			Standard/ sample	Valve turned to position 3 to select the first standard or sample line.
14	Reverse			The first standard or sample zone is drawn up into the extraction coil.
15	Off			Pump 1 stops.
16			Extractant	Valve is turned to position 4 to select the extractant line.
17	Reverse			The extractant zone is drawn up into the extraction coil.
19	Off			Pump 1 stops.
20			Standard/sample	Valve is turned to position 5 to select the second sample or standard line.
21	Reverse			The second sample or standard zone is drawn up into the extraction coil.
22	Off			Pump 1 stops.
24			Acidic solution	Valve turned to position 6 to select the acidic solution line.
25	Reverse			The acidic solution is drawn up into the extraction coil.
26	Off			Pump 1 stops.
27			Air	Valve is turned to position 7 to select the second air inlet.
28	Reverse			Second air bubble is drawn up into the extraction coil.
29	Off			Pump 1 stops.
30			Holding coil	Valve is turned to position 8 to select the holding coil.

TABLE 9.1 continued Device sequence of the sequential injection system for determination of Hg and Cd.

Time (s)	Pump 1	Pump 2	Valve	Description
31	Reverse		Holding coil	Extraction step 1: the acidic solution and sample 2 are mixed to ensure correct pH for Hg extraction and then extracted into the thin layer of CCl_4 (with Dithizone) which coated the Teflon walls of the tubing.
66	Forward			Extraction step 2: the flow is reversed and the acidic mixture moves back through the organic thin layer. The alkaline solution and sample 1 was also mixed during the previous step and this mixture is now also propelled through the organic layers and the analyte is extracted into the CCl_4 (with Dithizone). The second air bubble collect the organic layer again and the aqueous phase together with the first air bubble are pumped into the holding coil.
105	Off			Pump 1 stops.
106			Detector	Valve is turned to position 9 to select the detector line.
107	Forward			The organic zone with the extracted product and the second air bubble are propelled into the detector line.
110	Off			Pump 1 is stopped immediately after the bubble entered the detector line.
110		Forward		Pump 2 is switched on and the CCl_4 carrier is used to propelled the organic zone through the detector.
111			Holding coil	Valve is turned to position 10. This port of the valve is connected (by means of a T-piece) with a short piece of Teflon to the holding coil. This means that the holding coil is now selected.
112	Forward			The holding coil is now flushed with clean water to eliminate any sample carry-over.
186	Off	Off		Both pumps are stopped. End of analytical cycle.

9.3.1.4 Sample preparation

Sample collection: Urine samples were collected in polypropylene flasks which had previously been cleaned by rinsing with dilute nitric acid and water. The samples were quickly frozen after collection with minimum air space above the urine. Soil samples

were taken from a maize farm in the northern Free State and stored in polypropylene containers.

Before analysis, the frozen urine was allowed to reach room temperature and thoroughly mixed. All water samples were analysed directly. Representative soil samples of 20.00 ± 0.05 g were dried at 30°C for 8 - 10 hours. 5.00 ± 0.01 g of the air-dried soil was weighed into a beaker and 50 mℓ of a 0.43 mol/ℓ CH_3COOH solution was added. The suspension was stirred for 30 min and then filtered. The filtrate was analysed directly (pH corrections were done on-line).

9.4 Method optimisation

9.4.1 Physical parameters

A number of physical parameters can influence the degree of dispersion and extraction in the manifold. To obtain the highest sensitivity and precision it was necessary to optimise these parameters.

9.4.1.1 Zone sequence

Since two different reactions at different pH-values were taking place the zone sequence was of utmost importance. Different zone sequences were evaluate to find the sequence resulting in less interference and optimum extraction. The following sequence was first evaluated: extractant zone followed by the acidic zone, then the sample zone and finally the alkaline buffer. This sequence resulted in a neutralisation reaction when the acidic and basic zones overlap. This happened because the sample zone separating the two buffer zones was not large enough to prevent overlapping of the acidic and basic zones. When the organic extractant zone was placed behind the aqueous zones insufficient extraction took place as the aqueous zones only moved through the organic zone after the flow was reversed. The optimum zone sequence was found to be: an air bubble (separating extraction zones from carrier), the alkaline

buffer solution, sample zone 1, extractant zone (Dithizone reagent), a second sample zone, the acidic zone followed by another air bubble.

9.4.1.2 Introduction of air bubbles

Although it was feared that the introduction of air bubbles into a flow system would have led to irreproducible results, this was to a major extent not the case. The first bubble separated the extraction zones from the surrounding carrier solution. Preventing, in the first place, excessive dilution of the sample zones and secondly, it was used to 'collect' the thin layer of organic solvent again. This bubble was also pumped into the reaction coil and was removed by the debubbler prior to detection. The second bubble was used to separate the extraction zones from the solution in the holding coil, thereby preventing any carry-over between successive samples. In this way, a total recovery of the organic phase and the dispensing of the use of a separation device were achieved.

9.4.1.3 Removal of air bubbles

As important it was to introduce the air bubbles, it was even more important to remove them effectively prior to detection. Initially a debubbler in the form of a dialyser with a Spectrapor 1 membrane was used. The membrane (vol/cm = 8 mℓ, MW cutoff = 6 000 - 8 000, dry cylinder diameter = 31.8 mm and dry thickness = 0.030 mm) was insoluble in CCl_4. The membrane was mounted on a 16 cm x 5 cm perspex block with a flow path of 10 cm x 30 mm x 25 mm. The extraction product together with a small residue of aqueous solution and the first air bubble were pumped through the dialyser. This was aimed to achieve the removal of the excess water as well as the air bubble. Unfortunately, the lifetime of the membrane was not that long (maximum of two days) and deterioration of the membrane resulted in small leakages. The CCl_4 leaking through the membrane caused the iron screws to rust and that contaminated the system.

A piece of porous silicon tubing (length 30 cm, i.d. 0.75 mm and o.d. 1.25 mm) was then

introduced as debubbler. This would be effective, provided that there was ample back pressure on the air bubble, caused by the use of a flow restricter, or by simply elevating the outlet tube. The pressure placed on the bubble is then greater than atmospheric pressure and this difference force the air bubble through the porous tubing [32]. The pressure inside the SIA manifold was however not sufficiently high to push the air bubble through the pores. Eventually an h-shaped glass debubbler was placed in the reaction coil. A 50 cm (0.8 mm i.d.) piece of Teflon tubing connected the debubbler to a pump, operating at 0.8 mℓ/min, to pump away the air bubbles. Care was taken that the bubble was remove effectively, but that not too much of the product zone was removed. This debubbler proved to be the most effective and was incorporated into the SIA manifold.

9.4.1.4 Flow rate

Since two pumps were used in these application two different flow rates were to be considered. The first pump controlled the volumes of the different zones as well as the extraction process, whilst the second pump was used to propel the formed product zone to the detector. Table 9.2 and Fig. 9.3 illustrate the results obtained for the various flow rates evaluated. It shows clearly that lower flow rates needed to be used during the extraction process and faster flow rates to propel the product zone through the detector. Initially both pumps were set on the same speed. At flow rates higher than 2.64 mℓ/min the organic zone tended to break up and formed small organic bubbles in the aqueous phase. This lead to very irreproducible results. The optimum flow rate for pump 1 (using water as carrier) was therefore chosen to be 2.40 mℓ/min.

Faster flow rates result in less dispersion and it was therefore necessary to optimise this parameter further. An optimum flow rate of 3.8 mℓ/min was obtained for pump 2 (using carbon tetrachloride as carrier). The faster flow rate was also needed to flush out the fine suspension of water droplets inside the flow cell. These droplets resulted from the small amount of aqueous phase still present in the organic phase when it was pumped to the detector. The faster rinsing time also favoured shorter analysis time and

therefore a higher sample throughput.

TABLE 9.2 Influence of the individual flow rates of the two pumps on the sensitivity and precision

Flow rate (mℓ/min)		Relative peak height		%RSD	
Pump 1	Pump 2	Pump 1	Pump 2	Pump 1	Pump 2
1.35	1.35	2.65	2.65	5.75	5.75
1.50	1.50	2.96	2.96	6.21	6.21
1.75	1.75	3.42	3.42	5.20	5.20
2.40	2.40	4.52	4.52	1.79	1.79
2.64	2.64	5.28	5.28	2.79	2.79
3.00	3.00	6.77	6.77	10.3	10.3
2.40	3.00	4.52	7.13	-	2.08
2.40	3.50	4.52	7.58	-	1.98
2.40	3.80	4.52	8.25	-	1.85
2.40	4.20	4.52	8.13	-	2.06
2.40	4.50	4.52	8.06	-	3.26

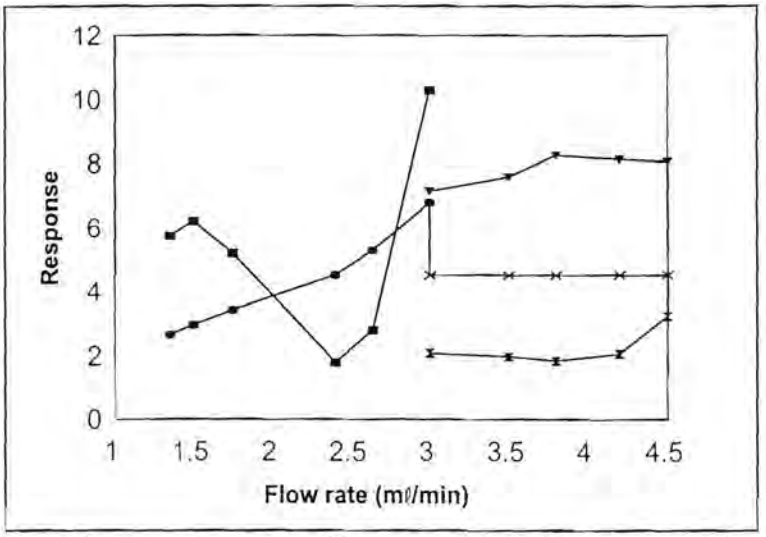

Fig. 9.3 Influence of flow rate on sensitivity and precision for both pumps. -●- = relative peak height when both pumps operate at the same flow rate, -■- = %RSD when both pumps operate at the same flow rate. To show the effect of the flow rate of pump 2 on sensitivity, -▼- = relative peak height of pump 2 alone, while pump 1 was kept constant (-✕-). The %RSD of pump 2 is represented by -▲-.

9.4.1.5 Sample volume

Sample zones were present on both sides of the organic zone. It was important to optimise this parameter to ensure that effective mixing with the buffer solutions was obtained as well as to ensure maximum analyte to be extracted into the organic phase. The two sample zones were evaluated independently. Table 9.3 and Fig. 9.4 shows the influence of different sample volumes on the sensitivity and reproducibility of the different test runs. For sample 1 (the zone between the alkaline solution and the organic phase) an optimum volume of 220 $\mu\ell$ (%RSD - 0.79) was established. It seemed from Fig. 9.4 that even bigger sample zones would led to higher sensitivity. These values were however ruled out due to their poor reproducibility. The volume of sample 1 was significantly higher than the optimum volume of 90 $\mu\ell$ (%RSD - 0.96) used for the second sample zone (the zone between the organic phase and the acidic solution).

The different results can easily been explained in terms of the different dispersions that the zones undergo. Smaller zones result in bigger dispersion, and therefore in better zone overlap [33, 34]. This explains why the second sample zone, which spends a shorter residence time in the extraction coil, needs to have a smaller volume than the first sample zone which spends a longer time in the extraction coil.

TABLE 9.3 Influence of the two sample zones on the precision and reproducibility of the SIE system

Sample volume ($\mu\ell$)		Relative peak height		%RSD	
Sample 1	Sample 2	Sample 1	Sample 2	Sample 1	Sample 2
45	45	2.66	3.25	3.54	2.05
90	90	3.49	2.03	3.92	1.79
135	135	3.92	1.79	3.63	2.11
180	180	4.17	1.20	3.35	2.51
225	-	4.31	0.79	-	-
270	-	4.42	2.12	-	-

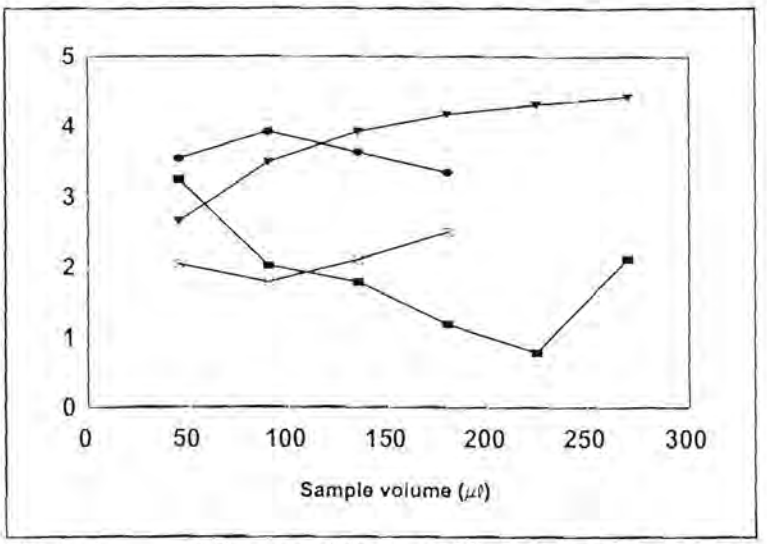

Fig. 9.4 Influence of the two different sample zones on the precision and sensitivity of the determination. ■ = %RSD for sample volume 1, ▼ = relative peak height for sample volume 1, ● = relative peak height for sample volume 2 and ✕ = %RSD for sample volume 2

9.4.1.6 Extractant volume and extraction time

This volume is dependant on a critical parameter called the zone inversion length. Zone inversion length refers to the distance travelled by the zones from the load position (where the organic zone was situated in the extraction coil after aspiration), to the position where the aqueous phase (AQ 2) has moved through the organic phase and reached the tail of AQ 1 (refer to Fig. 9.2). At this point the organic zone has been deposited on the tubing as a film, allowing maximum contact between the two phases. The volume of the extractant zone influence both the time of the extraction as well as the length of the extraction coil.

Different extractant volumes were evaluated. Larger volumes not only produced an excess of reagent, which greenish colour interfered in the determination, but also lead to unnecessary long extraction times. Taking the 50 μℓ used by Peterson *et al.* [35] as guideline a volume of 45 μℓ was found to be the optimum. Smaller volumes gave very irreproducible results due to the fact that extractant volume was not reproducibly drawn into the extraction coil. For volumes smaller than 45 μℓ, aspiration times of less than

a second were needed. Because of the imperfect flow dynamics of the pump (start up and stopping are not instantaneous) [34], these small volumes were not aspirated reproducibly.

It took 35 s for zone inversion to take place whereafter the flow was reversed and the aqueous sample moved through the organic film into the holding coil. This step took 39 s, which accounted for a total extraction time of 74 s. During this step the organic phase was collected again by the second air bubble. Shorter extraction times lead to incomplete zone inversion and lower sensitivity as can be seen in Table 9.4.

Table 9.4 The effect of various extraction times on the sensitivity and reproducibility of the SIE method.

Time needed for zone inversion (s)	Time needed to collect organic phase (s)	Total extraction time (s)	Relative peak height	%RSD
23	29	52	1.80	2.67
25	31	56	2.15	3.63
27	33	60	2.29	3.05
29	34	63	2.80	3.59
31	36	67	3.02	3.12
33	37	70	3.61	2.33
35	39	74	4.26	1.53
37	41	78	4.27	3.77

9.4.1.7 Volumes of acidic and alkaline buffer solutions

Due to the pH dependancy of the different extraction procedures, the volumes of the buffer zones were evaluated using sample to buffer volume ratios. A known volume of sample was taken and known amounts of buffer solution was added till the correct pH was reached. These ratios were then used to estimate the volume of buffer to be drawn into the extraction coil. The following ratios were found manually: Alkaline buffer : sample = 1 : 5 and sample : acidic solution = 2 : 1. Due to the difference in dispersion

which the two buffer zones undergo, these parameters were also evaluated by aspirating different volumes of each buffer zone individually. The optimum volumes were found to be 45 $\mu\ell$ for both buffer solutions (Table 9.5), which corresponded excellently with the predicted ratios.

Table 9.5 Influence of buffer zone volumes on the extraction efficiency and sensitivity of the method.

Volume of buffer solution ($\mu\ell$)	Ratio Buffer : sample* (alkaline)	Ratio Buffer : sample# (acidic)	Relative peak height	%RSD
45	1 : 5	-	3.44	2.96
90	1 : 2.5	-	3.13	3.39
135	1 : 1.6	-	2.98	3.24
45	-	1 : 2	3.44	2.96
90	-	1 : 1	3.29	3.18
135	-	1 : 0.67	3.04	3.78

The optimum sample volume was used to determine the buffer to sample ratios.
* sample volume = 220 $\mu\ell$
# sample volume = 90 $\mu\ell$

9.4.1.8 Organic film thickness

The thickness of the organic film influences extraction by affecting the mass transfer of analytes into the film [36]. Relative film thickness per unit length (d_f) can be predicted using the equation [35]

$$d_f = kd_t(u\eta/\gamma)^a \qquad 9.1$$

where u represents flow rate (velocity) and d_t tubing diameter. The solvent characteristics also play an important role and are included in the equation. Viscosity of the solvent is represented by η and surface tension by γ, k and a are constants between ~1/2 and ~ 2/3. From the equation it can be seen that film thickness is directly proportional to viscosity and inversely proportional to surface tension. As colligative

properties, it is appropriate to consider either interfacial or surface tension to viscosity as a film thickness parameter, η/γ [35]. The film thickness parameter for CCl_4 was calculated to be 3.26×10^{-2} (η = 0.88 cP and γ = 27.00) [37].

Slower flow rates resulted in longer zone inversion times and therefore thinner films. Faster flow rates, on the other hand, resulted in thick films with high extraction capacity, but analyte recovery was only partly because the contact time with the extractant was shortened. Under optimum running conditions the relative film thickness was calculated to be 7.5 μm.

9.4.1.9 Diameter and length of tubing

Extraction coil: The length of the extraction coil depends on the zone inversion length. Thickness of the wetting film is directly proportional to the inner diameter of the coil [38]. As a result, the extraction capacity (volume of the wetting film) is larger for wider and longer extraction coils. Using an extractant volume of 45 $\mu\ell$ an extraction coil of 2.8 m was needed. To ensure that none of the zones reached the pump conduit and became deformed, an extraction coil of 4 m was used. An inner diameter of 1.02 mm ensured good axial dispersion and zone overlap.

Holding coil: A 1 m long (0.8 mm i.d.) Teflon coil was used to allow the flow of the aqueous carrier to propel the extraction zones inside the extraction and holding coils. The relative large diameter was chosen to ensure minimum back pressure when the aqueous zones were pumped from the extraction coil to waste. It was important to rinse the holding coil after every analysis to avoid sample carry-over.

Reaction coil: Porous silicon tubing (30 cm, 0.75 mm i.d.) was used as reaction coil. This was done mainly to debubble the carrier solution prior to entering the flow cell. Unfortunately, this did not have the desired result and an h-shaped glass debubbler was installed. The debubbler was connected to pump 3 by means of a 50 cm (0.8 mm i.d.) piece of Teflon tubing. The pump was operating at a flow rate of 0.8 mℓ/min to ensure

effective removal of the air bubbles. The spectrophotometer should be positioned as close to the debubbler as possible. Longer distances between the debubbler and detector led to higher dispersion, longer rinsing times and ultimately lower sample throughput.

9.4.2 Chemical parameters

9.4.2.1 pH

Dithizone forms complexes with all the heavy metals as well as some other metals, such as Fe and Al [18]. To ensure high selectivity in determinations using Dithizone, pH control is of the utmost importance. Mercury forms a primary dithizonate in the acidic range (pH 1 - 4) [18], while cadmium forms a orange-red dithizonate in the alkaline range (pH 8.5 - 10.5) [30]. Preliminary experiments showed that the optimum extraction pH for mercury would be 3.5 and for cadmium extraction about 9. To ensure that these pH values were achieved in the flow system a sample to buffer volume ratio was used.

It was also important that the acidic extraction should have taken place first due to the stability of the $Hg(HDz)_2$. The cadmium dithizonate is however not very stable in acidic solutions [18] and the alkaline buffer was therefore carefully evaluated. Ammonia and sodium hydroxide were chosen as possible alkaline buffer solutions. Results obtained with ammonia proved to be not only very irreproducible (%RSD = 7.68), but also less sensitive than the same NaOH concentration. Various NaOH concentrations were then evaluated and a 2% m/v solution was chosen as optimum (relative peak height - 3.44 and %RSD - 3.67). Addition of this solution did improve the sensitivity with 14.8%, but reproducibility was still not satisfactory. Addition of 2% m/v NaKtartrate solution to the NaOH solution solved the problem to a great extend. Although the sensitivity did not improve much, the relative standard deviation dropped to 1.66%.

9.4.2.2 Choice of organic solvent

The choice of solvent or the solvent composition is a critical parameter for the successful application of sequential injection extraction, since it determines the difference in flow velocity between the organic and aqueous phases, the chemical selectivity and efficiency of the extraction [35]. Solvents with low viscosities do not offer a sufficient difference in flow velocity when compared to water and make SIE less effective as it requires more time and longer extraction coils. On the other hand, highly viscous solvents are difficult to wash out of the tubing.

CCl_4, with an intermediate viscosity of 0.88 cP, was chosen as solvent not only because of its film forming ability, but also because of Dithizone's high solubility and stability in the organic solvent. Dithizone, as well as its metal dithizonates are all highly soluble in chlorinated solvents [27]. The visible absorption spectrum of Dithizone is very sensitive to the organic solvent in which it is dissolved [39]. Dissolved in CCl_4, $Hg(HDz)_2$ and $Cd(HDz)_2$ absorbed at almost the same λ_{max}. Experimental values for λ_{max} are 485 nm and 488 nm for $Hg(HDz)_2$ and $Cd(HDz)_2$ respectively. Detection was done at 486 nm.

One disadvantage about CCl_4 is that it is highly carcinogenic and has ozone depleting properties [40]. Using the solvent in a SIE system ensured a closed system and no atmospheric contact. The CCl_4 waste was collected and recycled by adsorption on charcoal, water washing and distillation.

9.4.2.3 Concentration of Dithizone

Since solutions of Dithizone of any but the lowest concentration are deeply coloured, and often almost opaque, it is quite difficult to be certain whether excess solid is present in contact with a saturated solution. Special care is needed to ensure that metallic impurities are not introduced by the filtering medium, especially when the concentration is to be calculated afterwards from the absorbance of a suitably diluted aliquot and a

knowledge of the molar (decadic) absorption coefficient, ε [27]. A 100 mg/ℓ stock solution of Dithizone in CCl_4 was prepared. Several dilutions, using CCl_4, were made and evaluated. Most of these solutions could not been used due to the deep green colour of the unreacted Dithizone. A solution containing 0.10 mℓ of the stock solution, made up to 50 mℓ with CCl_4, produced a extractant solution with an absorbance in the range 0.4 - 0.6 (10 mm cell). This solution was used throughout the whole procedure as optimum Dithizone concentration. The solution had to be prepared daily.

9.5 Evaluation of the system

The proposed sequential extraction method was evaluated under optimum running conditions with regard to linearity of the two analytes respectively, sample frequency, reproducibility, sample interaction, detection limits, accuracy and major interferences.

9.5.1 Linearity

Evaluation under optimum running conditions delivered analytical curves for the extraction of Cd(II) and Hg(II) with Dithizone as shown in Table 9.6 and Fig. 9.5. The curves for the individual metals are linear between 50 μg/ℓ and 3 mg/ℓ for both metals. For cadmium r^2 = 0.9914 and for mercury r^2 = 0.9875. Peak height was used to evaluate the analytical signal.

TABLE 9.6 Calibration values for the individual metals analysed with the SIE system

Concentration (mg/ℓ) of both analytes	Relative peak height measured for Hg^{2+}	Relative peak height measured for Cd^{2+}
0.025	0.001	0.002
0.05	0.011	0.039
0.10	0.019	0.078
0.50	1.02	0.59
1.0	2.01	1.22
2.0	3.99	2.39
3.0	6.02	3.58
4.0	7.41	4.43
5.0	8.52	4.82
10.0	9.40	6.02

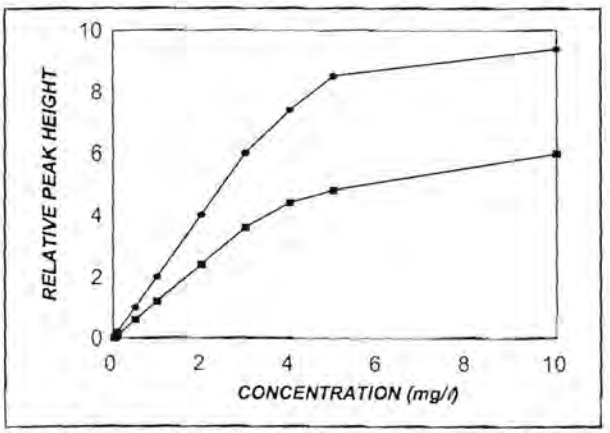

Fig. 9.5 Calibration curves for both Hg^{2+} and Cd^{2+} individually. -●- = Hg^{2+} and -■- = Cd^{2+}.

9.5.2 Accuracy

To investigate the accuracy of the SIE system a calibration curve for each individual metal were constructed. Because absorbance is additive two equations are obtained which should yield the required unknown concentrations when solved simultaneously [41]. The equations for the calibration curves obtained experimentally were:

Calibration curve for Hg(II): $A = 1.37[Hg] + 0.021$

Calibration curve for Cd(II): $A = 0.602[Cd] + 0.017$

Addition of the two equations gave:

$$A = 1.37[Hg] + 0.602[Cd] + 0.038$$

The same procedure was followed as described in Chapter 8. The above data represents the value of the peak maximum as determined by the FlowTEK program (refer to it as A). The other value was found by retrieving the data points of the specific peak profile into Quattro Pro and using the absorbance value recorded one second before the peak maximum was reached (refer to it as A'). The calibration data at this time were as follow:

For mercury: $A' = 1.24[Hg] + 0.001$ $r^2 = 0.9878$

For cadmium: $A' = 0.427[Cd] + 0.008$ $r^2 = 0.9789$

Addition of the equations give: $A' = 1.24[Hg] + 0.427[Cd] + 0.009$

Solving these two equations (A and A') simultaneously give the desired concentrations.

Three different aqueous mixtures, three urine mixtures and two soil extracts were analysed. The results are listed in Table 9.7. The percentage recovery was calculated for the aqueous samples and soil extracts, whilst standard addition to the urine samples showed that the urine did not contain any Cd(II) or Hg(II). The percentage recovery yielded satisfactory results in most cases.

Table 9.7 Evaluation of the accuracy of the proposed SIE method.

Sample	Known concentration in mg/ℓ		Concentration obtained with SIE in mg/ℓ		% Recovery	
	$[Cd^{2+}]$	$[Hg^{2+}]$	$[Cd^{2+}]$	$[Hg^{2+}]$	$[Cd^{2+}]$	$[Hg^{2+}]$
Aqueous 1	0.25	2.0	0.23	2.15	92	108
Aqueous 2	0.75	0.75	0.70	0.67	93.3	89.3
Aqueous 3	1.5	0.5	1.65	0.45	110.5	90
Urine 1	0.1	1.0	0.12	0.84	120	84
Urine 2	1.0	0.5	0.94	0.58	94	116
Urine 3	2.0	2.5	2.21	2.32	110.5	92.8
Soil 1	1.0	2.5	0.82	2.45	82	98
Soil 2	2.5	0.5	2.40	0.6	96	120

9.5.3 Reproducibility

The results obtained (Table 9.8) when using the proposed system revealed surprisingly good reproducibility. It is expected when using air bubbles in the flow system, that the reproducibility will deteriorate due to the irregular stretching and compressing of the bubble. Signals obtained for the two metals, in the standard solutions as well as the samples analysed, show relative standard deviations lower than 2.5% for ten measurements at each concentration or sample.

TABLE 9.8 Reproducibility of the proposed sequential injection extraction system

Standard/sample ([ ] in mg/ℓ)	%RSD
0.05	2.41
0.5	2.10
1	1.57
2	1.91
3	1.51
Aqueous 1	2.15
Aqueous 2	2.12
Aqueous 3	2.11
Urine 1	1.22
Urine 2	2.10
Urine 3	1.85
Soil 1	1.63
Soil 2	1.58

9.5.4 Sample frequency

It took 186 s to complete one whole extraction cycle, including the time needed for detection and to rinse the extraction coil. This resulted in a sample frequency of 19 samples per hour. Although the sample frequency seemed a little low, the fact that two analytes were determined during the analytical cycle, increased the importance of the system.

9.5.5 Sample interaction

Some carry-over between more concentrated samples was experienced. The sample interaction was calculated to be about 2% using the equation

$$Interaction = \frac{(A_3 - A_1)}{A_2} \times 100$$

where

A_1 = the true peak height of a sample with a low analyte concentration (0.1 mg/ℓ),

A_2 = the true peak height of a sample containing ten times more analyte (1 mg/ℓ), and

A_3 = the peak height for an interacted sample containing the same amount of analyte as A_1.

Rinsing of the extraction coil with a small amount of CCl_4, after every twentieth run, eliminate this problem.

9.5.6 Detection limits

The detection limits, estimated as three times the signal-to-noise ratio [42], was equal to 50 and 60 μg/ℓ for Cd(II) and Hg(II), respectively. These detection limits are acceptable, since a concentration of 50 μg/ℓ for both metals individually gave clearly recognisable peaks.

9.5.7 Interferences

Possible interferents were tested using a solution containing 1 mg/ℓ of both analytes. The following substances did not interfere with the determination of cadmium and mercury ions: 250 mg/ℓ SO_4^{2-}, 10 mg/ℓ PO_4^{3-}, 0.5 mg/ℓ Al^{3+}, 50 mg/ℓ Mg^{2+} and 400 mg/ℓ Ca^{2+}.

Chloride up to 14 g/ℓ (0.4 mol/ℓ) did not interfere in the mercury determination as long as the H_2SO_4 concentration did not exceed 2 mol/ℓ, while chloride concentrations of up to 20 g/ℓ could be tolerated in the cadmium determination. Bromide, cyanide and thiocyanate interfere in the mercury determination, since they complex mercury more strongly than Dithizone. These anions could be tolerated up to 10 mg/ℓ. Anions could

be removed by using anion exchange columns in the sample uptake tubes.

The metals normally present in urine, *viz.* Co(II), Fe(II), Ni(II), Pb(II) and Zn(II), were also tested as possible interferents. The metals were individually added to two different urine samples which contained 1 mg/ℓ Cd(II) and 1 mg/ℓ Hg(II) respectively. Although variation in pH usually is the most important way to eliminate interferences from metal cations, the cations still interfere at the optimum pH for the extractions. The interferences were less for the mercury determination. The extent of interference for the different metals are listed in Table 9.9.

TABLE 9.9 Effect of metal ions normally present in urine sample on the determination of Hg(II) and Cd(II)

Interferent	Influence on cadmium signal	Influence on mercury signal
Co(II)	Increase peak height with 5.2%	No interference
Fe(II)	Increase peak height with 10.8%	Increase peak height with 1.8%
Ni(II)	Increase peak height with 3%	No interference
Pb(II)	Increase peak height with 11.5%	Increase peak height with 2.5%
Zn(II)	Increase peak height with 7.5%	Increase peak height with 0.8%

These interferences can however be masked by addition of a mixture of hydroxylamine (1 mol/ℓ), sodium potassium tartrate (0.75 mol/ℓ and potassium hexacyanoferrate(II) (1.5 mol/ℓ) [17]. 2 mℓ of this solution was added to 5 mℓ urine samples. These mixtures were then diluted to 10 mℓ with distilled water prior to introduction into the sequential injection extraction system.

9.6 Conclusion

The sequential injection extraction system described allows the automated extraction of aqueous samples while keeping the organic solvent volume to a minimum and does not compromise repeatability or recovery as compared to conventional glassware

extraction with the same volumes. It operates without phase separators or segmenters by stacking the reagents in such a way that the faster moving phase overcome the slower one as the two travel through the tubing. In addition, as a completely enclosed system, SIE isolates potentially hazardous organic solvents from the operator and reduces contact with biohazardous samples. The robustness of design and ease of changing reagents make SIE a useful technique for automating batch analysis of liquid-liquid extractions and is therefore applicable to many fields.

9.7 References

1. N. N. Greenwood and A. Earnshaw, **Chemistry of the Elements**, Pergamon Press, 1986.
2. T. W. Clarkson, J. C. Smith, D. O. March and M. D. Turner, in P. A. Krenkel (ed), **Heavy Metals in the Aquatic Environment**, Pergamon Press, Oxford, pp 1 - 12.
3. K. Nomiyama, in P. A. Krenkel (ed), **Heavy Metals in the Aquatic Environment**, Pergamon Press, Oxford, pp 15 - 23.
4. I. Drabœk and Å. Iverfeldt in Quevauviller, Maier and Griepink (eds), **Quality Assurance for Environmental Analysis**, Elsevier Science, 1995.
5. H. A. McKenzie and L. E. Smythe, **Quantitative Trace Analysis of Biological Materials**, Elsevier, 1988, pp 543 - 561.
6. W. Dickinson Burrows, in P. A. Krenkel (ed), **Heavy Metals in the Aquatic Environment**, Pergamon Press, Oxford, pp 51 - 61.
7. O. Haase, M. Klare, J. A. C. Broekært and K. Krengel-Rothensee, **Analyst**, **123** (1998) 1219.
8. G. Tao, S. N. Willie and R. E. Sturgeon, **Analyst**, **123** (1998) 1215.
9. X. Yin, W. Frech, E. Hoffmann, C. Ludke and J. Skole, **Fresenius J. Anal. Chem.**, **361** (1998) 761.
10. C. E. C. Malgalhaes, F. J. Krug, A. H. Fostier and H. Berndt, **Jour. Anal. Atom. Spec.**, **12** (1997) 1231.
11. A. Ali, H. Shen and X. Yin, **Anal. Chim. Acta**, **369** (1998) 215.
12. E. Beinrohr, J. Dzurov, J. Annus and J. A. C. Broekært, **Fresenius J. Anal. Chem.**, **362** (1998) 201.
13. R-B Shi, K. Stein and G. Schwedt, **Fresenius J. Anal. Chem.**, **357** (1997) 753.
14. I. A. Gurév and N. V. Kuleshova, **Jour. Anal. Chem.**, **53** (1998) 15.
15. B. Romberg and H. Műller, **Anal. Chim. Acta.**, **353** (1997) 165.
16. P. C. Rudner, A. G. de Torres, J. M. C. Pavon and E. R. Castellon, **J. Anal. Atom. Spec.**, **13** (1998) 243.
17. J. L. Burguera and M. Burguera, **Anal. Chim. Acta.**, 153 (1983) 207.

18. J. Fries and H. Getrost, **Organic Reagents for Trace Analysis**, E. Merck Darmstadt, 1977.

19. R. P. Sartini, J. A. G. Neto, T. I. M. S. Lopes and E. A. G. Zagatto, **Quimica Analitica, 15** (1996) 161.

20. E. A. Jones, **Mintek Report**, No. M111, (1983) 1.

21. O. Klinghoffer, J. Růžička and E. H. Hansen, **Talanta, 17** (1980) 169.

22. P. Ruiz, T. H. Cordoba, M. M. Lozano and C. Sanchez-Pedreno, **Quimica Analitica, 4** (1985) 72.

23. M. D. Mateo, R. Forteza and V. Cerdà, **Int. Jour. Environ. Anal. Chem., 41** (1990) 39.

24. E. Janssen, **CANAS'95 Colloquium Analytsche Atomspektroskopie**, (1996) 257.

25. X. Peng, Q. Mao and J. Cheng, **Fresenius J. Anal. Chem., 348** (1994) 644.

26. J. C. Gage, **Analyst, 86** (1961) 457.

27. H. M. N. H. Irving, **Dithizone**, The Chemical Society, London, 1977.

28. M. F. Enriques-Domingues, M. C. Yebra-Biurrun and M. P. Bermejo-Barrera, **Analyst, 123** (1998) 105.

29. M. Lui and S. Xu, **Atomic Spectroscopy, 18** (1997) 195.

30. M. Trojanowicz, P. W. Alexander and D. Brynn Hibbert, **Anal. Chim. Acta, 370** (1998) 267.

31. G. D. Marshall and J. F. van Staden, **Anal. Instrum., 20** (1992) 79.

32. G. B. Martin, H. K. Cho and M. E. Meyerhoff, **Anal. Chem., 56** (1984) 2612.

33. G. D. Marshall and J. F. van Staden, **Process Control and Quality, 3** (1992) 251.

34. R. E. Taljaard, **Application of Sequential Injection Analysis as Process Analyzers**, MSc-Thesis, University of Pretoria, 1996.

35. K. L. Peterson, B. K. Logan, G. D. Christian and J. Růžička, **Anal. Chim. Acta., 337** (1997) 99.

36. C. A. Lucy, **Anal. Chem.**, 61 (1989) 101.

37. P. W. Atkins, **Physical Chemistry**, fourth ed., Oxford University Press, Oxford, 1990, pp 293 - 969.

38. Y. Luo, S. Nakano, D. A. Holman, J. Růžička and G. D. Christian, **Talanta**, **44** (1997) 1563.

39. A. T. Hutton, **Polyhedron**, **6** (1987) 13.

40. S. Nakano, Y. Luo, D. Holman, J. Růžička and G. D. Christian, **Microchemical Journal**, **55** (1997) 392.

41. A. Fernandez, M. D. Luque de Castro and M. Valcarcel, **Anal. Chem.**, **56** (1984) 1146.

42. I. Facchin, J. J. R. Rohwedder and C. Pasquini, **Journal of Automatic Chemistry**, **19** (1997) 33.

CHAPTER 10

Determination of Lead(II), Copper(II), Zinc(II), Cobalt(II), Cadmium(II), Iron(III) and Mercury(II) using Sequential Injection Extractions

10.1 Introduction

The use of certain metals has increased tremendously in our modern society. An increase in population density has inevitably led to ecological problems, due to the increased availability of these metals in the environment. These metals can have toxic effects on plants, animals and eventually men when absorbed in excess amounts. According to Adriano [1] metals could be present in one or more of the following species in soil or sediments:

1. Dissolved in soil solutions
2. On exchange positions of organic solids or inorganic compounds
3. Included in ground minerals
4. Precipitated together with other compounds in soil and sediments
5. Included in biological matter

The first two species are mobile and available to plants, while the last three are non mobile. They can however become mobile and plant available with time and other external factors, like leaching.

Metals, which are captured in river or dam sediments, are potentially dangerous as it can influence the quality of the water with which they are in contact. These metals can be released into the water when certain changes in the water environment take place.

These changes include pH changes, change in redox potential and/or oxygen deficiency, the presence of complexing agents (e. g. EDTA) or surfactants and microbiological transformations [2].

There are several sources of metals in nature, but metals are also added to soils as part of fertilisers, pesticides, fungicides and sewage. Metal pollution of water in a water scarce country like South Africa could become an economical hazard, since purification of water and solving problems associated with the procedures are quite expensive. Although mining is a huge part of the South African economy, it is also one of the main producers of metal pollution of dams and rivers. It is therefore crucial that the amount of dissolved metals in effluent streams must be monitored carefully.

Metals are never found in isolation in nature. Cobalt is invariably associated with nickel, and often also with copper and lead, and is usually obtained as a byproduct or co-product of the recovery of these metals. The production of cobalt is usually subsidiary to that of copper, nickel or lead and the details of its extraction depends on which of these it is associated with [3]. The bulk production of copper is from sulphide ores containing iron [4]. Cadmium on the other hand is closely related to zinc and is usually found to be associated with zinc and lead [2, 3]. Zinc is also associated with minerals that are rich in iron [2]. Mercury is seldom present in nature in metallic form, but occurs in several other forms, e.g. inorganic mercury and organic mercury compounds [5]. Lead and mercury form methyl compounds which are more toxic than the metals itself [2].

These associations between different metals usually complicate the analytical determination of individual metals. Metals associated or closely related to other metals are difficult to remove from samples prior to analysis and sometimes removal of interfering species is impossible. Cation exchange columns are useless when faced with these interferences, since they all carry positive charges in the ionic form and the analyte will therefore also be removed. To find the correct masking agent to eliminate interferences can also be cumbersome and may change the chemical environment of

the analyte and influence the determination. In this study a sequential injection extraction system with which seven metal ions can be detected without prior separation, is proposed. Lead, zinc, copper, iron, cobalt, cadmium and mercury can be quantitatively analysed by the SIE system. The procedure involves the extraction of these metal ions with dithizone and the subsequent detection of the formed dithizonates by diode array spectrophotometry. The bioavailability of the metals in soil and water samples as well as the use in clinical analysis of urine are highlighted.

10.2 Uses and biological importance of the different metals

The car and construction industries are the main consumers of lead. Lead is used in alloys, batteries, silencers, in paint, as additive to petrol and, for clinical applications, as a shield against radio active rays [2]. Lead is present in almost every sphere of our daily life. Humans ingest Pb from food and drink, and inhale it in the form of aerosols and particulates from air. Organo-lead compounds can also enter the body through the skin. Under normal conditions, food accounts for nearly 70% of the total Pb intake. There is no Pb-free food because there is a background Pb level in food according to the background Pb level in soil. Lead contamination of food can also occur through poorly soldered cans, food wrappers, and storage of food in lead-glazed pots. Other important non-food sources of Pb intake, particularly in children, are lead-containing paints, multicolored printed paper, cosmetics and household and playground dust [6].

Lead is generally considered to be a non-essential toxic element which accumulates in the organism. Although Pb in the skeleton is physiologically inert, the Pb in blood and soft tissues has identifiable toxic effects. The general order of susceptibility to the toxic effects of Pb is men < women < children < fetuses. According to the US Centre for Disease Control (CDC), a blood-Pb level < 240 μg/ℓ is 'normal' (Class I), while blood-Pb levels of 250 - 490 (Class II), 500 - 690 (Class III), and > 700 (Class IV) μg/ℓ fall into the 'moderate risk', 'high risk' and 'urgent risk' categories respectively [6].

Symptoms of lead poisoning include distinct neurobehavioral and learning disabilities in children. Lead also effects the hematopoetic system, peripheral nerve conduction, kidneys, gastrointestinal system, gingival tissues, brain, embryo and bone marrow [6].

Zinc is extensively used in the electrical, car and hardware manufacturing industries. It also found use in paints, domestic items, cosmetics, powders, ointments, antiseptic agents, linoleum, rubber, glass, tyres, television screens and dry batteries [2]. Other applications are as micro nutrients, fertilisers and pesticides for agricultural use, as well as hardeners in cements.

In contrast with lead, zinc is biologically one of the most important metals and is apparently necessary to all forms of life. The body of an adult human contains about 2 g of Zn, mainly as Zn enzymes which are present in most body cells [3]. The two Zn enzymes which have received most attention are carboxypeptidase A and carbonic anhydrase. Carboxypeptidase A catalyses the hydrolysis of the terminal peptide bond in proteins during the process of digestion, while carbonic anhydrase is used to catalyse the reaction:

$$CO_2 + H_2O \leftrightharpoons HCO_3^- + H^+$$

The forward (hydration) reaction occurs during the uptake of CO_2 by blood in tissue, while the backward (dehydration) reaction takes place when the CO_2 is subsequently released in the lungs [3].

Copper is mainly used in the manufacturing of wire and copper alloys. Electrical industries are major consumers of copper for the manufacturing of electrical wires and apparatus. Due to its high thermal conductivity and relative inertness, copper is used in stove pipes, car radiators and cooking devices. Copper is used in the agricultural industry as fertiliser, pesticide and fungicide [2].

Copper occurs in all bodily tissues. The distribution varies with age, species and diet. The liver, heart, brain, kidneys and hair contain high concentrations of copper compared to other tissues. A adult human contains around 100 mg of copper, mostly attached to

protein, an amount exceeded only by iron and zinc among transition metals. The required daily intake of copper is about 3 - 5 mg [4].

Abnormally high copper levels in the liver are characteristic of certain disease states in humans. Conditions that manifest increased copper content in the liver include tuberculosis, hemachromatosis, cirrhosis and yellow atrophy of liver. Wilson's disease is also characterized by abnormally high copper levels and is ascribed to the congenital inability to excrete copper, resulting in its accumulation.

Although copper occurs naturally in human organs, the ingestion of copper through other means can also result in the increase of its levels in humans and animals. An example is the ingestion of water. Drinking water that originates from natural sources could contain elevated concentrations of copper due to, e.g. the use of copper salts to control plant growth in reservoirs or from the corrosion of copper, brass or bronze pipe fittings. Drinking water that contains abnormal high amounts of copper could cause ptyalism, nausea, vomiting, epigastric burning and diarrhea [4].

Iron is used in various types of steels and alloys. Iron and its compounds are used in paints, colourants, in the electronic industry, as cover material for magnets and as catalysts. Iron salts are also used as flockulants in water purification [2, 3].

Biologically, iron plays crucial roles in the transport and storage of oxygen and also in electron transport and it is safe to say that, with only a few possible exceptions in the bacterial world, there would be no life without iron [3]. Iron is the most important transition element involved in living systems, being vital to both plants and animals. The stunted growth of the former is well known on soils which are either themselves deficient in iron, or in which high alkalinity renders the iron too insoluble to be accessible to the plants. In case of man, iron was the first minor element to be recognised as being essential when, in 1681, it was used to treat anaemia. The adult human body contains about 4 g of iron of which about 3 g are in the form of haemoglobin and this level is maintained by absorbing a mere 1 mg of iron per day - a remarkably economical

utilization [3].

Cobalt is mainly used as pigment in the ceramic and paint industries, but also serves, along with aluminium and nickel, in the manufactory of magnetic alloys [3].

Cobalt is essential for microorganisms fixing molecular N_2 and thus for higher plants relying on symbiotic nitrogen assimilation [7]. Cobalt is important for living species as complexed vitamin B_{12}. Vitamin B_{12} is present in human and animal cells in the forms of adenosylcobalamin(III) and methylcobalamin(IV). The deficiency of cobalt in ruminants usually results in different types of anaemia [3]. Despite of its essential biological role, high concentrations of cobalt can be very dangerous. Toxicological effects of large amounts of cobalt include vasodilation, flushing and cardiomyopathy in humans and animals [7].

Cadmium is used for electroplating, in alloys and in batteries (Ni/Cd batteries). Cadmium compounds are also used in glazing, as stabilisers in polyvinyl plastics and in the tubes of colour television sets [2]. Cadmium, as well as mercury, are extremely toxic and has no vital biological role to play [3]. Cadmium inhibits renal function, increases loss of calcium due to depression of proximal reabsorption and leads finally to osteomalacia [8]. Serious symptoms of cadmium poisoning include lumbago, followed by the later development of pseudo fractures and a waddling gait. Other symptoms due to cadmium poisoning are: (i) emphysema of the lungs, (ii) dysfunction of the kidneys and (iii) low molar mass proteinuria.

Mercury is widely used in the fields of science, agriculture and industry. The element is also used in paints, as catalyst, in pharmaceutical products and in the paper industry. Agricultural applications include the use of mercury as fungicide against plant diseases, which make pollution due to mercury unavoidable [2].

All forms of mercury are considered poisonous, but methyl-mercury is of particular concern since it is extremely toxic and is frequently found in the environment [5]. Due

to *(i)* the toxicity of mercury, *(ii)* the fact that organo-mercury compounds can be formed in nature (methyl-mercury and probably dimethyl-mercury), and *(iii)* the bio-accumulation of methyl-mercury, there is a great need for the accurate determination of mercury. These determinations are not only needed to locate polluted areas, but definitely to prevent mercury pollutants to enter the environmental chain by controlling industrial and research effluents.

10.3 Methods of determination

10.3.1 Conventional methods of detection

Simultaneous determination of trace amounts of heavy metals usually employ one of the following methods: AAS, cold vapour AAS or flame-AAS [11, 12, 15], ICP-OES [9], potentiometry (ion-selective electrodes) [10], anodic stripping voltammetry [19], chromatography (usually HPLC) [14], chemiluminescence detection, ETA [16], gravimetric detection [16] or photometry [4, 16 -18]. Several of these techniques were already adapted to FIA systems. Most of the systems already adapted included photometric determination of the analyte. Several reagents can be used to determine metal ions in various matrixes [11]. Many of the systems employ on-line separation of the analyte from specific interferences. These systems may include dialysis [20, 21] or extractions [11, 22 - 25].

All of the seven metals analysed with the proposed system, are so-called dithizone metals [11, 26]. They form intensely coloured complexes with the reagent dithizone. Extraction at a neutral pH of 7 - 7.5 with dithizone was therefore chosen for the quantitative determination of the seven metals.

10.3.2 Reactions with diphenylthiocarbazone (dithizone)

Distinction is made between primary and secondary dithizonates, according to whether the metal ion reacting with dithizone only replaces the imide hydrogen and forms the so-

called keto complex or also reacts with the hydrogen of the thiol compound and form a so-called enol complex [11]. All seven elements can be extracted at a pH 7 - 7.5. Most of the metals form primary dithizonates, but depending on reaction conditions cobalt, copper and mercury can form either primary or secondary dithizonates [11]. Table 10.1 lists the different metals, their resulting dithizonates, pH ranges for formation of the dithizonates and their absorption maxima. The absorption maxima of the dithizonates in ethanol were determine experimentally.

TABLE 10.1 Properties of the different metal dithizonates

Cation	Dithizonate complex	Primary/ secondary	pH range	Absorption maxima (λ_{max} in nm)
-	Dithizone (H_2Dz)	-	-	435 590
Cd	$Cd(HDz)_2$	primary	6 - 14	436
Co	$Co(HDz)_2$	primary	6.5 - 10.5	519
Cu	Cu(Dz)	secondary	7 - 14	447
Fe	$Fe(HDz)_3$	primary	7.5 - 8.5	402
Hg	Hg(Dz)	secondary	7 - 14	519
Pb	$Pb(HDz)_2$	primary	6.5 - 10.5	500
Zn	$Zn(HDz)_2$	primary	6.5 - 9.5	571

Primary dithizonates follow the reaction scheme represented in Fig. 10.1, while the secondary dithizonates follow the reaction scheme represented in Fig. 10.2 [27]. Dithizone also formed complexes with organometallic complexes, like methyl mercury or methyl lead [26]. This reaction scheme is represented in Fig. 10.3.

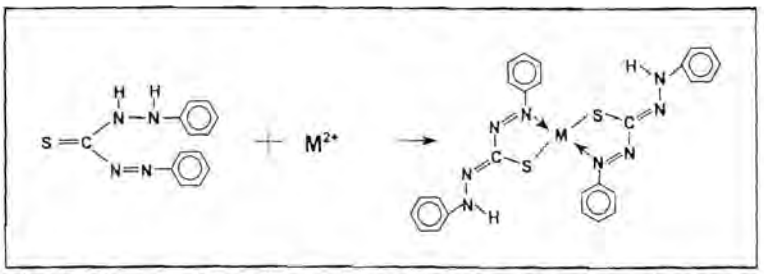

Fig. 10.1 Reaction scheme for the formation of primary dithizonates. M^{2+} - Pb, Zn, Co, Cd and Fe.

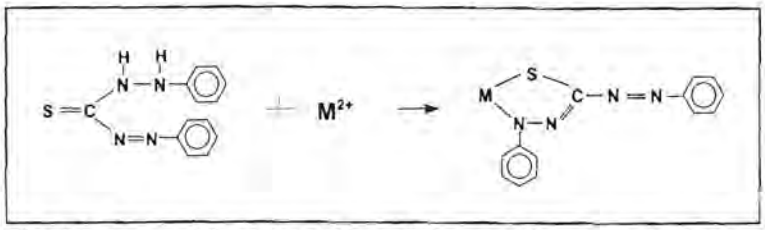

Fig. 10.2 Representation of the reaction scheme for the formation of secondary dithizonates. M^{2+} - Hg and Cu.

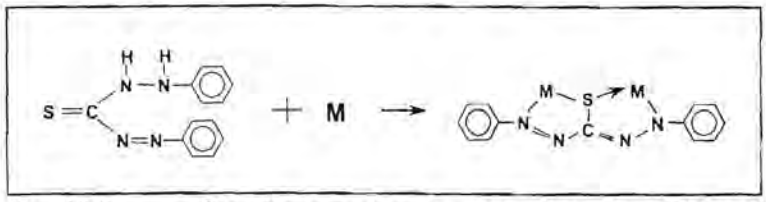

Fig. 10.3 Reaction scheme for the formation of organometallic dithizonates. M - HgR^{+} or PbR^{+}. R = methyl or ethyl group.

10.4 Simultaneous determination of Pb(II), Cu(II), Zn(II), Co(II), Cd(II), Fe(III) and Hg(II) with sequential injection extraction

10.4.1 Experimental

10.4.1.1 Reagents and solutions

All solutions are prepared of analytical grade reagent unless specified otherwise. Deionised water from a Modulab system (Continental Water Systems, San Antonio, TX, USA) was used to prepare all aqueous solutions and dilutions. The water used as carrier was degassed before use.

Extractant: 0.05 g of dithizone (Hopkin & Williams Ltd.) was dissolved in 250 mℓ ethanol to produce an emerald green stock solution. The solution was filtered using a Whatman no. 4 filter paper to remove all undissolved dithizone particles. Stored in a cool place (5°C) and protected from light this solution was stable for up to ten days. Working solutions are obtained by suitable dilution of the stock solution with ethanol.

Metal stock solutions: The following 1000 mg/ℓ metal stock solutions were prepared:

- *Lead(II):* 0.1609 g $Pb(NO_3)_2$ (PAL Chemicals) was dissolved in 1 ℓ deionised water.
- *Copper(II):* Pure Cu metal coarse chips were used in the preparation of the Cu(II) stock solution. The copper metal was cleaned to remove any oxides and dissolved by heating 1.0 g of the copper metal in 10 mℓ 55% (m/m) HNO_3 and *ca.* 10 mℓ of water. The resulting solution was cooled and then diluted to 1 ℓ with deionised water.
- *Zinc(II):* Pure Zn metal was cleaned with diluted HCl and the stock solution was prepared by dissolving 1.093 g Zn metal in 50 mℓ concentrated HCl. The solution was then diluted to 1 ℓ with deionised water.
- *Cobalt(II):* 0.4036 g $CoCl_2 \cdot 6H_2O$ (Riedel-de Haën AG) was dissolved in 1 ℓ deionised water.
- *Cadmium(II):* 2.744 g $Cd(NO_3)_2 \cdot 4H_2O$ (Merck) was dissolved in 1 ℓ deionised water.
- *Aluminium(III):* Pure Al metal was cleaned with a mixture of diluted HCl and HNO_3. The stock solution was prepared by dissolving 1.0833 g Al metal in 60 mℓ concentrated HCl and 10 mℓ concentrated HNO_3 and then diluting the solution to 1 ℓ with deionised water.
- *Iron(III):* 0.702 g $Fe(NH_4)_2(SO_4)_2 \cdot 6H_2O$ was dissolved in *ca.* 20 mℓ of water together with 1.1 mℓ of 18.4 mol/ℓ H_2SO_4 (98%, m/m). The final solution was diluted to 100 mℓ with deionised water.
- *Mercury(II):* 1.71 g $Hg(NO_3)_2.2H_2O$ (Merck) was dissolved in 1 ℓ of deionised water.

Distilled water was used as carrier solution. A 0.43 mol/ℓ acetic acid solution was used as eluent during the soil extractions. For pH corrections either a 1 mol/ℓ NH_3 solution or a 0.5 mol/ℓ H_2SO_4 solution was used.

10.4.1.2 Instrumentation

The sequential injection extraction (SIE) manifold is illustrated in Fig. 10.4. It was constructed from a Gilson Minipuls peristaltic pump (operating at 18 rpm), a 4 m long extraction coil (1.02 mm i.d.) made of Teflon (PTFE) tubing (SUPELCO) and a 10-port electrically actuated VICI selection valve (Model ECSD10P) (Valco Instruments, Houston, Texas). Acidflex pump tubing was used. The reaction coil was constructed using 45 cm of 0.25 mm i.d. Teflon tubing. Device control were achieved using a PC30-B interface board (Eagle Electric, Cape Town, South Africa) and an assembled distribution board (MINTEK, Randburg, South Africa). The FlowTEK [28] software package (obtainable from MINTEK) was used throughout the procedure. An Hewlett Packard UV-VIS diode array spectrophotometer (HP 8453), equipped with a 10 mm Hellma flow-through cell (volume 80 $\mu\ell$), was used for measuring the absorbance and data acquisition. The single component analysis program was used to record the linear ranges of the analytes individually and the multi component analysis program was used to record spectra of the seven analytes in mixed standards as well as in the different samples. Spectra were recorded over a wavelength range from 340 - 750 nm with intervals of 5 nm each when using the sequential injection system and intervals of 1 nm each when hand extractions were done to confirm the performance of the system. The calibration program was used for data analysis.

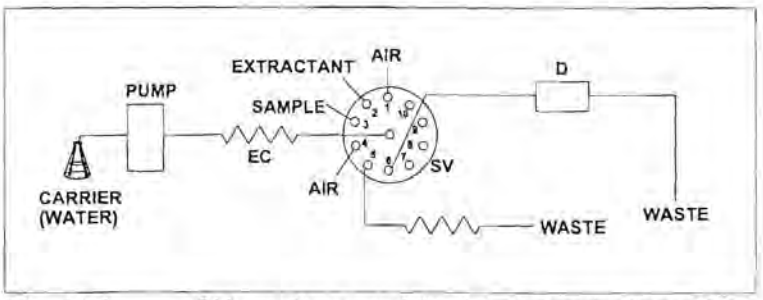

Fig. 10.4 SIA system used in the determination of the seven analytes. EC - extraction coil, SV - selection valve, HC - holding coil and D - detector.

10.4.1.3 Procedure

A small air bubble was drawn up to separate the extraction zones from the carrier solution (ethanol). Thereafter the extractant zone (dithizone in ethanol) and the sample zone (containing some of or all seven analytes) were drawn up into the extraction coil. Another air bubble was drawn up to separate these zones from the carrier in the holding coil. By reversing the flow, extraction took place into the thin organic layer formed by the dithizone zone whose flow was impeded due to the hydrophobic interactions with the walls of the Teflon coil. Since ethanol and water is miscible in all ratios no separation step was needed and after flow reversal the product peak was measured directly. No removal of the air bubbles was necessary, since the product zone was stopped inside the flow cell prior to detection. At this stage the second bubble (drawn up second, therefor reaching the detector first) was already propelled through the flow cell, while the first bubble did not yet entered the flow cell.

The spectrophotometer used three different files to store data (BLANK, STANDARD and SAMPLE) and therefore it was needed to construct three different programs which enable FlowTEK to sent the correct signal at the desired time. These programs were all basically the same and differ only in the command given to the spectrophotometer. This command was received by the spectrophotometer via a macro which enabled the computer to read the signal coming from FlowTEK. The program used by FlowTEK to control the devices is given in Table 10.2.

TABLE 10.2 Device sequence for the proposed sequential injection extraction system

Time (s)	Pump	Valve	Detector	Description
0	Off	Air ①		Pump off, valve is turned to select first air inlet.
4	Reverse			Draw up air bubble
4.5	Off			Pump stop
5.5		Extractant ②		Select extractant line
6.5	Reverse			Draw up extractant solution
10.5	Off			Pump stop
11.5		Standard/ sample ③		Select standard/sample line
12.5	Reverse			Draw up standard/sample solution
16.5	Off			Pump stop
17.5		Air ④		Select second air inlet
18.5	Reverse			Draw up second air bubble
19	Off			Pump stop
20		Holding coil ⑤		Select holding coil
21	Reverse			Extraction step 1: Zones are drawn back into extraction coil to ensure effective mixing and extraction.
26	Forward			Extraction step 2: Pump stack of zones forward until the bubble reached a position just in front of the valve.
31	Off			Pump stop
32		Detector ⑥		Select detector line
33	Forward			Pump stack of zones to detector until the second bubble is visible outside the flow cell. This ensure that the product zone is entirely inside the flow cell.
43	Off			Pump stop, a waiting period is now installed to ensure that there will be no interferences due to mirages that occur when ethanol and water are mixed.
93			BLANK/ STANDARD/ SAMPLE	A signal is sent to the diode array spectrophotometer to do either a blank, standard or sample spectra.
103	Forward			Stack of zones are pump to waste.
153	Off			Pump stop, end of analytical cycle.

10.4.1.4 Sample preparation

Sample collection: Urine samples were collected in polypropylene flasks which had previously been cleaned by rinsing with dilute nitric acid and water. The samples were quickly frozen after collection with minimum air space above the urine. Soil samples were taken from a maize farm in the northern Free State and stored in polypropylene containers.

Before analysis, the frozen urine was allowed to reach room temperature and thoroughly mixed. Urine samples were diluted 1:3 with deionised water. All water samples in the pH range 7 - 7.5 were analysed directly. For other water samples the pH was first corrected by using either NH_3 or H_2SO_4 solution. Representative soil samples of 20.00 ± 0.05 g were dried at 30°C for 8 - 10 hours. 5.00 ± 0.01 g of the air-dried soil was weighed into a beaker and 50 mℓ of a 0.43 mol/ℓ CH_3COOH solution was added. The suspension was stirred for 30 min and then filtered. Since the pH of the reaction mixture needed to be 7.5, a 25% (m/m) NH_3 solution, was used to correct an 50 mℓ aliquot of the filtrate. The solutions were then made up to 100 mℓ using deionised water. *10 mℓ acetone (AR) was added to every working solution (standard) and sample prepared.*

10.4.2 Optimisation

10.4.2.1 Physical parameters

A number of physical parameters can influence the degree of dispersion and extraction in the manifold. To obtain the highest sensitivity and precision it was necessary to optimise these parameters. Most of the optimization of the physical and chemical parameters was done using the same sequential injection system as in Chapter 8. This was done, because of the simplicity of the detection system employed. When using the diode array spectrophotometer, a BLANK run must be done every time a parameter is changed - even if the parameter is changed only slightly. Except for increasing the

analysis time to double the original time, it also make comparisons between different results obtained very difficult. The optimisation was done with a standard solution containing 1 mg/ℓ of every analyte. Absorption was measure at 500 nm, since most of the dithizonates show absorption at that wavelength and the reagent show minimum absorbance at 500 nm (Fig. 10.5). It was not surprisingly that almost exactly the same optimum conditions were found for the two systems. Only two parameters were optimize using the diode array spectrophotometer - the duration of the waiting period and the addition of acetone to the standard and sample solutions.

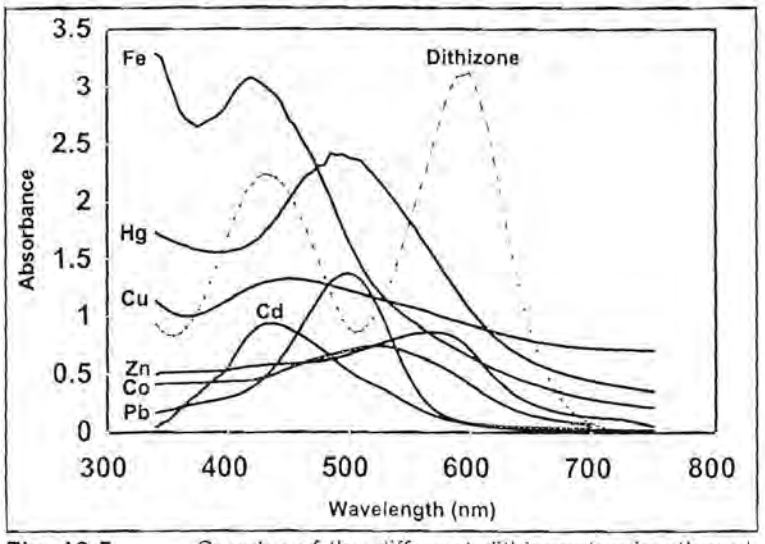

Fig. 10.5 Spectra of the different dithizonates in ethanol. Optimisation of the sequential injection system was done at 500 nm.

10.4.2.1.1 Introduction and removal of air bubbles

Air bubbles are highly undesirable in flow and sequential injection systems, not only because they led to spurious results, but also because it decreased the reproducibility of the procedure. Although it was feared that the introduction of air bubbles into a flow system would have led to irreproducible results, this was to a major extent not the case. The bubbles separated the extraction zones from the surrounding carrier solution, preventing excessive dilution of the extraction zones.

No removal of bubbles took place in this procedure, since the product zone was halted inside the flow cell during detection. Flow was stopped as soon as the second bubble was just outside the flow cell. Because the extraction zones were so big, the first bubble had at that stage not yet entered the flow cell. This ensured that the whole product zone was inside the flow cell when absorbance measurements were done. After measurements were completed, the product zone as well as the bubbles were flushed to waste.

10.4.2.1.2 Flow rate

From previous experiments (Chapters 8 and 9), it was clear that slower flow rates improve the mass transfer from aqueous to organic phase, while faster flow rates were needed to propel the formed product zone through the detector. The faster flow rates through the detector was necessary to eliminate excess dilution of the product zone as well as to prevent peak tailing in the detector. During this application absorbance measurements were not made while the product zones were propelled through the detector. The product zone was stopped inside the flow cell and after a waiting period of 50 seconds, the absorbance was measured. Thereafter the product zone was flushed to waste. Pump rate was therefore only optimise to ensure optimum extraction.

Slower flow rates result in thinner organic film and inevitably in longer extraction times. Thinner films are useful when back extractions are employed, but for single extractions, thicker films resulted in better extraction efficiency, since they have higher capacities [29]. Flow rates between 1.5 and 3 mℓ/min were evaluated and the results are listed in Table 10.3. Flow rate was determined as the mass of the volume of water delivered by the pump in one minute, divided by the density of water at 25°C. The average of three determinations was used.

TABLE 10.3 Influence of different flow rates on sensitivity (extraction efficiency) and precision

Flow rate (mℓ/min)	Sensitivity (Relative peak height)	Precision (%RSD)
1.51	2.96	2.21
1.73	3.42	2.63
1.97	3.65	1.75
2.41	4.29	2.01
2.64	5.28	1.79
2.97	5.77	2.30

An optimum flow rate of 2.4 mℓ/min was chosen, due to its sensitivity and good reproducibility. Although higher flow rates delivered better sensitivities, it was ruled out due to their poor precision.

10.4.2.1.3 Sample volume

Smaller sample zones lead to bigger dispersion and ultimately to lower sensitivity. The sample volume was therefore carefully evaluated to obtain maximum sensitivity and reproducibility. The results obtained in the evaluation are schematically represented in Fig. 10.6.

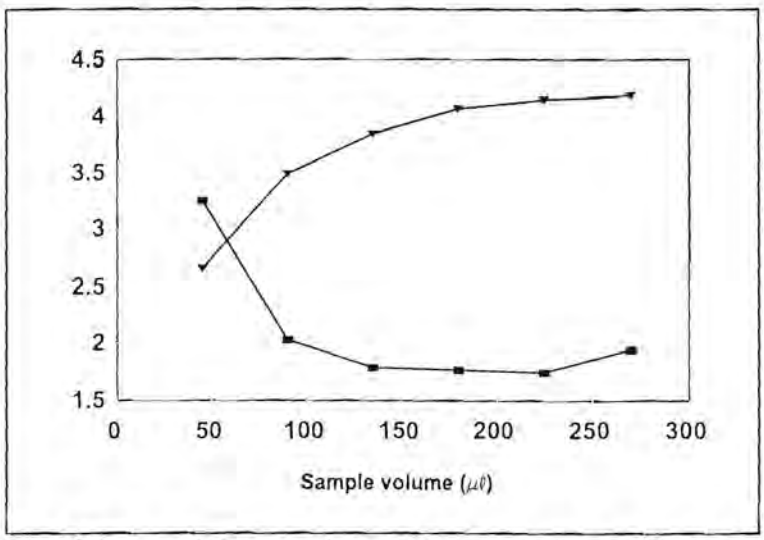

Fig. 10.6 Influence of sample volume on the sensitivity and reproducibility of the SIE method.

Larger sample volumes led to better sensitivity until a plateau was reached. Since the flow was stopped inside the flow cell, a large enough extraction zone must be created to allow that the whole product zone would be situated inside the flow cell during measurements. The reproducibility of the method decreased with volumes bigger than 180 $\mu\ell$. This is because of insufficient zone overlap, because larger volumes led to smaller axial dispersion which decrease the zone penetration [30, 31]. An optimum sample volume of 180 $\mu\ell$ was thus chosen for the system.

10.4.2.1.4 Extractant volume and extraction time

Although the extractant volume is dependant on a critical parameter called the zone inversion length, it also governs the linear ranges of the different analytes determined as well as the number of analytes that can be analysed. Because the organic solvent, ethanol, is miscible with water in all ratios, optimal mixing rather than film thickness will be optimised. Since extraction still has to take place, longer extraction time will be allowed for the reaction. The volume of the extractant zone influence both the time of the extraction as well as the length of the extraction coil.

Extractant volumes between 45 $\mu\ell$ and 180 $\mu\ell$ were evaluated (Fig. 10.7). Smaller volumes gave very irreproducible results, because of the imperfect flow dynamics of the pump (start up and stopping are not instantaneous) [30, 31], these small volumes were not aspirated reproducibly. A plateau is reached in peak height at volumes bigger than 135 $\mu\ell$. The optimum extractant volume was chosen to be 180 $\mu\ell$ due to the good precision and sensitivity it delivered. This also contributed towards the larger product zone inside the flow cell during measurements.

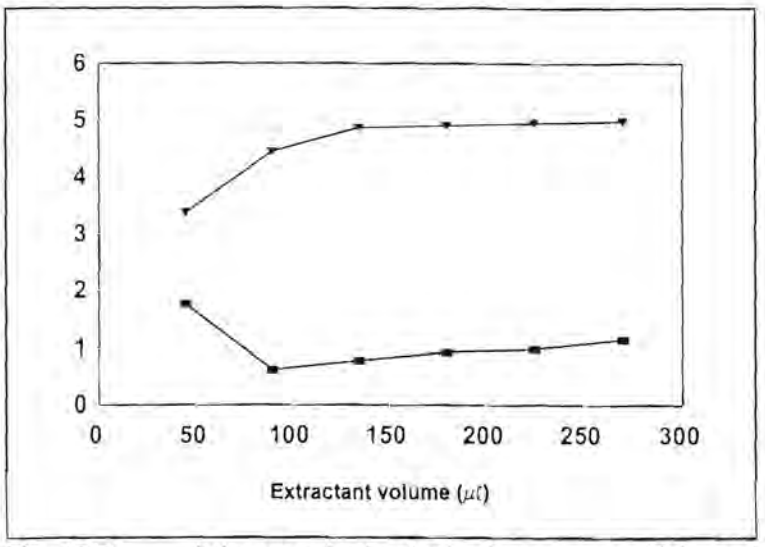

Fig. 10.7 Influence of extractant volume on sensitivity and precision. ▼ = relative peak height and ■ = %RSD.

Several extraction options, including multiple flow reversals to obtain thorough mixing of the zones were evaluated in Chapter 8. This study revealed that an extraction step consisting of only one flow reversal and extraction time of 17.5 seconds resulted in peaks with the desired Gaussian shapes. Longer extraction times were evaluated for the proposed SIE system, but did not have any effect on the sensitivity of the technique. This might be due to the waiting period incorporated prior to detection. This allow the reactions to reach a certain level of equilibrium. Extraction times shorter than 11 seconds led to a decrease in sensitivity and 11 seconds were therefor chosen as optimum extraction time.

10.4.2.1.5 Organic film thickness

Relative film thickness per unit length (d_f) can be predicted using the equation [29]

$$d_f = kd_t(u\eta/\gamma)^a$$

where u represents flow rate (velocity) and d_t tubing diameter. The solvent characteristics also play an important role and are included in the equation. Viscosity

of the solvent is represented by η and surface tension by γ, *k* and *a* are constants between ~1/2 and ~ 2/3. From the equation it can be seen that film thickness is directly proportional to viscosity and inversely proportional to surface tension. As colligative properties, it is appropriate to consider either interfacial or surface tension to viscosity as a film thickness parameter, η/γ [29]. The film thickness parameter for ethanol was calculated to be 4.64 x 10^{-2} (η = 1.06 cP and γ = 21.80) [32]. The thickness of the organic film is very important since it influences extraction by affecting the mass transfer of analytes into the film [33]. Under optimum running conditions the relative film thickness was calculated to be 9.4 μm.

10.4.2.1.6 Diameter and length of tubing

Extraction coil: The length of the extraction coil depends on the zone inversion length. It was found that during the extraction step a reverse step of 5 seconds was used. This time multiplied with the flow rate 5.38 x cm/s (2.64 mℓ/min), resulted in a zone inversion length of 26.9 cm. Due to dispersion in the flow conduit, these zones occupy about 9 times the inversion length. Thickness of the wetting film is directly proportional to the inner diameter of the coil [34]. As a result, the extraction capacity (volume of the wetting film) is larger for wider and longer extraction coils. Using an extractant volume of 180 μℓ an extraction coil of 3.8 m was needed. To ensure that none of the zones reached the pump conduit and became deformed, an extraction coil of 4 m was used. An inner diameter of 1.02 mm ensured good axial dispersion and zone overlap.

Reaction coil: The spectrophotometer should be positioned as close to the debubbler as possible. Longer distances between the debubbler and detector led to higher dispersion, longer rinsing times and ultimately lower sample throughput. Wider tubing also contribute to dispersion and undesired dilution of the product zone. Since no removal of bubbles was needed, a 45 cm 1.25 mm i.d. Teflon reaction coil was used. This length of tubing was needed as it represent the shortest distance between the valve and the spectrophotometer.

10.4.2.1.7 Waiting period and measuring intervals

Because the diode array spectrophotometer is so extremely sensitive, it was very difficult to obtain smooth analytical curves therewith. When the water and ethanol were mixed due to the flow in the manifold conduit, mirages were created in the process. These mirages led to very spurious peaks. To reduce the effect of the mirages to a great extent, a waiting period was incorporated into the flow programming. As it is known that stop and start in flow and sequential analysis systems are not instantaneous [30, 31], the waiting period allow the product peak to come to a standstill within the flow cell. It was difficult to evaluate the influence of the waiting period on sensitivity and precision, because of the high noise experience with none or short waiting periods. As this parameter was evaluated on the diode array spectrometer itself, different backgrounds were needed for different waiting periods. Initially the background value was very unstable, but with increasing waiting time length, it stabilised to give a background value as shown in Fig. 10.8. Waiting periods longer than 50 seconds did not improve the shape and smoothness of the peaks and only increased the analysis time. The waiting period was then taken as 50 seconds.

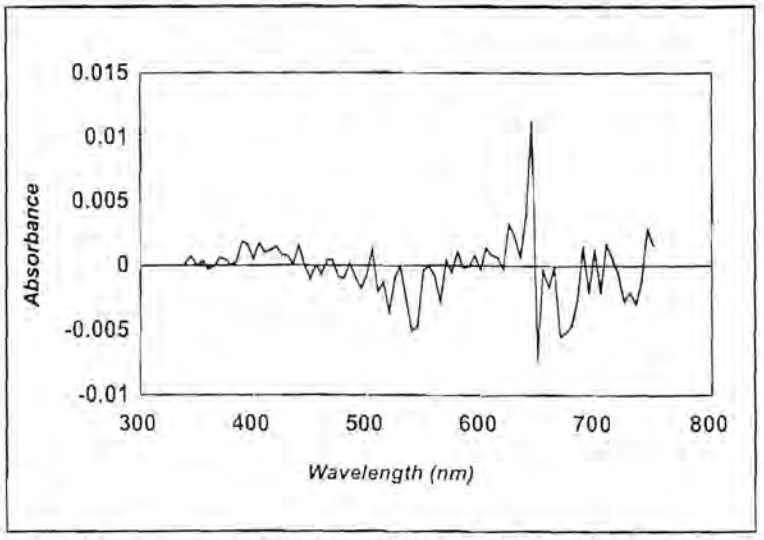

Fig. 10.8 Background obtained with a blank solution containing 10% acetone when employing a 50 second waiting period into the flow programming.

It was necessary to do a blank measurement after every ten runs, to ensure smooth peaks. The necessity of a new blank became visible in especially the region between 600 and 750 nm, when very 'spiky' peaks were obtained. This was probably due to the difference in the refractive index, n_r, of the different phases. The refractive index of a medium is the ratio of the speed of light in a vacuum to its speed in the medium [32]:

$$n_r = \frac{c}{v}$$

The refractive index is related to the molecular polarizability because the propagation of light through a medium can be imagined as occurring by the incident light inducing an oscillating dipole moment, which then radiates light of the same frequency. The newly formed radiation is delayed in phase relative to the incident radiation, so the light propagated more slowly through the medium as through a vacuum. Since photons of high frequency light carry more energy than those of low frequency light, they can distort the electronic distributions of the molecules in their path more effectively. Therefore, it is expected that the polarizabilities of molecules, and hence the refraction index, will increase with increasing frequency [32].

The different refractive indices for both ethanol and water are given in Table 10.4. Although the refractive indices of the two solvent do not vary much at the respective wavelengths, light moves faster through ethanol than water, which is the reason for the mirages obtained.

TABLE 10.4 Refractive indices relative to air at 20°C [32]

Solvent	434 nm	589 nm	656 nm
Ethanol	1.3700	1.3618	1.3605
Water	1.3404	1.3330	1.3312

Δ refractive indices ≈ 0.03

Another option to smooth the analytical curve was to reduce the number of measurements. Initially measurements were done at every wavelength (1 nm intervals). This was reduced to measurements at every fifth nanometre. Experiments with measurements at intervals of 10 nm, resulted in very poor reproducibility and sensitivity. Measurements at intervals of five nanometres were chosen for measurements done by the sequential system. Stationary measurements (hand extractions) were still taken with measurements at 1 nm intervals.

10.4.2.2 Chemical parameters

10.4.2.2.1 pH

The formation of all dithizonates is pH dependant and when employing different pH values, differentiation between different metals is possible. In Table 10.1 it was shown that a pH between 7 and 7.5 allowed the extraction of all seven metal ions as dithizonates. The pH of clean drinking water falls into this range. The pH of all samples that were analysed with this system were therefore measured and corrected to pH 7.5 with 1 mol/ℓ ammonia solution or 0.5 mol/ℓ sulphuric acid solution. Ammonia was chosen to eliminate any interference of NaOH due to the formation of less soluble hydroxides [35].

10.4.2.2.2 Choice of organic solvent

Except for the flow rate, the viscosity and surface tension of the organic solvent also play a major role in the film thickness and therefore in the extraction efficiency. Solvents with low viscosities do not offer a sufficient difference in flow velocity when compared to water and make SIE less effective as it requires more time and longer extraction coils. On the other hand, highly viscous solvents are difficult to wash out of the tubing. With less dense solvents, phase separation may present problems, although there may be cases where the use of a diluent not much less dense than water has special advantages [26]. As described earlier, there are several factors, including

economical factors, that influence the choice of organic solvent used.

Dithizone, as well as its metal dithizonates are all highly soluble in chlorinated solvents and the most common solvent used in extractions are carbon tetrachloride and chloroform [26, 36]. One disadvantage about CCl_4 is that it is highly carcinogenic and has ozone depleting properties [37]. To avoid the use of toxic organic solvents such as CCl_4 and $CHCl_3$ [24], ethanol was used as solvent for the dithizone reagent.

The major reasons used to justify the use of ethanol as solvent were highlighted in Chapter 8. Firstly, since ethanol and water are miscible in all ratios, the use of phase separators were omitted and the mixture of aqueous and organic liquids containing the reaction product was determined directly. Secondly, according to the physical properties of ethanol, it was calculated that it would produce the thickest extraction film, when compared to a few other solvents. The film thickness parameter, as calculated for ethanol was 4.64×10^{-2}.

The visible absorption spectrum of dithizone is, however, very sensitive to the organic solvent in which it is dissolved [36]. The absorption maxima for the seven metal dithizonates in ethanol was determined experimentally and are listed in Table 10.1 and represented in Fig. 10.5.

10.4.2.2.3 Concentration of dithizone

Dithizone is only sparingly soluble in ethanol, with a solubility of 0.3 g/ℓ at 20°C [26]. Since solutions of dithizone of any but the lowest concentration are deeply coloured, and often almost opaque, it is quite difficult to be certain whether excess solid is present in contact with a saturated solution. Special care is needed to ensure that metallic impurities are not introduced by the filtering medium, especially when the concentration is to be calculated afterwards from the absorbance of a suitably diluted aliquot and a knowledge of the molar (decadic) absorption coefficient, ϵ [26].

A stock solution containing 0.05 g of dithizone in 250 mℓ ethanol was prepared. Since most of the primary dithizonates favoured a 1:2 metal:dithizone ratio, excess reagent was needed in the determinations. The solution was first used undiluted, but this resulted in very 'spiky' peaks. Because of the sensitivity of the detector, the undissolved dithizone reagent interfered in the determination. Filtering of the reagent through a Whatman no. 4 filter paper solved this problem. The reagent was however too concentrated and resulted in deformed peaks. Several dilutions, using ethanol, were made and evaluate. A 1:1 dilution gave smooth peaks and allow the determination of slightly more concentrated samples. This solution was used throughout the whole procedure as optimum dithizone concentration. The solution had to be prepared daily, but the stock solution was stable for up to two weeks when stored in the refrigerator and protected from light.

10.4.2.2.4 Addition of acetone

As stated earlier, the mirages originating from the mixing of ethanol and water, created huge problems during measurements. The difference in surface tension between ethanol and water are relatively big (Δ surface tension = 0.05 N/m), which could have an influence on the mixing of the two phases. The addition of acetone to the aqueous sample lower the surface tension of the water which resulted in better mixing and reduction of the effect of the mirages. Different acetone concentrations were evaluated. For concentrations up to 10% the smoothness of the peak was enhanced, while for concentrations higher than 10% no additional enhancement was observed. Preparation of sample and standard solutions therefore included the addition of 10% acetone.

10.4.3 Evaluation of the system

The proposed sequential extraction method was evaluated under optimum running conditions with regard to linearity of the individual analytes, sample frequency, reproducibility, sample interaction, detection limits, accuracy and major interferences.

10.4.3.1 Linearity

Analytical curves for the different metals were difficult to obtain, since the unreacted dithizone reagent interfere at low concentrations. At these concentrations the shape of the dithizone reagent was very recognisable. The spectra obtained for different concentrations of the individual metals as well as the calibration curves obtained are given in Figs. 10.9 to 10.22 Concentrations up to 20 mg/ℓ were evaluated. At 20 mg/ℓ there was still excess reagent present, since most dithizonates react in a 1:2 metal:reagent ratio.

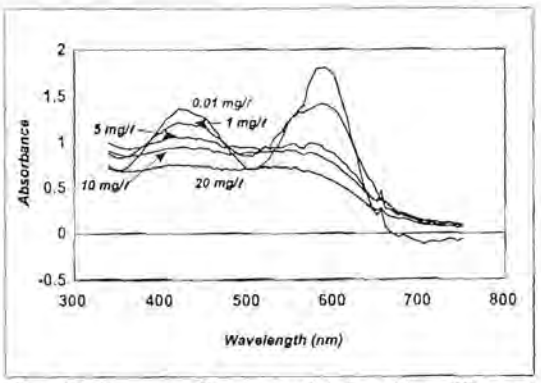

Fig. 10.9 Spectra obtained for different Co concentrations.

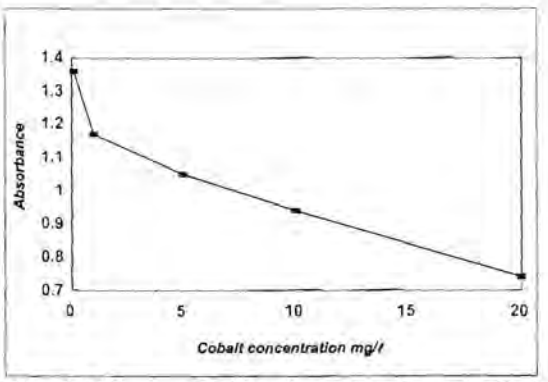

Fig. 10.10 Calibration curve for cobalt at 420 nm.

At 519 nm, the absorbance maximum for cobalt, difficulties were experience in finding the correct absorbance value for the cobalt dithizonate. This was mainly because of the excess reagent present when smaller concentrations were determined. The calibration curve was constructed from the absorbance values at 420 nm (Fig. 10.10). This represent the decrease in reagent with increasing cobalt concentration. The calibration curve was linear between 1 and 20 mg/ℓ Co. The equation of the line was:

$$A_{Co} = -0.022[Co] + 1.169; \quad r^2 = 0.9955$$

For mercury it was even more difficult to set up an calibration curve, since the peak shape changed and the absorbance maximum shifted with increasing mercury concentration (Fig. 10.11). The decrease in reagent concentration, with increasing analyte concentration, was monitored at 430 nm. This plot gave a linear range for

mercury between 1 and 10 mg/ℓ (Fig. 10.12).

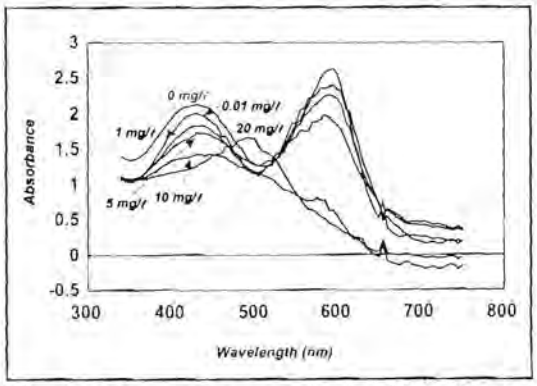

Fig. 10.11 Spectra obtained for different mercury concentrations.

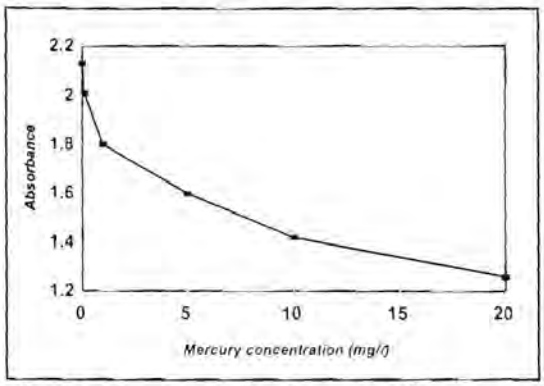

Fig. 10.12 Calibration curve for mercury at 430 nm.

As with mercury, the iron peak form changed when higher concentrations were analysed. It seems as if there were different linear sections on the calibration curve which corresponded with a certain peak form (Figs. 10.13 and 10.14). The linear range for iron was taken between 1 and 10 mg/ℓ. The small analytical range can be ascribed to the fact that the iron-dithizone complex favours a 1:3 metal:reagent ratio.

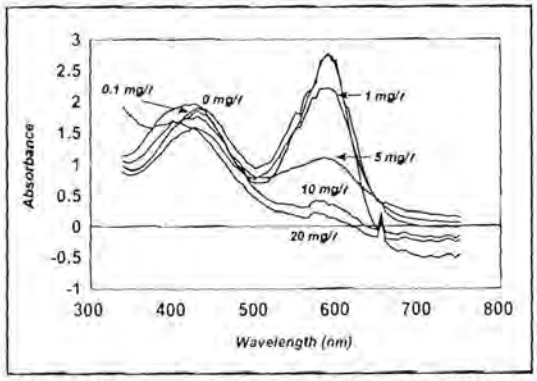

Fig. 10.13 Spectra obtained for different iron concentrations.

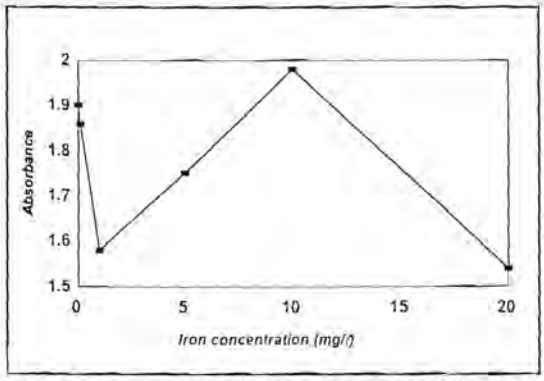

Fig. 10.14 Calibration curve(s) for iron at 430 nm.

For copper it was impossible to use decrease of reagent to construct the calibration curve, because the spectra of the different concentrations overlap tremendously, especially at the wavelengths were dithizone absorb. The calibration curve was therefore constructed from the absorbance readings at 490 nm. This resulted in a linear range between 1 and 20 mg/ℓ copper. The equation of the line was:

$$A_{Co} = 0.028[Cu] + 1.009; \quad r^2 = 0.9976$$

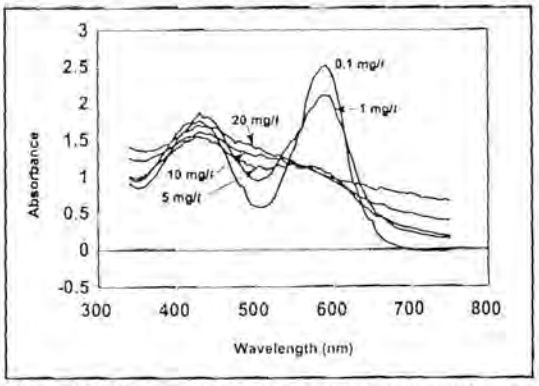

Fig. 10.15 Spectra obtained for different copper concentrations.

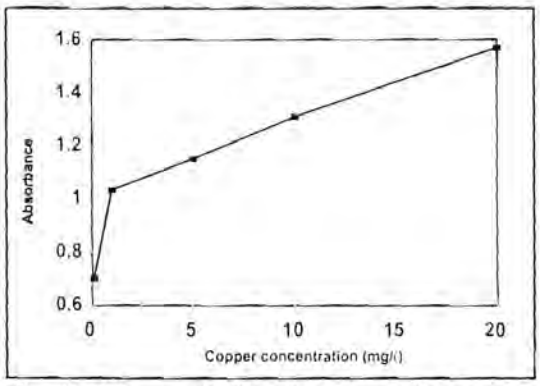

Fig. 10.16 Calibration curve for copper at 490 nm.

Again the peak shape seemed to determine the linear range. Lower concentrations of zinc showed peaks with an dithizone shape, due to the excess of the reagent and for this peak shape the calibration curve was linear between 1 and 10 mg/ℓ. Higher concentrations of zinc showed peak profiles with maximum absorbance close to 571 nm. The calibration curve was linear between 10 and 20 mg/ℓ for these peak profiles.

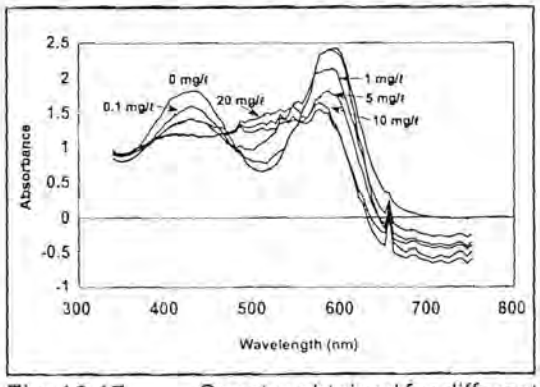

Fig. 10.17 Spectra obtained for different concentrations of zinc.

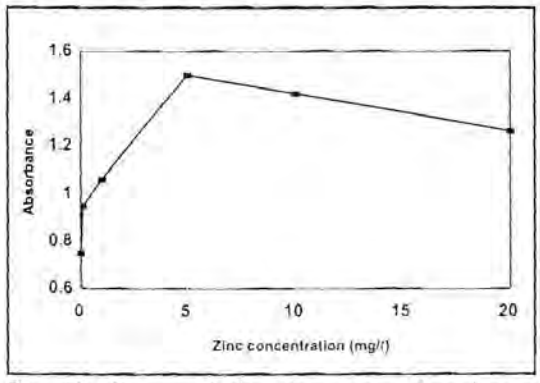

Fig. 10.18 Calibration curve for zinc at 525 nm.

No change in peak shape was observed for lead. The difference in the absorbance between the different concentrations were noticeable, but very small. Virtually no distinction could be made between the blank and a 0.1 mg/ℓ solution. The graph shows linearity between 1 and 20 mg/ℓ when reading the absorbance at 525 nm. The calibration graph's equation was as follow:

$$A_{Pb} = 0.015[Pb] + 0.807;\ r^2 = 0.9974.$$

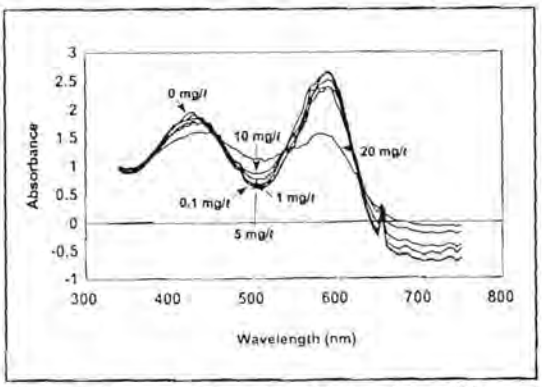

Fig. 10.19 Spectra obtained for different concentrations of lead.

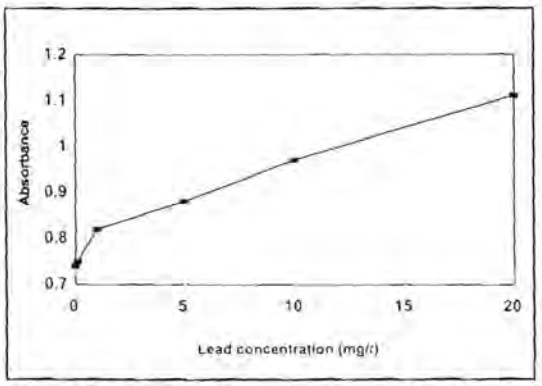

Fig. 10.20 Calibration curve for lead at 525 nm.

The calibration curve for cadmium was constructed of measurement values taken at 435 nm. Two different linear ranges could be found: between 1 and 5 mg/ℓ and between 5 and 20 mg/ℓ. As in the case with the other metals, the peak shape were different for higher concentrations of the analyte.

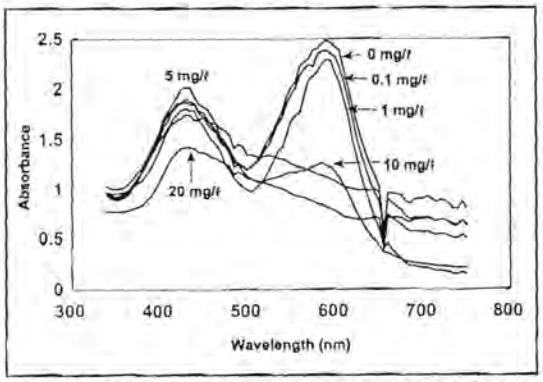

Fig. 10.21 Spectra obtained for different cadmium concentrations.

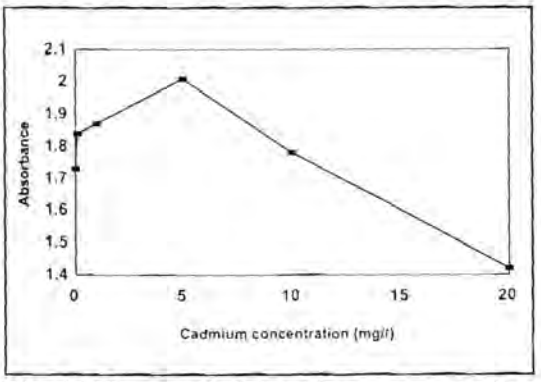

Fig. 10.22 Calibration curve for cadmium at 435 nm.

10.4.3.2 Accuracy and precision

To evaluate the accuracy of the sequential injection system, three soil samples, three urine samples, two tap water samples and one synthetically prepared aqueous test solution were evaluated. Seven standard which contain six of the seven analytes as

well as one standard containing all seven analytes were prepared. The standard solutions prepared are listed in Table 10. 5.

TABLE 10.5 Standard solutions prepared to construct calibration data

Standard	Analyte (mg/ℓ)						
	Pb^{2+}	Cu^{2+}	Zn^{2+}	Co^{2+}	Cd^{2+}	Fe^{3+}	Hg^{2+}
1	7	6	5	4	3	1	0
2	6	5	4	3	2	0	7
3	5	4	3	2	1	7	6
4	4	3	2	1	0	6	5
5	3	2	1	0	7	5	4
6	2	1	0	7	6	4	3
7	1	0	7	6	5	3	2
8	5	5	5	5	5	5	5

The results were verified using results obtained by conventional hand extractions at the same pH. Figs. 10.23 and 10.24 show the spectra obtained for the standard solutions using the conventional extraction (Fig. 10.23) and using the sequential injection extraction system (Fig. 10.24).

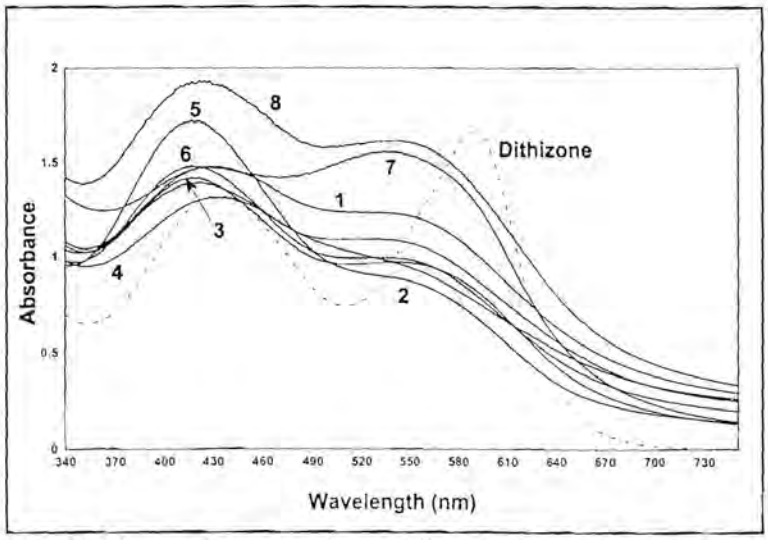

Fig. 10.23 Spectra of the different standard solutions to create calibration data. Analyses were done by traditional hand extractions.

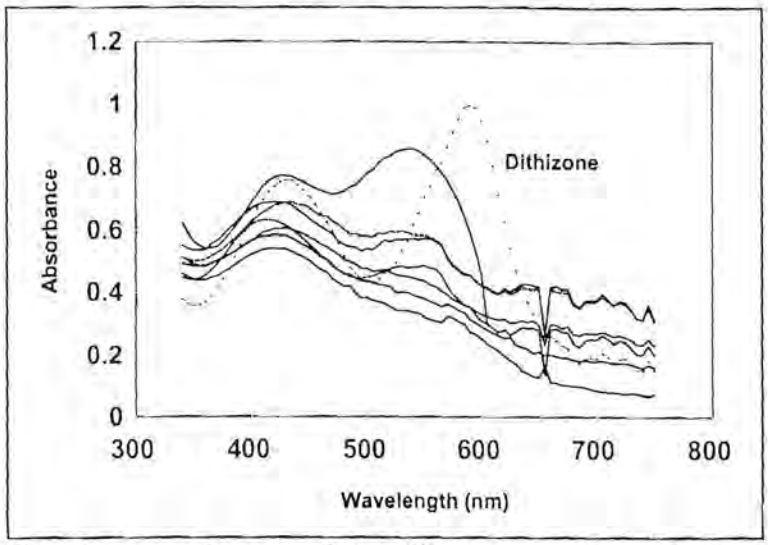

Fig. 10.24 Spectra of the different standard solutions to create calibration data. Analyses were done by using the sequential injection analyser.

It can be observed that the sensitivity of the spectra obtained with the sequential injection system was much lower compared to the spectra obtained with traditional hand extractions. Because the sensitivity of the SIE system was so low, it was difficult to distinguish clearly between the different spectra of the standards. Figs. 10.25 to 10.33 were therefore created to show the peak shapes and the difference in sensitivity for every standard solution.

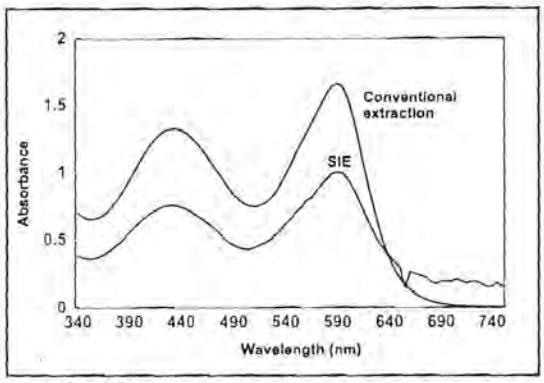

Fig. 10.25 Blank spectra (only dithizone) using conventional extraction and sequential injection extraction (SIE).

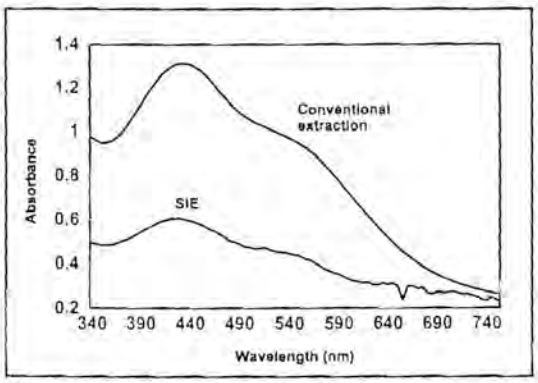

Fig. 10.26 Spectra of standard 1 using conventional extraction and sequential injection extraction (SIE).

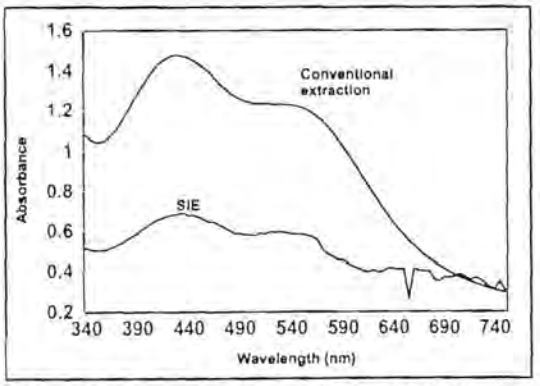

Fig. 10.27 Spectra of standard 2 using conventional extraction and sequential injection extraction (SIE).

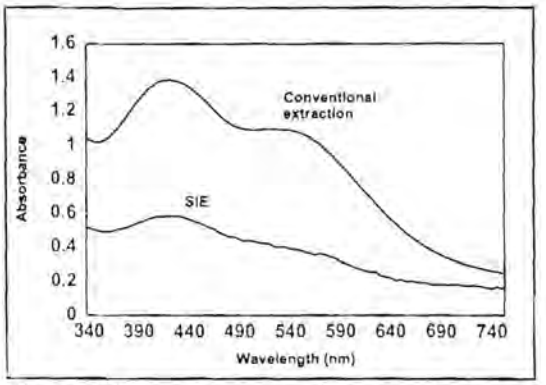

Fig. 10.28 Spectra of standard 3 using conventional extraction and sequential injection extraction (SIE).

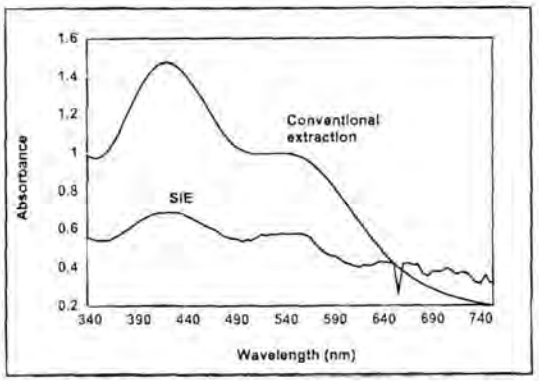

Fig. 10.29 Spectra of standard 4 using conventional extraction and sequential injection extraction (SIE).

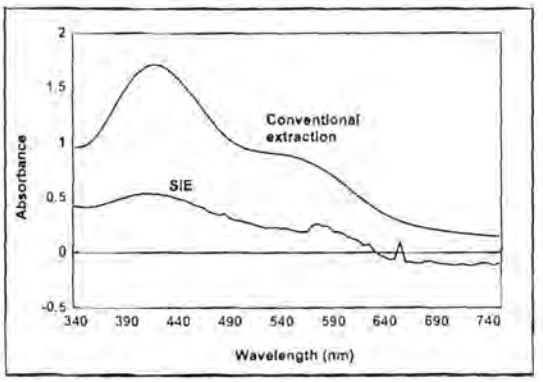

Fig. 10.30 Spectra of standard 5 using conventional extraction and sequential injection extraction (SIE).

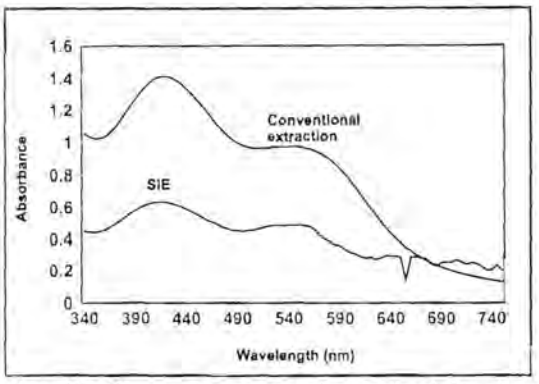

Fig. 10.31 Spectra of standard 6 using conventional extraction and sequential injection extraction (SIE).

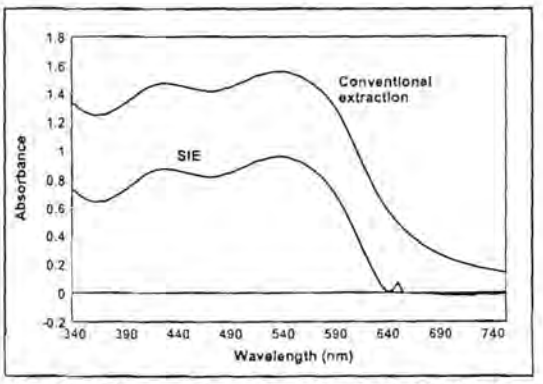

Fig. 10.32 Spectra of standard 7 using conventional extraction and sequential injection extraction (SIE).

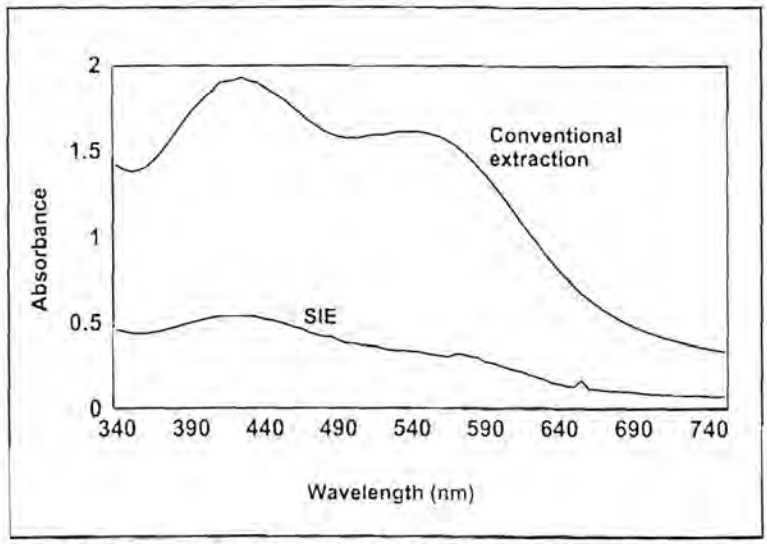

Fig. 10.33 Spectra of standard 8 using conventional extraction and sequential injection extraction (SIE).

The reproducibility of the two systems were evaluated and the percentage relative standard deviation as calculated for each individual analyte, are given in Tables 10.6 and 10.7. Calculations were done by the calibration program of the diode array spectrophotometer.

TABLE 10.6 Relative standard deviation obtained for each individual analyte in a standard solution. Results were obtained with the sequential injection system.

Standard	%RSD						
	Pb^{2+}	Cu^{2+}	Zn^{2+}	Co^{2+}	Cd^{2+}	Fe^{3+}	Hg^{2+}
1	1.43	2.07	0.17	0.97	0.34	1.93	0.49
2	1.92	2.06	0.81	0.69	0.53	0.92	0.64
3	1.74	1.51	0.31	0.62	0.62	0.51	0.32
4	0.65	2.41	0.21	0.25	0.52	1.70	0.43
5	1.57	1.83	0.47	0.86	1.46	0.75	1.86
6	1.62	1.47	0.76	0.78	1.51	1.42	1.91
7	2.03	1.65	0.95	0.77	1.09	1.54	1.40
8	2.09	1.67	0.89	0.87	0.94	1.61	1.64

TABLE 10.7 Relative standard deviation for each individual analyte in the standard solutions. %RSD obtained when employing conventional hand extraction methods.

Standard	%RSD						
	Pb^{2+}	Cu^{2+}	Zn^{2+}	Co^{2+}	Cd^{2+}	Fe^{3+}	Hg^{2+}
1	1.44	0.78	1.94	1.21	0.31	1.31	1.08
2	0.42	0.83	1.41	1.30	0.97	0.62	1.16
3	0.68	0.58	1.17	0.91	1.82	0.67	0.81
4	0.46	0.75	1.61	0.88	1.76	1.05	0.78
5	1.15	1.37	1.91	1.25	1.28	1.71	1.66
6	1.28	1.47	1.95	1.41	1.34	1.58	1.80
7	1.95	1.36	1.54	0.41	1.34	1.78	1.06
8	1.79	1.48	1.58	0.44	1.23	0.61	1.60

The samples that were analysed with the sequential injection extraction system are listed in Table 10.8. Standard additions are indicated as well.

TABLE 10.8 Sample solutions analysed with the SIE system and conventional hand extraction methods to evaluate the accuracy of the SIE system

Sample	Analyte added (mg/ℓ)						
	Pb^{2+}	Cu^{2+}	Zn^{2+}	Co^{2+}	Cd^{2+}	Fe^{3+}	Hg^{2+}
Soil 1	-	-	-	-	7	5	2
Soil 2	5	6	-	-	4	-	4
Soil 3	-	-	5	5	1	-	1
Tap water 1	-	-	-	-	-	-	-
Tap water 2	-	2	-	2	-	5	4
Urine 1	-	-	-	-	-	-	-
Urine 2	-	-	-	-	5	-	2
Urine 3	-	-	-	-	-	5	7
Control	5	5	5	5	5	5	5

The results obtained with the conventional hand extractions are shown in Fig. 10.34, while the results obtained using the SIE system are highlighted in Fig. 10.35.

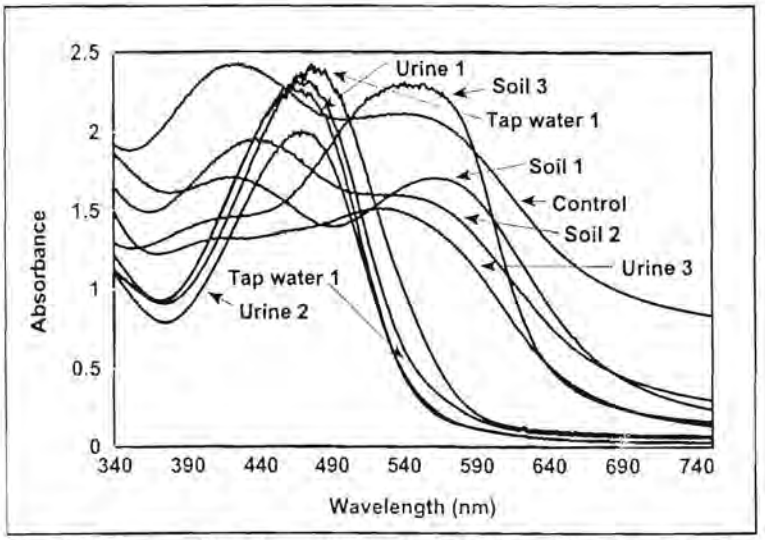

Fig. 10.34 Spectra obtained for the different samples analysed. Conventional extractions were used to obtain the dithizonates.

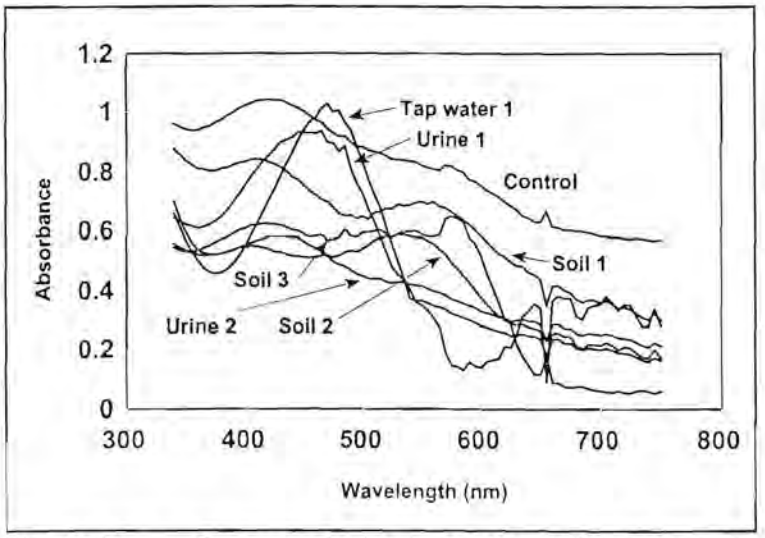

Fig. 10.35 Spectra obtained for the different samples analysed. The sequential injection extraction system were used to obtain the dithizonates.

Using the multivariate calibration option of the diode array spectrophotometer, the concentration of the various analytes as well as the percentage relative standard

deviation of each determination could be obtained. These values are listed in Table 10.9 and 10.10, while the results obtained with the conventional hand extractions are listed in Table 10.11 and 10.12.

TABLE 10.9 Results obtained employing sequential injection extraction system

Sample	Analyte concentration found (mg/ℓ)						
	Pb^{2+}	Cu^{2+}	Zn^{2+}	Co^{2+}	Cd^{2+}	Fe^{3+}	Hg^{2+}
Soil 1	4.60	3.18	0.66	22.56	1.30	9.69	2.52
Soil 2	7.29	5.99	5.58	17.37	5.83	8.67	6.25
Soil 3	3.74	0	4.74	17.56	4.74	9.30	1.22
Tap water 1	8.49	7.67	11.08	23.62	12.93	46.82	0.29
Tap water 2	4.96	5.62	17.49	27.00	13.20	46.20	0.47
Urine 1	8.34	6.43	5.31	19.54	13.48	4.93	0.74
Urine 2	7.05	5.19	5.80	25.36	11.96	439	2.40
Urine 3	0	2.61	3.58	14.05	13.19	4.28	6.43
Control	4.91	5.01	4.89	5.42	5.04	5.11	4.79

TABLE 10.10 Relative standard deviations obtained for samples analysed with the sequential injection extraction system

Sample	%RSD						
	Pb^{2+}	Cu^{2+}	Zn^{2+}	Co^{2+}	Cd^{2+}	Fe^{3+}	Hg^{2+}
Soil 1	0.81	0.19	0.34	0.49	0.78	0.41	1.08
Soil 2	0.21	0.14	0.26	0.32	0.58	0.31	0.81
Soil 3	0.76	0.80	1.46	1.86	1.37	1.76	1.66
Tap water 1	0.98	1.04	1.90	1.94	1.36	1.28	1.06
Tap water 2	0.78	0.85	1.54	1.97	1.54	1.85	1.88
Urine 1	0.96	1.07	1.93	1.44	1.44	1.34	1.13
Urine 2	0.87	0.94	1.70	1.15	1.91	1.95	1.40
Urine 3	0.52	0.28	0.50	0.68	1.17	0.62	1.63
Control	0.64	0.75	0.67	0.47	0.28	0.58	0.84

TABLE 10.11 Results obtained using the conventional hand extractions

Sample	Analyte concentration found (mg/ℓ)						
	Pb^{2+}	Cu^{2+}	Zn^{2+}	Co^{2+}	Cd^{2+}	Fe^{3+}	Hg^{2+}
Soil 1	4.26	3.64	0.31	23.17	1.09	10.59	2.40
Soil 2	7.15	5.99	5.52	17.02	5.33	8.85	5.61
Soil 3	3.74	2.12	4.74	18.21	5.45	11.19	1.46
Tap water 1	8.60	7.67	1.18	13.09	13.00	47.80	0.74
Tap water 2	5.56	5.24	1.74	27.88	13.41	47.23	0.58
Urine 1	8.45	6.40	5.31	3.97	13.56	4.92	1.46
Urine 2	7.05	5.19	5.80	3.56	12.01	4.38	1.32
Urine 3	0	2.62	3.58	1.48	10.70	2.87	5.73
Control	4.95	5.09	4.99	4.87	5.01	5.18	5.08

TABLE 10.10 Relative standard deviations obtained when using conventional hand extractions

Sample	%RSD						
	Pb^{2+}	Cu^{2+}	Zn^{2+}	Co^{2+}	Cd^{2+}	Fe^{3+}	Hg^{2+}
Soil 1	0.17	0.20	0.35	0.46	0.83	0.44	1.16
Soil 2	0.13	0.14	0.25	0.31	0.57	0.30	0.78
Soil 3	0.74	0.83	1.51	1.91	1.47	1.82	1.80
Tap water 1	0.95	1.07	1.94	1.46	1.48	1.34	1.18
Tap water 2	0.77	0.86	1.56	1.97	1.58	1.87	1.95
Urine 1	0.97	1.06	1.92	1.42	1.41	1.31	1.08
Urine 2	0.86	0.94	1.70	1.15	1.91	1.05	1.40
Urine 3	0.26	0.28	0.50	0.64	1.16	0.61	1.60
Control	0.18	0.17	0.19	0.34	0.49	0.78	0.41

10.4.3.3 Sample frequency

To complete the whole analytical cycle, including the extraction and detection, took 135 seconds. This resulted in a sample frequency of 27 samples per hour. When

considering that seven analytes were determined simultaneously, the sample frequency is quite remarkable for a sequential injection system.

10.4.3.4 Sample interaction

Sample carry-over was evaluated employing a Unicam 8625 spectrometer, to avoid the effect of deteriorating blank signals. Negligible carry-over between samples was experienced when employing this system. A sample with low analyte concentration (1 mg/ℓ) was analysed, followed by a sample with analyte concentration five times higher than the first. To evaluate sample interaction the first sample was analysed again. Sample carry-over was then calculated according to the difference between the two peak height values [18]. The percentage carry-over calculated were low enough to be ignored. The sample interaction was calculated to be about 0.05%.

10.4.3.5 Detection limits

The detection limit is both a function of sensitivity and noise. The lowest concentration, that could be determined without doubt, would be considered the detection limit of the system. Due to the excess of reagent, detection limits were difficult to obtain. Low concentrations of the analyte showed peak profiles similar to those of the reagent alone, while the peak shape changed with higher analyte concentrations. Since the most of the linear ranges started at 1 mg/ℓ, this concentration was taken as limit of detection for all seven analytes.

10.4.3.6 Interferences

Possible interferents were tested using a solution containing 1 mg/ℓ of all seven analytes. The following substances did not interfere in the determination: 500 mg/ℓ SO_4^{2-}, 10 mg/ℓ PO_4^{3-}, 2 mg/ℓ Al^{3+} (Al do not react with dithizone under neutral to alkaline conditions), 50 mg/ℓ Mg^{2+} and 400 mg/ℓ Ca^{2+}.

The mercury determination was more vulnerable to interferences. Chloride up to 14 g/ℓ (0.4 mol/ℓ) did not interfere in the mercury determination as long as the H_2SO_4 concentration did not exceed 2 mol/ℓ. Bromide, cyanide and thiocyanate also interfered seriously in the mercury determination, since they complex mercury more strongly than dithizone. These anions could be tolerated up to 10 mg/ℓ. Thiocyanate and cyanate were used to mask interferences due to cobalt and interfered seriously in the determination of cobalt. Anions could be removed by using anion exchange columns in the sample uptake tubes. The other metals did not experience any interference due to the anions present in the solution.

Since the metals normally present in urine, *viz.* Fe(II), Ni(II), Pb(II) and Zn(II), were also analysed with the SIE system, they were ruled out as interferents. Variation in pH could be used to separate the different metals from one another to allow individual analysis, but at the pH used all the analytes were extracted into the organic layer.

10.5 Conclusion

A simplified, automated extraction system is described which employ a non toxic solvent, ethanol. This makes the technique much more environmental and operator friendly. The technique can be applied without the use of phase separators or segmenters. This fact highlights the durability and robustness of the technique, since less maintenance will be needed. The sequential injection system is fully computerised and allow the determination of seven metal ions (lead, zinc, copper, iron, cobalt, cadmium and mercury) in the same sample without prior separation. A sample frequency of 27 samples per hour place it ahead of other SIA systems, where the main drawback usually is the low sample throughput. Coupling sequential injection extraction with a diode array spectrophotometer resulted in high sample throughput and a sensitive method to determine related species without the need of tedious analyte separations.

10.6 References

1. D. C. Adriano, **Trace Elements in the Terrestrial Environment**, Springer-Verlag-New York Inc., **1**, pp 1.496.
2. L. van der Merwe, **Ondersoek na Bepalings van Geselekteerde Metale in Riviersedimente met behulp van 'n pH-afhanklike Ekstraksieprocedure**, MSc-Thesis, University of Pretoria, 1992.
3. N. N. Greenwood and A. Earnshaw, **Chemistry of the Elements**, Pergamon Press, 1984.
4. A. Botha, **Sequential Injection Analysis: Evaluation of Operational Parameters and Application to Process Analytical Systems**, MSc-Thesis, University of Pretoria, 1999.
5. I. Drabœk and Å. Iverfeldt in Quevauviller, Maier and Griepink (eds), **Quality Assurance for Environmental Analysis**, Elsevier Science, 1995.
6. H. A. McKenzie and L. E. Smythe, **Quantitative Trace Analysis of Biological Materials**, Elsevier, 1988, pp 589 - 603.
7. A. I. Yuzefovsky, R. F. Lonardo, M. Wang and R. G. Michel, **Jour. Anal. Atom. Spec.**, **9** (1994) 1195.
8. K. Nomiyama, in P. A. Krenkel (ed), **Heavy Metals in the Aquatic Environment**, Pergamon Press, Oxford, pp 15 - 23.
9. P. C. Rudner, A. G. de Torres, J. M. C. Pavon and E. R. Castellon, **Jour. Anal. Atom. Spec.**, **13** (1998) 243.
10. I. A. Gurév and N. V. Kuleshova, **Jour. Anal. Chem.**, **53** (1998) 15.
11. J. Fries and H. Getrost, **Organic Reagents for Trace Analysis**, E. Merck Darmstadt, 1977.
12. O. Haase, M. Klare, J. A. C. Broekært and K. Krengel-Rothensee, **Analyst**, **123** (1998) 1219.
13. G. Tao, S. N. Willie and R. E. Sturgeon, **Analyst**, **123** (1998) 1215.
14. A. Ali, H. Shen and X. Yin, **Anal. Chim. Acta**, **369** (1998) 215.
15. C. E. C. Malgalhaes, F. J. Krug, A. H. Fostier and H. Berndt, **Jour. Anal. Atom. Spec.**, **12** (1997) 1231.

16. L. W. Potts, **Quantitative Analysis. Theory and Practice**, Harper and Row, New York, 1987.

17. **Cobalt in Potable Waters**, Methods for the Examination of Waters and Associated Materials, HMSO, 1981.

18. R. E. Taljaard, **Sequential Injection Analysis as Process Analyzers**, MSc-Thesis, University of Pretoria, 1996.

19. A. Ivaska and W. W. Kubiak, **Talanta**, **44** (1997) 713.

20. J. L. F. C. Lima, A. O. S. S Rangel and M. M. S. Roque da Silva, **Cienca e Technica Vitivinicola**, **9** (1990) 121.

21. J. F. van Staden, H. du Plessis and R. E. Taljaard, **Anal. Chim. Acta**, **357** (1997) 141.

22. J. L. Burguera and M. Burguera, **Anal. Chim. Acta**, **153** (1983) 207.

23. O. Klinghoffer, J. Růžička and E. H. Hansen, **Talanta**, **27** (1980) 169.

24. M. H. Memon and P. J. Worsfold, **Analyst**, **113** (1988) 769.

25. E. A. Novikov, L. K. Shpigun and Y. A. Zolotov, **Anal. Chim. Acta**, **230** (1990) 157.

26. H. M. N. H. Irving, **Dithizone**, The Chemical Society, London, 1977.

27. G. Iwantscheff, **Das Dithizon und seine Andwendung in der Mikro- und Spurenanlyse**, Verlag Chemie, Weinheim, 1958.

28. G. D. Marshall and J. F. van Staden, **Anal. Instrum.**, **20** (1992) 79.

29. K. L. Peterson, B. K. Logan, G. D. Christian and J. Růžička, **Anal. Chim. Acta.**, **337** (1997) 99.

30. M. Valcarcel and M. D. Luque de Castro, **Flow Injection Analysis. Principles and Applications**, Ellis Horwood, Chichester, 1987.

31. J. Růžička and E. H. Hansen, **Flow Injection analysis**, 2nd ed, John Wiley & Sons, New York, 1988.

32. P. W. Atkins, **Physical Chemistry**, fourth ed., Oxford University Press, Oxford, 1990, pp 293 - 969.

33. C. A. Lucy, **Anal. Chem.**, 61 (1989) 101.

34. Y. Luo, S. Nakano, D. A. Holman, J. Růžička and G. D. Christian, **Talanta**, **44** (1997) 1563.

35. L. W. Potts, **Quantitative Analysis. Theory and Practice**, Harper and Row, New York, 1987.

36. A. T. Hutton, **Polyhedron**, **6** (1987) 13.

37. S. Nakano, Y. Luo, D. Holman, J. Růžička and G. D. Christian, **Microchem. Jour.**, **55** (1997) 392.

CHAPTER 11

Summary

The development of analysers capable of on-line monitoring, with a high sample throughput, minimum sample and reagent consumption that are robust, reliable and requires a low frequency of maintenance became a necessity in many laboratories. Flow injection analysis was only moderate successful in complying the strict requirements of precise timing and low sample and reagent consumption. Furthermore, FIA manifolds require physical manipulation of the manifold when changing from one configuration to another. Very often multiple lines are required that make the system inconvenient to operate and more prone to failures. Simply changing a chemistry can be very time consuming.

The attributes of flow-injection analysis (FIA): speed, solution containment, capability of miniaturization, automated standardization, sample dilution, matrix removal, analyte preconcentration and the ability to control the time/concentration domain of any solution chemistry under investigation, are, however, well recognized and exploited by the world wide community of flow injection enthusiasts.

The introduction of SIA was an attempt to make injection techniques more rugged for process control application. This single-line system that is completely computer controlled, can be configured to perform most operations of conventional flow injection analysis with no or minimal physical reconfiguration of the manifold. This system contributes considerably to reducing reagent and sample configuration which is one of its greatest attributes. The simplicity of the SIA system is attributed to the multi-port selection valve by which the samples, reagents, reactions lines and detector line(s) are accessed. Adaption of chemistries to SIA is also (in most cases) an easy task, as it can be based on the practice and the theory of flow injection methodology, which provide guidelines for the design of sequential injection systems.

The inherent flexibility of SIA makes it an ideal tool for monitoring bioprocesses where sample matrix changes with time and different conditions of analysis may be required. Another advantage of SIA is the possibility of clustering standards around the multi-position valve, so that the system might be automatically recalibrated as required. The detector is only exposed to the potentially harsh sample for a short time, the rest of the time, the detector is exposed to the wash solution. There is also the possibility of two assays being performed with an unique SIA system.

It is unlikely that SIA in its present form will replace FIA. Few sample manipulation techniques match FIA in flexibility. The only requirement for successful implementation in FIA is a repeatable flow pattern. In SIA careful planning and method design is required. Attention must be given to ensure that zones are contained within the reaction coil and that device events are carefully synchronized. This requires closer attention during the method development phase. Nevertheless, once a method has been developed, SIA tirelessly and slavishly repeats the device sequence which generates the desired analytical results.

Important guidelines were established to assist in the design of SIA manifolds. Of course, these guidelines must be interpreted in the light of the application at hand; it may not always be desirable to maximize sensitivity.

The development of sequential injection analysis is aimed at providing the industrial, agricultural, clinical and pharmaceutical fields with reliable, precise and cost-effective instrumentation for performing the analyses required. The increasing awareness regarding environmental pollution and the regulation of the effluents that are released into the environment, places an enormous responsibility on analysts to develop methods that can be effectively applied to determine the actual amount of polluting elements that are discharged.

A wide range of successful applications of SIA are already described by various researchers. Unfortunately, most of these applications involved the determination of

only one analyte at a time. Simultaneous analysis (or multi-component analysis) employing sequential injection analysis seems to be more complicated or less feasible than single-component analyses. This might be described to the fact that most multi-component determinations require extractions and the subsequent separation of the aqueous and organic phases, establishment of pH gradients or effective pH control, long and complex procedures, complex mathematical and statistical calculations and/or multiple detectors. Systems that only use one detector for multi-component detection are more complex to program and manipulate, but are much more cost effective than multi-detector systems. In this study, various single detector systems for multi-component analysis were illustrated and evaluated.

The methodology developed during this study demonstrates the suitability of sequential injection analysis for sequential and simultaneous determinations. A novel tandem technique for the determination of iron and sulphate in the same or different samples were described. It was possible by using an optimised sequence of samples and reagents and the kinetics of the two reactions to determine to analytes in one analytical cycle. The zones of the slower turbidimetric determination of sulphate were first introduced into the holding coil, followed by the zones of the faster iron-tiron reaction. This arrangement allowed ample time for both reactions to develop to a desired stage before photometric detection at the same wavelength took place.

The same reactions were also used to evaluate a sandwich technique based on the introduction of a very large sample zone sandwiched between the two reagents. The volume of the sample zone was crucial to eliminate any interference of the two reactions on one another and to ensure sufficient resolution between the two reagent peaks obtained. The latter was necessary for convenient measurement of the respective peak heights.

Due to the discontinuous nature of sequential injection analysis, a multi-component determination based on differential kinetics were successfully adapted from FIA. The simultaneous determination of nickel(II) and cobalt(II) were based on the different

reaction rates of the two analytes with a non-selective reagent, PAR. Since SIA is a discontinuous technique, stopped flow periods are easily incorporated to ensure longer reaction times for slower reactions.

Three different extraction procedures were developed for determination of two or more metal ions in soil extracts, clinical samples and aqueous samples. The first sequential injection extraction (SIE) system described a common extraction method. The sample in the aqueous phase was mixed with the reagent (dithizone) in the organic phase. Since the organic solvent used was ethanol and because ethanol and water are miscible in all ratios, no separation of the phases was necessary prior to detection. Cobalt(II) and mercury(II) were determined with this SIE method with acceptable accuracy and reproducibility.

Since no phase segmenters or separators are needed in a sequential injection extraction system, the manifold is much simpler and easier to construct than those of flow injection extraction systems. SIE is a flow-based extraction method where an aqueous sample and organic solvent are injected sequentially into an extraction coil, then mixed and separated due to the differential flow velocities of the aqueous and organic phases.

Dithizone was also used for the second extraction process, but this time it was dissolved in carbon tetrachloride. Specific metal dithizonates are formed at specific pH values. For the extraction of mercury(II) and cadmium(II) a pH gradient was established in the extraction coil to ensure maximum extraction of both analytes into the organic phase. The acidic extraction product ($Hg(HDz)_2$) was formed first, due to its stability in dilute alkaline solutions and therefore did not decompose when the flow was reversed to allow the alkaline extraction of the cadmium dithizonate. The organic phase containing both analytes was determined photometrically employing only one detector.

In the third extraction method, seven metal ions (Pb(II), Zn(II), Cu(II), Fe(III), Co(II), Cd(II) and Hg(II)) were determined using a single detector. The metal ions were extracted into an organic phase (ethanol) containing dithizone. No separation of phases was necessary due to miscibility of the two phases. The flow was stopped in the flow-through cell in the detector and the spectra were recorded with a diode array spectrophotometer. Spectra were recorded between 350 and 750 nm. The method proved to be accurate, sensitive and reproducible.

Since simultaneous or multi-component analysis allow the measurement of more than one analyte or parameter at a time, it increases the sample throughput of SIA systems tremendously. This study also proved that the sequential injection analysers developed, are compatible with analysis of samples in different forms and from different application fields. It can therefore be expected that multi-component sequential injection analysers will be proliferated in modern chemical, biochemical, metallurgical and environmental applications.

ADDENDUM A

ADDENDUM A

Method construction

Sequential injection analysis is dependant on precisely timed operations which took place in a preprogrammed sequence. These programming was done using the FlowTEK [1, 2] program, developed by Marshall [3]. The method used for the determination of seven metal ions in one sample (described in Chapter 10) is used to explain the construction of methods and procedures in FlowTEK.

The analytical cycle used in the determination consisted of the following operations: the sequential introduction of an air bubble, the extractant, the sample and a second air bubble, the extraction step itself, detection of the formed products and rinsing of the manifold.

A Hewlett Packard 8543 diode array spectrophotometer was use as detector and for data acquisition and manipulation. The FlowTEK program was used to control the different devices. (A device is defined as an analytical instrument or component which must be controlled by the software package. These devices must be compatible with TTL or switch control signals [2].) FlowTEK was also used to send a signal to the diode array after the product was stopped in the flow-through cell. The signal from FlowTEK was recognised by a macro (UMACINIT.MAC) written especially for this application. Three different signals could be recognised by the diode array spectrophotometer, *viz.* BLANK, STANDARD and SAMPLE. Since there was no program or device option in FlowTEK to send these signals, it was first necessary to define this device.

It was needed to use two pairs of outputs, one which combined the BLANK and STANDARD signal as well as one which combined the SAMPLE and a STOP signal. Both pairs of outputs were placed in a single method rather than two, this was necessary because, when changing one pair the other pair must not be changed as

well. This is accomplished only when both pairs of outputs are in the same method. It was also needed to initialise the digital outputs (from the interface) to the inactive state. This was done by selecting the **Startup** option on the *method* menu. The value **240** was entered there. The value was obtain from the fact that the digital outputs of ports **5**, **6**, **7** and **8** of the interface were al set to **1** (16 + 32 + 64 + 128 = 240). This meant that the end of the pulse (when defining the device) should be set to **11** (by typing **3** at the end of the configuring device process). The method was saved (using the option **File** on the *method* menu and typing **S** for save). It was needed to exit FlowTEK and restarted it to initialise the new dev.cfg (device configuration file).

To define the device, the option **Config devices** on the *method* menu was chosen. The questions or commands which followed were answered as follow:

Enter device defn number:	**8**	
Enter device name:	**BS**	(BLANK and STANDARD)
Enter number of device actions:	**2**	
Enter action narration for action 1:	**BLANK**	
Enter digital output for action BLANK:	**1**	
Enter hotkey for BLANK:	**B**	
Enter action narration for action 2:	**STAND**	
Enter digital output for action STAND:	**2**	
Enter hotkey for STAND:	**S**	
Enter pulse length (0 for continuous):	**0.5**	
Enter digital output for pulse:	**3**	(The end of the pulse is given as 11 on the *notepad* page - see Fig. 2)

Enter device defn number:	**9**	
Enter device name:	**SS**	(SAMPLE and STOP)
Enter number of device actions:	**2**	
Enter action narration for action 1:	**SAMPL**	
Enter digital output for action SAMPLE:	**1**	

Enter hotkey for SAMPLE:	**S**
Enter action narration for action 2:	**STOP**
Enter digital output for action STOP:	**2**
Enter hotkey for STOP:	**Z**
Enter pulse length (0 for continuous):	**0.5**
Enter digital output for pulse:	**3**

The device descriptions can be viewed under the *notepad* menu (Fig. 1). The first six device definitions are supplied with the software package. There are six more devices than can be user specified. Number 8 and 9 were used for the diode array spectrophotometer. The letter **N** must be typed to view the second page of the device configurations (Fig. 2). For sequential injection analysis the device configuration data of the Gilson pump (GP) and the selection valve (SV) are used (see Fig. 1).

Next Page Hard Copy RED Print MET Print PDR Print Quit

```
Board : PC30-B
Experiment time :    154.0
Zoom min time :      0.0
Zoom max time :      154.0
Start acquisition : 150.0
I/O port for GP :    1
I/O port for SV :    3
I/O port for BS :    5
I/O port for SS :    7
Save profile : Yes
Abridged profile : Yes
Regression on Height
Detector displ : Paged
Inject mode : Auto
Startup :   (0)
Rescale Y-axis : Fixed
Min : 0.00    Max :10.00

F1 : Displ Analog input
F2 : Displ Digital input
F3 : 010000000000 (2)
F4 : 110000000000 (3)
F5 : 000000000000 (0)
F6 : 000100000000 (8)
F7 : 001100000000 (12)
F8 : 000000000000 (0)
F9 : 000000000000 (0)
F10 : Directory
```

Detector	1	2	3	4
A/D channel	1			
Transformation	None			
Auto Zero	None			
AZ time	0.0			
AZ offset	0.000			
Min Integ Lim	150.0			
Max Integ Lim	154.0			
Width Height	0.000			
Peak Time	@ Pk max			

```
Path :                          c:\flowtek\PHD\EXTRAC\
Main Procedure file :           MULTIEXT.PDR
Method file :                   MULTIEXT.MET
Reduced data file :             3AUG.RED
Experiment Profile Root :       3AUG
Calibration file :              DEFAULT.CAL
```

Name	AP	GP	IV	SV	AS	SW
Action	FWD REV OFF	FWD REV OFF	INJ LOAD	ADV HOME	NEXT	TRUE FALSE
Hotkey	F R O	F R O	I L	A H	N	T F
Output	01 (1) 10 (2) 00 (0)	10 (2) 11 (3) 00 (0)	01 (1) 10 (2)	10 (2) 01 (1) 00 (0)	1 (1) 0 (0)	1 (1) 0 (0)
Pulse	0.00	0.00	0.00	0.30	5.00	0.00

Fig. 1 Schematic representation of the FlowTEK notepad screen (page 1 for device descriptions).

Name	SP	BS	SS	0	0	0
Action	2 REV OFF	BLANK STAND	SAMPL STOP			
Hotkey	F R O	B S	S Z			
Output	0 (0) 1 (1) 0 (0)	01 (1) 10 (2) 11 (3)	01 (1) 10 (2) 11 (3)			
Pulse	0.00	0.50	0.50	0.00	0.00	0.00

Fig. 2 Schematic representation of the FlowTEK notepad screen (page 2 for device descriptions).

For the extraction method four different devices were used, *viz.* the Gilson pump (GP), the selection valve (SV) and the two newly configured devices (BS and SS). These four devices were selected using the option **Type** (of) **device** on the *method* menu. The questions or commands which followed were answered as follow:

Enter number of devices:	**4**	
Enter type device 1:	**GP**	
Enter digital point for GP:	**1**	(This represent the first position the device occupy on the interface board)
Enter type device 2:	**SV**	
Enter digital point for SV:	**3**	
Enter type device 3:	**BS**	
Enter digital point for BS:	**5**	
Enter type device 4:	**SS**	
Enter digital point for SS:	**7**	

The screen is now divided into four panels, each containing a straight line in the middle of the panel. The position of these lines represent the 'OFF' position of each device. Programming of each device are now allowed. Device events are entered by choosing the option **Insert** in the *method* menu. It is important to switch on **NUM LOCK** when

using the **Insert** or **Delete** options. The programming for the different operations needed were done as follows:

Insert

Device number:	**2**	(selection valve)
Enter time of event:	**0**	
Hotkey (A H):	**H**	(Select HOME position - connected to the first air inlet)

Insert

Device number:	**1**	(Gilson pump)
Enter time of event:	**4**	
Hotkey (F R O):	**R**	(Switch pump on in the reverse direction)

Insert

Device number:	**1**	(Gilson pump)
Enter time of event:	**4.5**	
Hotkey (F R O):	**O**	(Switch pump off)

Insert

Device number:	**2**	(selection valve)
Enter time of event:	**5.5**	
Hotkey (A H):	**A**	(Select second port - extractant solution)

Insert

Device number:	**1**	(Gilson pump)
Enter time of event:	**6.5**	
Hotkey (F R O):	**R**	(Switch pump on in the reverse direction)

Insert

Device number:	**1**	(Gilson pump)
Enter time of event:	**10.5**	
Hotkey (F R O):	**O**	(Switch pump off)

Insert

Device number:	**2**	(Selection valve)
Enter time of event:	**11.5**	

Hotkey (A H):	**A**	(Select third port - standard or sample solution)
Insert		
Device number:	**1**	(Gilson pump)
Enter time of event:	**12.5**	
Hotkey (F R O):	**R**	(Switch pump on in the reverse direction)
Insert		
Device number:	**1**	(Gilson pump)
Enter time of event:	**16.5**	
Hotkey (F R O):	**O**	(Switch pump off)
Insert		
Device number:	**2**	(Selection valve)
Enter time of event:	**17.5**	
Hotkey (A H):	**A**	(Select fourth port - second air inlet)
Insert		
Device number:	**1**	(Gilson pump)
Enter time of event:	**18.5**	
Hotkey (F R O):	**R**	(Switch pump on in the reverse direction)
Insert		
Device number:	**1**	(Gilson pump)
Enter time of event:	**19**	
Hotkey (F R O):	**O**	(Switch pump off)
Insert		
Device number:	**2**	(Selection valve)
Enter time of event:	**20**	
Hotkey (A H):	**A**	(Select fifth port - holding coil)
Insert		
Device number:	**1**	(Gilson pump)
Enter time of event:	**21**	
Hotkey (F R O):	**R**	(Switch pump on in the reverse direction)

Insert

Device number:	**1**	(Gilson pump)
Enter time of event:	**26**	
Hotkey (F R O):	**F**	(Switch pump on in the forward direction)

Insert

Device number:	**1**	(Gilson pump)
Enter time of event:	**31**	
Hotkey (F R O):	**O**	(Switch pump off)

Insert

Device number:	**2**	(Selection valve)
Enter time of event:	**32**	
Hotkey (A H):	**A**	(Select sixth port - detector)

Insert

Device number:	**1**	(Gilson pump)
Enter time of event:	**33**	
Hotkey (F R O):	**F**	(Switch pump on in the forward direction)

Insert

Device number:	**1**	(Gilson pump)
Enter time of event:	**43**	
Hotkey (F R O):	**O**	(Switch pump off - waiting period)

Insert

Device number:	**3**	(BLANK or STANDARD)
Enter time of event:	**93**	
Hotkey (B S):	**B or S**	(Depending on the solution in the flow-through cell at that moment a BLANK or a STANDARD signal is send to the diode array spectrophotometer for data acquisition.)

OR

Insert

Device number:	**4**	(SAMPLE or STOP)
Enter time of event:	**93**	
Hotkey (B S):	**B or S**	(Sample solution must be present in the flow-through cell at that moment. A SAMPLE or STOP signal is send to the diode array spectrophotometer for data acquisition.)

Insert

Device number:	**1**	(Gilson pump)
Enter time of event:	**103**	
Hotkey (F R O):	**F**	(Switch pump on in the forward direction)

Insert

Device number:	**1**	(Gilson pump)
Enter time of event:	**153**	
Hotkey (F R O):	**O**	(Switch pump off - end of analytical cycle)

To delete any existing event, the option **Delete** on the *method* menu must be used. The time of the event needed to be erased must be typed in when asked for it. The procedure to delete an event is the same as the procedure needed to insert an event.

To ensure that no redundant data will be stored, data acquisition could be started only a few moments after the valve was switched to select the detector line. This will result in the collection of only the peak profile and relevant data. To accomplish this the option **Expt time** on the *method* menu must be selected and the time to start data acquisition must be typed in. Because data acquisition and manipulation was performed using the software of the diode array spectrophotometer, this option was not use in the method constructed. The final method is represented schematically in Fig. 3.

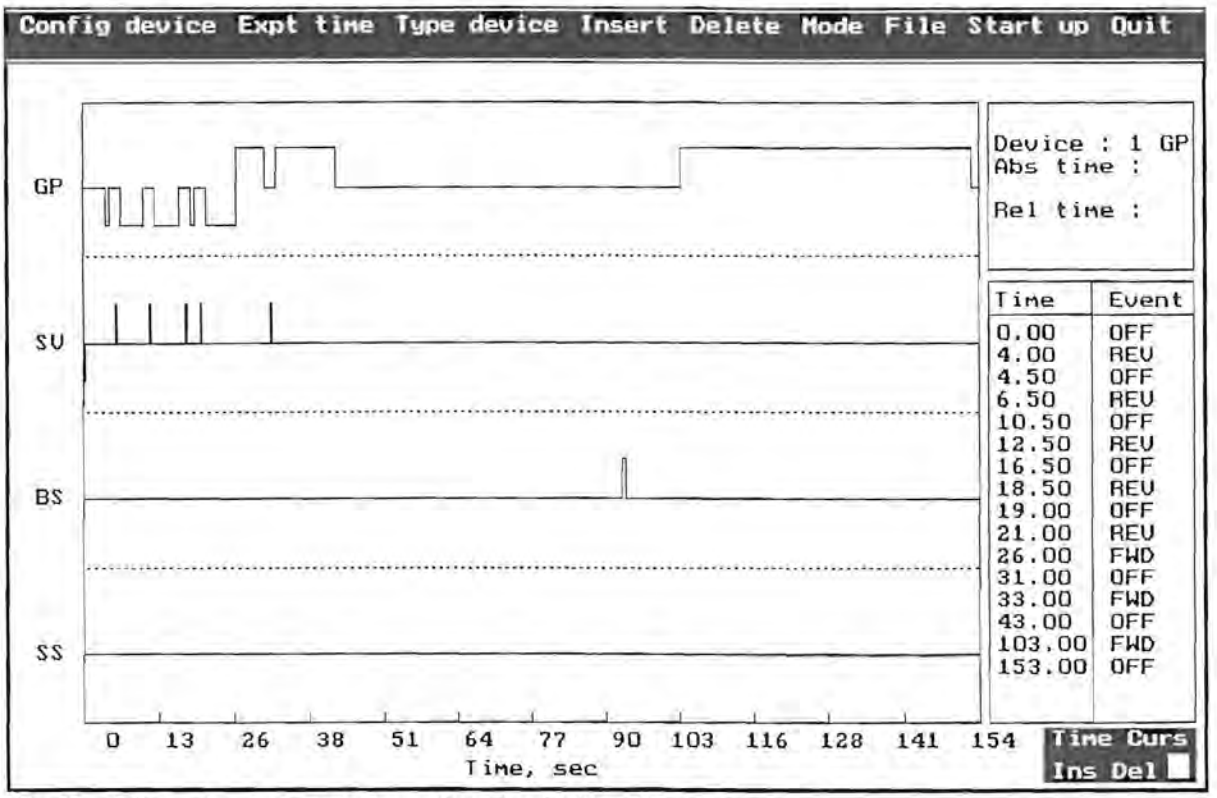

Fig. 3 Schematic representation of the FlowTEK method screen.

After a method is constructed, the option **File** on the *method* menu is used to safe (**S**) the method under an appropriate name. The method file used for the multi-component extraction was saved as **multiext.met**. When the method must be repeated a fixed number of times it is best to write a *procedure* to carry out the repetitions. Five repetitions of the method were used during the final evaluation of the SIE system.

To create a *procedure*, the option **Repeated** on the *main* menu must be selected. The option **Build Proc** on the *repeated* menu is used to create a procedure. The procedure was named multiext.pdr. It was necessary to specify whether a method file (.met) or another procedure file (.pdr) was used in this application. The following commands or questions must be answered:

Enter main procedure:	**C:\FLOWTEK\PHD\EXTRAC\MULTIEXT.PDR**
Enter method or procedure file:	**MULTIEXT.MET**
Enter number of repetitions:	**5**

If more methods or procedures are to follow, the process must be repeated till all the methods together with their number of repetitions are listed. Otherwise **ESC** terminates the procedure definition. To use this main procedure file, the option **Main Proc** on the *method* menu must be chosen. The name of the main procedure file must then be typed in. The option **Red. Data file** on the *Repeated* menu selects a reduced data file for saving each experiments' peak parameter data and relative experiment identification information. The experiment number counter is reset to 1 when the reduced data file name is changed **or when the program was exited**. Every time the program is restarted a **new** reduced data file must be opened, otherwise the previous data would be lost. The option **Profile file** on the *Repeated* menu selects the file root name for storing the profile data. The file name extension gives the number of the experiment number. If no profile root is chosen, profile files are not saved.

To execute the *Main procedure* the option **Go!** on the *Repeated* menu must be chosen. The option **Once** on the *Main* menu is chosen if only one run is needed. The *Main procedure* can be aborted by pressing **ESC**.

Simplified method

To construct a basic method for a simple application employing only sample and one (or more reagents) (Fig. 4) the following procedure is needed:

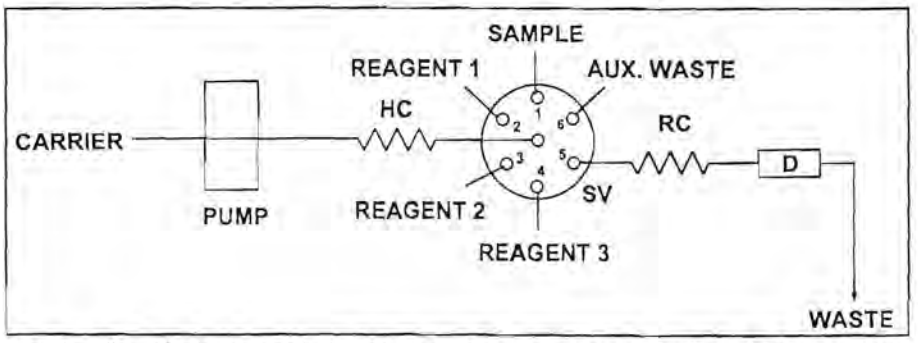

Fig. 4 A typical sequential injection system used to determine single analytes (components). HC - holding coil, SV - selection valve, RC - reaction coil and D - detector.

Since the device definitions for both the pump and the valve are supplied with the software, it does not need any programming. The pump (GP) and valve (SV) can just be selected from the *notepad* (see Fig. 1). From the *main menu* the letter **M** must be typed to obtain the *method menu*. The two devices needed can be selected using the option **Type** (of) **device**. The questions or commands which followed can be answered as follow:

Enter number of devices:	**2**	
Enter type device 1:	**GP**	
Enter digital point for GP:	**1**	(This represent the first position the device occupy on the interface board)
Enter type device 2:	**SV**	
Enter digital point for SV:	**3**	

The screen is now divided into two panels, each containing a straight line in the middle of the panel. The position of these lines represent the 'OFF' position of each device. Programming of each device are now allowed. Device events are entered by choosing the option **Insert** in the *method* menu. It is important to switch on **NUM LOCK** when using the **Insert** or **Delete** options. The programming for the different operations needed can be done as follows:

Insert

Device number:	**2**	(selection valve)
Enter time of event:	**0**	
Hotkey (A H):	**H**	(Select HOME position - connected to the sample inlet)

Insert

Device number:	**1**	(Gilson pump)
Enter time of event:	**4**	
Hotkey (F R O):	**R**	(Switch pump on in the reverse direction)

Insert

Device number:	**1**	(Gilson pump)
Enter time of event:	**6**	
Hotkey (F R O):	**O**	(Switch pump off)

Insert

Device number:	**2**	(selection valve)
Enter time of event:	**7**	
Hotkey (A H):	**A**	(Select second port - reagent 1)

Insert

Device number:	**1**	(Gilson pump)
Enter time of event:	**8**	
Hotkey (F R O):	**R**	(Switch pump on in the reverse direction)

Insert

Device number:	**1**	(Gilson pump)
Enter time of event:	**10**	
Hotkey (F R O):	**O**	(Switch pump off)

Insert

Device number:	**2**	(Selection valve)
Enter time of event:	**11**	
Hotkey (A H):	**A**	(Select third port - reagent 2)

Insert

Device number:	**1**	(Gilson pump)
Enter time of event:	**12**	
Hotkey (F R O):	**R**	(Switch pump on in the reverse direction)

Insert

Device number:	**1**	(Gilson pump)
Enter time of event:	**14**	
Hotkey (F R O):	**O**	(Switch pump off)

Insert

Device number:	**2**	(Selection valve)
Enter time of event:	**15**	

Hotkey (A H):	**A**	(Select fourth port - reagent 3)
Insert		
Device number:	**1**	(Gilson pump)
Enter time of event:	**16**	
Hotkey (F R O):	**R**	(Switch pump on in the reverse direction)
Insert		
Device number:	**1**	(Gilson pump)
Enter time of event:	**18**	
Hotkey (F R O):	**O**	(Switch pump off)
Insert		
Device number:	**2**	(Selection valve)
Enter time of event:	**19**	
Hotkey (A H):	**A**	(Select fifth port - detector)
Insert		
Device number:	**1**	(Gilson pump)
Enter time of event:	**20**	
Hotkey (F R O):	**F**	(Switch pump on in the forward direction - to pump stack of zones through detector)
Insert		
Device number:	**1**	(Gilson pump)
Enter time of event:	**60**	
Hotkey (F R O):	**O**	(Switch pump off - end of analytical cycle)

the auxiliary waste port can be use to rinse the manifold. The rest of the procedure are the same as described on pages 308 and 309.

References

1. G. D. Marshall, **Analytical Instrumentation**, **20**(1) (1992) 79.
2. **FlowTEK Reference Manual, Device Control and Data Acquisition software, ver 1.1**, Mintek, 1993.
3. G. D. Marshall, **Sequential-Injection Analysis**, PhD-Thesis, University of Pretoria, 1994.

ADDENDUM B

ADDENDUM B

Publications and Presentations

Publications

1. R. E. Taljaard and J. F. van Staden, *Simultaneous Determination of Cobalt(II) and Ni(II) in Water and Soil Samples with Sequential Injection Analysis*, **Anal. Chim. Acta**, **366**, (1998) 177.
2. R. E. Taljaard and J. F. van Staden, *Application of Sequential Injection Analysis as Process Analysers*, **Lab. Rob. Autom.**, **10** (1998) 325.
3. R. E. Taljaard and J. F. van Staden, *Simultaneous Determination of Cadmium(II) and Mercury(II) in Aqueous, Urine and Soil Samples using Sequential Injection Extraction (SIE)*, **S. Afr. J. Chem.**, **52** (1999) 36.
4. R. E. Taljaard and J. F. van Staden, *Tandem Sequential Injection Analysis: Determination of Iron and Sulphate*, **Anal. Chim. Acta**, In Press.
5. R. E. Taljaard and J. F. van Staden, *Simultaneous Determination of Mercury(II) and Cadmium(II) in Aqueous, Soil and Biological Solutions using a Simple Sequential Injection Extraction Method*, In Preparation.
6. R. E. Taljaard and J. F. van Staden, *Determination of Lead(II), Copper(II), Zinc(II), Cobalt(II), Cadmium(II), Iron(III) and Mercury(II) using Sequential Injection Extraction*, In Preparation.

Presentations

1. Simultaneous Determination of Cobalt(II) and Ni(II) in Water and Soil Samples with Sequential Injection Analysis

   R. E. Taljaard

   Flow Analysis (FIA 7), Piracicaba, Brazil. 26 August 1997.

2. Simultaneous Determination of Cadmium(II) and Mercury(II) in Aqueous, Urine and Soil Samples using Sequential Injection Extraction (SIE)
R. E. Taljaard and J. F. van Staden
7th International Chemistry Conference in Africa and 34th Convention of the South African Chemical Institute. Durban. South Africa. 6 - 10 July 1998.

3. Simultaneous Determination of Cadmium(II) and Mercury(II) in Aqueous, Urine and Soil Samples using Sequential Injection Extraction (SIE)
R. E. Taljaard and J. F. van Staden
ICFIA 98. Ninth International Conference on Flow Injection Analysis. Seattle. Washington. USA. 23 - 27 August 1998.

4. Simultaneous Determination of Cadmium(II) and Mercury(II) in Aqueous, Urine and Soil Samples using Sequential Injection Extraction (SIE)
R. E. Taljaard and J. F. van Staden
Euroanalysis X. Working Party on Analytical Chemistry of the Federation of European Chemical Societies and the New Swiss Chemical society. Basel. Switzerland. 6 - 11 September 1998.

5. Simultaneous Determination of Cadmium(II) and Mercury(II) in Aqueous, Urine and Soil Samples using Sequential Injection Extraction (SIE)
R. E. Taljaard and J. F. van Staden
SCAR'98 XIVth National Conference on Analytic Chemistry. Division of Analytical Chemistry of the Federation of European Chemical Societies and the Roman Society of Analytical Chemistry. Piatra Neamt. Romania. 24 - 26 September 1998.

6. Simultaneous Determination of Cadmium(II) and Mercury(II) in Aqueous, Urine and Soil Samples using Sequential Injection Extraction (SIE)
R. E. Taljaard and J. F. van Staden

ANALYTICA'98. Third National Symposium on Analytical Science. S A Chemical Institute. Midrand. South Africa. 12 - 14 October 1998.